The Dissertation Committee for Eric Michael Compher
certifies that this is the approved version of the following dissertation:

Long-Term Low-Level Arctic Aerosol Trends, Analysis, and Climatological Correlations at Alert, Canada

Committee:

_____
Sheldon Landsberger, Supervisor

_____
Steven R. Biegalski, Co-Supervisor

_____
Derek A. Haas

_____
William S. Charlton

_____
Philip K. Hopke

Long-Term Low-Level Arctic Aerosol Trends, Analysis, and Climatological Correlations at Alert, Canada

by

Eric Michael Compher

Dissertation

Presented to the Faculty of the Graduate School

of the University of Texas at Austin

in Partial Fulfillment

of the Requirements

for the Degree of

Doctor of Philosophy

The University of Texas at Austin

August 2018

Dedicated to
my wife, Yoon Kyoung,
and our daughter,
Abigail Lee

Acknowledgments

I would like to first thank my committee members, Dr. S. Landsberger, Dr. S. Biegalski, Dr. D. Haas, Dr. W. Charlton and Dr. P. K. Hopke for taking time out of their busy schedules. Of particular importance on my committee is my supervisor, Dr. S. Landsberger who not only convinced me to initially apply for the program but assisted me every step of the way thereafter, and my co-Supervisor Dr. S. Biegalski who helped get things going in the early stages, and whose work formed the beginning of my own.

Others from the University of Texas who deserve recognition are first and foremost the students who performed and are performing Neutron Activation Analysis on the Arctic samples used herein. These students include Richard Lara and Taylor Glover. Next, the graduate students who have come before me who provided, through their work, both a path of investigation, and a body of literature. Most notable is M. Shamsuzzha Basunia.

Environment Canada must be acknowledged for supplying the samples on which this research is based. Dr. Sangeeta Sharma was instrumental in obtaining the data, and the primary contact at Environment Canada who helped with questions along the way.

Finally, many people at Bettis Laboratory, as well as everyone at home, have given me the time and support needed to complete this work. I owe them all a debt of gratitude.

Long-Term Low-Level Arctic Aerosol Trends, Analysis, and Climatological Correlations at Alert, Canada

by

Eric Michael Compher, Ph.D.

The University of Texas at Austin, 2018

SUPERVISOR: Sheldon Landsberger

CO-SUPERVISOR: Steven R. Biegalski

Three decades of weekly winter low-level Arctic aerosol samples from Alert, Canada, are analyzed using Neutron Activation Analysis (NAA) in the TRIGA reactor at the University of Texas. The samples are from the longest currently-running Arctic aerosol data collection project and have received only limited analysis to date. The elemental composition (Aluminum, Bromine, Calcium, Chlorine, Copper, Iodine, Magnesium, Manganese, Sodium, Titanium, and Vanadium) is determined for each sample. The elemental results are characterized statistically and the results are compared to climatological data including temperature data, sea ice data, ice shelf data, and snow cover data. Positive Matrix Factorization (PMF) is performed on the complete data set to determine primary sources of the aerosol pollution. Other data from Alert,

including Methanesulphonic Acid (MSA), Iron, and Sulphate data, is compared to the NAA results, and additional PMF is performed with the additional data. Results show many expected as well as unexpected trends and correlations including correlations with ice cover and temperature trends, correlations to decreasing anthropogenic pollution, and long-term trends of sea components and sea-component ratios in the aerosol. PMF results conclude that there are 5 predominant sources of the Arctic aerosol including two sea sources, two predominant anthropogenic sources (combustion and industrial), and a crustal component. This particular area of inquiry represents completely new information in the growing body of climate science and may influence studies that relate to the Arctic climate and environment, and should have an impact on the particular fields of Arctic Aerosol Monitoring, Atmospheric Transport, Global Diffusion and Dispersion, Arctic Climate Science, and Pollution Monitoring.

Table of Contents

Table of Figures

Table of Tables

1. Introduction

Arctic aerosol pollution has wide ranging implications from enhanced melting of Arctic ice to toxic chemical dispersion. Ground-level Arctic aerosol samples have been collected for decades at various locations across the Arctic to study the trends and effects of these constituents. Significant conclusions from the aerosol sampling have been reached including showing a strong correlation to the melting of Arctic sea ice [Becagli et al., 2016]. Other observations regarding aerosol samples include a notable decrease in lead aerosols as unleaded gasoline became the norm over several decades [Krachler et al., 2005]. The industrial activities (and subsequent fall) of the Soviet Union can even be tracked in the Arctic aerosol record as the industrial components markedly decreased as the Russian economy dealt with the new realities of an open economy [Gong & Barrie, 2005; Sirois & Barrie, 1999].

Other trends in the Arctic aerosol record include increased sea components due to increasing air temperatures in the Arctic and subsequent decrease in sea-ice cover [Browse et al., 2014; Nilsson et al., 2001; Struthers et al., 2011]. In addition, certain anthropogenic pollution constituents such as mercury and black carbon (soot) have been seen to significantly decrease in recent decades [Stone et al., 2014; Cole & Steffen, 2010] as the world has become more environmentally conscious. Such trends may also be related to certain ratios of sea components such as Cl/Na and Mg/Na ratios in the aerosol

record as seen in data from Maenhaut et al. [1996]. Snow cover trends in the Northern Hemisphere and other uncorrelated climatological changes in the Arctic could produce unpredicted and unseen changes in the Arctic aerosol record as well. There remains a great deal more that can be learned from studying Arctic aerosol compositions.

1.1 Problem Statement

Weekly low-level aerosol samples have been taken for the past four decades at Alert, Canada. Environment Canada provided portions of each weekly sample to the University of Texas at Austin. This is the longest currently-running Arctic aerosol data collection project and has received only limited analysis to date. There is a great deal that can be learned from analyzing this sample set and subsequently comparing the results to other results and local pollution and environmental trends. Trends, correlations, and information can be identified found by performing an in-depth study of this sample set.

As with any long-term data collection project, much can be learned that may not expected when the analysis begins. In addition, there is a growing level of interest worldwide in information pertaining to the global climate and specifically, the Arctic climate, its changes, and any additional data that may help to understand the inner-workings of the environment.

1.2 Background

Environment Canada has an Arctic aerosol collection program (the Canadian Arctic Air Pollution Program (CAAPP)) in place at Alert, Canada. Weekly samples are collected, divided, and sent to the University of Texas at Austin, with the understanding that the samples will be analyzed and results will be provided to Environment Canada. The University of Texas has a research reactor (a TRIGA [Training, Research, Isotopes, General Atomics] reactor) that is well-suited to neutron activation analysis (NAA). NAA on such samples which provides volumetric elemental composition through a process detailed herein.

1.3 History

Throughout the 1800s many explorers commented on the “metallic soot” that settled continuously over the Arctic, and hypothesized that the dust was transported from more southern lands. The “Arctic Haze” from which the soot precipitated was noted during numerous US Air Force weather reconnaissance missions during the 1940s and 1950s. Air Force meteorologist J. Murray Mitchell Jr. was credited with the first official diagnosis of this “Arctic Haze” in 1957. From an aircraft, he noted that the striations and colors of the haze indicated particle size of <2 μm. In 1972 a researcher from the University of Alaska, Glen Shaw, formally attributed the haze to aerosol pollution from regions beyond, and

therefore south of, the Arctic. [Garrett & Verzella, 2008] It was ultimately determined that the largest component of Arctic Haze is Sulphate aerosol, which is largely comprised of anthropogenically-generated constituents [Quinn et al., 2007].

With the early belief that the haze was in part attributed to anthropogenic pollution (which was later confirmed) many organizations began researching the Arctic aerosol composition to identify the constituents of the aerosol and identify both events and locations that attributed a large amount of any single component of the aerosol.

The first Arctic aerosol composition analysis was completed in 1976. The results showed that the pollution contained components derived both from oil combustion and from various natural components that included dust from the Gobi desert. [Garrett & Verzella, 2008] In 1980, the Arctic haze was determined to be predominately Sulphate aerosol, and thus largely anthropogenic [Rahn & McCaffrey, 1980]. In the years since the first studies were conducted, studies have been conducted across the Arctic region showing more detailed elemental compositions including contributions from smelters and coal combustion, as well as leaded gasoline combustion and agricultural activities [Krachler et al., 2005].

1.4 Literature Review

Much has been written and published relating to Arctic Aerosols and related topics over the past several decades. This section includes the most relevant and recent information of interest. Additional information to that provided in this section is included throughout the other sections where such information is most appropriate and relevant.

1.4.1 General Review

Multiple sample locations around the Arctic have been used to sample data in the decades since pollution was first attributed to the Arctic aerosol. Different types of air samplers, filters, and subsequent analysis was performed on the various data sets. Sampling locations of interest include Kevo, Finland [Laing et al., 2014; Yli-Tuomi et al., 2003a]; Burnt Island, Egbert, Canada [Biegalski et al., 1998]; Point Petre, Canada [Biegalski et al., 1998]; Barrow, Alaska [Quinn et al., 2009], and Alert, Canada [Landsberger et al., 1990], to name only a few.

1.4.2 Review of Alert Aerosol Trends

The composition of the Alert, Canada aerosol has been reported in multiple publications [Cheng et al., 1991; Ping, 1996; Sirois & Barrie, 1999]. Other literature reports on the composition at other locations throughout the Arctic [Basunia, 2002; Yli-Tuomi et al., 2003a; Yli-Tuomi et al., 2003b], all to be compared with the data in this particular study. However, understanding the composition of the Arctic aerosol samples at different locations is not enough to understand the source or relevance of the elemental composition. There are time-varying components as well that must be understood to fully realize the implications of various compositions.

Much of the research over the past few decades has focused on various trends around the Arctic. Quinn et al. [2009] noted that the decadal trends of certain chemical compositions at Barrow, Alaska, have increased at a rate of around 10% per year. Quinn et al. also indicated that the Mn/V ratio (a useful anthropogenic pollution metric described in Section 6.3) has decreased over the past few decades. Overall, Quinn et al. indicates that chemical species contributing to the Arctic haze decreased at Barrow, Alaska between 1976 and 2008. [Quinn et al., 2009] Similarly, Bodahaine & Dutton [1993] noted that the Arctic Haze at Barrow, Alaska showed a long-term decrease since its relative maximum in 1982 [Bodahaine & Dutton 1993] which is consistent with the decrease of at least 50% in black carbon [Stone et al., 2014]. Other researchers

such as Sprovieri et al. [2004] studied the atmospheric concentration of Mercury at Terra Nova in Antarctica and reached the conclusions that mercury (and implied related anthropogenic pollution levels) were higher in the Arctic than in the Antarctic.

Sirois & Barrie [1999] showed a strong seasonal dependence on Sodium, Chlorine, Copper, Bromine, Iodine, xV (non-crustal Vanadium), xMn (non-crustal Manganese), and Magnesium. Aluminum and Calcium, however, showed minimal seasonal variation in Sirois & Barrie's work. Other research has shown a weak yearly cyclical trend in Aluminum [Basunia, 2002], and it has been noted that a slight seasonal trend may, in fact, exist for Calcium [Barrie & Hoff, 1985]. It is also seen in Sirois et al.'s work that both Vanadium and Manganese show a long-term decreasing trend, as does Copper, whereas Iodine has a long-term increase (albeit small). A sea-salt trend is finally shown in Sirois & Barrie with peaks around 1981 and 1993, although no long term trend (ending at 1995) is apparent. [Sirois & Barrie, 1999]

In other literature, Quinn et al. [2007] compared the seasonal and long-term trends between Barrow, Alaska and Alert, Canada, showing some interesting similarities and distinct differences. Another study [Gong & Barrie, 2005] that shows a marked decrease in xV and xMn also states that there is no observable long-term trend in Magnesium, Calcium, or Sodium at Alert (our results show an increase in Sodium). Gong & Barrie further comment that Aluminum and Titanium show a decrease between 1995 and 2000. Finally, Gong

& Barrie comment that Zn, Cu, as well as xV and xMn all show a decline between 1980 and the 1990s. Perhaps the most interesting revelation from Gong & Barrie is that the northern portions of Russia still contribute the majority of anthropogenic aerosol pollution to the station at Alert, Canada.

Bromine concentrations in the Arctic Aerosol were studied by Biegalski et al. [1997]. The sampling location was at Burnt Island in Lake Huron, Canada. The results showed a seasonal trend, consistent with, but weaker than Arctic Bromine trends noted elsewhere. However, it is stated that although there is a cyclical trend in natural Br, the anthropogenic component does not display a seasonal variation. Other research into aerosol components at Alert shows seasonal variations as well [Barrie et al., 1994].

For additional details regarding reported trends of the included aerosol components, see Chapter 3 of this paper.

1.4.3 Other Arctic Aerosol Trends

Russian Arctic aerosol pollution has been explicitly studied, as it is well known that northern Russia is a primary contributor to overall Arctic aerosol pollution [Gong & Barrie, 2005]. One such study, conducted by Shevchenko et al. [2003] concluded that the values reported around the Arctic for Arsenic, Vanadium, Zinc, and other anthropogenic pollution was comparable to what can be directly measured in the Russian Arctic.

The longest study related to this work was published Laing et al. [2014a; 2014b], in which 47 years of weekly aerosol data from Kevo, Finland was analyzed for both chemical composition and trend analysis. Results published showed clear seasonal trends for most species, as has been reported in most similar studies, but also noted that the concentrations of anthropogenic contributors were higher than other Arctic sources due to the proximity of Kevo to Eurasian sources. Laing et al. considered that Vanadium and Manganese (among other elements not considered for this study) should be considered as markers of stationary fuel combustion. Finally, a 92% reduction in Lead is noted over the 47 years due to the reduction in the use of Lead in gasoline.

1.4.4 Climatological Correlation Review

Speculation has arisen in some climatological fields as to the effect on climatological changes on not only ice, snow, and temperature, but the subsequent impacts to the Arctic aerosol record. Sea salt aerosols (including Sodium, Chlorine, Magnesium, Bromine, Potassium, and Iodine) are typically thought to be emitted from open water, from breaking waves and wind, with little to no contribution from ice-bound salts [Browse et al., 2014]. The prominent mechanism of sea-salt aerosol generation is therefore believed to be salt entrained in air-bubbles on whitecaps and other wind-driven waves, bursting into the wind. With this understanding, sea-salt aerosol emissions should be inversely

correlated to sea-ice cover [Struthers et al., 2011]. However, it is well known that local peaks in aerosol sea salt components tend to occur in the winter when the local ocean is iced over [Huang & Jaeglé, 2017].

There is also the potential that sea-salt aerosols are not just driven by the climate, but that the aerosols provide a feedback and actually influence the climate as well. Specifically, the aerosol changes the optical properties of the climate, changing the radiative balance in the region. [Struthers et al., 2011] As an example, clean air standards enacted during the 1970s have reduced Sulphate pollution in the Arctic, which may also be related to increasing Arctic temperatures as well as an increase in Chlorides as Sulphates not only tend to cool the atmosphere, but also scrub Chlorides from the air resulting in higher levels of sea-salt aerosol [Samset, 2018; Voiland, 2009]. In addition, the feedbacks may include changes in cloud of fog intensity or lifetimes [Nilsson et al, 2001]. It has been noted additionally that the Arctic Haze reached a maximum in 1992, and was decreasing as of 1993 [Bodahaine & Dutton, 1993].

The mechanisms that drive the Cl/Na aerosol ratio from 1.73 in the seawater to values much lower over land and ice appear to have one main driver that appears to be volatilization of Chlorine by air pollution. One possible pollutant that may remove chloride from aerosol sea salt is H_2SO_4. The Cl/Na ratio has been inversely correlated to SO_4 in previous literature. Increased pollution has been seen explicitly in some samples in conjunction with depressed Cl/Na ratios. [Shaw, 1991]

All other factors being equal, higher pollution should correlate with a reduced Cl/Na ratio in the Arctic aerosol sample. Increased wind from open water, or increased open water for a consistent wind, should also result in an increase in the Cl/Na ratio. An additional ratio that may have some relevance is the Ca/Cl ratio.

There is less of an understanding of the Mg/Na ratio, but the Mg/Na ratio has been noted to be higher over ice than near open water. [Maenhaut et al., 1996] Thus, an increase of wind from open water, or a lessening of ice in the upstream direction of the wind should correlate with a decrease of the Mg/Na ratio.

Ongoing Arctic aerosol studies are still being conducted, as are seasonal studies. One final recent study of interest was conducted recently in the Arctic on board a Chinese research vessel. In 2015, a Chinese research expedition collected Arctic aerosol over the seas and noted that Methanesulphonic acid (MSA) concentrations over the ocean were highly correlated to sea surface temperature. MSA concentrations were compared to other reported MSA concentrations including those at Alert, Canada. [Ye et al., 2015]

2. Alert, Canada, Climate and Environment

This body of work is based on sampling and elemental data obtained at Alert, Canada by Environment Canada. The Alert station includes one of the longest running sets of Arctic aerosol data. Weekly samples have been formally collected since 1980, and continue to be collected to this day. The samples are divided and shipped to multiple locations around the world for analysis, including the University of Texas at Austin. To truly understand certain trends and other data included herein, it is first important to outline some relevant details about Alert, including its geography, weather, and climate.

2.1 Alert, Canada

The Canadian Archipelago consists of many islands, with the northernmost being Ellesmere Island. This large Arctic island as seen in Figure 1 has an area of nearly 200,000 km^2, which makes it the third largest island in Canada and the tenth largest island in the word. Ellesmere Island is a polar desert which includes mountains, plains, glaciers, and ice. [Ellesmere, 2017]

Alert, Canada, as seen in Figure 2 lies near the northernmost tip of Ellesmere Island. Alert is the northernmost permanently inhabited place on earth, being closer to the north pole than it is to the Arctic Circle (Alert is at 82.5018° N, 62.3481° W; for reference, the Arctic Circle is at ~66º North, and the North Pole

is at 90º north). The sky is perpetually dark for a large part of the year. The sun rises around February 28th; from mid-April until September, the sun never sets. The permanent Alert population of approximately 60 people (mostly scientists and researchers) collect data, monitor the Arctic climate, and performing a whole host of other duties including taking ice-core samples for various research projects. [Alert, 2017]

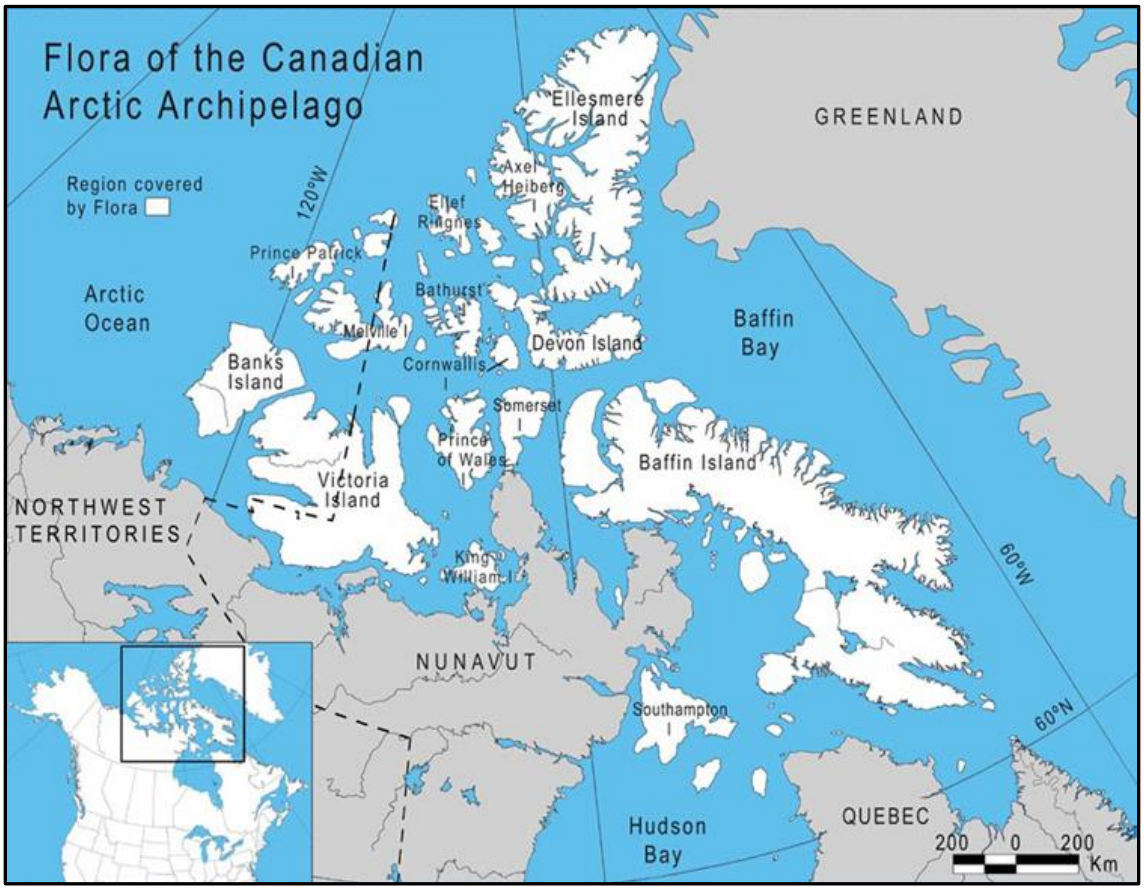

Figure 1 - Canadian Archipelago [www.nature.ca]

Figure 2 - Alert, Canada [www.ec.gc.ca]

Near Alert are a host of interesting coastal and oceanographic features. Approximately 200 miles to the southwest lies Yelverton Bay at a longitude of approximately 82°20'N. Yelverton Bay is typically iced over into the Yelverton inlet as well as the Kulutingwak Fiord. Along the coast from Yelverton bay towards Alert are numerous ice shelves and a large amount of landfast sea ice, including a great deal of multi-year landfast sea ice. The entire region is characterized by permafrost and nearly year-long ice cover, while only some of the ice disappears in the warmer months.

The extremely low yearly temperatures at Alert can be seen in the Figure 3 and in Table 1.

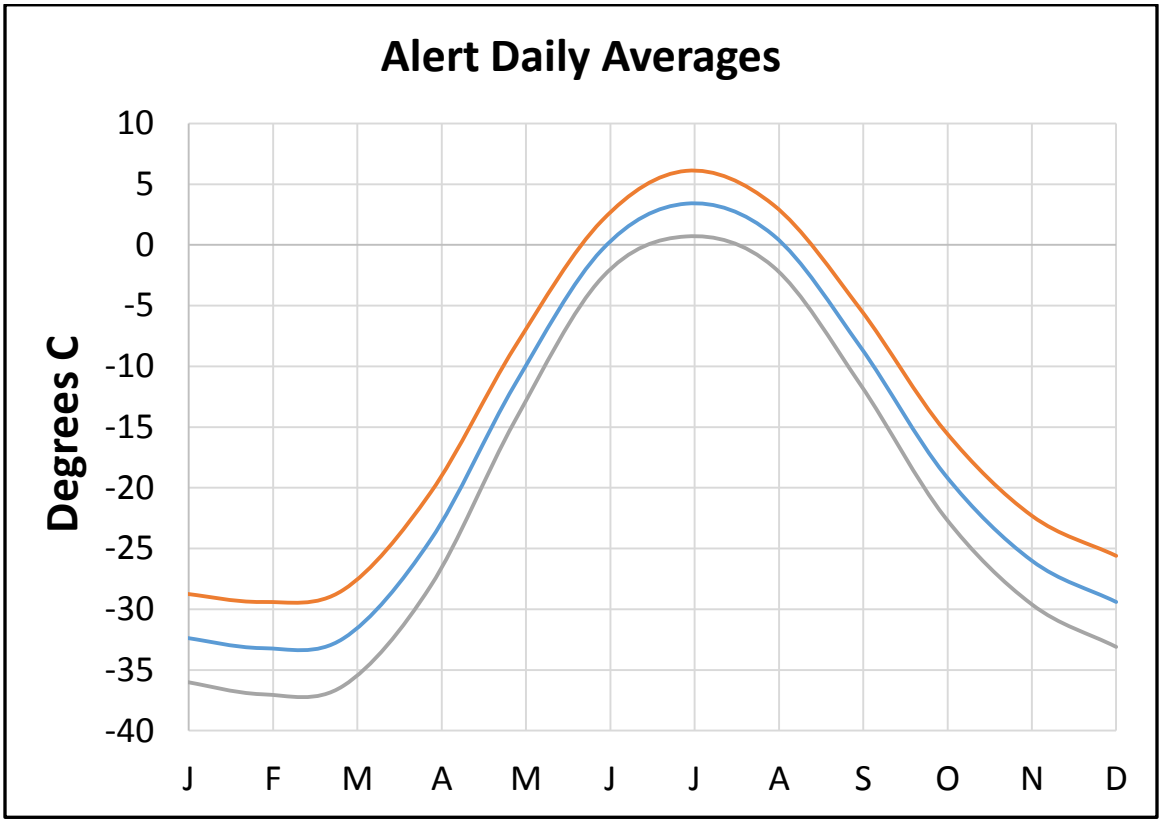

Figure 3 - Alert Daily Temperatures

Table 1 - Alert Daily Temperatures in ˚C

	Daily Mean	Daily Max	Daily Min
JANUARY	-32.2	-28.6	-35.8
FEBRUARY	-33.2	-29.4	-37
MARCH	-32.4	-28.4	-36.3
APRIL	-24.3	-20.4	-28.1
MAY	-11.5	-8.4	-14.5
JUNE	-0.4	2	-2.7
JULY	3.4	6.1	0.7
AUGUST	0.8	3.3	-1.8
SEPTEMBER	-8.4	-5.3	-11.5
OCTOBER	-18.9	-15.3	-22.4
NOVEMBER	-26	-22.3	-29.6
DECEMBER	-29.4	-25.6	-33.1

2.2 Sea Ice

Sea ice covers the overwhelming majority of the Arctic during winter months and a great deal of the Arctic during the summer. The freeze-up at Alert typically occurs between late August and mid-September, although the exact date is a function of the average daily temperature in a given August [Bilello, 1961]. Sea ice coverage and thickness are both at their lowest during the month of September [Rothrick et al., 1999], before the refreeze/freeze-up occurs as temperatures drop and the sun sets for the season. It is also possible that sea-ice coverage may be correlated to Arctic aerosol sea components. There was a strong decrease in total sea coverage for every month from 1979 until at least

2007 [Sezzere et al., 2007], roughly the same time span as the Arctic aerosol sample span in this study.

The primary drivers for sea-ice loss have long been considered to be ocean and atmospheric temperatures. Precipitation, although a major factor in snow-pack and glacier formation (and maintenance), is less important where the sea surface must actually freeze over in the colder and darker months. Increasing atmospheric temperatures and sea water temperatures are therefore important to understand trends in sea ice duration, thickness, and extent. There is some debate about the primary drivers of sea-ice coverage, but a clear decreasing trend has been seen through the 1980s and 1990s where interranual changes in sea-ice coverage are not clearly correlated to interranual atmospheric changes [Maslanik et al., 2007]. The clear long-term trend shows a decadal decrease in coverage which is correlated to the trend in local and Arctic low-level atmospheric temperatures as a whole.

One possible factor relating to reduced ice coverage is the relationship between sea ice thickness and potential salinity contribution in the Arctic aerosol record. This relationship is seen in a study of ice core samples. It was seen that salinity drastically increases about 150 cm into the sea ice. [Pope et al., 2012] Therefore, as ice is sublimated from the top due to lack of precipitation, more salinity would be exposed to the ice surface and thus to the wind.

It has been projected that the September sea-ice coverage may completely vanish by the year 2100, as there was a noted 25% decrease in

coverage, or about 100,000 km^2 decrease per year during September [Boé et al., 2009]. Other studies have shown that the mean thickness of the existing Arctic sea ice decreased to 2 meters in the 1990s, down from 3 meters 2-4 decades earlier [Rothrick et al., 1999]. Such a thinning would only tend to exacerbate net coverage loss.

Landfast sea ice is a particular stationary type of sea ice that is attached to a shoreline. This type of ice is the defining characteristic of the Arctic coast. It fills the channels and inlets around islands in the arctic. It can extend into the ocean from a few kilometers to hundreds of kilometers. [Yu et al., 2014] Whereas most sea ice shifts or flows throughout a season, landfast sea ice does not move. As with other types of sea ice, variations in Arctic landfast ice shows a strong seasonal cycle. At the end of the winter season, thickness can be near 2 meters thick. This type of sea ice may then completely melt in the summer, yet most Arctic landfast ice remains on the water for 7-9 months each year.

Multiyear landfast sea ice remains in place year after year and is prevalent along the northern coast of the Canadian Arctic Archipelago in relatively close proximity to Alert. It has been noted in literature that multiyear landfast sea ice has broken up in the summer multiple times since 1998 at Nansen Sound (south of Alert), and summer survival has become less common. The observed trend in landfast sea ice thickness at Alert from 1957-2014 is -4.44±1.6 cm/decade. [Howell et al., 2016] Over the entire Arctic, the observed trend of landfast sea ice extent is -7%/decade since the 1970s [Yu et al., 2014]. Other research has

shown trends in Arctic multiyear landfast sea ice that range as high as -12.4% per decade. The years 2007 through 2011 included the lowest Arctic sea ice extent (in September, before the freezeup) in the existing satellite imagery (the only reliable measurement of sea ice extent). [Pope et al., 2012]

Reported regional ice coverage trends on the northern Canadian Arctic Archipelago are around -6%/decade from 1979-2008. Yelverton bay, in relatively close proximity to Alert, has shown a drastic reduction in ice coverage over the past few decades. [Pope et al., 2012]

Landfast sea ice thickness trends, unlike other sea ice trends, are more strongly correlated to snowfall and snow depth than they are to temperature changes, although the temperature changes may be statistically significant. Regardless, atmospheric forcing is more strongly correlated to landfast ice thickness than are deep ocean influences. [Howell et al., 2016]

Table 2 provides a summary of sea ice trends in the Arctic. The data can be seen explicitly in Figure 91 of the Appendix.

Table 2 - Arctic Ice Cover Trend Summary

Source	Ice Coverage Trend	Notes
[Yu et al., 2014]	-7%/decade	1970s-2014, landfast sea ice
[Howell et al., 2016]	-4.44±1.6 cm/decade	1957-2014, landfast sea ice
[Boé et al., 2009]	100,000 km2 decrease per year during September	25% total loss in coverage per records
[Rothrick et al., 1999]	33% decrease in total ice cover	From 1960s (3m average sea ice thickness) until 1990s (2m average sea ice thickness)
[Pope et al., 2012]	As high as -12%/decade; -6%/decade at Alert from 1979-2008	
[Ellesmere, 2017]	90% loss in ice shelves from 1906 - 2017	

2.3 Ice Shelves

Ice shelves (the extension of a glacier or land-ice into the ocean), once prominent around Northern Ellesmere Island, have been collapsing and will likely continue to collapse given current climate conditions [Copland et al., 2007]. Over 90% of the total area of ice shelves reported in 1906 has been lost [Ellesmere, 2017].

An example of the loss of ice-shelves in northern Ellesmere Island is the Ayles Ice Shelf, located ~180 miles west of Alert, Canada, and about 40 miles

northeast of Yelverton Bay (Figure 4). This large ice shelf (~25 mi^2) broke away in August of 2005. The breakup was likely due to an extremely warm summer in 2005, combined with atmospheric warming trends, wind patterns, and ocean current trends [Copland et al., 2007].

Figure 4 - Ayles Ice Shelf Breaking Away [NASA, 08/13/2005]

2.4 Long-Term Temperature Trends

Publicly available historical temperature data is available from monitoring points at Alert, and summarized in Table 3. Arctic trends are somewhat consistent regardless of the location in the Arctic, and the trends are similar to global temperature trends for the observed periods. Alert was seen to cool at a rate of 0.3 ºC/decade from the 1950s into the 1970s, and then warmed, consistent with other Arctic sites, from the 1970s onward with a rate of ~0.5 ºC/decade [Throop et al., 2010].

Using a least-squares regression on the Alert data (gathered from http://climate.weather.gc.ca/climate_normals/index_e.html), there is an overall increase of 0.014 ºC/year, which is equivalently 0.14 ºC/decade and 1.4 ºC/century (Table 3) However, the time span of our analysis is 1979-2010. From 1979-2006 (the last year for the temperature set in question), the least-squares regression provides a temperature increase of 0.06 ºC/year, or 0.6 ºC/decade which is much more dramatic. This is also consistent with a study using borehole analysis at Alert, which demonstrated a warming trend of ~0.5 ºC/decade [Throop et al., 2010], and fits very well with noted trends throughout the northern Asia and Russia [Ma et al., 2017]. This recent decadal trend (that tapered off after this data set completed) is a relatively dramatic change considering long-term and pre-1970s available trends do not show such a strong temporal change. [Ma et al., 2017] It is likely that the strong up-trend is related to cleaner air

standards implemented during the 1970s as lower Sulphates result in a faster heating of the air from the sun [Samset, 2018; Voiland, 2009].

Table 3 - Arctic Temperature Trend Summary

Location	Temperature Trend(s)
Alert, Canada [This Work] - Air temperature data, Environment Canada (see Figure 90 of the Appendix)	+0.014 ºC/year from 1950s-2006; regression +0.06 ºC/year from 1979-2006; regression
Alert, Canada [Throop et al., 2010] - Borehole Analysis	+0.5 ºC/decade from 1975-2010
Ayles Ice Shelf, Ellesmere Island [Pope et al., 2012; Copland et al., 2007]	+0.37 ºC/decade from 1948-2006 +3.7 ºC total increase from 1972-2007
Arctic [Copland et al., 2007]	+0.4 ºC/decade from 1966-2003

Finally, it should be noted that the aerosol data used in this study is winter data only. The Alert winter averaged temperatures show a Pearson Correlation value to time of 0.36, meaning the correlation of the winter-averaged temperatures per year may not be statistically significant from 1980-2006, or, that the winter temperature trend at Alert for that timeframe may be statistically insignificant.

2.5 CO_2 Trends and Misc. Gaseous Trends

Other gaseous information is continuously collected at Alert. The data can be found at the following URL: https://www.ec.gc.ca/mges-ghgm/default.asp?lang=En&n=3150486A-1. The specific information collected and available can be seen in Table 4. This information is included because there remains an area where future work may be performed. Comparing the aerosol record with gaseous trends in the local record for possible correlations and causalities would potentially provide a great deal of insight.

Table 4 - Gaseous Data Available from Alert

Measurement	Sampling Frequency	Sampling Record
Carbon Dioxide (CO2)	Weekly Flask	1975 - Present
Carbon Dioxide (CO2)	Hourly	1988 - Present
Methane (CH4)	Hourly	1988 - Present
Chlorofluorocarbons (CFC-11 and CFC-12)	Hourly	1995 - 2009
Carbon Monoxide (CO)	Hourly	1998 - Present
Hydrogen (H2)	Hourly	1998 - 2002
CO2, CH4, CO, N2O, SF6, H2, 13C, and 18O in CO2	Weekly Flask	1998 - Present
Sulphur Hexafluoride (SF6)	Hourly	2000 - 2006
Nitrous Oxide (N2O)	Hourly	2000 – 2006

3. Arctic Aerosol Sampling

3.1 Background

Aerosols in the atmosphere consist of particles that can be either liquid or solid and are suspended in atmospheric gas. The true definition of “particulate matter” is matter that consists of “aggregations… that are larger than molecules.” Sources of atmospheric aerosols include combustion, volcanoes, cultivation of land, and the natural interactions between the seas and the atmosphere. [Randerson, 1984]

Coal and other combustion releases many toxic elements and compounds in both gaseous and particulate form. Fly ash, dust, smoke, and mists can all be emitted both from combustion as well as from other anthropogenic sources. Gaseous emissions from combustion generally react in the atmosphere to form more particulate matter. Once particulate matter has been emitted into, or created within the atmosphere, multiple factors affect its behavior in the air. These factors include, but are not limited to: wind speed, thermal gradients, weather patterns, particulate size, and particulate shape. [Randerson, 1984] Less prominent sources exist as well, such as desert winds [Garrett & Verzella, 2008] and miscellaneous industrial processes such as smelting.

The sampling station that includes the longest currently running set of data in the Arctic is operated by the Canadian Arctic Aerosol Sampling Network

(CAASN) at Alert, Canada. In early 1978 the Canadian Arctic Air Pollution Program (CAAPP) was established due to concern about air pollution in the Canadian Arctic. Aerosol sampling thus began in 1979, and became part of a larger, international Arctic monitoring program [Barrie et al., 1980]. Samples have been formally collected at Alert since 1980, and continue to be collected to this day. The samples are divided and shipped to the University of Texas.

3.2 Specific Method

The Alert samples in this study are gathered by drawing air, at ground level, through a Whatman® 41 air filter (Figure 5) for one week at a specified rate which results in approximately 16,000 m^3 of air passed through one filter [Barrie et al., 1980].

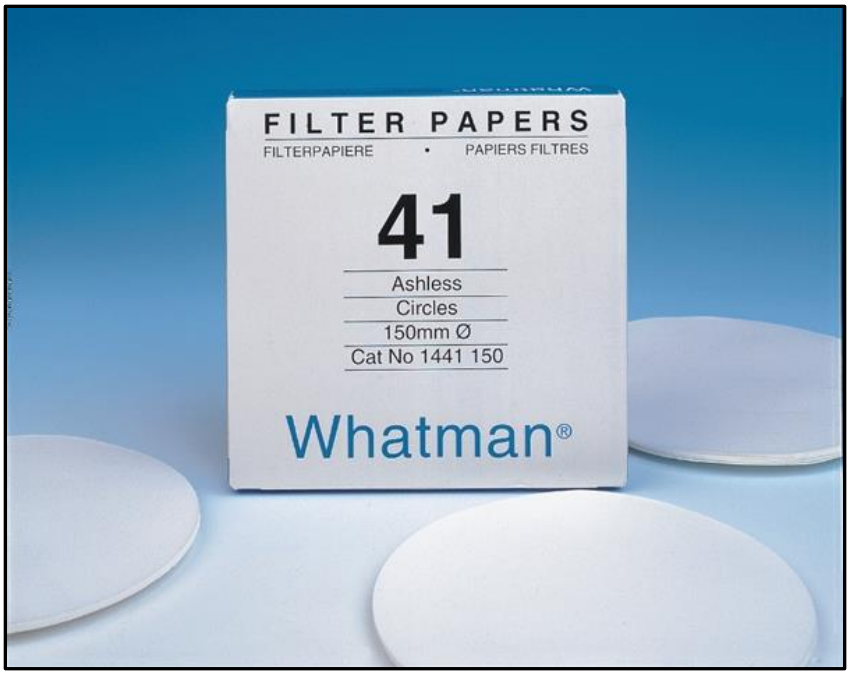

Figure 5 - Whatman® 41 Filter papers [www.camlab.co.uk]

Particulate matter in the atmosphere is thus captured in the Whatman® filters where it remains until analysis can later be accomplished. The amount of particulate matter in the sample is proportional to the amount in a volume of air equal to the volume drawn through the sample. A constant of proportionality may be used to estimate factors such as the percentage of particulate matter not captured in the filter due to size incompatibility and other issues such as chemical instabilities and the extended shelf time before some samples can be analyzed. Due to the coarseness of the Whatman® 41 filters, no particle size discrimination is attempted. Despite heated debates during the mid-1980s on the

use of Whatman® 41 filter papers for particulate sampling regarding collection efficiency and consistency [Lodge, 1986], it was determined that for high-volume sampling, depending on the application, the Whatman® 41 filter media is sufficient [Lowenthal & Rahn, 1987]. Furthermore, the Alert data has used the Whatman® 41 filter media since its inception and should be changed mid-course if long-term trends are to be valid. Interestingly, one study that involved 47 years of Arctic aerosol filter samples did change the type of filters used twice, and recorded only a small change in results due to the filter swaps [Laing et al., 2014a].

Particulate aerosol matter captured by the ground-level sampling is not typically in pure elemental form, but rather in the form of salts and other chemical compounds. The shapes of the particulate matter captured varies based on the type of particle. Sea salt particles are cubic, whereas fly ash tends to be spherical, and metallurgical fumes tend to be condensation flocs. [Randerson, 1984] The size and shape of the particles undoubtedly have some effect on the ability to capture the particulate matter in the filter that is being used.

Neutron Activation Analysis (NAA, described in Section 4) cannot discern information about particular chemical forms that the elements are bound in, so only the elemental composition of the sample is of interest. Explicit chemical or other types of analysis and information would be used if the chemical composition of a sample was of primary concern. Elemental concentrations, however, still provide a wealth of information about pollution sources and emitter

trends.

Due to the limitations inferred from Sections 3 and 4, such as incompatible half-lives and molecular size issues that render certain elements immeasurable with NAA, only 11 elements of interest are analyzed in this study. The 11 elements that are analyzed are each described in detail as relevant to their probable source. Each of the 11 elements is useful to deliver specific clues about the environment and potential pollution sources. The elements are listed in the sections that follow categorized by their primary contribution source. Additionally, several elements and molecules are listed in the section that follows due to the additional Canadian Arctic Baseline Measurements (CABM) data described in Section 7 for comparison in later sections.

3.3 Elemental Information

The elements in this study are grouped broadly into three categories as seen in Table 5 with the addition of the CABM data:

Table 5 - Aerosol Component Primary Source

Crustal	Anthropogenic	Sea
Al	V	Na
Ti	Cu	Br
Ca	(Pb, CABM)	Cl
Mn	(S, CABM)	I
Mg	(NH4, CABM)	(MSA, CABM)
(Fe, CABM)	(N, CABM)	

The groupings are not definite; for example, some research groups Magnesium as a sea-salt component and Manganese as an anthropogenic component [Barrie et al., 1985]. Essentially all crustal elements are found in sea water due to erosion and other natural processes depositing them in the sea. All elements herein can also be emitted from anthropogenic sources as well. Additional information about each element, its sources and well-documented trends are found on the following pages. The groupings in Table 5, however, are considered the most relevant as related to pollution tracking, and represent correlations to known elements such as Aluminum and Sodium, but are not exclusive.

Table 6 includes the 2 most common reference values [Wedepohl, 1967; Lide, 2000] for crustal and sea elemental compositions of the elements included in this study. It is clear from these values what the most important elements are for each source, which is Sodium and Chlorine for the sea, and Aluminum for crustal. “CABM” elements, described in Section 7, are included herein also.

Table 6 - Elemental Composition in Crust and Sea

Element	Concentration as % of Crust	Wedepohl Crustal Data for Comparison	Concentration as % of Seawater	Wedepohl Sea Data for Comparison
Aluminum (Al)	8.2E0	7.8E0	1.9E-7	1.0E-7
Bromine (Br)	2.4E-4	2.9E-4	6.5E-3	6.5E-5
Calcium (Ca)	4.2E0	2.9E0	4.0E-2	4.0E-2
Chlorine (Cl)	1.5E-2	3.2E-2	1.9E0	1.9E0
Copper (Cu)	6.0E-3	3.0E-3	2.4E-8	2.0E-7
Iodine (I)	4.5E-5	5.0E-5	5.8E-6	5.0E-6
Magnesium (Mg)	2.3E0	1.4E0	1.3E-1	1.3E-1
Manganese (Mn)	9.5E-2	6.9E-2	1.9E-8	4.0E-7
Sodium (Na)	2.4E+0	2.5E0	1.1E0	1.1E0
Titanium (Ti)	5.7E-1	4.7E-1	9.7E-8	1.0E-7
Vanadium (V)	1.2E-2	9.5E-3	2.4E-7	2.0E-7
Iron (Fe, CABM)	5.6E0	N/A	2.0E-7	N/A
Sulphur (S, CABM)	3.5E-2	N/A	8.8E-2	N/A
Lead (Pb, CABM)	1.4E-3	N/A	2.9E-9	N/A
Nitrogen (N, CABM)	1.9E-3	N/A	4.9E-5	N/A

What follows is a detailed description of the 11 elements that compose this study. Included are known important sources, trends, literature, and other relevant information.

Aluminum (Al)

Aluminum is a crustal component [Lide, 2000] and may also be attributed to smelter activity. In addition, Aluminum is released from coal burning power plants and tends to stay in the gaseous phase after emission [Randerson, 1984]. Of the crustal components, it is perhaps the most dominant regarding aerosol sampling. Somewhat weak yearly cyclic trends have been noted with a peak in winter and a trough in summer in the Finnish Arctic aerosol record [Basunia, 2002]. This trend matches a similar trend in Titanium [Barrie et al., 1985], another strong crustal aerosol component (Aluminum and Titanium are highly correlated throughout this and other Arctic aerosol sample sets, as is Iron). One study of Northern Hemisphere Arctic aerosol notes a possible long-term decrease in this element [Gong & Barrie, 2005]. The data used in this study appears to show a long-term decrease as well when observing the time-series moving average, although the Pearson's time correlation does not confirm a statistically significant decrease. The CABM Section 7 data shows a seasonal variation where the highest concentrations are seen in September and October, and the lowest in January and February (September is ~4x January).

Bromine (Br)

Bromine is primarily a sea component, with seawater containing approximately 85 ppm of it [Lide, 2000]. This element is also released from anthropogenic activity, specifically from fumigation and leaded gasoline combustion (leaded gasoline is nearly phased out worldwide at the current time, but was still widely used when the Alert samples began). Bromine reacts with ozone and other oxygen compounds in the atmosphere, so it is considered detrimental to the ozone layer. However, the majority of atmospheric Bromine is primarily from sea emissions (75%-95% of the emissions even when leaded gasoline combustion was still widespread). [Wofsy et al., 1975] A strong seasonal trend has been noted in atmospheric Bromine, with the peak being late winter/early spring [Biegalski et al., 1997; Sirois & Barrie, 1999; Barrie et al., 1994]. The jump is as much as an order of magnitude from the trough to the peak [Barrie et al., 1994]. A possible cause of this seasonal trend is photo-induced production of particulate Bromine that occurs in the spring, or rather when the Arctic sunrise takes place [Biegalski et al., 1997]. No long-term visual or strong statistical trend is seen in the data used in this study, although there is a notable increase between February and March, which corresponds to the Arctic sunrise at Alert, and is consistent with the aforementioned studies.

Calcium (Ca)

Calcium is a crustal element, and weathering is the primary source of this

element in aerosol form. In addition to wind entrainment, Calcium is released from coal-fired power plants in gaseous form [Randerson, 1984]. An increase in the Arctic aerosol concentration of this element has been noted from the late 1970s with no noticeable seasonal trend [Basunia, 2002]. A possible, but not definitive seasonal trend is seen in other literature [Barrie & Hoff, 1985] which is possibly a result of some Calcium being introduced into the air via the ocean which is covered by ice in the winter [Pacyna & Ottar, 1988].

There is no monthly trend in the winter months used for this study. The CABM Section 7 data shows a seasonal trend with the highest levels being in September and October. The data herein does show a very strong long-term decrease beginning around 1992 and continuing until the end of the sample space at 2010. Although the trend is not apparent from 1980 until 1992, this is in stark contradiction to other research that comments on the lack of any long-term trend in this element [Gong & Barrie, 2005]. As the trend does not occur prior to 1992, it is possible that some previously unknown regional change or spike around 1992 led to this phenomena, or it may be dependent on specific location in the Arctic.

Chlorine (Cl)

Chlorine is a sea component, and very little cyclic variation has been previously noted in its Arctic aerosol contribution. There has been at least one report in the Canadian Arctic of chlorine being at its highest between December

and January [Barrie & Hoff, 1985] with a sharp drop around the polar sunrise [Barrie et al., 1994]. The CABM Section 7 data shows seasonal variation with the lowest levels being seen in the summer (daylight) months. Other Arctic data shows no obvious seasonal trend [Basunia, 2002]. The data used in this study shows a strong long-term increase over the sample space as confirmed by a Pearson Correlation value of >0.5 as well as a potential drop between February and March averages. The CABM Section 7 data confirms this trend in our data.

Copper (Cu)

Copper is an important element for tracing smelter activity, particularly Copper and Nickel smelters. Copper is a very high-risk element for anthropogenic pollution [Bowen, 1966] and is emitted as pollution not just from smelting, but also from coal combustion. Very little seasonal variation has been noted in the Arctic aerosol contribution from his element [Basunia, 2002]. The CABM Section 7 data shows essentially no monthly or seasonal trend. A long-term decreasing trend in this element was noted at Alert, Canada from ~1985 through at least 1996, which may be attributed to the collapse of the Soviet Union [Sirois & Barrie, 1999]. Other research indicates that this element decreased from 1980 until around 1995 and then began to increase again until at least 2000 in the northern hemisphere [Gong & Barrie, 2005]. There are several regions of interest which are large sustained spikes in this element that may warrant further investigation.

Iodine (I)

Iodine is found to be the highest in winter with broad cyclic variation. Natural Iodine is purely I-127, which is useful for NAA [Lide, 2000]. Iodine is common in seawater, and high levels may coincide with Bromine [Basunia, 2002]. The Alert data does not show such a correlation; in fact, it shows that they are definitively not correlated. A long-term increase in Iodine aerosol was noted in at least one previous study at Alert, Canada [Sirois & Barrie, 1999]. Another study showed a correlation between Bromine and Iodine in regards to seasonal variation (with a peak between March and April) [Barrie & Hoff, 1985]. This uptick begins around the Arctic sunrise and remains in place until fall [Barrie et al., 1994]. This study shows a slight uptick between February and March averages which agrees with the noted study. There is also a long-term statistically-significant increase, as demonstrated with the statistical correlations, although not visually apparent in the time-series data.

Magnesium (Mg)

Magnesium is a minor crustal element that is also found in seawater. Mg has been linked to industrial activity [Lide, 2000], and is released from coal burning power plants in its gaseous form [Randerson, 1984]. Although previously linked to industrial activity, the potential for anthropogenic pollution of Mg is low [Bowen, 1966]. As noted by Gong & Barrie in 2005, there is no long-term trend apparent in Alert concentrations. There appears to be an increase from around

1980 until around 1995, and then a decrease from around 1995 until the end of this study. This trend has not been noted elsewhere. The overall trend in this study is a long-term decrease. A seasonal trend is seen in the CABM Section 7 data, which is ~4x greater in the winter than in the summer.

Manganese (Mn)

Manganese is not found as a free element in nature [Lide, 2000], but is a common emission from coal burning power plants [Basunia, 2002; Randerson, 1984]. It can be a marker of stationary fuel combustion [Liang et al., 2014a]. Additionally, Manganese is a product of agricultural activity, as it is essential for all plant life. As such, some Manganese in the aerosol is potentially from soil erosion, and is therefore a sea component as well. Manganese is also released from nonferrous smelting [Sirois & Barrie, 1999].

A seasonal trend in Arctic aerosol Manganese concentrations has been reported, with the peak value occurring in late September [Barrie & Hoff, 1985]. Other research shows the peak in Manganese in the Finnish Arctic aerosol record to occur instead during winter months [Basunia, 2002; Ping, 1996]. This discrepancy in time of the peak could be indicative of a regional trend difference related to different pollution sources as the three studies were performed on data from three separate locations in the Arctic. Regardless of the date of occurrence, a winter maxima in the seasonal variation is well documented in other research [Gong & Barrie, 2005], and is seen in the CABM Section 7 data as having a peak

in September and October. The data in this study shows a possible long-term deceasing trend.

Sodium (Na)

Sodium is a common sea-spray component. Sea-salt is made primarily from NaCl, so a strong correlation between Sodium and Chlorine is expected in any Arctic aerosol data set. Sodium is added to the oceans at a faster rate than it is removed, and is similarly mined at a greater rate than the ocean can naturally remove it [Bowen, 1966]. For the Northern Hemisphere, no long-term trend can be seen between at least 1980 and 2000 [Gong & Barrie, 2005]. In addition to being a sea component, Sodium is released from coal-burning power plants in its gaseous form [Randerson, 1984], although no correlation to this fact is seen in any Arctic data used for this study. There is also no strong monthly trend in this element noted in other Arctic aerosol data [Basunia, 2002], although there may be a maximum in winter in the northern hemisphere [Gong & Barrie, 2005]. The CABM Section 7 data shows a seasonal variation with a high in the winter, and a low in the summer. This study shows a long-term increasing trend in this element.

Titanium (Ti)

Titanium is a minor crustal element that is often used as a basis for elemental enrichment (Section 6.1). In addition to being entrained by wind, Titanium is released in its gaseous form from coal burning power plants [Randerson, 1984]. Typically, Aluminum and Titanium (and Iron) are strongly correlated, although some research has failed to illustrate that correlation [Basunia, 2002]. Furthermore, Titanium runs a high potential in a sample of being anthropogenic pollution, whereas Aluminum poses only a moderate potential [Bowen, 1966]. Titanium tends to display a slight seasonal variation, with the peak occurring around December [Barrie & Hoff, 1985]. A minimal long-term decrease in aerosol Titanium levels in the northern hemisphere has been noted previously [Gong & Barrie, 2005]. There is no long-term trend noted in this data set, nor is there any other trend of interest. A visual inspection of the data seems to show a slight decrease, but the Pearson's Correlation value for this potential decrease determines it likely to be insignificant.

Vanadium (V)

Vanadium is a trace element in the earth's crust, but in the aerosol samples, Vanadium is mainly due to oil and coal combustion [Basunia, 2002]. It can be a marker of stationary fuel combustion [Liang et al., 2014a]. Vanadium is perhaps only significantly emitted as pollution from the burning of oil [Rahn, 1981], but is also released in gaseous form during coal combustion [Randerson,

1984]. A strong trend in Vanadium, or a strong correlation between Vanadium and Manganese, may be highly indicative of the presence of, or of changes in, oil-burning activity. A very strong seasonal trend, with the highest values in late winter, was seen in both Finnish Arctic aerosol samples and Canadian Arctic aerosol samples [Ping, 1996; Yli-Tuomi et al., 2003a; Barrie & Hoff, 1985; Sirois & Barrie, 1999].

The Northern Hemisphere aerosol record confirms a seasonal trend with the minimum being in summer and the maximum being in winter [Gong & Barrie, 2005]. Another reference records the variation to peak in spring or late winter, and shows the difference between the late winter peak and the summer minimum to be a very strong factor of 5 when the data was collected with Whatman® 41 air filters, as was the data in this study [Shevchenko et al., 2003]. This study shows a very strong decrease in this element with time. The Pearson's value for the decrease is -0.9 which is more significant than anything found in other literature. In fact, the trend seems to asymptotically approach a lower limit of detectability. If the sensitivity NAA was higher (lower limits of detection), this decreasing trend may be even stronger than it appears here. Table 7 shows previously reported concentrations for these 11 elements.

Table 7 - Previously Reported Concentrations (ng/m^3)

	Data*	Al	Ti	Na	Cl	Mn	V	I	Br	Cu	Ca	Mg
This Work	M	55	3.4	230	200	0.8	0.4	0.2	8.9	2.2	110	94
	GM	42	2.2	200	140	0.6	0.3	0.2	6.7	0.7	100	76
Alert 1	M	65.8	-	-	-	0.99	0.66	-	-	-	-	-
Alert 2	GM	58.4	5.2	71.1	51.3	0.7	0.2	-	1.5	-	70.6	-
Alert 3	M	38.6	10.4	234.5	406.5	0.8	0.3	1.0	18.5	-	62.6	-
Finland	M	42.9	7.2	281.4	116.0	1.6	0.8	0.9	3.1	15.0	56.1	-
	GM	34.4	5.4	249.5	73.1	1.2	0.4	0.9	2.1	12.7	37.5	

* M = Mean; GM = Geometric Mean
Alert 1 = [Ping, 1996], Winter Only, Excluding 1982-1983
Alert 2 = [Polissar et al., 1998]
Alert 3 = [Landsberger et al., 1990]
Finland = [Basunia, 2002]

Other Alert data results, for comparison, are shown in Table 8. The data in Table 8 uses inductively-coupled plasma (ICP) spectroscopy, instrumental neutron activation (INA) analysis, and ion chromatography (IC) methods, and the results reported are all in units of ng/m^3 [Cheng et al., 1991]. Note that these results include all elements in this study with the exception of Copper. The paper also assumes the data to be lognormally distributed, as is the data used herein.

Table 8 - Alert ICP Data and Other Results (ng/m^3)

Element (meth)	Mean	Median	Mode	Skew	Kurtosis	Stdev (σ)	Log-Normal Mean	Log-Normal Stdev
Al (INA)	128.4	58.9	46.9	3.1	11.4	192.3	123.7	201.2
Br (INA)	7.1	2.9	0.3	2.8	9.8	10.8	8.6	29.0
Ca (ICP)	129.6	61.1	3.8	2.5	6.4	170.8	140.0	252.5
Cl (IC)	170.0	81.3	4.0	2.4	6.5	237.3	270.6	1255.2
I (INA)	0.4	0.4	0.0	1.0	1.1	0.3	0.4	0.5
Mg (ICP)	84.7	54.3	1.9	2.4	8.0	93.8	97.6	175.8
Mn (INA)	1.3	0.8	1.0	2.5	9.0	1.4	1.4	2.0
Na (IC)	153.6	117.7	2.8	1.2	1.2	144.4	220.4	591.5
Ti (ICP)	0.6	0.4	0.1	2.1	5.5	0.6	0.6	0.8
V (ICP)	0.4	0.1	0.1	2.7	9.3	0.6	0.4	1.0

3.4 Additional Elemental and Molecular Information

Several additional molecular and elemental data sets are compared to the data studies herein. The additional (CABM) data is described in Section 7, and the additional components are described in the following section.

Lead (Pb)

Lead has a very high potential for anthropogenic pollution, and is added to water and air at rates faster than it can be removed by natural processes [Bowen, 1966]. Its primary pathways of seawater pollution were historically runoff from roadways and pollution from mines into rivers [Bowen, 1966]. Lead was widely used in gasoline for automotive use at the beginning of the sample span (1980) [Lide, 2000]. Lead was eventually phased out, and now is essentially gone worldwide from combustion engines. Similarly, Lead was widely used as a paint additive for the better part of the 20th century [Lide, 2000], but has since been eliminated due to environmental and childhood ingestion risk. Industrial emissions are now limited in the United States, although globally there are countries that do not have the same stringent requirements on emissions. There is a strong seasonal trend in the Arctic aerosol record with the summer levels being the lowest levels [which is confirmed by CABM Section 7 data], and there is a very strong decrease since at least 1980 due to the reductions in automobile emissions and paint additives [Gong & Barrie, 2005].

Iron (Fe)

Iron is a major crustal element, and has a high potential for anthropogenic pollution. As a major crustal contributor, Iron is typically strongly correlated with the other major crustal elements, Aluminum and Titanium (which is confirmed with CABM Section 7 data). The toxicity of Iron, especially as compared to lead, is very low. Iron is, in fact, necessary for all living organisms. Iron is responsible for the color of nearly all soils, and is thus omnipresent. It can be removed from seawater at rates faster than it is added by pollution through natural processes. [Bowen, 1966] Iron is, however, associated with many types of industrial activity. There is no strong seasonal variation noted in the Iron component of the Arctic aerosol record, although a minor variation is seen in the CABM Section 7 data, with the peak concentrations occurring in September and October. There is a strong long-term decrease as evidenced in the record starting in 1980 or before [Gong & Barrie, 2005]. This decrease is also validated with the CABM Section 7 data.

Sulphur (S)

Sulphate pollution is caused both by natural (marine) sources, as well as industrial activity. Increased pollution has been seen explicitly in some samples in conjunction with depressed Cl/Na ratios. [Shaw, 1991] Approximately 2/3 of sulphates in the arctic record are anthropogenic [Fisher et al., 2011]. It was also

found that the majority of the “Arctic Haze” is largely composed of Sulphate aerosol [Quinn et al., 2007]. In certain literature, Cl/Na was shown to be inversely correlated to SO_4 [Shaw, 1991]. A strong seasonal variation is seen in the CABM Section 7 data, with the lowest concentrations occurring in the summer, and the highest in winter.

Nitrogen (N)

Nitrogen is common in air, making up approximately 78% of the air on the planet (78.084% of the air at sea level [Lide, 2000]). However, in the aerosol record, gaseous Nitrogen cannot become trapped in a filter. Nitrates, however, are molecules made up of Nitrogen and Oxygen, are not gaseous, and can become trapped in an aerosol filter. Nitrates are used in large quantities as fertilizer, and are common pollutants in rivers and waterways from sewage and agricultural runoff [Lide, 2000]. Typically existing in salt form, Nitrates tend to be water-soluble and behave similarly to other salts. Thus seasonal variations that correlate to ice cover may be seen. A strong seasonal variation is seen in the CABM Section 7 data, with the lowest concentrations occurring in the summer, and the highest in winter, which validates the hypothesis. High levels of Nitrate aerosols may be expected during strong wind patterns from areas with high agricultural activity.

Methanesulphonic Acid (MSA)

Methanesulphonic Acid (MSA) in the Arctic aerosol is primarily from marine biogenic emissions, and thus of natural origins [Chang et al., 2011; Ye et al., 2015]. MSA and other Sulphur compounds contribute approximately 1/3 of the Arctic haze [Barrie, et al. 1980]. It tends to be higher over open water and lower when ice cover is more expansive, and is highly correlated to sea surface temperature [Ye et al., 2015]. Thus, it should show an increase during the summer, and a decrease when the ice freezes over locally at Alert. Additionally, higher MSA concentrations are associated with warmer sea surface temperatures [Ye et al., 2015]. The CABM Section 7 data does, in fact, show a strong seasonal variation with the highest levels occurring in the summer. The highest month for MSA concentrations is May, which may be a result of a bloom or sea life after the arctic sunrise.

Ammonium (NH_4)

Ammonium, known by its chemical form NH_4, is a cation formed when ammonia (NH_3) connects gains a proton. Approximately 2/3 or ammonia emissions are anthropogenic, and thus it is important to study in conjunction with other Arctic aerosol constituents [Fisher et al., 2011]. In the CABM Section 7 data, ammonium peaks in December, and is the lowest over the summer. It is strongly correlated only with Sulphates in the CABM data.

4. Neutron Activation Analysis

Neutron Activation Analysis (NAA) is a method of characterizing the elemental constituents in a sample. NAA is among the most sensitive of all methods by which to perform such multielemental analysis. It is both faster and easier than chemical analysis. For these two reasons, as well as many others, NAA is the ideal method of sample analysis for a long-term Arctic aerosol study. [Landsberger et al., 1997]

The benefits of NAA compared to most other analytical methods are:

- very high precision,
- simple preparation of samples,
- ability to measure many elements simultaneously,
- very high levels of repeatability, and
- essentially non-destructive.

The primary disadvantage of NAA is the required neutron source. Neutron sources are not as readily available as they once were, and the number of research reactors in the United States has declined in recent decades. This disadvantage has caused NAA to fall out of favor as an analytical method, and it has been largely replaced by other methods. Other disadvantages relate to the nature of radioactivity: irradiating a sample with a neutron source not only causes

the sample to become radioactive, but results in radiological considerations that may add to the cost and complexity of the method. Although irradiating some materials will result in a sample that is only temporarily radioactive, irradiating other elements may result in samples that remain radioactive for long periods of time. The benefits, however, vastly outweigh these disadvantages when a neutron source (or a TRIGA reactor) is readily available.

4.1 General Method

A sample of interest is prepared, placed into an inert container, and subsequently irradiated by a neutron flux of a known energy spectrum and density (typically inside of a reactor). Some nuclei in the sample will absorb neutrons during the irradiation period, based on probabilities governed by their relative cross-sections, forming compound nuclei that will subsequently decay with characteristic half-lives. During the decay, radiation will be emitted primarily in the form of betas and gammas. The gamma spectrum from an irradiated sample is monitored and analyzed with specialized monitoring equipment and computer software such as NADA92 [Landsberger et al., 1994].

4.2 NAA Theory

During the neutron irradiation, a neutron combines with a nucleus to form a compound nucleus which emits a prompt gamma ray. In normal NAA, the prompt gamma is not used because it occurs before the sample can be placed in the counting chamber. The radiative capture reaction is used for most NAA (n,ɣ) is as follows:

$$n + {}^{A}Z \rightarrow {}^{A+1}Z^{*} \rightarrow {}^{A+1}Z + \gamma$$

where:

n = 1 neutron

^{A}Z = Original nuclide

$^{A+1}Z^{*}$ = Original nuclide after capturing 1 neutron (still excited)

^{A+1}Z = A+1 nuclide after falling to ground state

ɣ = 1 (or more) gamma released in the beta decay.

The neutron-rich ground-state ^{A+1}Z atom will typically later decay and release one or more characteristic gammas at a time determined by the half-life of the new nuclide. The characteristic gammas are the ones described that give a fingerprint of which elements were activated by the neutron capture reaction.

The rate of production of a specific isotope, *R*, can be expressed in the following way [all equations and information that follows in this section are from Koch, 1960]:

$$R = \emptyset n \sigma_{\gamma} = \frac{\emptyset m N^{\circ} f \sigma_{\gamma}}{A}$$

Where:

Φ = the neutron flux (n/cm^2-sec)

n = the number of target atoms

m = the mass of the trace element in the sample (gm)

A = the atomic weight of the trace element (gm/gm-atom)

f = the fractional isotope abundance of the target nuclide

N˚ = the Avagadro's Constant: 6.022E23 atoms/mole

σ_{γ} = the radiative capture cross-section (cm^2/atom)

The decay rate, D (disintegrations/sec), for some finite amount of a radioactive isotope is typically expressed as:

$$D = \lambda N$$

where:

N = the number of atoms of the nuclide in question, and

λ = the decay constant of the nuclide (sec^{-1})

The rate of change of the quantity of the activation product in the sample during irradiation can then be understood as the combination of the production and decay equations:

$$\frac{dN}{dt} = R - D = \frac{\emptyset m N° f \sigma_{\gamma}}{A} - N\lambda$$

Finally, the disintegration rate after some irradiation time, D(t), becomes:

$$D(t) = \frac{\emptyset m N° f \sigma_{\gamma}\left(1 - e^{-\lambda t}\right)}{A}$$

After a very long irradiation time, the exponential term goes to zero and the relation becomes:

$$D^{\infty} = \frac{\emptyset m N^{\circ} f \sigma_{\gamma}}{A}$$

which is called the “Saturation Activity,” or the amount at which no more will ever exist.

Alternately, this relation can be expressed as:

$$D(t) = D^{\infty}\left(1 - e^{-\lambda t}\right)$$

which is also known as the “buildup” equation.

Only a fraction of the gammas emitted can be detected. Therefore, for a specific decay a more useful expression for the relationship to the number of decays to the number of detected gamma of a specific energy is given by:

$$D(t) = \frac{\emptyset m N° f \sigma_{\gamma}\left(1 - e^{-\lambda t}\right)}{A} * \xi P_{\gamma} C$$

where:

ξ = Detector Efficiency

P_{γ} = probability of emitting a characteristic gamma per the decay

C = counting time constant

4.3 Measurement Techniques

A gamma-ray is uncharged and creates no direct ionizations if it passes through a detector. Therefore, gamma rays can only be measured if they interact with an electron (or atom) in a specialized absorbing material where they can transfer all or part of their energy to that material. The interactions of primary interest result in the release of fast electrons. These fast electrons can be measured, and the energy of the electrons provides information about the energy of the incident photon. [Knoll, 2000]

The three useful interactions that a gamma can have with an electron, including their usefulness to gamma ray spectroscopy are as follows [Knoll, 2000]:

1) Photoelectric absorption, also known as the Photoelectric Effect, is an interaction where a gamma is completely absorbed by an atom. The absorption may result in an excited state that then returns to ground releasing a gamma (or gammas) or the electron may then have enough energy to be ejected from its orbit given the following relation:

$$E_{e-} = h\nu - E_b$$

where:

E_e- is the kinetic energy of a liberated electron,

$h\nu$ is the energy of the incident gamma, and

E_b is the binding energy the liberated electron originally possessed.

The vacancy left by the liberated electron is quickly filled by electron rearrangements that may give off x-ray radiation or an Auger electron (an electron liberated by the capture of the x-ray energy). This (the energy of liberated electrons) is the only event that can actually be measured in gamma-ray spectroscopy.

2) Compton scattering, where the gamma transfers a fraction of its energy to an electron that is not liberated, and then continues on in a different direction with a different energy. The subsequent gamma energy in this process is not necessarily indicative or the initial gamma energy. However, since this interaction is happening in the detector, further interactions can be attributed to the initial gamma, and an initial energy may still be able to be deduced.

3) Pair Production. During this interaction, a photon glances a charged nucleus at a particular angle, and splits into an electron and a positron. The electron and positron rapidly annihilate, forming a new photon with a new trajectory. Again, other interactions can occur from the new photon, and all interactions occur within the detector. Therefore, the initial energy may still be able to be determined. Annihilation photons often occur and are always seen as 511 keV in energy.

To monitor the emitted photons from a sample, the irradiated samples are placed into a chamber used for gamma ray spectroscopy. This must be done in a short amount of time based on the half-lives of the isotopes being analyzed.

Software is used to take the input from the detector(s) and automatically output an amount of an isotope per sample based on the characteristic photons

emitted, irradiation time, neutron flux, and all other relevant information that was entered into NADA92 [Landsberger et al., 1994].

4.4 Germanium Detectors

A common type of detector used for NAA gamma-ray spectroscopy is a Hyper-Pure Germanium (HPGe) gamma-Ray detector. A germanium detector is a simple junction and surface-barrier detector. To overcome limitations imposed by typical semiconductor impurity levels, a “superpure” semiconductor is used, and then the detector is maintained at extremely low temperatures to prevent drift of impurities that would occur at room temperature. [Knoll, 2000] Thus, temperature is reduced to ~77 K using liquid nitrogen and the device shown in the following two Figures (6 and 7).

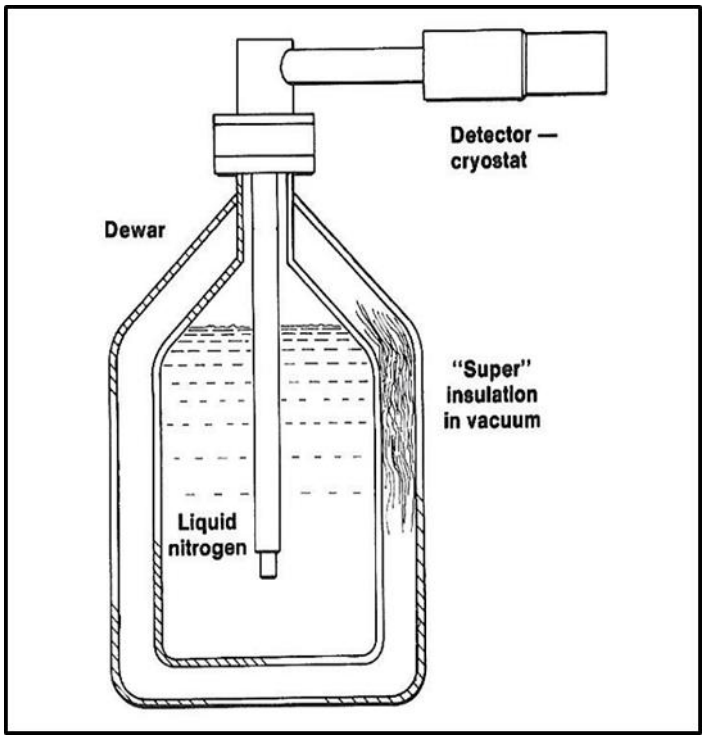

Figure 6 - Ge Detector Dewar [Knoll, 2000]

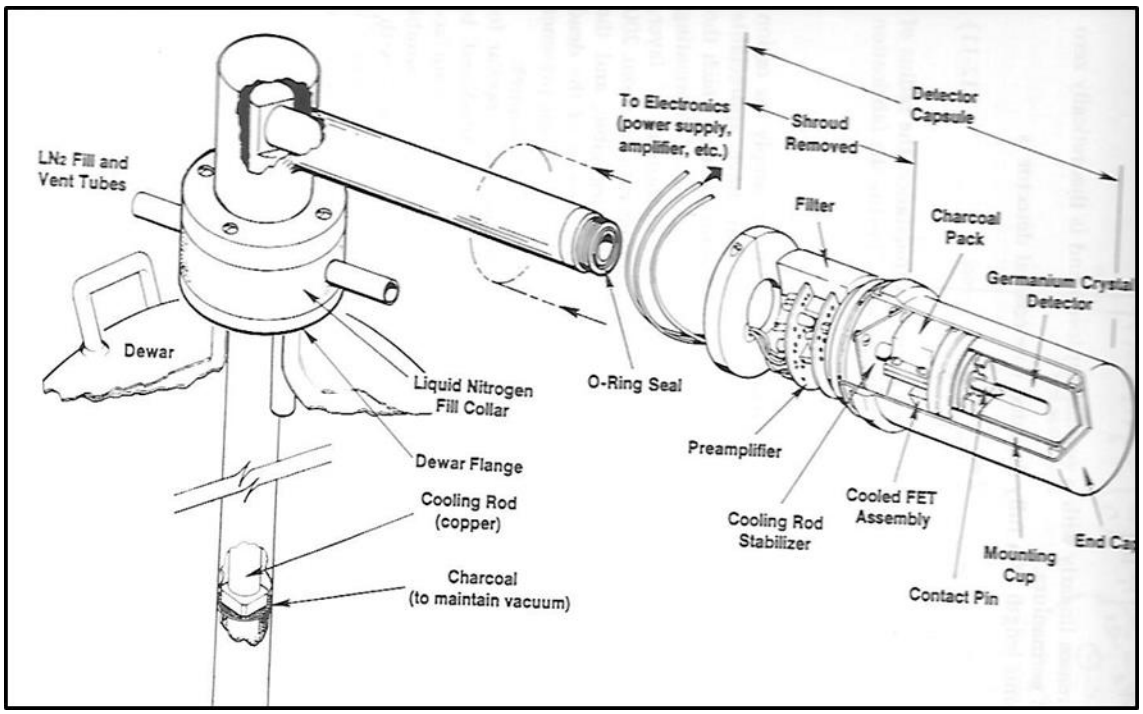

Figure 7 - De Detector Setup [Knoll, 2000]

The resolution of the germanium detector, using the liquid nitrogen, is excellent, and much better than most other types of detectors. This drastically improved resolution over similar types of detectors is the reason that such a detector is used at the University of Texas as well as many other similar facilities.

4.5 Compton Suppression

Compton suppression, also called “anticoincidence,” is a technique used to account for scattered gammas to help refine results from an NAA analysis. Detectors are essentially placed around the primary germanium detector such that gammas that are scattered out of the initial detector (via Compton scattering wherein the scattered photon has a different energy from the incident photon) are detected coincident with a detector event (Figure 8). The two interactions can be used to understand what the initial gamma’s incident energy had been. Due to the placement of the secondary detectors, the scattering angle can be inferred, and the incident photon energy can be calculated using the following relation [Knoll, 2000]:

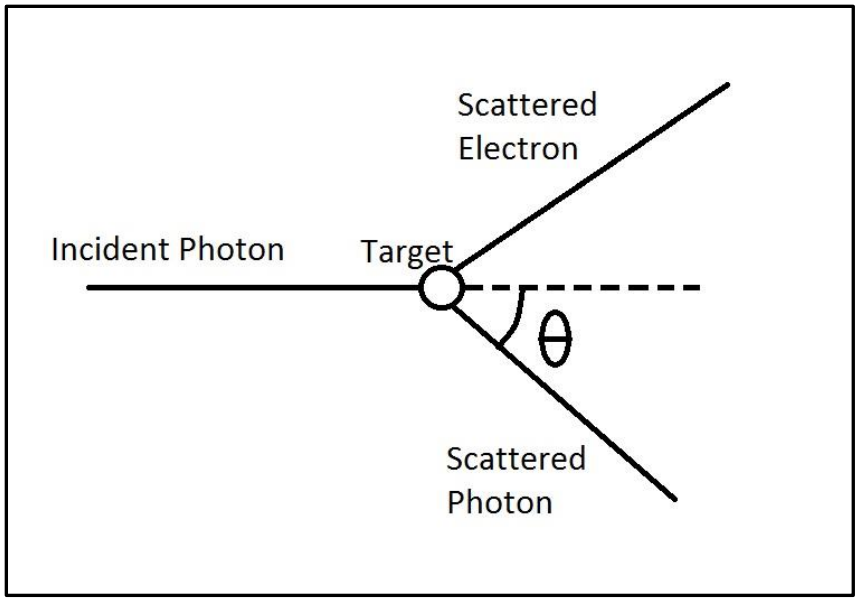

Figure 8 - Compton Scattering Diagram

$$h\nu' = \frac{h\nu}{1 + \left(\frac{h\nu}{m_0 c^2}\right) * \left(1 - cos(\theta)\right)}$$

where:

h = Plank's constant

v = gamma frequency (v' is the gamma frequency after scattering)

m_0 = the fundamental mass

c = the speed of light

Thus, knowing the scattering angle and energy of the photon captured in the detector, after scattering, will give the initial energy of the gamma.

This method of accounting for Compton scattering (Compton suppression) is a feature included in the equipment and is used for all the results gathered for this study.

4.6 Specific Application

Samples of filter paper from the Alert, Canada station (see Section 3) are first prepared by being cut into a specific size (1/10 or the original Whatman® 41 filter paper as described in Section 3). The piece of filter paper is carefully folded and/or rolled and placed into a clean polyethylene container. The containers and samples are handled carefully with gloved hands as the oils and elements deposited by human hands could significantly alter the results from this type of analysis. Next, the polyethylene container is sent into the reactor via a pneumatic transport system that then returns the plastic container after a given amount of exposure time in the reactor.

The pneumatic system is located in the fume hood in the following photograph (Figure 9). The germanium detector that counts the gammas is located inside the pile of gray lead bricks.

Figure 9 - Counter and Transfer System

The region of the reactor where the sample is irradiated is well characterized regarding its neutron flux profile at a specific power. The reactor power used for irradiation of the samples is 100 kW, and the flux at the location in the core is 4.5E12 n/cm^2/s thermal at 950 kW.

A typical Arctic air filter gamma ray spectrum is shown below in Figure 10:

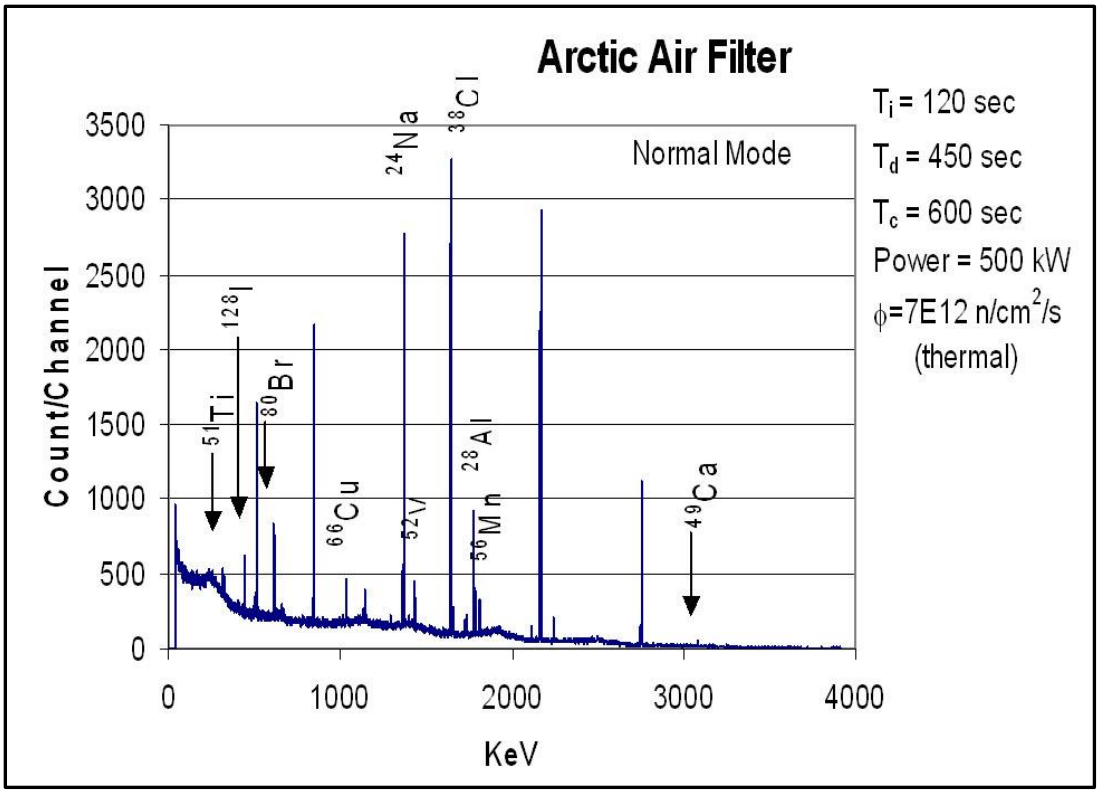

Figure 10 - Example Arctic Air Filter Gamma Spectrum

Note that the peaks are of particular interest can be determined in one irradiation.

4.7 Element-Specific NAA Information

A radiative capture involves a thermal capture cross section (σ_γ), an intensity of gamma released (I_γ) after some decay time denoted by its half-life ($T_{½}$), and specific characteristic gamma energy per decay of interest. If the half-life is too short, the decays cannot be detected as the transit time from the

reactor to the detector results in all the nuclides decaying away. A similarly long half-life would result in either low activity or a very long wait (activity is directly proportional to both quantity and half-life). The information that follows in Table 9 is therefore crucial to determine the composition in the irradiated sample, which includes the percent of natural abundance one nuclide useful to NAA. Elements with a very small thermal σ_γ are also not of use (although some may be evaluated separately with epithermal NAA). The spectroscopic characteristics of the elements are shown in Table 9.

Table 9 - Spectroscopy Information

Element (primary isotope for (n,γ), natural abundance)	I_γ/σ_γ*	Gamma Energy (keV)*;	T ½ *
Ca (Ca48, 0.2%)	0.51	3084.4	8.72m
V (V51, 99.8%)	0.55	1434.1	3.76m
Na (Na23, 100%)	0.60	1368.6	14.97h
Ti (Ti50, 5.2%)	0.62	320.1	5.76m
Mg (Mg26, 11.0%)	0.64	843.8	9.45m
Al (Al27, 100%)	0.74	1779.0	2.25m
Cl (Cl37, 24.2%)	0.74	1642.4 (2167.7)**	37.20m
Cu (Cu65, 30.9%)	1.01	1039.3	5.10m
Mn (Mn55, 100%)	1.05	1810.8 (846.8)**	2.58h
Br (Br81, 49.3%)	19.24	776.5	1.47d
I (I127, 100%)	24.19	442.9	25.00m

* [Baum et al., 2009]; Multiple gammas; primary listed

** True primary is in parenthetical, secondary [Basunia, 2002], is listed first

4.8 NAA Results

The first 28 years of winter samples collected at Alert, Canada, were independently analyzed using thermal NAA by students at the University of Texas at Austin in the TRIGA reactor and tabulated in an Excel spreadsheet by the same students who performed the NAA. Detection limits were noted, as were airflow correction factors and air volumes. The final NAA results were provided to the author of this dissertation for further study and analysis via a shared folder.

The results were checked for obvious errors and other anomalies and inconsistencies. The following three sets of data were first removed from the overall collection of data for the reasons listed:

1) Sample A-22-15 (formally row #309) is first removed as 10 of 11 elements are below minimum detectable, and the 10 all read “0.00” when normalizing the data set.
2) Sample A-1- 4 (formally row #5) is removed as 6 of 11 elements are high “1” and produced a significant outlier in Vanadium. As data before 1985 will ultimately not be included in the long-term yearly trending due to monthly sample inaccuracies, this helps individual element sample trending.
3) The final removal is Sample A-26-11 (now row 365) as 4 of 11 elements are low below minimum detectable, and this is a significant outlier (low below minimum detectable) for Vanadium.

The detailed results from the NAA are shown both explicitly and implicitly in other sections herein, specifically in the next section’s statistical analysis results). A short summary validating our results follows, comparing geometric means and means with other selected work is shown in Table 7 in the previous section (common-sense check).

In addition, the data included limits of detection, and as such are tabulated

below. Three elements showed significant numbers of samples below detectable. Of the three, Titanium is believed to be recorded and measured adequately because Titanium matches well with Al in the correlations, the scatterplots, and with the PMF model. Even the enrichment factor is in the expected range for the reasons given in Table 10:

Table 10 - Limits of Detection

	% of Samples Below	Mean Detectable Level	Median Detectible Level	Comparison to Other Literature	Notes
Al	0%	1.2	0.5	Lower than Ref 1	
Br	85%	18.3	7.9	Much higher than any previously noted	Not well resolved with PMF
Ca	0%	7.2	6.0	Lower than Refs 1&2	
Cl	0%	1.7	1.5	Lower than Refs 3&4	
Cu	89%	4.1	1.3	Consistent with Ref 1&2	Poor resolution in all PMF results
I	0%	0.002	0.002	Consistent with Ref 2	
Mg	0%	10.8	4.9	Unknown	
Mn	1%	0.13	0.03	Consistent with Ref 3	
Na	0%	1.6	1.5	Lower than Refs 1 or 3	
Ti	100%	70.6	30.7	Lower than Ref 1	Likely an error in the lower limit method
V	0%	0.003	0.001	Consistent with Refs 3&4	

Ref 1: [Biegalski & Landsberger, 1995]
Ref 2: [Basunia, 2002]
Ref 3: [Yli-Tuomi et al., 2003a]
Ref 4: [Barrie et al., 1980]

5. Statistical Analysis

The data is given a basic statistical treatment, as well as some more advanced treatments that determine trends, times, and relationships of interest. Some specific treatment methods are described in the sections that follow.

5.1 General Statistical Methods and Considerations

Statistical analysis is important for understanding data in nearly all fields of quantitative science involving data sets. Depending on the type of data used for any particular study, descriptive statistical analysis can yield a large amount of information about the data in question.

5.1.1 Robustness and Resistance

Classical statistical techniques commonly assume a normal (Gaussian) distribution. Data gathered in the atmospheric sciences often falls outside of this type of distribution. For example, much of the aerosol data collected in the Arctic is more closely related to a log normal distribution as seen in other literature as well [Basunia, 2002; Cheng et al., 1991]. Many classical procedures produce poor or potentially misleading results if the data is, in fact, a distribution other than a Gaussian. For these reasons, classical techniques, as well as some non-

classical techniques (Sen's slope; Spearman's Rank Correlation) are used and compared.

5.1.2 Means, Medians, Quartiles, and Other General Analysis

Mean

The most common statistical measure is the mean. The mean, also known as the average, is the sum of the samples divided by the number of samples. The mean being the most common type of statistical device, it is included throughout the results herein to convey relations with other data as well as to convey a comfortable measure of the data. For a normal (Gaussian) distribution, the mean is a measure of the central tendency.

Median

Another measure of central tendency, or a way to compare the mean with the central tendency, is to calculate the second most common statistical measure: the median. The median is the middle value of a set of numbers. If the distribution of a large set of numbers is truly normal, the median is equal to the mean. If there is a divergence between the median and the mean, the implication is that the distribution is skewed in the direction of the mean.

Geometric Mean

The geometric mean is a way to convey the central tendency when a distribution is skewed away from normal by using a single number instead of the two values required when using the median and mean. There are several sources that use the geometric mean instead of the mean and median, so all three values are calculated and included in this research.

Minimum and Maximum

The maximum and minimum need no explicit definition herein due to their widespread use. They are very useful for several reasons when performing statistical analysis. They are used to define the bound of a data set, used to develop box-and-whisker plots, and may be considered outliers depending on the other facts surrounding the existence of certain extreme points.

Quartiles

Quartiles are a value above which a specified quarter, or quarters, of the data falls. For example, the second quartile is the median, and the third quartile falls where 25% of the data is greater and 75% is lower than the value. Quartiles are useful in statistical analysis because the shape of the distribution can be implied. If the quartiles are evenly spaced, that may imply a normal distribution, else the analyst will be informed as to the true nature of a distribution.

Skewness

The skewness is essentially asymmetry in a distribution. Generally speaking, the more skewed, or the greater the “skewness” of a set of numbers, the less likely the set of numbers is normally distributed. When used with kurtosis and a normality test, much can be learned about the distribution of a set of numbers.

Kurtosis

Put simply, kurtosis is a measure of the “sharpness” of a peak, particularly as it related to the distribution of a set of data. Used in conjunction with the other parameters herein, much can be learned about the distribution of a set of data when the kurtosis is paired with the other information in the statistical analysis tables herein.

Normality

Normality is the property of a set of data that is distributed in a “Gaussian” or “Normal” way. The most basic descriptive statistics are best understood when data is described in these terms, although understanding when data is not normally distributed is also instructive.

5.1.3 Normality Tests

There are multiple normality testing methods including the Kolmogorov-Smirnov normality test, the Shapiro-Wilk test, and the d'Augustino-Pearson test.

For this work, the software used to determine Kurtosis, Skewness, and Normality, is "Real-Statistics," an add-in for Excel downloaded for free from www.real-statistics.com. The Shapiro-Wilk and d'Augustino tests are built-in, and both were run for both the complete data and for the yearly-averaged data. Both the Shapiro-Wilk and the d'Augustino-Pearson tests are based on assumed values for normality, and scores the data as falling within the expected range or not.

5.2 Graphical Techniques for Single Data Sets

5.2.1 Box and Whisker Plots

First introduced as a technique in exploratory data analysis in 1977, the box-and-whisker plot is now widely used [Wilks, 2006]. This type of graphical tool allows data to be displayed in a form that does not allow outliers to significantly affect the usefulness or comprehension of the data set. The box-and-whisker plot allows the full range of data to be seen at first glance, while simultaneously highlighting the quartiles and median.

The “box” is set by using the upper quartile and lower quartile, where the separation between the two is the median. The “whiskers” extend from the box to the maximum and minimum values in the data set.

The primary disadvantage of this type of plot, however, is that outlier behavior cannot be gleamed as the outliers will all be buried in the tails [Wilks, 2006]. For large data sets, it is possible to take the whiskers only to the 5^{th} and 95^{th} percentiles, and then place the outliers on their own beyond the whiskers [Miller et al., 1990]. Other options include “fencing” the data such that the outliers are seen beyond the whiskers [Wilks, 2006]. Regardless of the specific method, the box-and-whisker plot provides a quick visual understanding of the general distribution of a data set.

5.3 Techniques for Paired Data Sets

5.3.1 Scatterplots

Scatterplots are a “nearly universal format for displaying paired data [Wilks, 2006].” Scatter plots simply plot one variable, or set, along the x-axis, and the other along the y-axis. Trends and correlations can be seen with the naked eyes using this technique. Although numerical techniques can give a more solid understanding of correlations, scatterplots also allow outliers to be immediately apparent for potential special treatment.

5.3.2 Pearson (Ordinary) Correlation

The Pearson Correlation is a measure of covariance, which is a way to understand how two variables change together. The Pearson's will show how closely two data sets match a linear relation.

$$Correl(x, y) = \frac{\sum(x - \acute{x})(y - \acute{y})}{\sqrt{\sum(x - \acute{x})^2 \sum(y - \acute{y})^2}}$$

The resulting value is bounded by -1 and 1. A value of |1| implies a perfect linear correlation, and a negative value implies negative linear correlation. A value of "0" means there is no mathematical correlation.

The Pearson Correlation is neither robust nor resistant as it does not show non-linear relationships between two variables, and it is extremely sensitive to outliers. However, the Pearson Correlation makes no assumption about normality of the data and works with most types of data. Used in conjunction with scatterplots that make outliers more apparent, the Pearson Correlation is an extremely useful scoping tool for interdependency between variables.

5.3.3 Spearman's Rank Correlation

The Spearman's Rank Correlation (or the Spearman Rank Correlation), unlike the Pearson Correlation, is both robust and resistant. Essentially, the Spearman Correlation first "ranks" the data from "1" to "n" and then uses the Pearson Correlation on the ranked data rather than on the true data. Converting values into ranks eliminates or normalizes extreme outliers, and thus turns the correlation into one which is robust. The Spearman Rank Correlation equation is as follows:

$$r_{rank} = 1 - \frac{6 * \sum_{i=1}^{n} D_i^2}{n(n-1)}$$

where:

D^i is the difference in ranks between the i^{th} pair of data values, and

n is the sample size.

Because of this method's inherent robustness and resiliency, it is used for all data herein and results are compared to the Pearson (ordinary) Correlation where possible. Significant differences between Spearman and Pearson correlations may indicate the presence of extreme outliers or inform the analyst as to some inherent property of the underlying data.

5.3.4 Correlation Matrices

The purpose of a correlation matrix is to display multiple correlations among more than two sets of matched data. With multiple variable, there are distinct parings of: [(k)(k-1)]/2, so that for 11 data sets (as in the case of this research, or 12 if time is included), there are (11)*(10)/2 = 55 distinct pairings. [Wilks, 2006] Much of the matrix is redundant, so it is typically displayed with all data above (or below) the diagonal removed, such that each distinct pairing is displayed only once. Correlation matrices of both the Spearman and the Pearson varieties inform the relative magnitude of each correlation to quickly identify the most significant. Applied “heat maps” make this process even faster. When a Spearman’s Rank Correlation matrix is compared alongside a Pearson Correlation matrix, other information related to outliers may also become evident.

5.3.5 Regression

Regression is the general process of fitting a function to a set of data. There are several methods to accomplish this task, including methods for both linear and non-linear regression. Linear regression is the most common type of regression, and the easiest to describe and perform. The common method by which linear regression is accomplished is called the “least-squares” method. The least-square method of this type of regression will provide a general

understanding of either a time trend of a data set, or provide a visual understanding of the interrelation of any two variables (such as two different elements in a single data set). A strong linear dependency can be seen when the linear regression line is plotted with the points in 2-dimensional space.

The method of least squares [Miller et al., 1990] involves the initial assumption that there is, in fact, a linear dependency between two variables, such that:

$$y(x) = mx+b.$$

Then, each data point in the set, or, rather, every (x_i, y_i) point can be visualized in a scattergram. The goal is to determine the constants “m” and “b” such that the sum of the differences between every (x_i, y_i) point and the line, y(x) = mx+b, is minimized. In other words,

$$\sum_{i=1}^{n} \left(y_i - (m * x_i + b)\right)^2$$

This “sum of squares” quantity should be minimized by varying “m” and “b,” hence the namesake of this method: “least-squares.” This is the most common type of regression, and is calculated automatically in Microsoft Excel when adding the default type of trend line to a set of data.

The least-squares method will work with non-linear trends that still follow a linear function as well. The theory is the same: that an equation is set up and the constants are determined by minimizing the sum of the squares of the differences between the function and each data point. Other built-in functions in Microsoft Excel perform such more complex operations, such as finding a polynomial of user-defined order. Logarithmic trends are also options for automatic calculation.

As with other types of analysis, the user must judge the fit of such trends and values and then make a determination if the type of trend is a good fit, and interpret the results appropriately.

5.3.6 Sen's Slope

The slope that simple linear regression may provide is greatly affected by extreme variance and outliers (see discussion on robustness and resistance). Therefore, it is sometimes desirable to understand the more general trend of a set of data. One method of inferring more about a slope than can be divined from linear regression is by using a tool called "Sen's slope." The Sen's slope, also known as the Theil-Sen method, among other terms, is a nonparametric slope estimate tool that is more robust than a simple regression line. Neither the slope nor the estimate, using this method, is significantly affected by outliers.

One particular disadvantage of this general type of trending (considering

the median slope) can be visualized when considering data that exhibits a saw-tooth or similar type of cyclical variation. If the saw-tooth is skewed, and the skew is a reversal of the general trend, the Sen's slope will exhibit a trend contradictory for the direction of the true trend. Other issues may arise when using this methods for various other distribution types as well. However, for more generally distributed data, there is often insight to be gleamed from considering the Sen's slope.

5.4 Statistical Analysis Results

In this section is displayed all the described general results as labeled in the Tables 11-15 that follow.

Table 11 - Yearly Averaged Statistical Results

	Al	Br	Ca	Cl	Cu	I	Mg	Mn	Na	Ti	V
Geomean	5.1E+01	9.1E+00	1.1E+02	2.0E+02	1.3E+00	2.1E-01	9.6E+01	7.6E-01	2.3E+02	3.1E+00	3.3E-01
Mean	5.4E+01	9.4E+00	1.1E+02	2.2E+02	2.3E+00	2.1E-01	9.8E+01	7.8E-01	2.3E+02	3.3E+00	3.8E-01
Median	5.0E+01	9.0E+00	1.1E+02	2.0E+02	1.1E+00	2.0E-01	9.8E+01	7.8E-01	2.3E+02	3.2E+00	3.4E-01
Std Mean Error	9.0E-01	1.3E-01	1.6E+00	3.8E+00	1.9E-01	1.7E-03	1.0E+00	9.7E-03	1.9E+00	5.6E-02	9.8E-03
Minimum	3.1E+01	4.8E+00	6.9E+01	1.2E+02	3.9E-01	1.5E-01	6.7E+01	4.6E-01	1.8E+02	1.2E+00	1.3E-01
Maximum	1.0E+02	1.7E+01	2.1E+02	3.9E+02	1.8E+01	3.0E-01	1.4E+02	1.1E+00	3.3E+02	6.2E+00	8.1E-01
Range	6.9E+01	1.2E+01	1.5E+02	2.8E+02	1.8E+01	1.5E-01	7.5E+01	6.8E-01	1.5E+02	5.0E+00	6.8E-01
Std Dev	1.8E+01	2.5E+00	3.1E+01	7.6E+01	3.8E+00	3.5E-02	2.1E+01	1.9E-01	3.8E+01	1.1E+00	2.0E-01
Variance	3.2E+02	6.4E+00	9.7E+02	5.8E+03	1.5E+01	1.2E-03	4.3E+02	3.7E-02	1.5E+03	1.3E+00	3.9E-02
1st Quartile	4.2E+01	8.4E+00	8.8E+01	1.6E+02	6.3E-01	1.9E-01	8.0E+01	6.0E-01	2.1E+02	2.7E+00	1.9E-01
3rd Quartile	6.3E+01	9.9E+00	1.2E+02	2.6E+02	1.9E+00	2.2E-01	1.0E+02	9.6E-01	2.5E+02	3.8E+00	5.7E-01

Table 12 - All Data Statistical Results

	Al	Br	Ca	Cl	Cu	I	Mg	Mn	Na	Ti	V
Geomean	4.2E+01	6.7E+00	1.0E+02	1.4E+02	7.2E-01	1.9E-01	7.6E+01	5.7E-01	2.0E+02	2.2E+00	2.9E-01
Mean	5.5E+01	8.9E+00	1.1E+02	2.0E+02	2.2E+00	2.1E-01	9.4E+01	7.6E-01	2.3E+02	3.4E+00	3.8E-01
Median	4.0E+01	6.4E+00	9.5E+01	1.2E+02	8.1E-01	1.8E-01	8.6E+01	6.7E-01	1.9E+02	2.6E+00	2.7E-01
Std Mean Error	2.6E+00	4.0E-01	2.9E+00	1.1E+01	5.2E-01	4.4E-03	2.7E+00	2.6E-02	6.6E+00	1.7E-01	1.5E-02
Minimum	1.3E+01	1.8E+00	4.7E+01	4.1E+01	9.4E-02	1.0E-01	7.2E+00	6.6E-02	6.5E+01	1.0E-01	9.4E-02
Maximum	4.9E+02	7.4E+01	6.2E+02	1.9E+03	2.0E+02	9.4E-01	3.8E+02	3.4E+00	1.0E+03	2.8E+01	1.4E+00
Range	4.8E+02	7.3E+01	5.7E+02	1.8E+03	2.0E+02	8.4E-01	3.7E+02	3.3E+00	9.6E+02	2.8E+01	1.3E+00
Std Dev	5.2E+01	8.1E+00	5.7E+01	2.1E+02	1.0E+01	8.7E-02	5.3E+01	5.2E-01	1.3E+02	3.3E+00	3.0E-01
Variance	2.7E+03	6.5E+01	3.3E+03	4.6E+04	1.1E+02	7.6E-03	2.8E+03	2.7E-01	1.8E+04	1.1E+01	8.9E-02
1st Quartile	2.5E+01	3.8E+00	7.2E+01	6.6E+01	1.7E-01	1.6E-01	6.3E+01	4.3E-01	1.3E+02	1.5E+00	1.5E-01
3rd Quartile	6.6E+01	1.1E+01	1.3E+02	2.6E+02	1.7E+00	2.2E-01	1.2E+02	1.0E+00	2.8E+02	4.2E+00	5.0E-01

Table 13 - All Data Kurtosis, Skewness, and Normality

	Al	Br	Ca	Cl	Cu	I	Mg	Mn	Na	Ti	V
Kurtosis	19.2	20.3	21.7	12.6	308.4	19.4	3.4	3.1	5.8	16.1	1.5
Skewness	3.6	3.4	3.5	2.9	16.7	3.6	1.2	1.3	1.9	3.3	1.4
Normal?	**No**	**No**	**No**	**No**	**No**	**No**	**No**	**No**	**No**	**No**	**No**

Table 14 - Yearly Averaged Data Kurtosis, Skewness, and Normality

	Al	Br	Ca	Cl	Cu	I	Mg	Mn	Na	Ti	V
Kurtosis	0.2	2.3	3.9	-0.3	16.7	0.9	2.2	0.9	1.1	0.4	-0.4
Skewness	0.6	0.3	1.5	0.6	3.9	0.9	-0.8	-0.8	-0.5	0.5	0.5
Normal? Shapiro/ d'Augustino	Yes/ Yes	No/ No	No/ No	Yes/ Yes	No/ No	No/ Yes	Yes/ No	Yes/ Yes	Yes/ Yes	Yes/ Yes	No/ Yes

Table 15 - Monthly Means

	Al	Br	Ca	Cl	Cu	I	Mg	Mn	Na	Ti	V
January	5.8E+01	5.0E+00	1.2E+02	2.8E+02	1.9E+00	1.7E-01	1.1E+02	8.7E-01	2.5E+02	3.4E+00	4.9E-01
February	4.1E+01	6.0E+00	1.0E+02	2.5E+02	1.4E+00	1.8E-01	9.6E+01	6.6E-01	2.4E+02	2.7E+00	3.8E-01
March	4.6E+01	1.2E+01	1.0E+02	1.8E+02	3.9E+00	2.6E-01	9.3E+01	7.4E-01	2.2E+02	2.9E+00	3.9E-01
April	7.7E+01	1.5E+01	1.2E+02	1.2E+02	1.8E+00	2.1E-01	9.6E+01	9.3E-01	2.1E+02	4.5E+00	3.0E-01

Notes on monthly trends, for comparison to information provided in Section 3, per element is shown in Table 16.

Table 16 - Comparison of Monthly/Winter Trends to Literature

Element	Trend(s)
Al	Possible long-term decrease as was noted in previous research [Gong & Barrie, 2005]. No other particular trends or regions of interest noted.
Br	Large jump in March [Biegalski et al., 1997] that may be as much as a full order of magnitude [Barrie et al., 1994]: this work verifies the March jump. The Arctic sunrise occurs Around March 1 at Alert, which corresponds with the increase.
Ca	No noted trends in this or other Arctic aerosol literature.
Cl	A drop beginning in March is consistent with other literature [Barrie & Hoff, 1985; Barrie et al., 1994].
Cu	A March excursion is apparent here yet is not noted in other literature.
I	An uptick in March is noted here and is consistent with other literature [Barrie & Hoff, 1985; Barrie et al., 1994].
Mg	No noted trends in this or other Arctic aerosol literature.
Mn	No noted trends in this or other Arctic aerosol literature.
Na	No noted trends in this or other Arctic aerosol literature (with the exception of an unseen seasonal trend).
Ti	No noted trends here in either this data set or in Arctic aerosol literature
V	Consistent with literature, there is a drop in late winter/early Spring [Barrie & Hoff, 1985]. Other literature also notes that Vanadium is highest in January for the entire year [Basunia, 2002].

The following Table 17 includes both the linear regression slope and the Sen's slope for all elements, using both yearly averaged data and sample data:

Table 17 - Sen's and Regression Results

Element	Yearly Averaged Data (per year)	Sen's Yearly Data (per year)	All Data (per sample)	Sen's All Data (per sample)
Al	-5.1E-02	-5.7E+00	-1.5E-02	-9.0E-01
Br	4.4E-02	-2.4E-01	6.6E-04	9.7E-02
Ca	-1.2E+00	-5.1E+00	-1.1E-01	3.9E-01
Cl	6.3E+00	2.2E-01	4.4E-01	-1.2E+00
Cu	-2.6E-02	-2.0E-01	-2.3E-03	-3.0E-03
I	2.7E-03	1.0E-03	1.9E-04	4.0E-04
Mg	3.4E-01	2.6E+00	-1.5E-02	1.0E-01
Mn	-2.7E-03	-1.3E-02	-5.2E-04	-1.4E-03
Na	3.0E+00	3.7E+00	1.7E-01	-1.2E+00
Ti	-2.4E-02	-7.5E-02	-1.7E-03	-1.2E-02
V	-1.9E-02	-1.0E-02	-1.2E-03	-2.6E-03

Regression of yearly averages with temperature is compared with Correlation results in Section 5.4.3. Note, however, that the strongest "slope" in the regression results does relate somewhat to the stronger correlations. They do not line up exactly for reasons to be explained later. Other items of interest are whether or not the sign of the slope is consistent across the 4 groupings for a single element, and to notice which elements bear similar values (for either yearly or all data) between the Sen's and regression slope.

5.4.1 Box Plots

Box and whisker plots are displayed in Figures 11-13 for each elemental sample set in log scale. Note that removing the outliers, or applying other methodology as in done in the subsequent section, allows the plots to appear “normal” in the log scale, which is the definition of a log-normal distribution. As is the stated disadvantage in a general box-and-whisker plot, the outliers are buried in, and give misleading whisker magnitudes to the plots [Wilks, 2006].

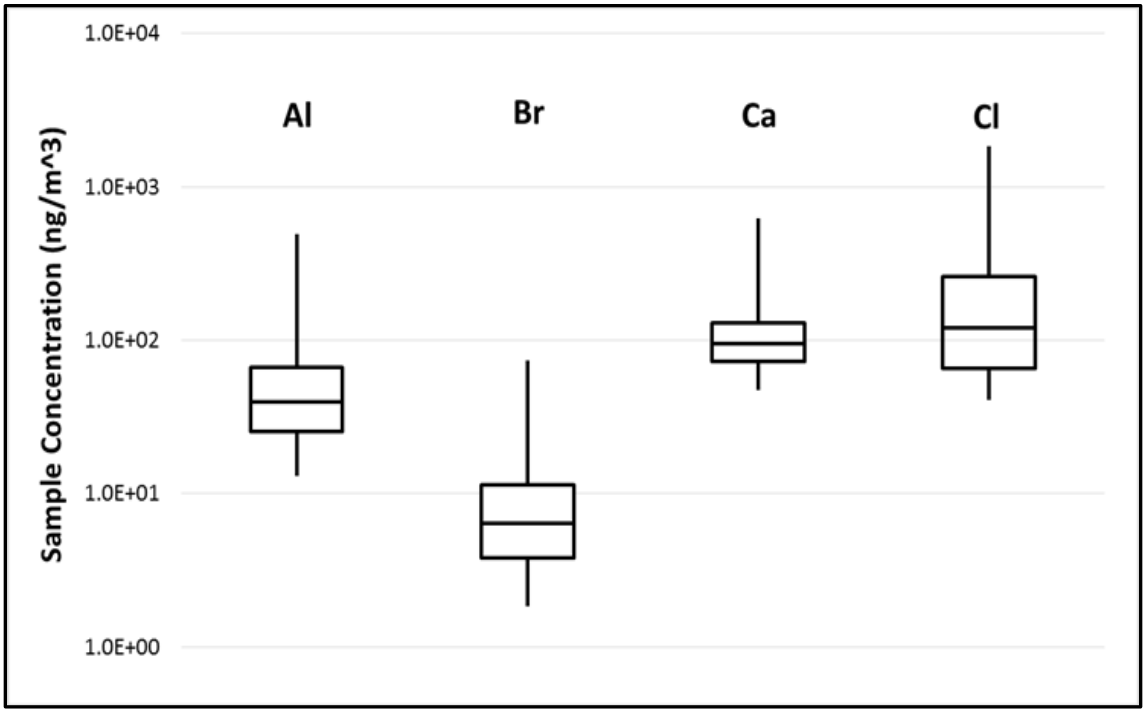

Figure 11 - Al, Br, Ca, Cl Log Box Plots

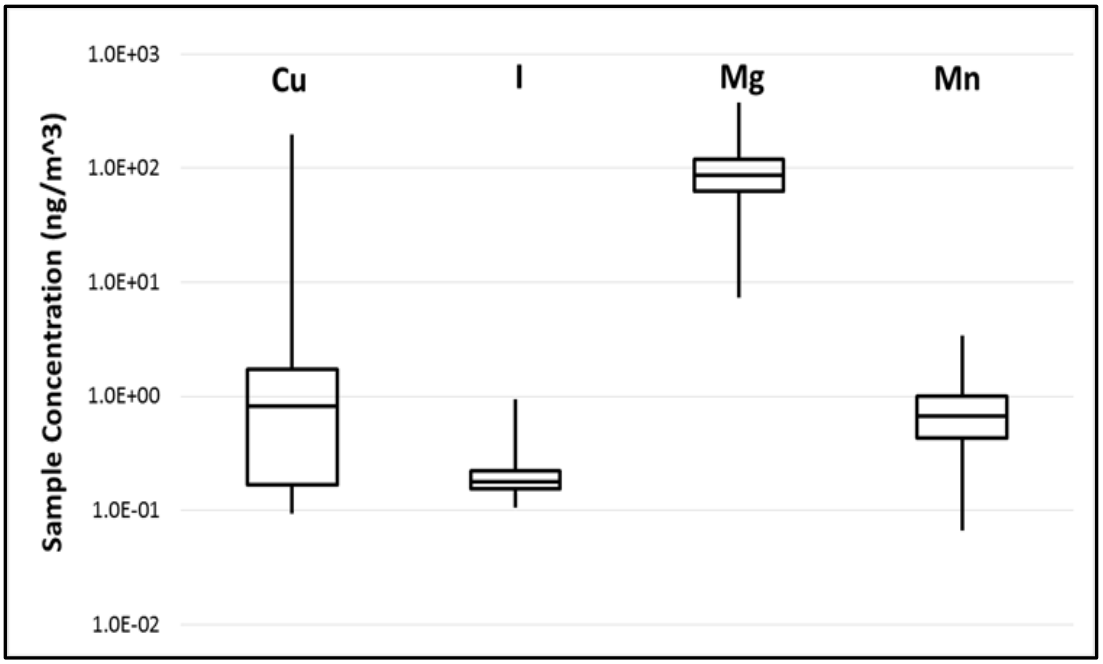

Figure 12 - Cu, I, Mg, Mn Log Box Plots

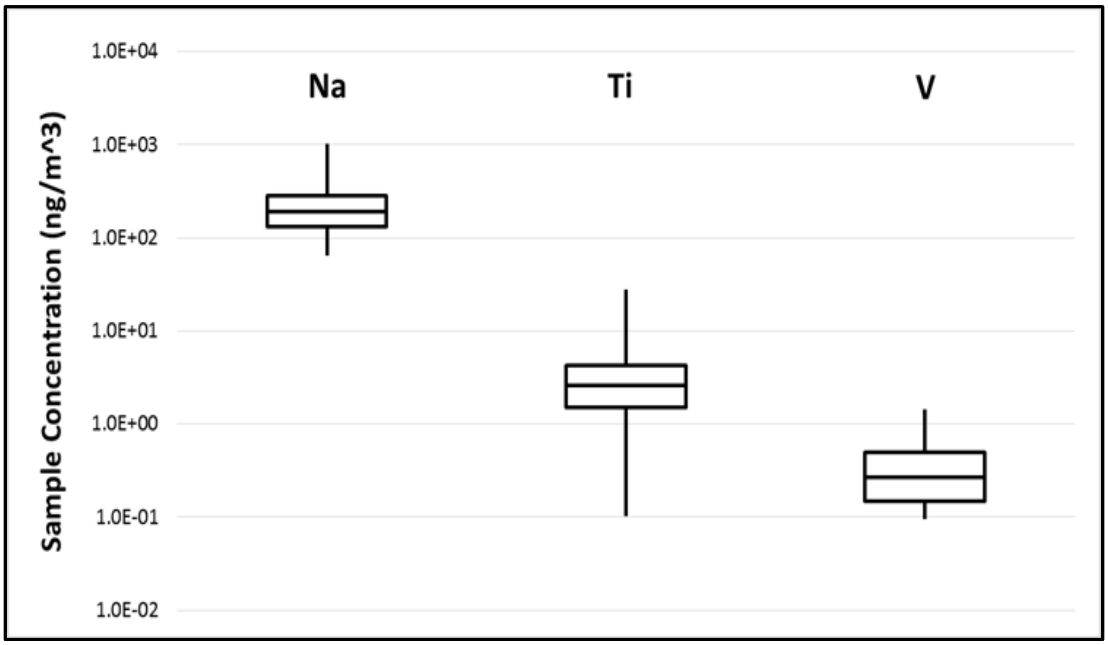

Figure 13 - Na, Ti, V Log Box Plots

The 2nd and 3rd quartile appear to be generally log-normally distributed for the elements in the preceding box plots. However, the whiskers do not. Therefore, the following plots are generated using whiskers that only extend to the 5th percentile and the 95th percentile, as is recommended for some data sets [Miller et al., 1990]. Note that Sodium, Vanadium, and Bromine appear to be almost perfectly log-normally distributed, and most of the others, especially Aluminum, appear more log-normally distributed than when the whiskers end at the max and min. Figures 14-16 show the Sans Outliers.

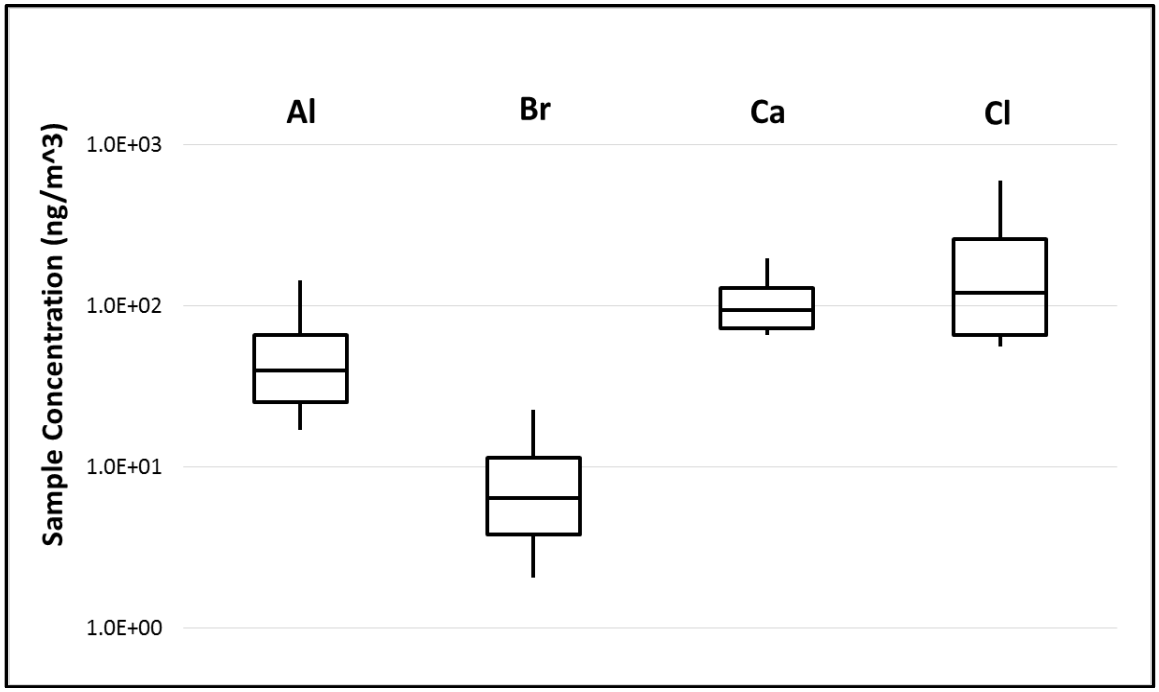

Figure 14 - Al, Br Ca, and Cl Log Box Plots Sans Outliers

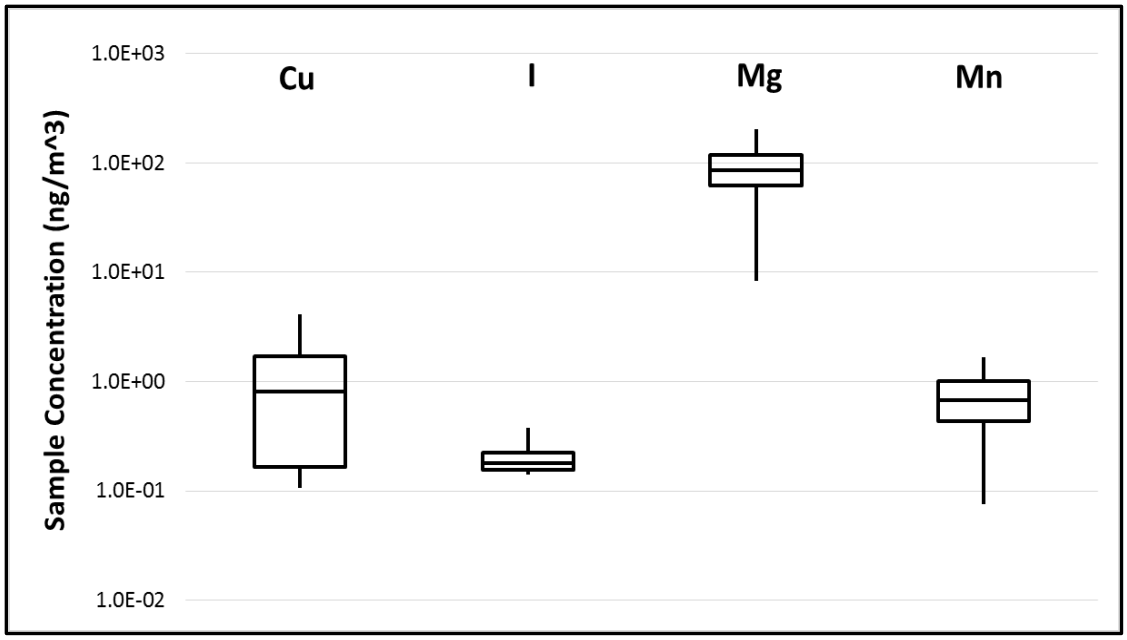

Figure 15 - Cu, I, Mg, and Mn Log Box Plots Sans Outliers

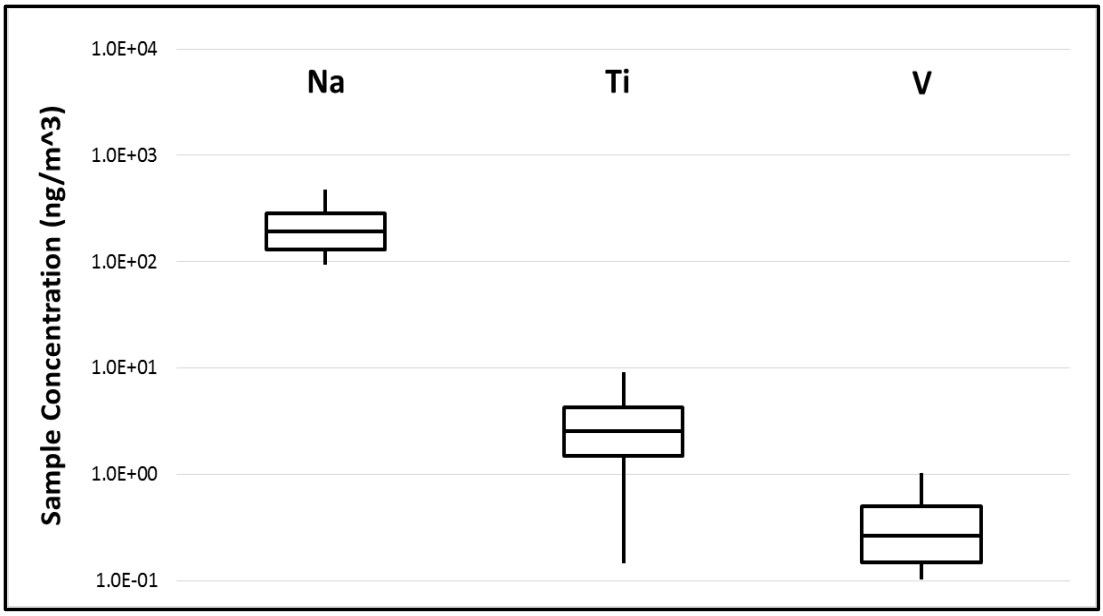

Figure 16 - Na, Ti, and V Log Box Plots Sans Outliers

5.4.2 Scatter Plots

Scatter plots for all 11 elemental combinations would equal 55 variations (or 110 if axial shifts were to be included), most of which would add little understanding of the underlying data. Therefore, only the 13 Pearson correlations greater than 0.5 are included. In addition, the next highest 2 are also included (Ti/Mg and Cu/I). In order of correlation from strongest to weakest (Figures 17-30):

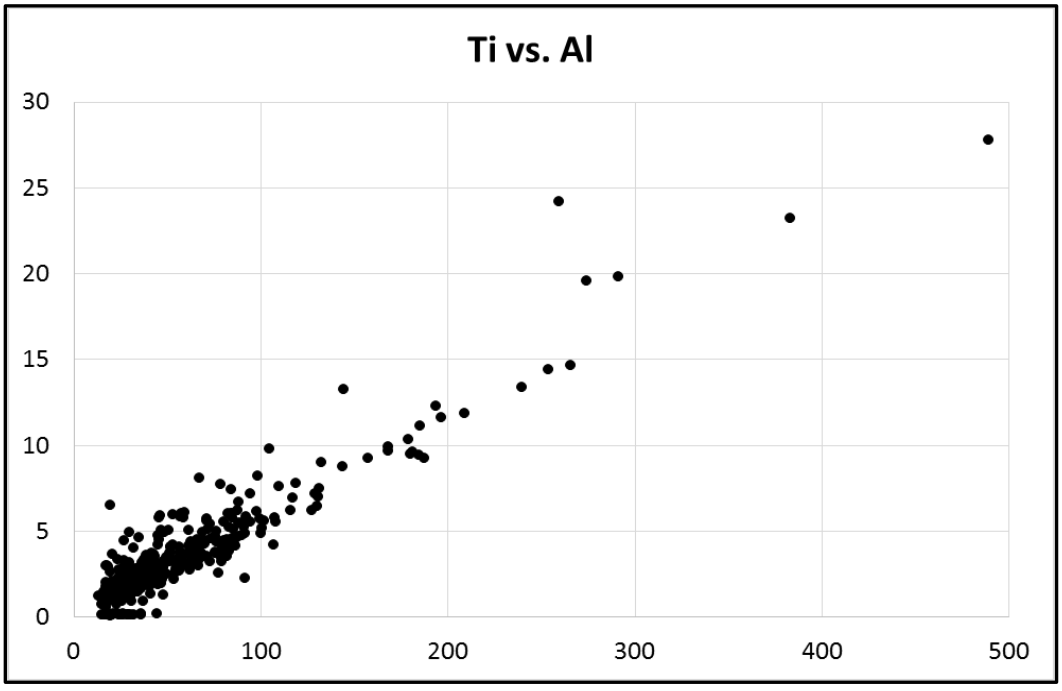

Figure 17 - Ti vs. Al Scatterplot

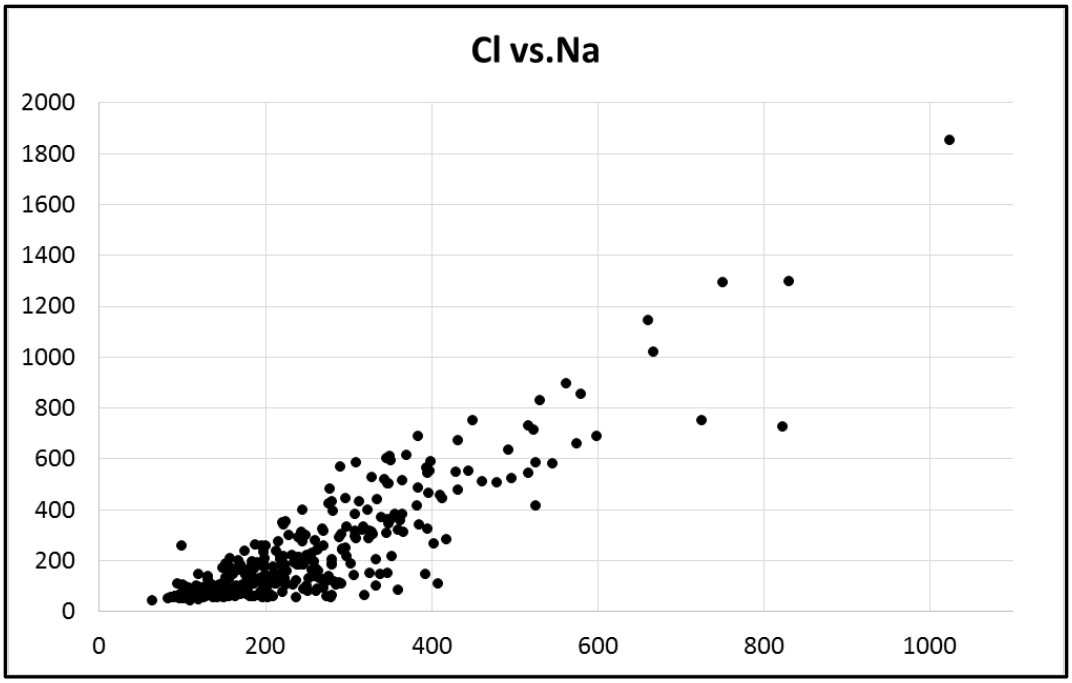

Figure 18 - Cl vs. Na Scatterplot

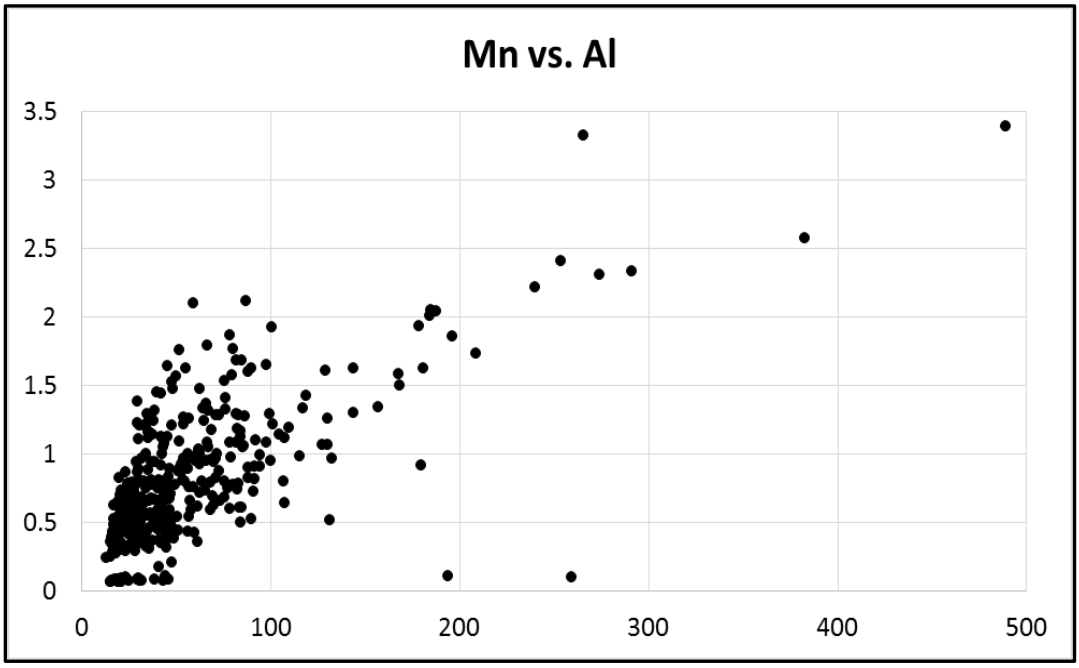

Figure 19 - Mn vs. Al Scatterplot

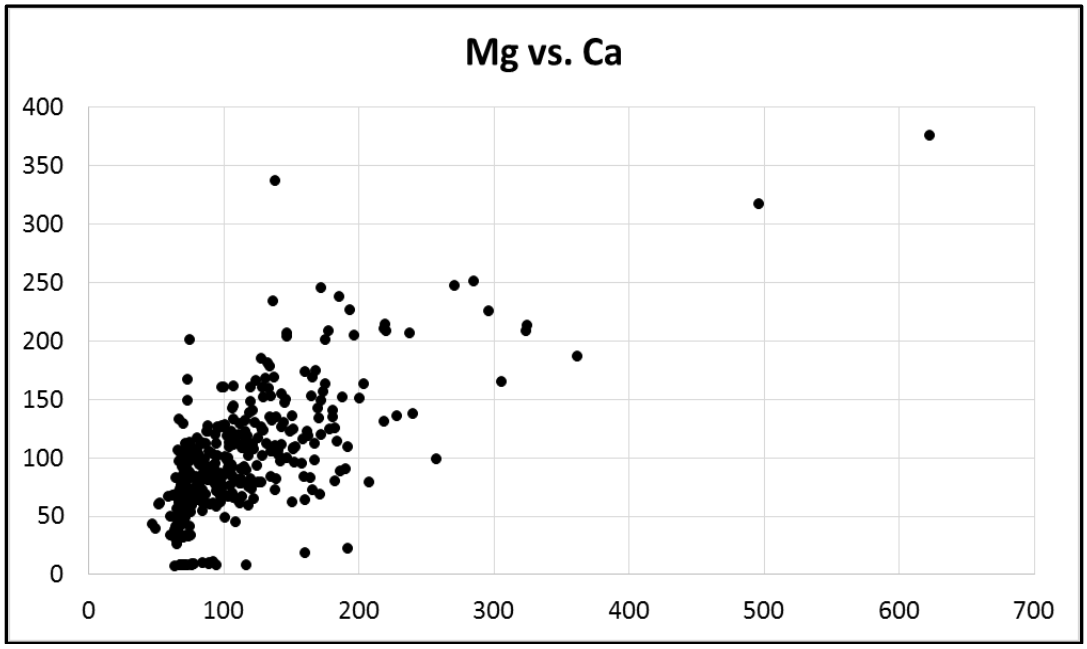

Figure 20 - Mg vs. Ca Scatterplot

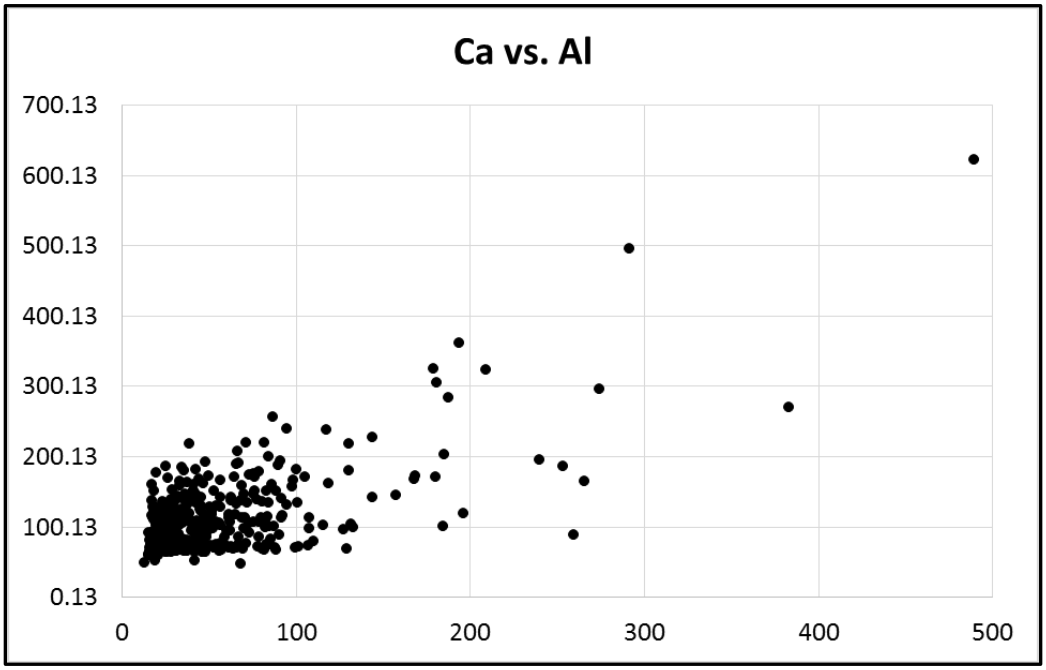

Figure 21 - Ca vs. Al Scatterplot

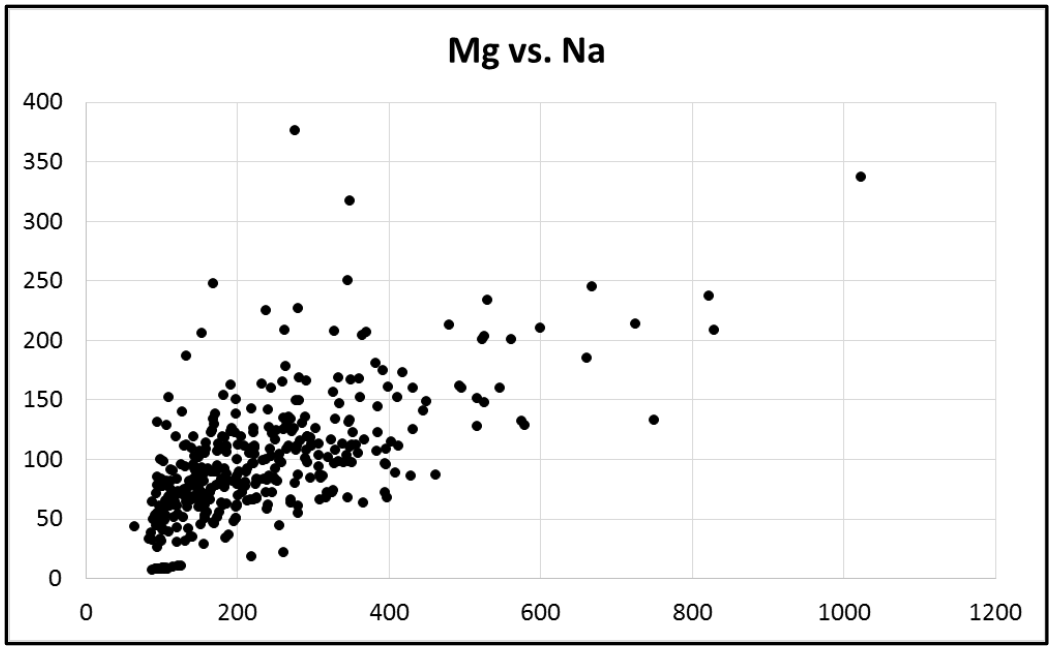

Figure 22 - Mg vs. Na Scatterplot

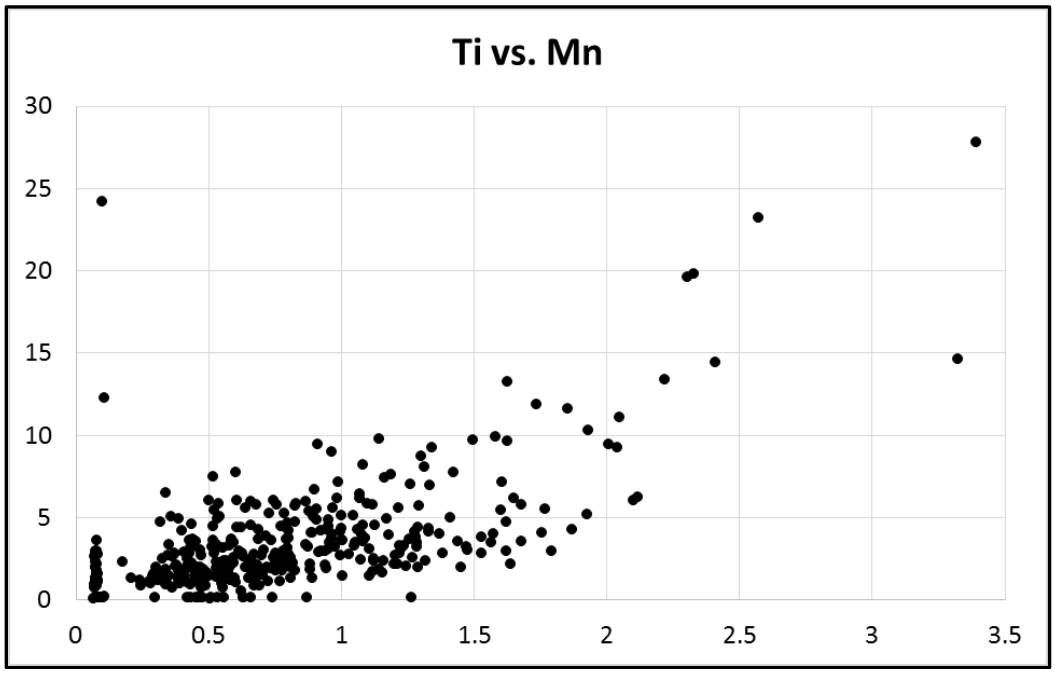

Figure 23 - Ti vs. Mn Scatterplot

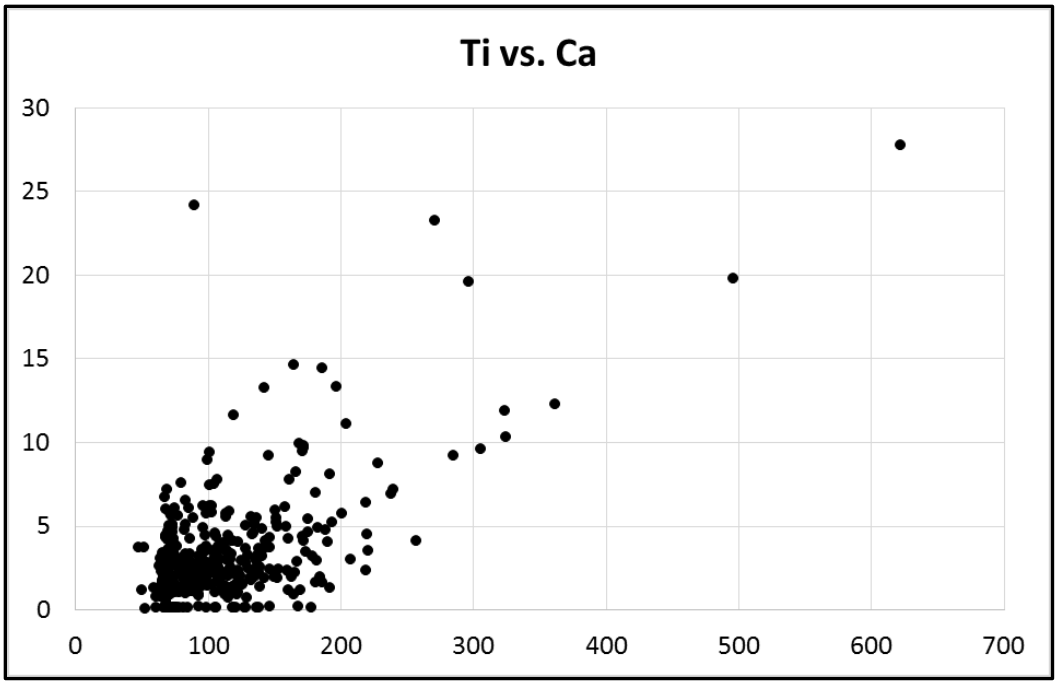

Figure 24 - Ti vs. Ca Scatterplot

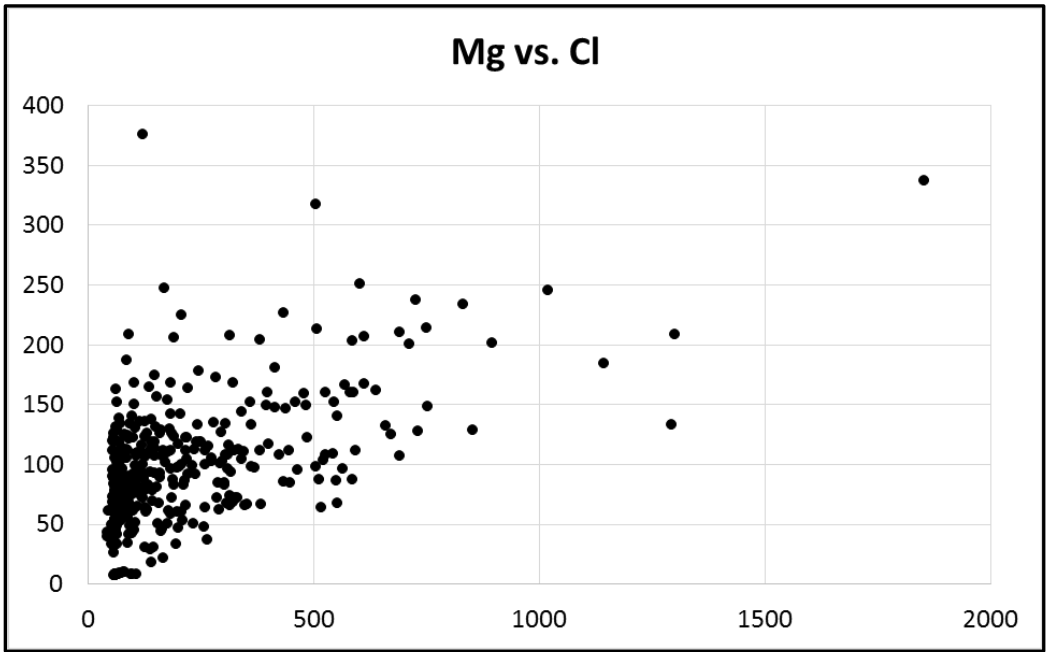

Figure 25 - Mg vs. Cl Scatterplot

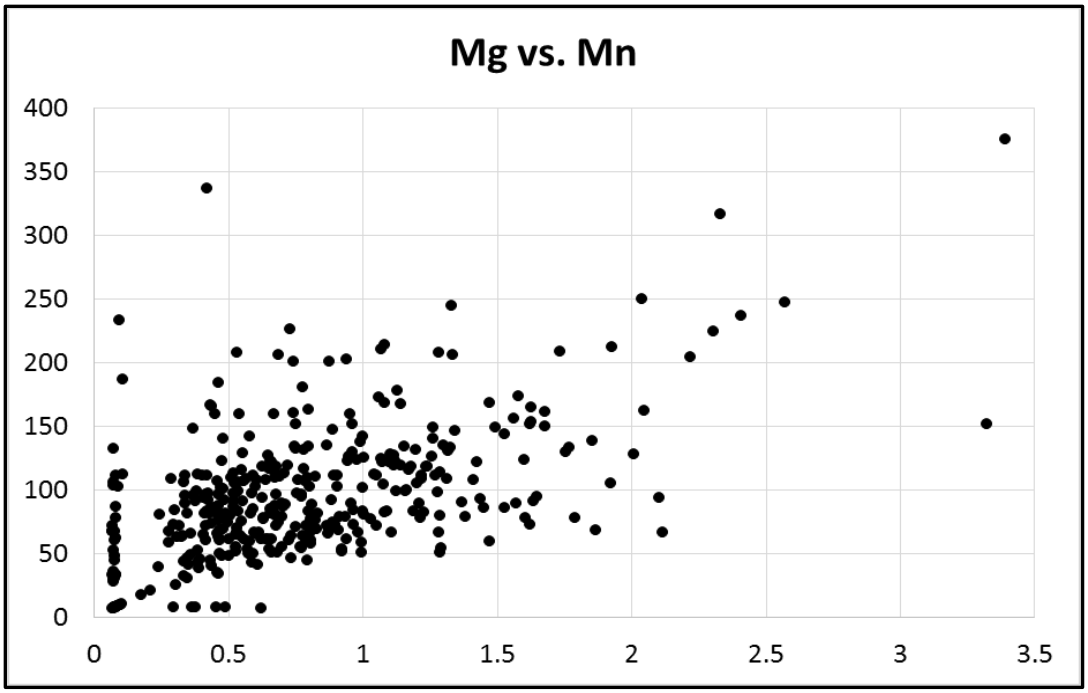

Figure 26 - Mg vs. Mn Scatterplot

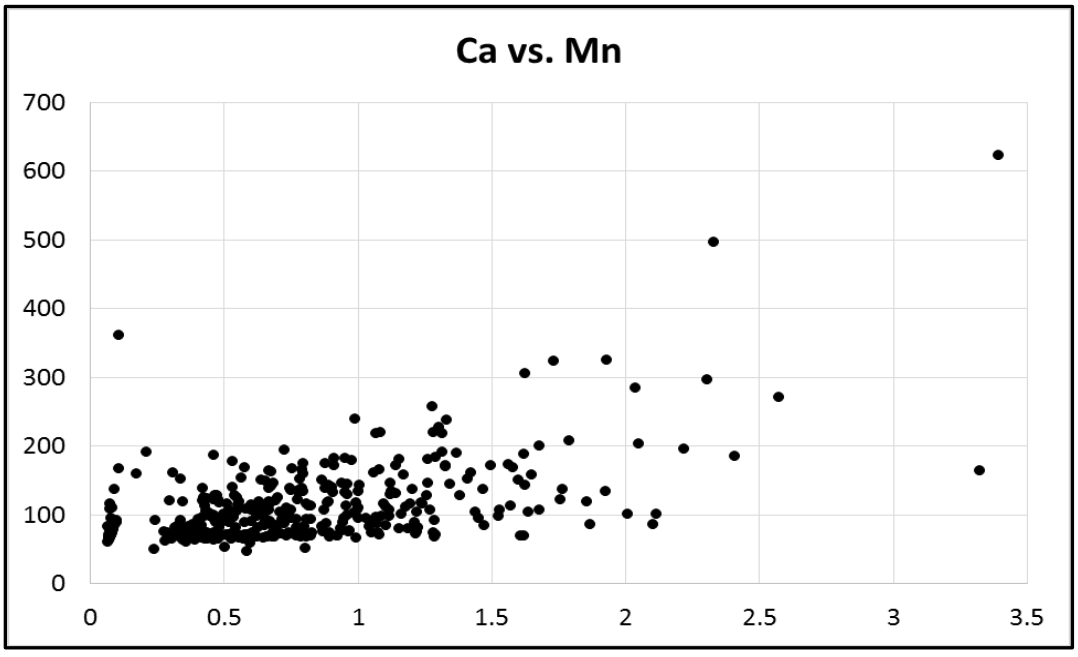

Figure 27 - Ca vs. Mn Scatterplot

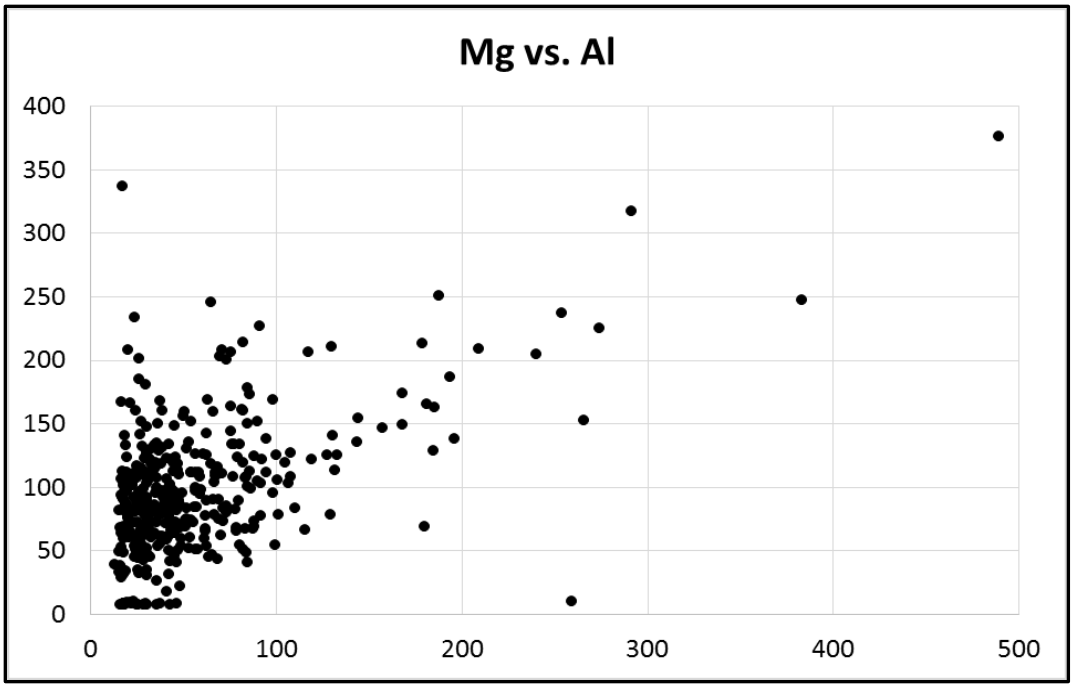

Figure 28 - Mg vs. Al Scatterplot

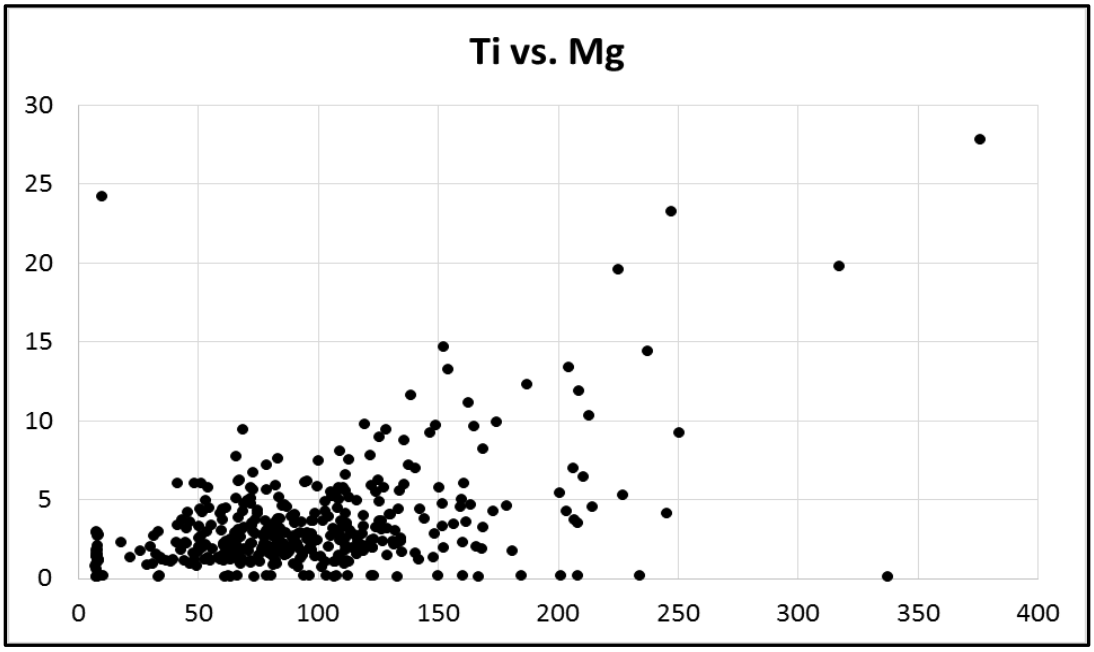

Figure 29 - Ti vs. Mg Scatterplot

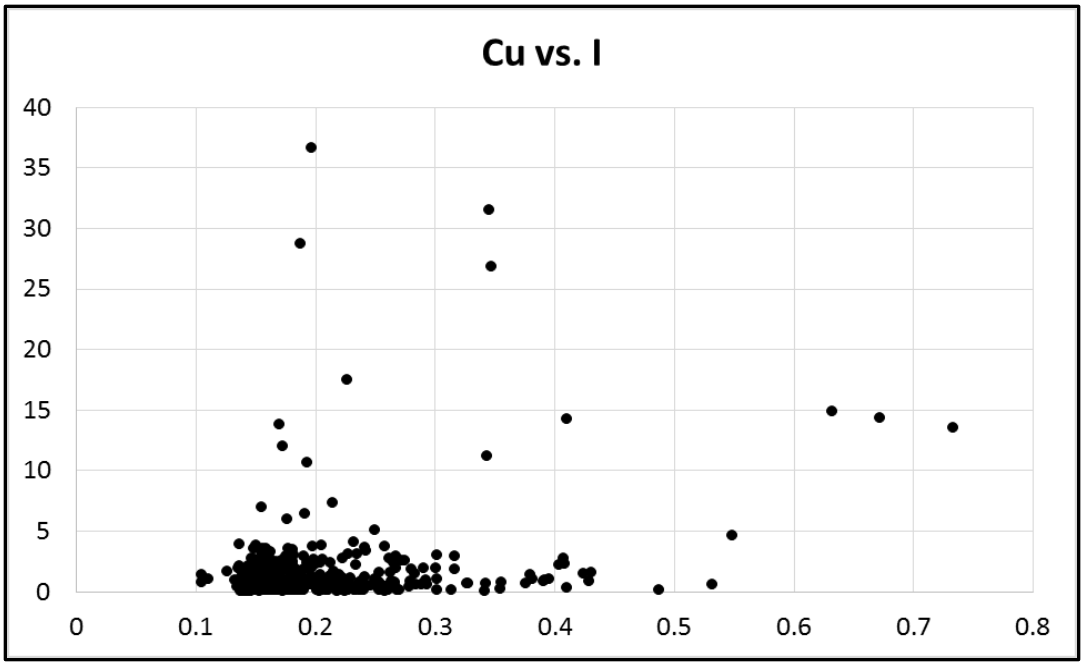

Figure 30 - Cu vs. I Scatterplot

5.4.3 Correlation Results

Correlation results for the 11 elements for all-data and yearly-averaged are given in Tables 18-20. Additional correlation results using monthly averages per year instead of yearly averages can be seen in Table 46 of the Appendix.

Table 18 - All-Data Pearson Correlation Heat Map

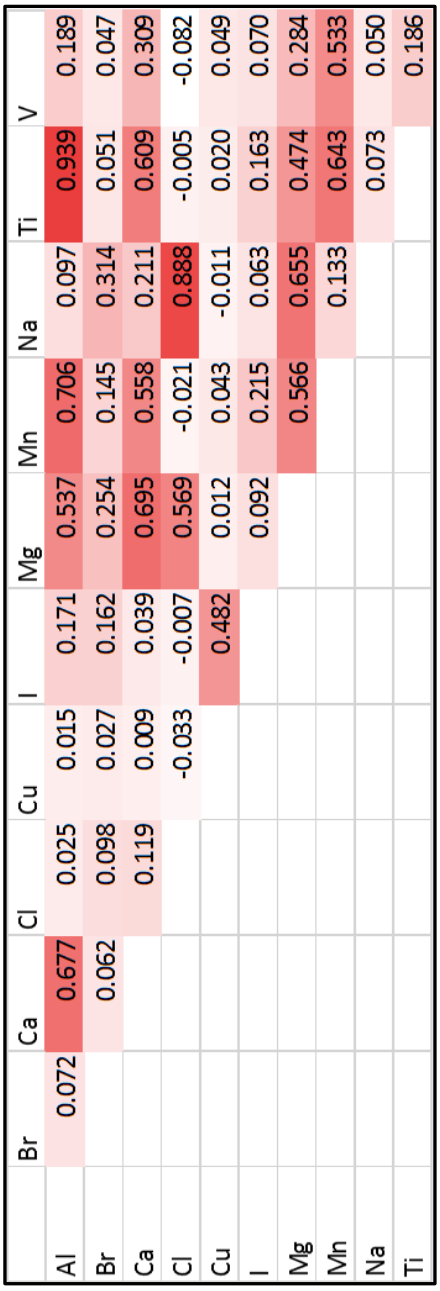

	Br	Ca	Cl	Cu	I	Mg	Mn	Na	Ti	V
Al	0.072	0.677	0.025	0.015	0.171	0.537	0.706	0.097	0.939	0.189
Br		0.062	0.098	0.027	0.162	0.254	0.145	0.314	0.051	0.047
Ca			0.119	0.009	0.039	0.695	0.558	0.211	0.609	0.309
Cl				-0.033	-0.007	0.569	-0.021	0.888	-0.005	-0.082
Cu					0.482	0.012	0.043	-0.011	0.020	0.049
I						0.092	0.215	0.063	0.163	0.070
Mg							0.566	0.655	0.474	0.284
Mn								0.133	0.643	0.533
Na									0.073	0.050
Ti										0.186

Table 19 - Yearly Averaged Data Pearson Correlation Heat Map

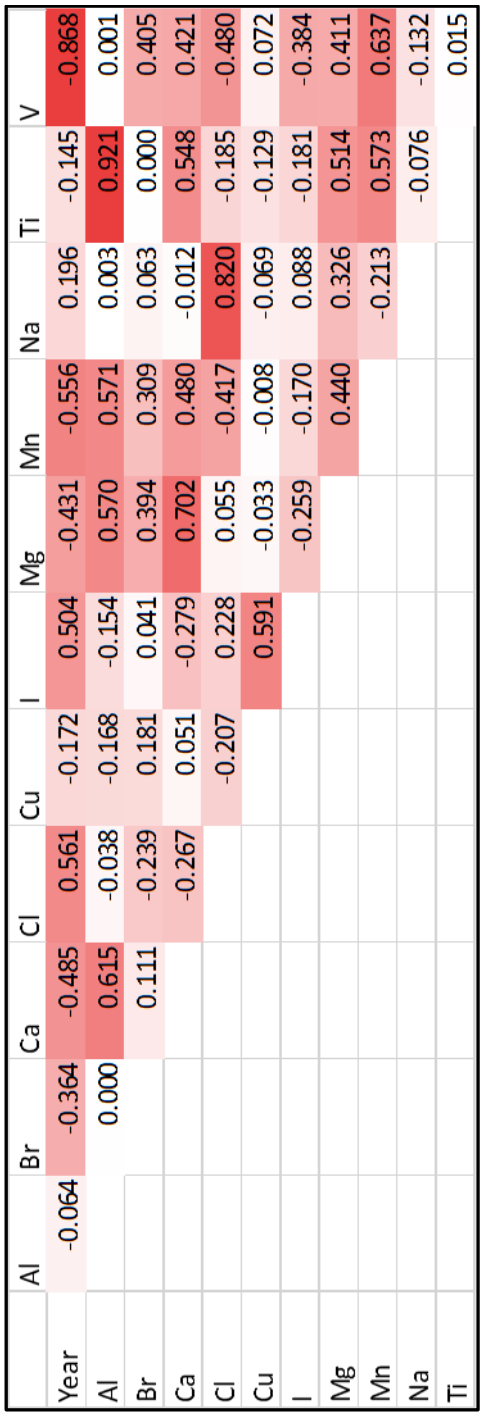

	Al	Br	Ca	Cl	Cu	I	Mg	Mn	Na	Ti	V
Year	-0.064	-0.364	-0.485	0.561	-0.172	0.504	-0.431	-0.556	0.196	-0.145	-0.868
Al		0.000	0.615	-0.038	-0.168	-0.154	0.570	0.571	0.003	0.921	0.001
Br			0.111	-0.239	0.181	0.041	0.394	0.309	0.063	0.000	0.405
Ca				-0.267	0.051	-0.279	0.702	0.480	-0.012	0.548	0.421
Cl					-0.207	0.228	0.055	-0.417	0.820	-0.185	-0.480
Cu						0.591	-0.033	-0.008	-0.069	-0.129	0.072
I							-0.259	-0.170	0.088	-0.181	-0.384
Mg								0.440	0.326	0.514	0.411
Mn									-0.213	0.573	0.637
Na										-0.076	-0.132
Ti											0.015

Table 20 - Spearman's Rank Correlation of Time-Averaged Data

	Al	Br	Ca	Cl	Cu	I	Mg	Mn	Na	Ti	V
Year	-0.048	-0.510	-0.510	0.637	-0.470	0.543	-0.519	-0.575	0.226	-0.151	-0.864
Al		-0.057	0.443	0.059	-0.135	-0.044	0.501	0.599	0.181	0.860	0.024
Br			0.087	-0.414	0.200	-0.116	0.329	0.325	-0.075	0.044	0.439
Ca				-0.270	0.057	-0.228	0.766	0.521	-0.005	0.342	0.615
Cl					-0.444	0.184	-0.157	-0.470	0.735	-0.226	-0.575
Cu						0.199	-0.053	0.299	-0.090	-0.100	0.401
I							-0.180	-0.065	0.141	-0.064	-0.348
Mg								0.536	0.248	0.456	0.557
Mn									-0.127	0.624	0.643
Na										-0.105	-0.179
Ti											0.078

Comparing these correlation results to the Sen's slope and regression values in the previous section, for the yearly averaged data, Chlorine has the strongest regression value, followed by Sodium and Calcium. Manganese has the weakest regression value. The Sen's value for the strongest positive values are for Aluminum, Calcium, and Sodium, and the weakest is for Iodine. While neither the regression values nor the Sen's values line up well with the time correlation values, each is still useful. A strong correlation to time, such as the one seen for Vanadium, does not necessarily mean that the regression, or Sen's slope, will be similar. In the case of Vanadium, the decrease is very strong, but it is not linear. The Sen's slope gives the mean slope between two years, as Vanadium experienced most of its decline early on in the data where the mean slope is less significant. Similarly, the regression value assumes a linear slope, which Vanadium does not exhibit. Thus, the time correlations are a more useful metric by which to determine which elements are decreasing absolutely or increasing absolutely over the sample space as a function of time.

5.4.4 Time Series Plots

Time series and moving averages for all 11 elements are given in Figures 31 through 52.

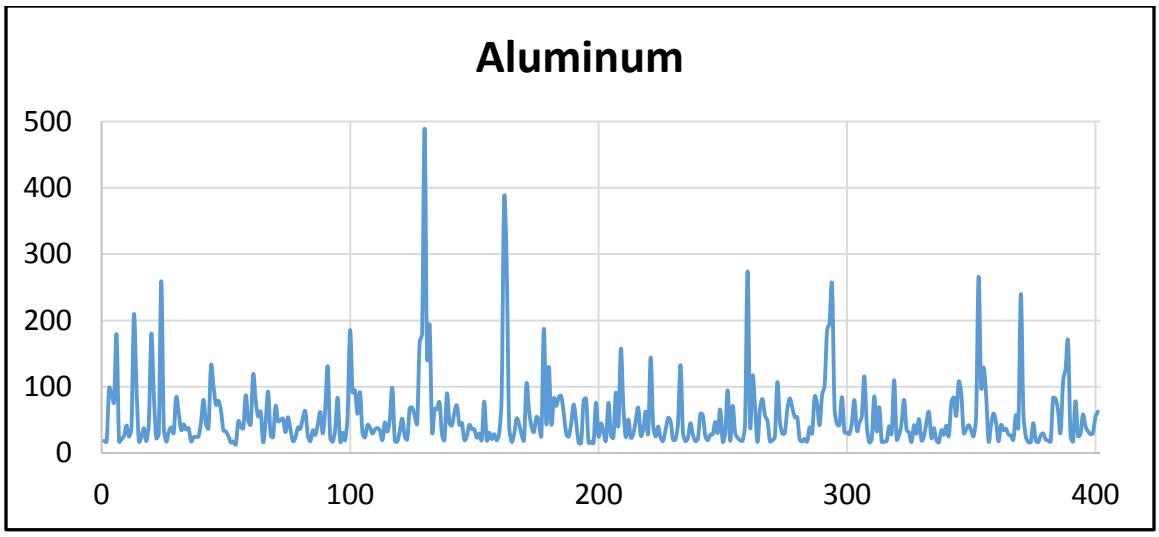

Figure 31 - Aluminum Time Series

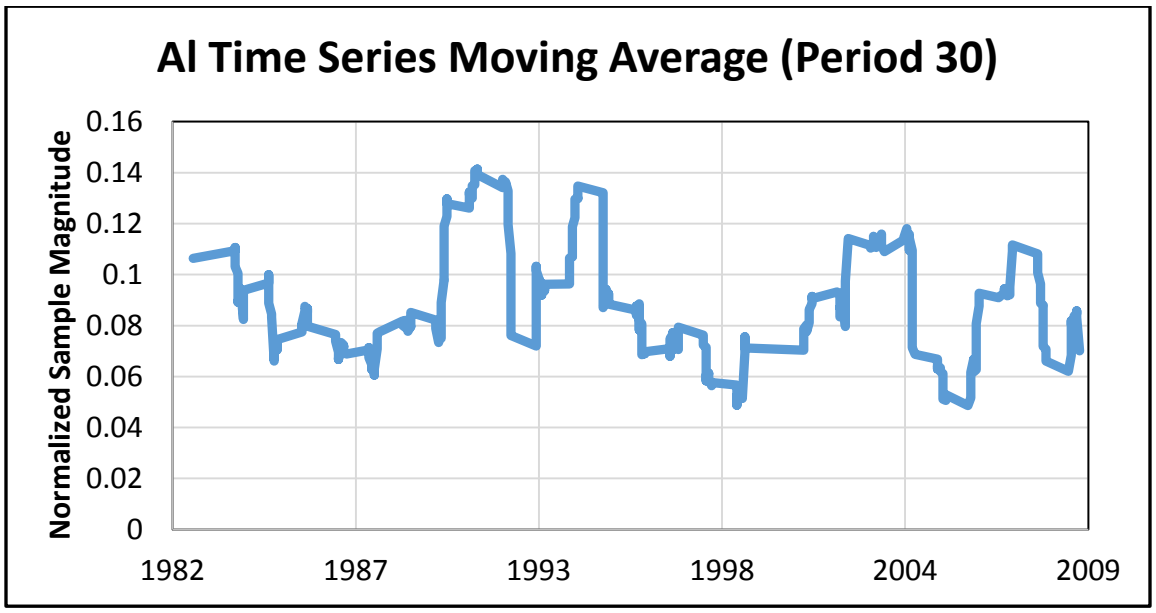

Figure 32 - Aluminum Time Series Moving Average

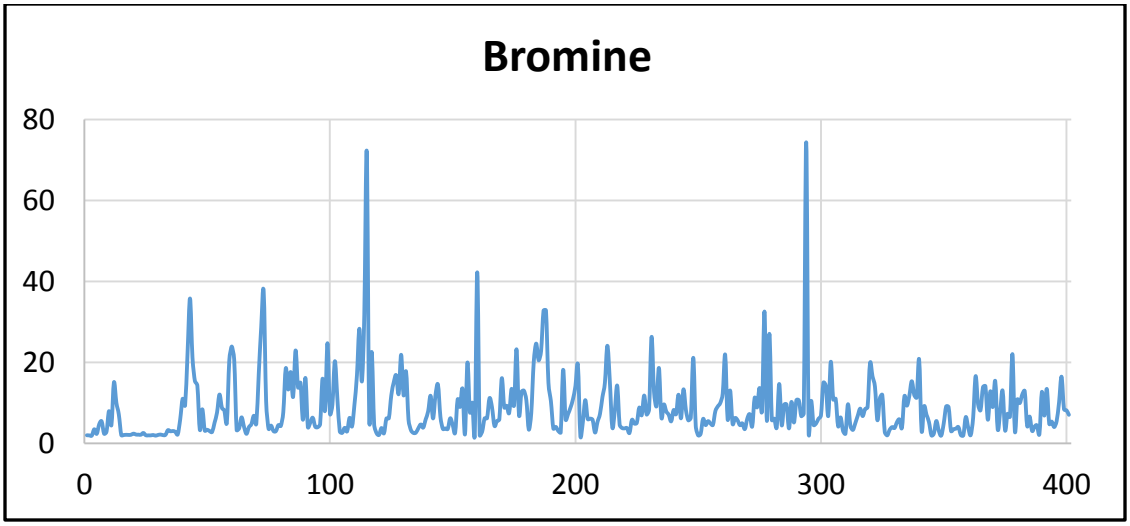

Figure 33 - Bromine Time Series

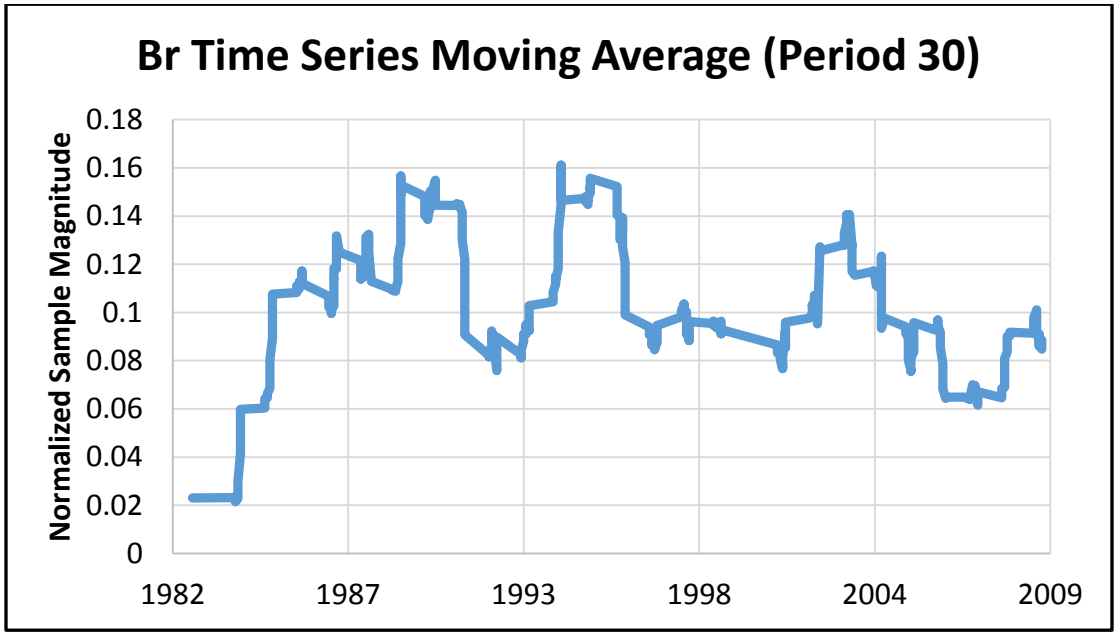

Figure 34 - Bromine Time Series Moving Average

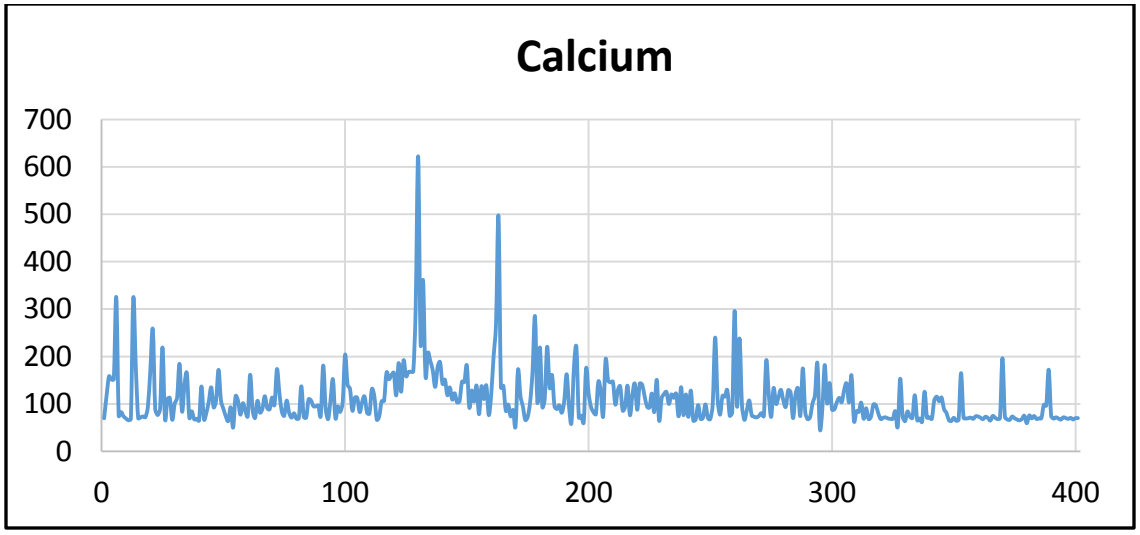

Figure 35 - Calcium Time Series

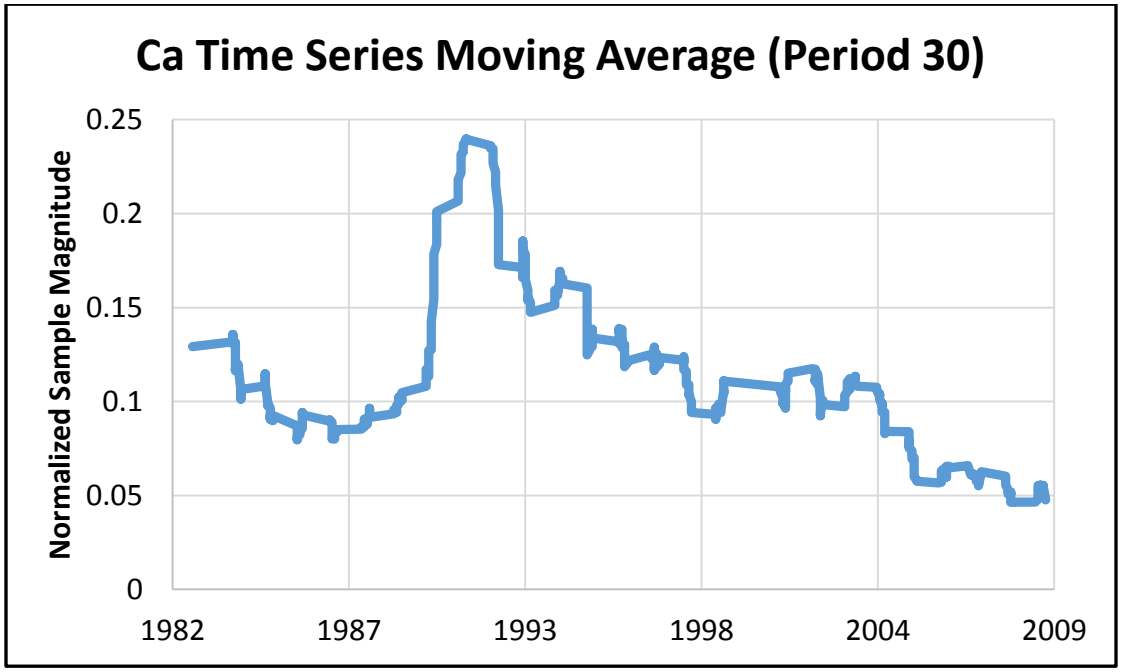

Figure 36 - Calcium Time Series Moving Average

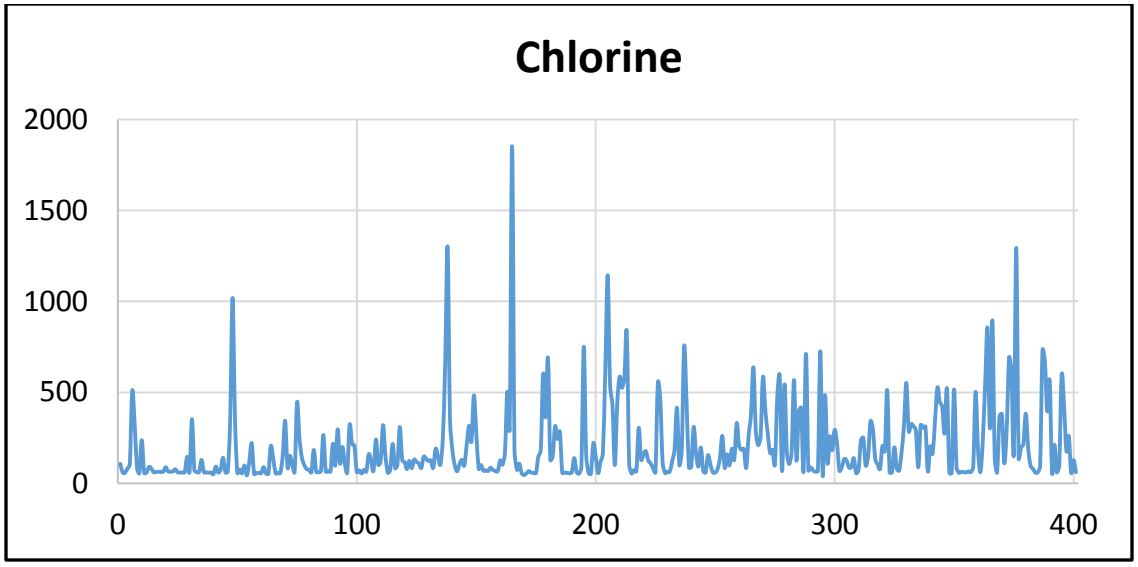

Figure 37 - Chlorine Time Series

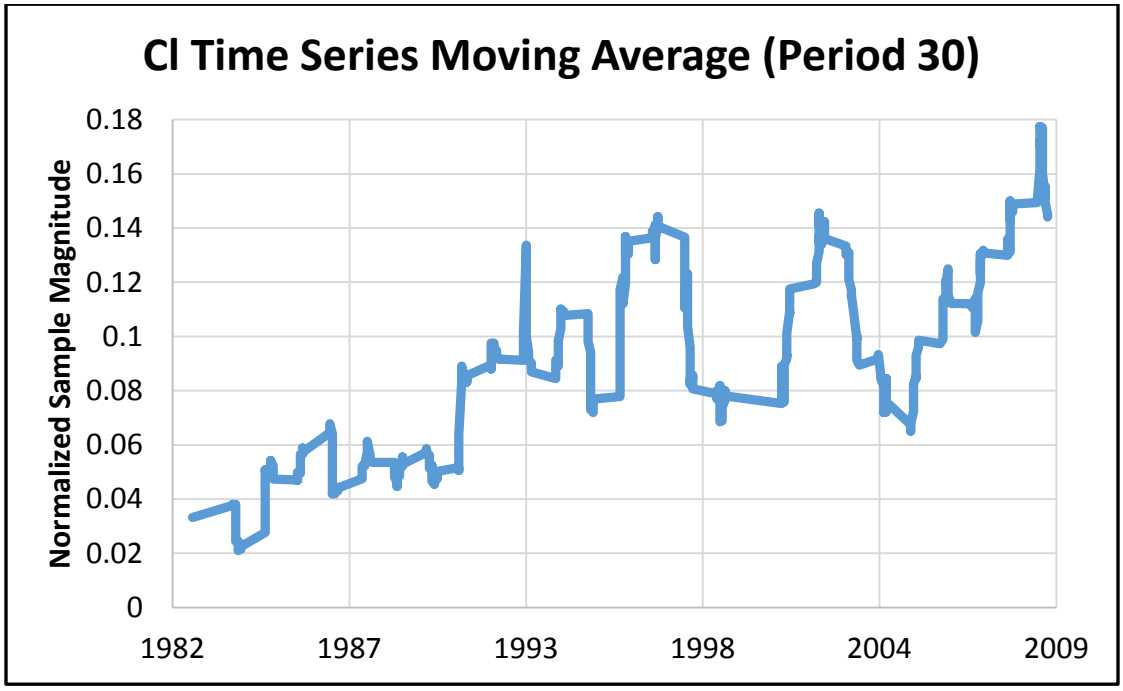

Figure 38 - Chlorine Time Series Moving Average

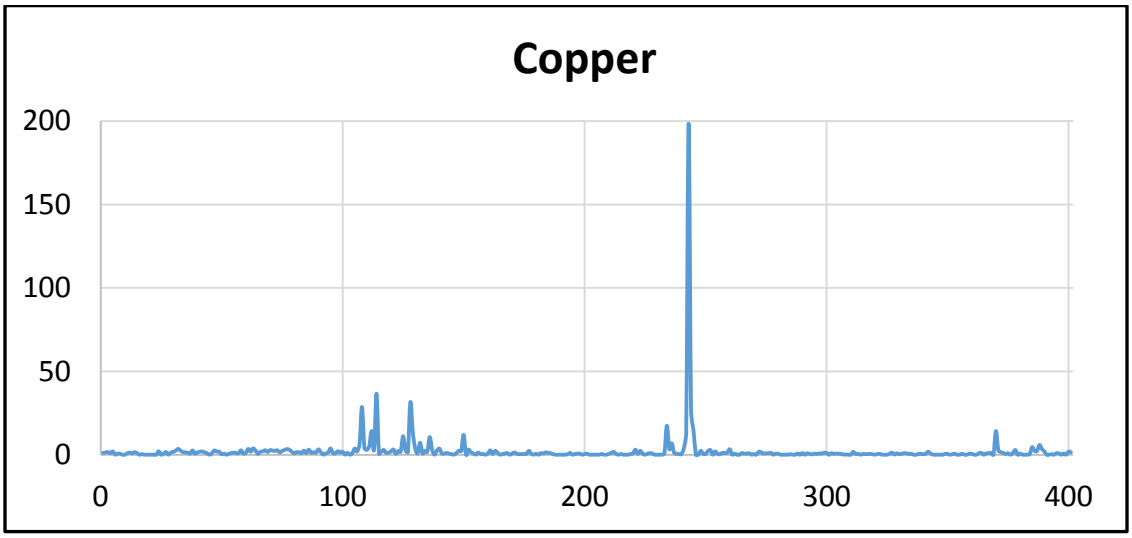

Figure 39 - Copper Time Series

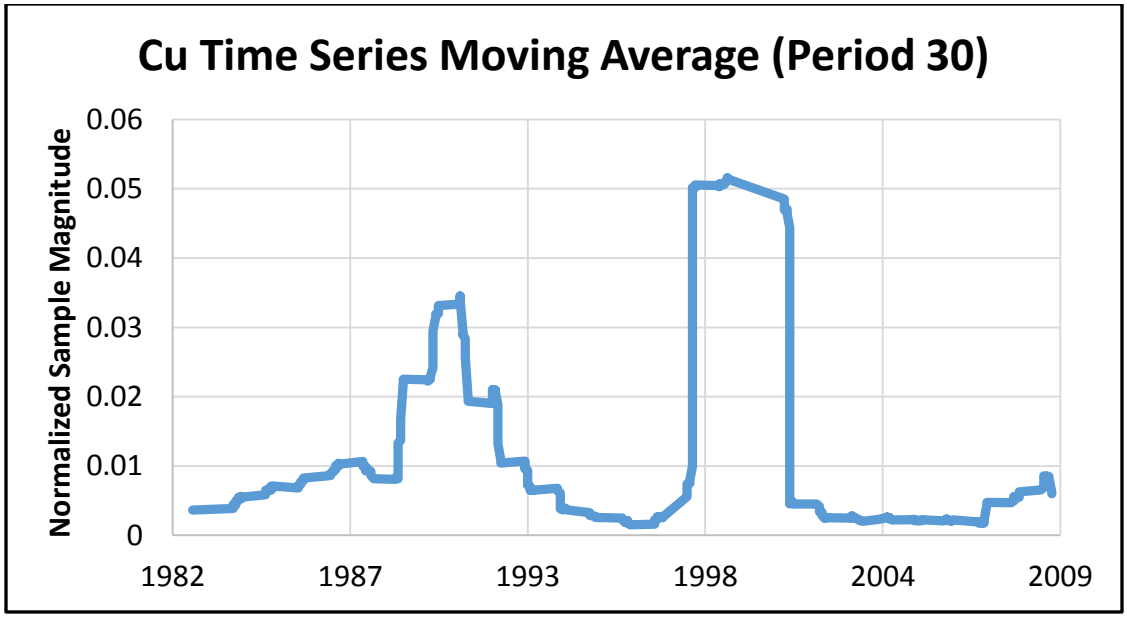

Figure 40 - Copper Time Series Moving Average

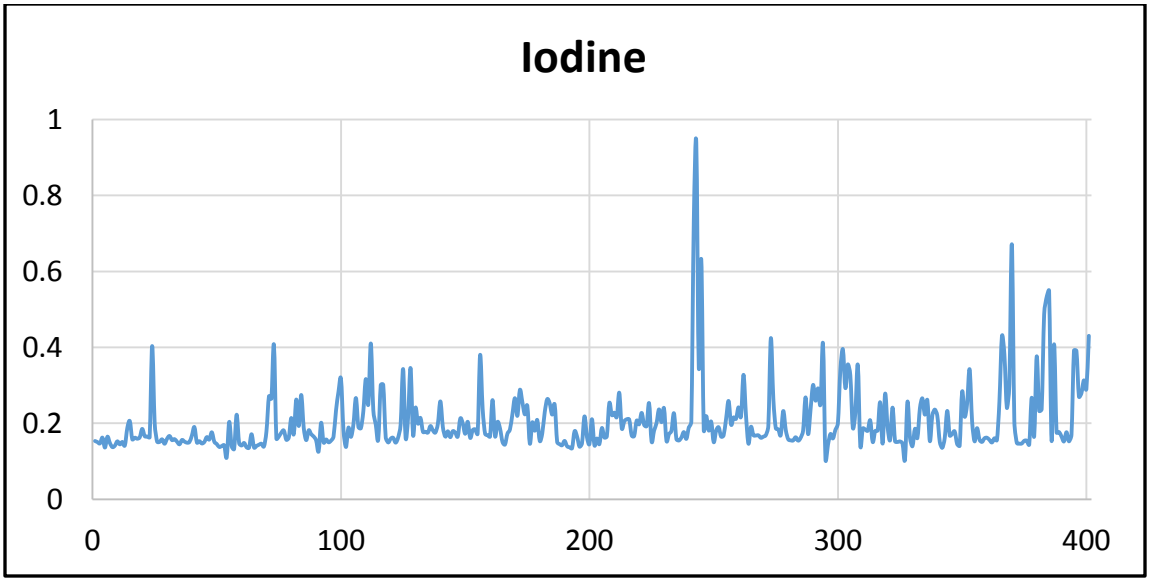

Figure 41 - Iodine Time Series

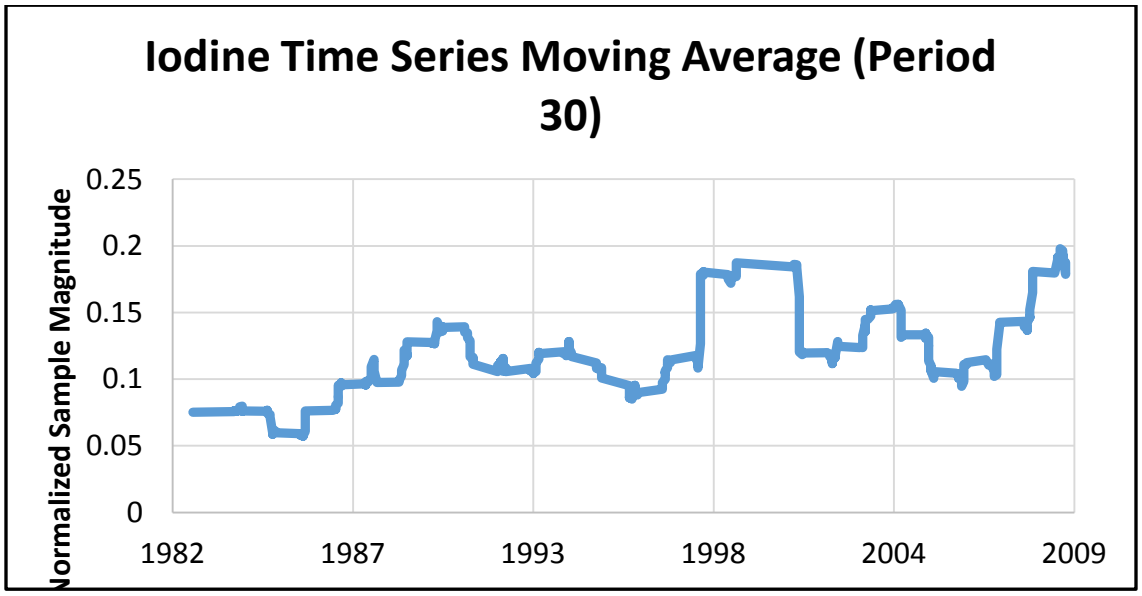

Figure 42 - Iodine Time Series Moving Average

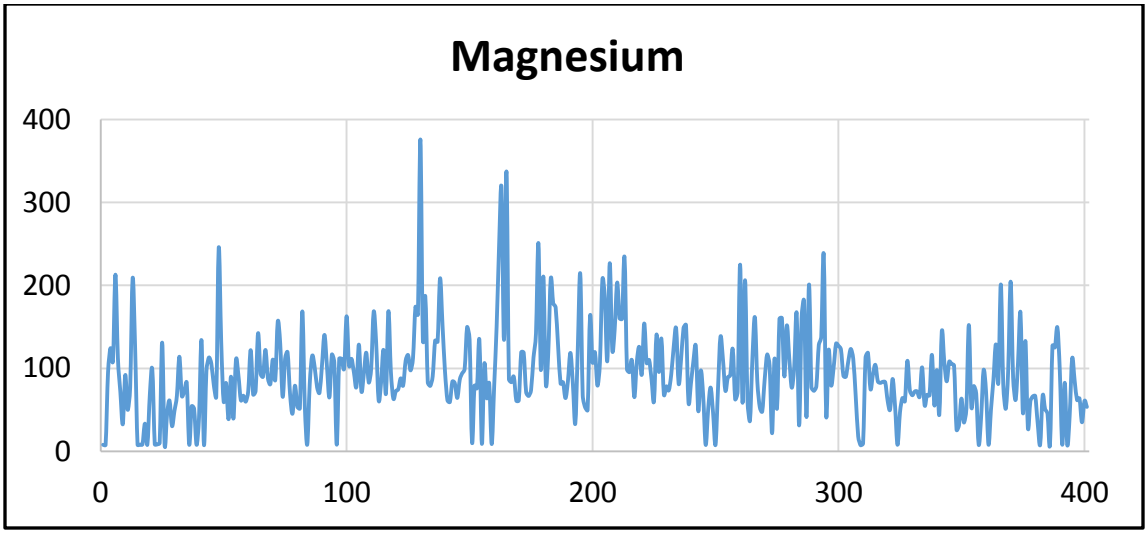

Figure 43 - Magnesium Time Series

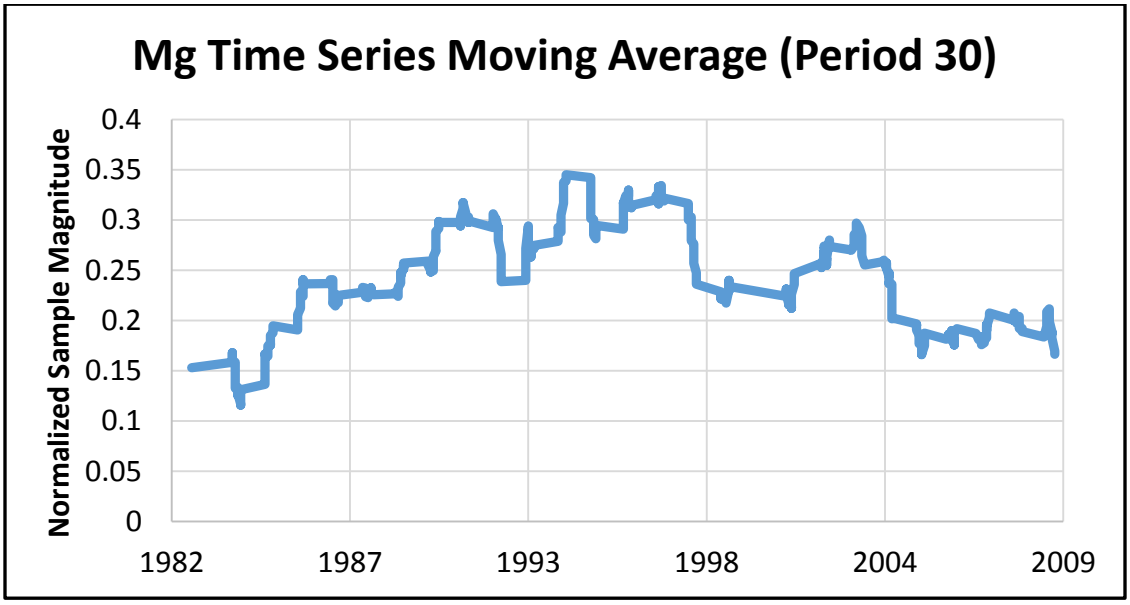

Figure 44 - Magnesium Time Series Moving Average

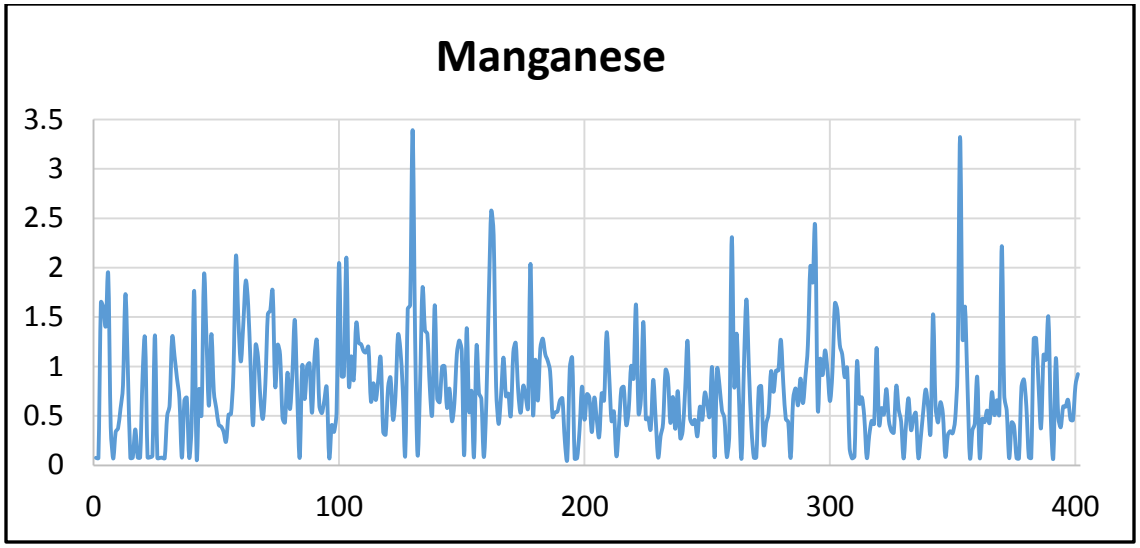

Figure 45 - Manganese Time Series

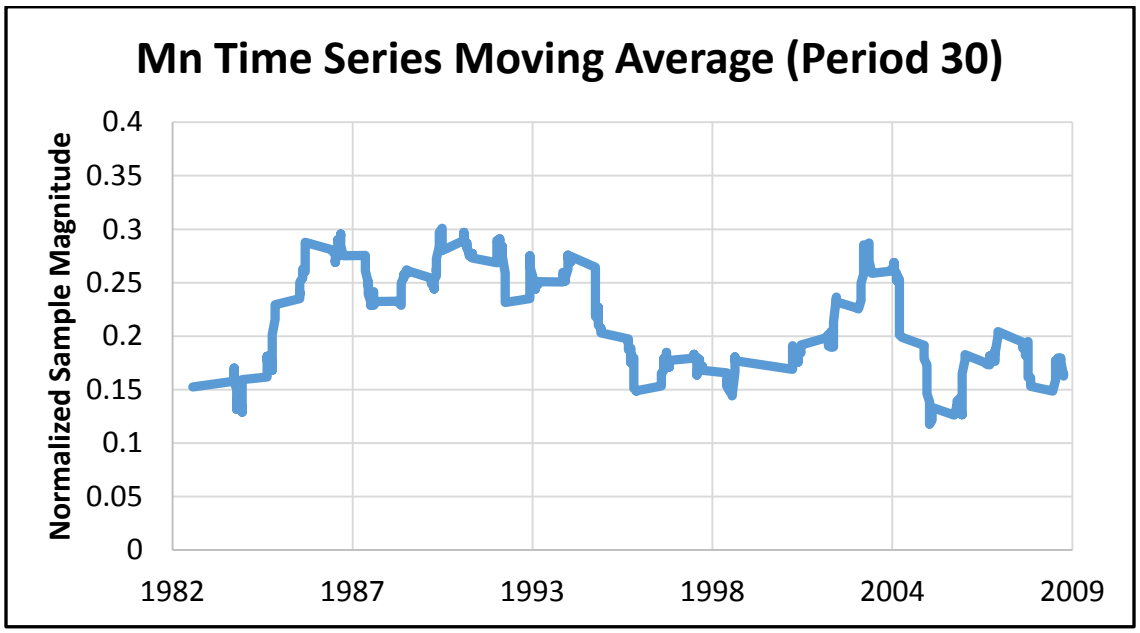

Figure 46 - Manganese Time Series Moving Average

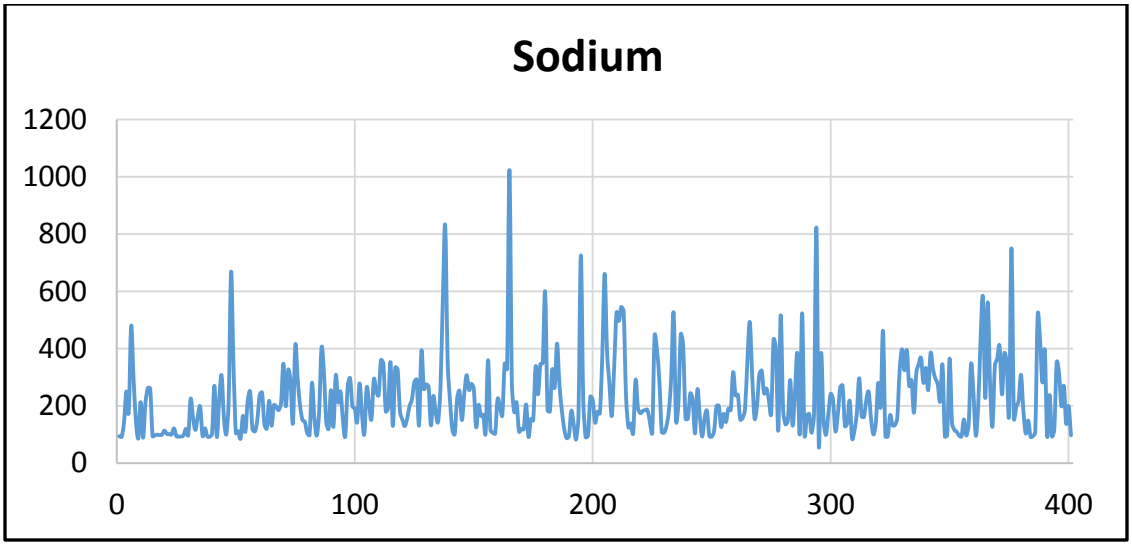

Figure 47 - Sodium Time Series

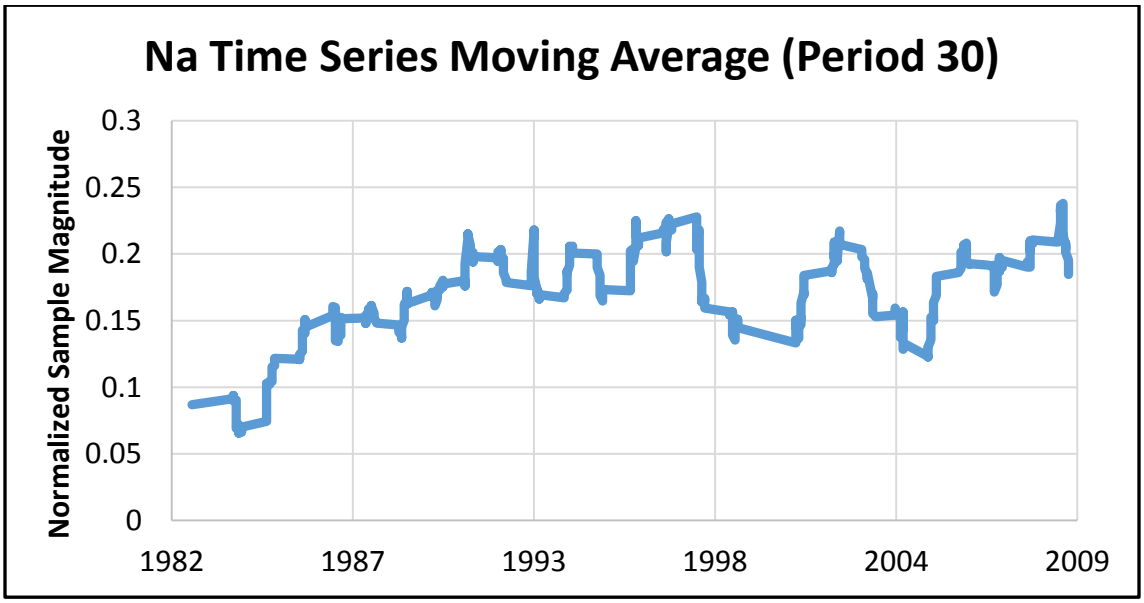

Figure 48 - Sodium Time Series Moving Average

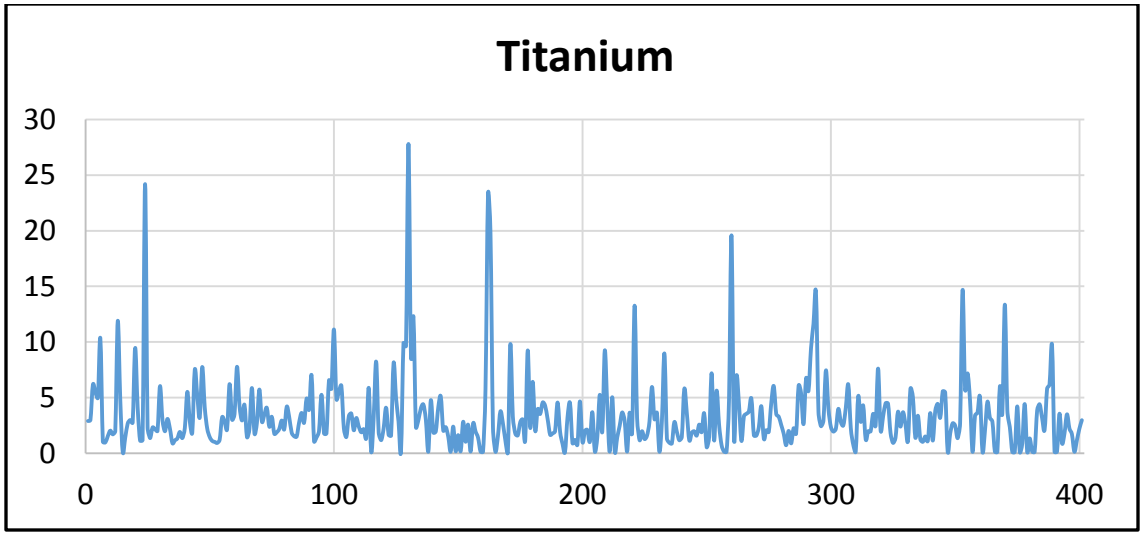

Figure 49 - Titanium Time Series

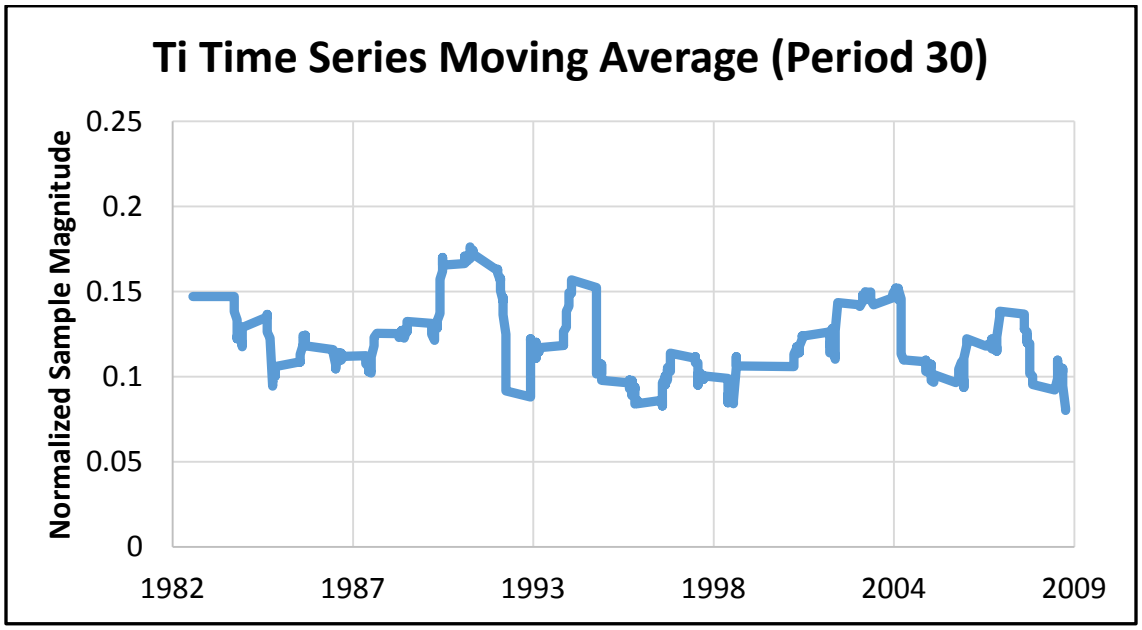

Figure 50 - Titanium Time Series Moving Average

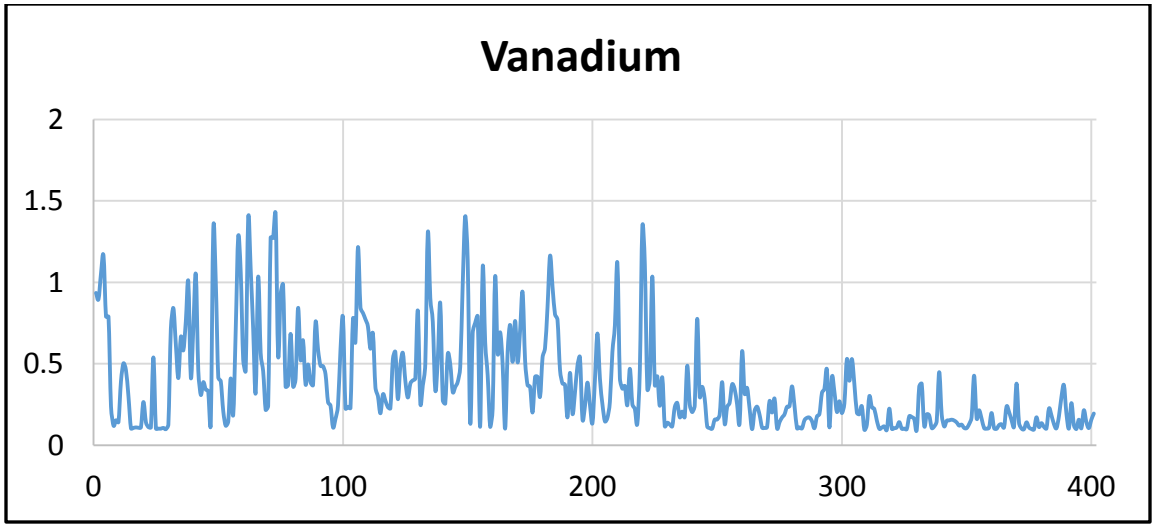

Figure 51 - Vanadium Time Series

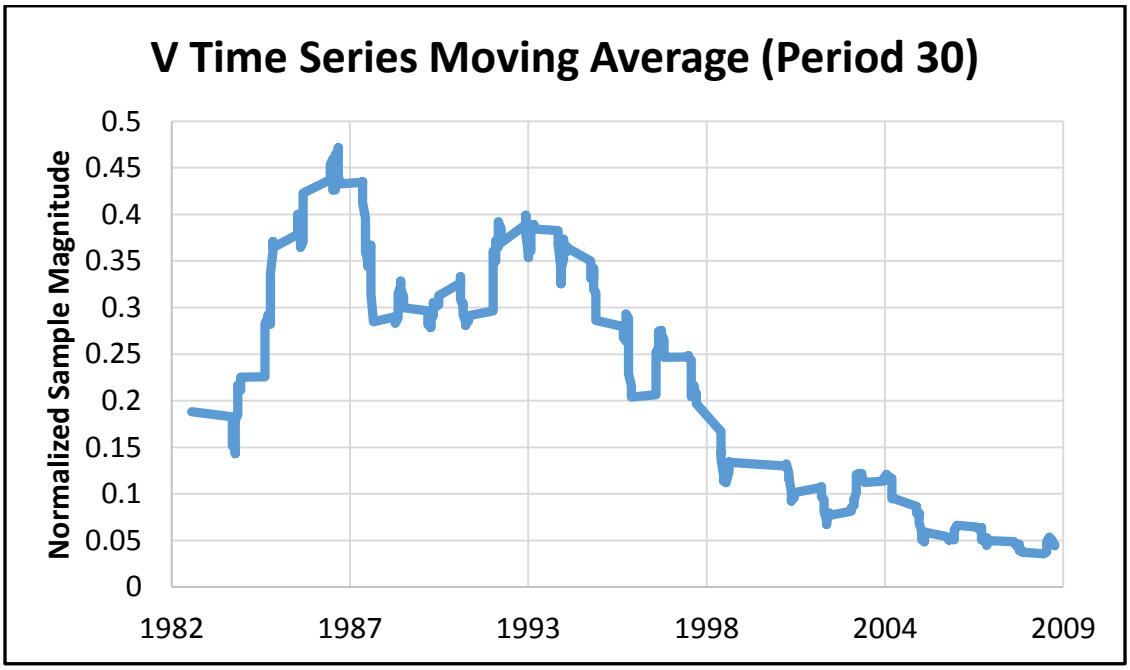

Figure 52 - Vanadium Time Series Moving Average

Summary information from Time Series plots are given below in Table 21:

Table 21 - Notable Time Series Observations

Al	- April 1990, Al, Br, Mg, Mn, and Ti all had large peaks that coincided with each other - No visual trend noted in Al
Br	- Minimum from 1982 through 1984 - No other visible trend - Maximum peaks in April 1989 and April 2002
Ca	- "Bulge" centered around 1990 (1989 through 1993) - Constant levels over the final 4 years of the data
Cl	- Visible increase as noted in the correlation data (and linear regression gives an increase of +0.44 ng/m^3 per sample across the entire set, which has a mean of 200 ng/m^3)
Cu	- There are 3 regions of visible interest for copper: - 1989-1992 (increased concentrations) - 1997-1998 (very large spike over this period) - 2007- end of data (slightly elevated concentrations)
I	- Large spike around 1997 - Slight increase (as noted in the correlation), regression value of +0.0002 ng/m^3 per sample across the entire set with a mean of 0.21 ng/m^3
Mg	- Strong parabolic trend over the sample space - The peak region for this time period is from 1988 through 2003
Mn	- No strong visible overall trend or obvious regions of interest, although a general decreasing trend may be present.
Na	- Visible increase as noted in the correlation values: regression shows +0.1692 ng/m^3 (mean of 230 ng/m^3) per sample over the entire sample space
Ti	- No general trends noted - Region increased concentration from February 2002 through February 2003. This region is interesting because it coincides with a similar increased region in Mn, Al, and V, and the peak coincides with a peak in Mn, Mg, I, Br (very strong), Al and Na.
V	- Strong decrease in the plot. Linear regression shows a decrease of -0.0012 ng/m3 per sample (with a mean of 0.38 ng/m^3). This correlates to ~0.5 ng/m^3 reduction from a beginning average of ~0.6 ng/m^3. Minimum detectable is ~0.1 ng/m^3. Most significant time trend in all the data available. Vanadium is primarily attributed to anthropogenic pollution; it should track with elements like Mercury that fell markedly during this study [Cole & Steffen, 2010].

5.4.5 Climatological Correlations

The following results include some correlations between elements and climatological information, believed not to be seen elsewhere (Tables 22 and 23). This section includes correlations between the elemental data with snow, ice, temperature, Cl/Na, Mg/Na, and wind speed. Ice, Snow, and Temperature trends can be seen independently in the Appendix in Figures 92, 93, and 94.

Table 22 - Time and Temperature Correlations

Element and Ratio	Correlation to Temperature	Correlation to Time	Notes
Cl	0.41	0.56	- Spearman's Rank Correlation with Time = 0.64; - Very significant time trend - Significant correlation to temperature
Na	0.32 Insignificant	0.20 Insignificant	- Spearman's Rank Correlation with Time = 0.23; - No significant correlation to either time or temperature
Mg	0.18 Insignificant	-0.43	- Evident negative correlation with time
Cl/Na	0.41	0.78	- Extreme significance to time -Evident correlation with temperature
Mg/Na	-0.11 Insignificant	-0.51	- Significant negative correlation with time

Table 23 - Ice, Wind, and Snow Pearson Correlations

	Winter Arctic Ice Cover	Yearly Arctic Ice Cover	Winter Northern Hemisphere Snow Cover	Yearly Northern Hemisphere Snow Cover	Winter Mean Wind Speed	Yearly Mean Wind Speed
Al	0.07	-0.01	-0.43	-0.23	0.19	0.48
Br	0.02	0.03	-0.30	-0.20	-0.46	0.19
Ca	0.35	0.36	-0.49	-0.31	-0.08	0.29
Cl	-0.61	-0.59	-0.04	0.01	0.26	0.26
Cu	0.19	0.14	-0.14	-0.11	-0.12	-0.05
I	-0.32	-0.45	-0.22	-0.20	0.33	0.20
Mg	0.00	0.03	-0.40	-0.09	-0.17	0.32
Mn	0.18	0.14	-0.27	-0.04	-0.28	0.27
Na	-0.48	-0.44	-0.24	-0.12	0.02	0.32
Ti	0.23	0.11	-0.27	-0.19	0.05	0.37
V	0.64	0.74	0.19	0.09	-0.71	-0.03
Cl/Na	-0.63	-0.65	0.12	0.13	0.45	0.13
Mg/Na	0.59	0.58	-0.23	-0.01	-0.32	0.00

Noteworthy items in the correlation results are as follows:

- Vanadium is strongly correlated to ice cover; Vanadium has been decreasing steadily while ice has been decreasing, and Vanadium is the only element strongly correlated to wind speed.
- No elements or ratios are strongly correlated to snow cover.
- Chlorine and Sodium are inversely correlated to ice cover, likely because the predominant source of both is wind blowing over the open water. Surprisingly, neither are strongly correlated to wind speed.
- Cl/Na is inversely correlated to ice cover. This is likely caused by 2 independent factors: 1) Cl/Na tends to decrease as the ocean becomes iced over as can be seen in the Cl/Na results in Chapter 6, and 2) the pollution that scavenges the Chlorine while ignoring the Sodium has been decreasing over the timespan of this data.
- Mg/Na is correlated to ice cover, possibly for reasons described in Chapter 2.

Splitting the Chlorine vs. Sodium scatterplot into light/dark months gives the following information (Table 24), including a breakdown of the scatterplots between light and dark months:

Table 24 - Light vs. Dark Months

Statistical Measure	January/February Cl vs. Na	March/April Cl vs. Na
Pearson Correlation	0.94	0.81
Regression Slope	1.33	0.54
Nonparametric Slope Estimate	1.65	1.10

Chlorine and Sodium are seen in this table to be more strongly correlated together during dark months, as can be seen in the preceding table. This is likely due to Chlorine being scavenged more readily once the artic sunrise occurs. The split can be visualized in the following Figures 53-55.

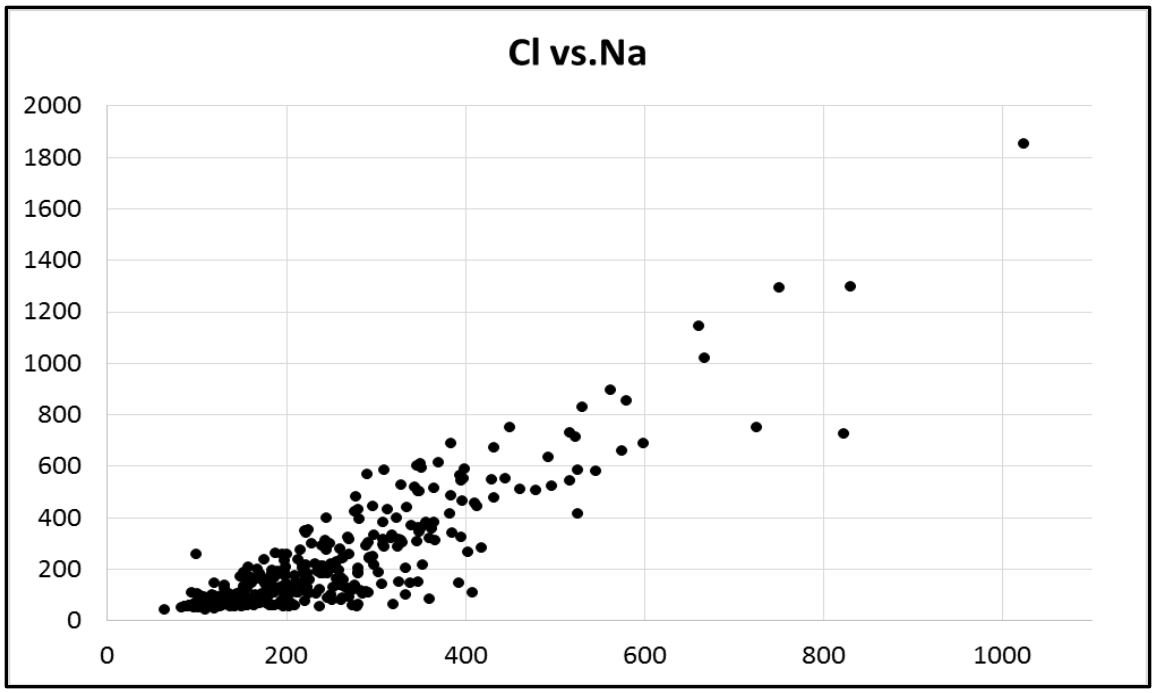

Figure 53 - Cl vs. Na Scatterplot (repeat)

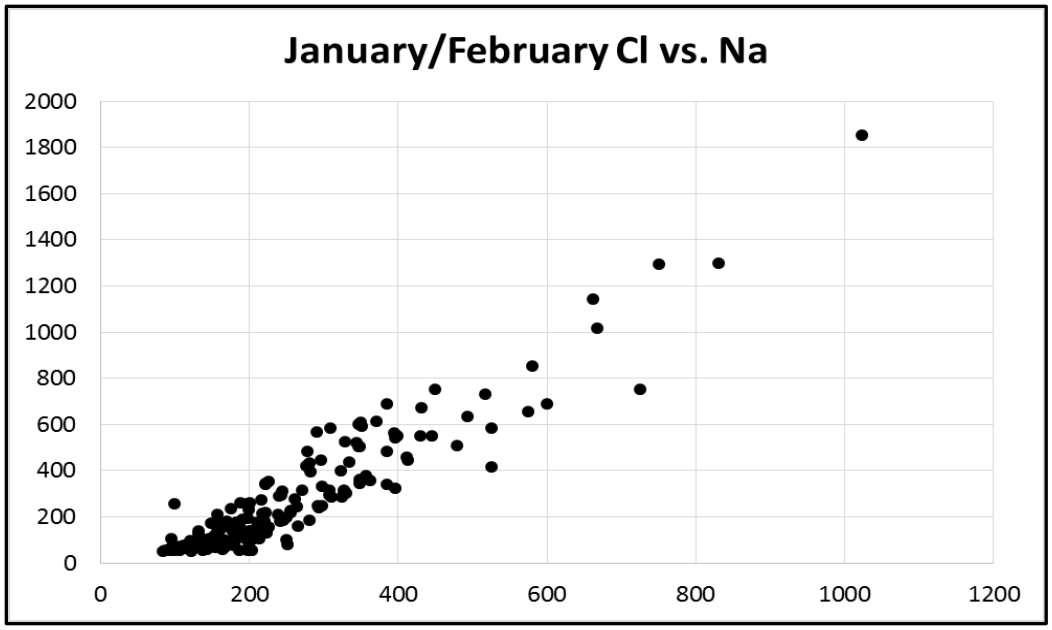

Figure 54 - Cl vs. Na Dark Months Scatterplot

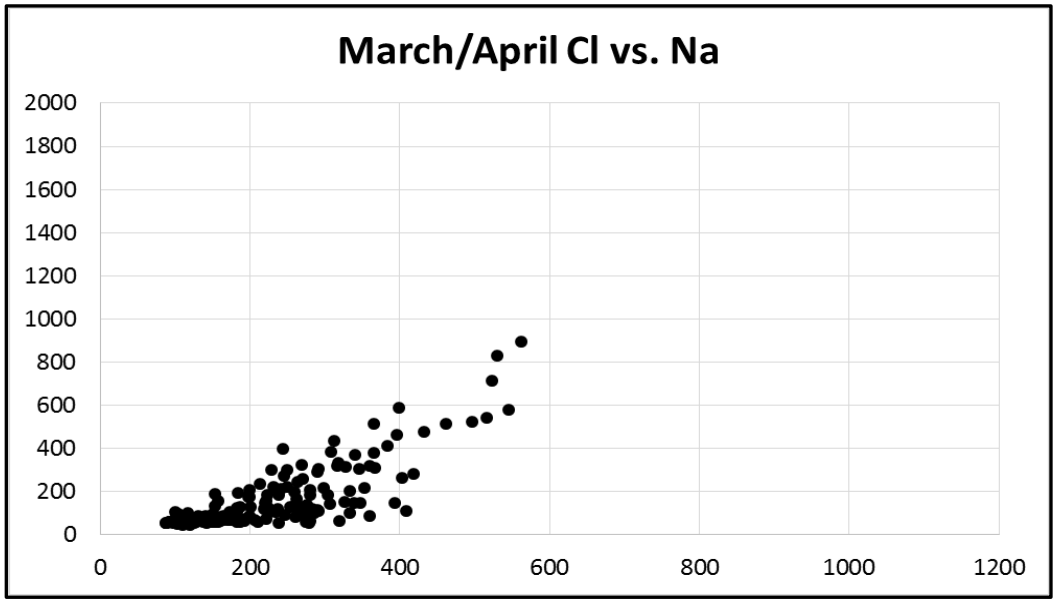

Figure 55 - Cl vs. Na Light Months Scatterplot

6. Miscellaneous Analytical Methods

This section includes analytical methods that have been used in other research. There is some debate as to the applicability and relevance of some of these methods, but they are performed on the data set at hand and results are compared to other research for both affirmation and validation of the data set.

6.1 Enrichment Factor Calculations

Several decades of research found that a useful method of tracking pollution and other potentially unnatural contributors to the Arctic aerosol involves using enrichment factors [Heidam, 1985; Landsberger et al., 1990]. A reference material is first selected, then elements are determined to be “enriched” relative to sea or crustal reference elements using a statistical correlation. Deviations from the enrichments are assumed to be due to pollution or other anthropogenic causes.

6.1.1 Enrichment Factors

The elemental concentration data of both the earth’s crust and seawater needed for enrichment factor calculations historically used data from two particular sources in most literature which are Wedepohl [1967]; and Bowen

[1966]. [Ping, 1996; Basunia, 2002; Landsberger et al., 1990]. Both sources are more than 45 years old, so a more recent reference, the CRC Handbook of Chemistry and Physics, is used to compare with the Wedepohl and Bowen data. The CRC data is identical to the Bowen data for both sea and crustal components. Although the reference cited in the CRC Handbook is not Bowen itself, Bowen is likely either the source of the CRC data or the Bowen data is taken from another common source. The values from Bowen (CRC) and Wedepohl are given in Table 25 as percentages by mass: mg/kg is used for crustal elements and mg/L is used for sea components. To convert the CRC seawater data into a percentage, the g/L for seawater (also taken from Bowen) is approximately 1.03E3 g/L for the range of temperatures of concern in the oceans. Thus the mg/L is converted to mg/g from the given mg/L. Wedepohl data is included in this table primarily because some research [Landsberger et al., 1990] exclusively uses Wedepohl for crustal component composition.

Table 25 - Crustal Elemental Composition

Element	Concentration as % of crust	Wedepohl Crustal Data for Comparison	Concentration as % of seawater	Wedepohl Sea Data for Comparison
Aluminum (Al)	8.2E+0	7.8E+0	1.9E-7	1.0E-7[(2)(3)]
Bromine (Br)	2.4E-4	2.9E-4	6.5E-3	6.5E-5
Calcium (Ca)	4.2E+0	2.9E+0	4.0E-2	4.0E-2
Chlorine (Cl)	1.5E-2	3.2E-2[(3)]	1.9E+0	1.9E+0
Copper (Cu)	6.0E-3	3.0E-3[(3)]	2.4E-8	2.0E-7[(2)(3)]
Iodine (I)	4.5E-5	5.0E-5	5.8E-6	5.0E-6
Magnesium (Mg)	2.3E+0	1.4E+0	1.3E-1	1.3E-1
Manganese (Mn)	9.5E-2	6.9E-2	1.9E-8	4.0E-7[(3)]
Sodium (Na)	2.4E+0	2.5E+0	1.1E+0	1.1E+0
Titanium (Ti)	5.7E-1	4.7E-01	9.7E-8	1.0E-7
Vanadium (V)	1.2E-2	9.5E-03	2.4E-7	2.0E-7

[(1)] All tabulated data from CRC [Lide, 2000] except Wedepohl [1967]

[(2)] Wedepohl only gives the ionic concentration for these two elements; overall, sea data is similar between Wedepohl and Bowen/CRC

[(3)] Significant difference between CRC/Bowen and Wedepohl

The decision to use an enrichment factor from either the sea or from the earth's crust would ideally be based on statistical data determining the correlation between elements in this research, but instead the grouping in Table 26 is used for ready comparison to previously published research. It is well known that Sodium and Chlorine are strong sea components, so any elements with a strong correlation to Sodium and Chlorine will likely be a sea component rather than a crustal component. The strongest crustal elements for correlating other "crustal" elements are typically considered to be Aluminum and Titanium, but Silicon and Iron can also be used [Heidam, 1985; Lawson & Winchester, 1979]. For example, Bromine, Carbon, and Iodine are not good for crustal component enrichments due to influence from sea and anthropogenic sources, but maybe useful to calculate sea salt excess levels.

Although this study incorporates Iron from the CABM data in Section 7, only Aluminum and Titanium are considered herein as they are both available to compare in other studies and are in the NAA data themselves. There are arguments to made for Titanium [Heidam, 1985], as well as Aluminum [Landsberger et al., 1990; Shelley et al., 2014]. Some studies have commented that Titanium did not correlate as expected with other crustal elements such as Aluminum [Basunia, 2002]. The choice of which element to use ultimately depends on sample element availability, calculated correlation to other elements in the sample, and specific application and other undefined study considerations.

Titanium and Aluminum (and Iron) are seen to be the strongest elements

correlated together in this particular study (correlation coefficient of >0.9). Previous studies [Landsberger et al., 1990] binned the inclusive 11 elements as can be seen in the following table; the same groupings are applied to the enrichment factor calculations herein.

Table 26 - Enrichment Factor Bases

Crustal	**Anthropogenic**	**Sea**
Al	**V** (enriched against Crustal components)	**Na**
Ti	**Br** (enriched against Sea components)	**Cl**
Ca	**Cu** (primarily anthropogenic; enriched against crustal components)	**I** (normally binned as Sea, but correlated primarily to Copper)
***Mn**		
***Mg**		

* Manganese and Magnesium are Crustal, Anthropogenic, and Sea components. They are enriched, however, only against crustal components to be consistent with other literature.

Once the elements are binned into one of three categories: Sea, Crustal, or Anthropogenic (Table 26), the calculations for enrichment factors are calculated as follows [Lawson & Winchester, 1979]:

$$EF(x) = \frac{\left(\frac{X}{C}\right)_{Aer}}{\left(\frac{X}{C}\right)_{Ref}}$$

where:

EF(x) = enrichment factor of element “x,”

X = element being enriched (aerosol sample or reference), and

C = concentration of the reference element, also aerosol sample.

6.1.2 Enrichment Factor Results

The enrichment factors results are shown below using Aluminum as the basis of enrichment (Figure 56). These enrichments are also be calculated against Titanium for comparison (Figure 57). Aluminum, however, tends to be a stronger trace element and should give more consistent results.

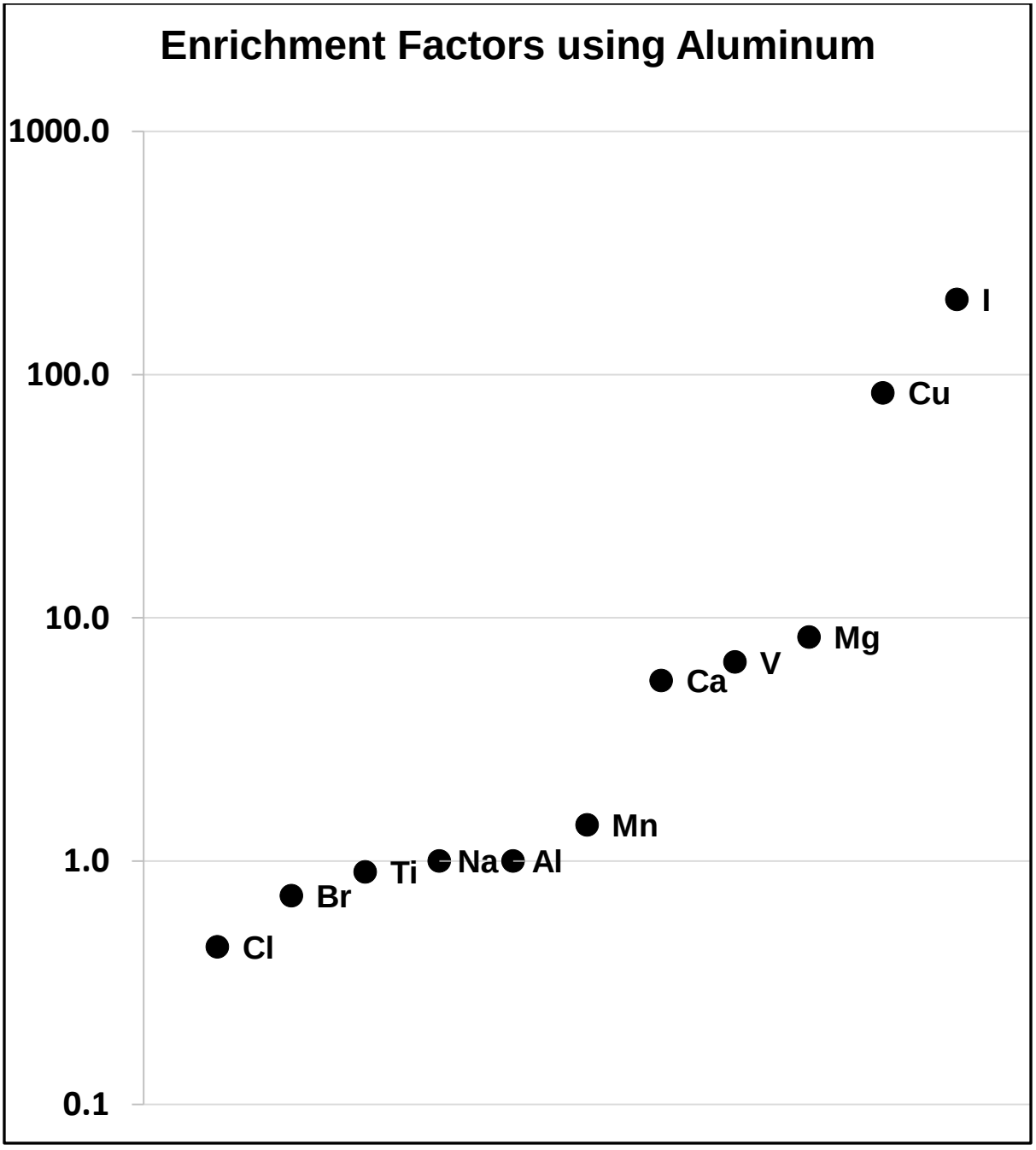

Figure 56 - Enrichment Factors using Aluminum

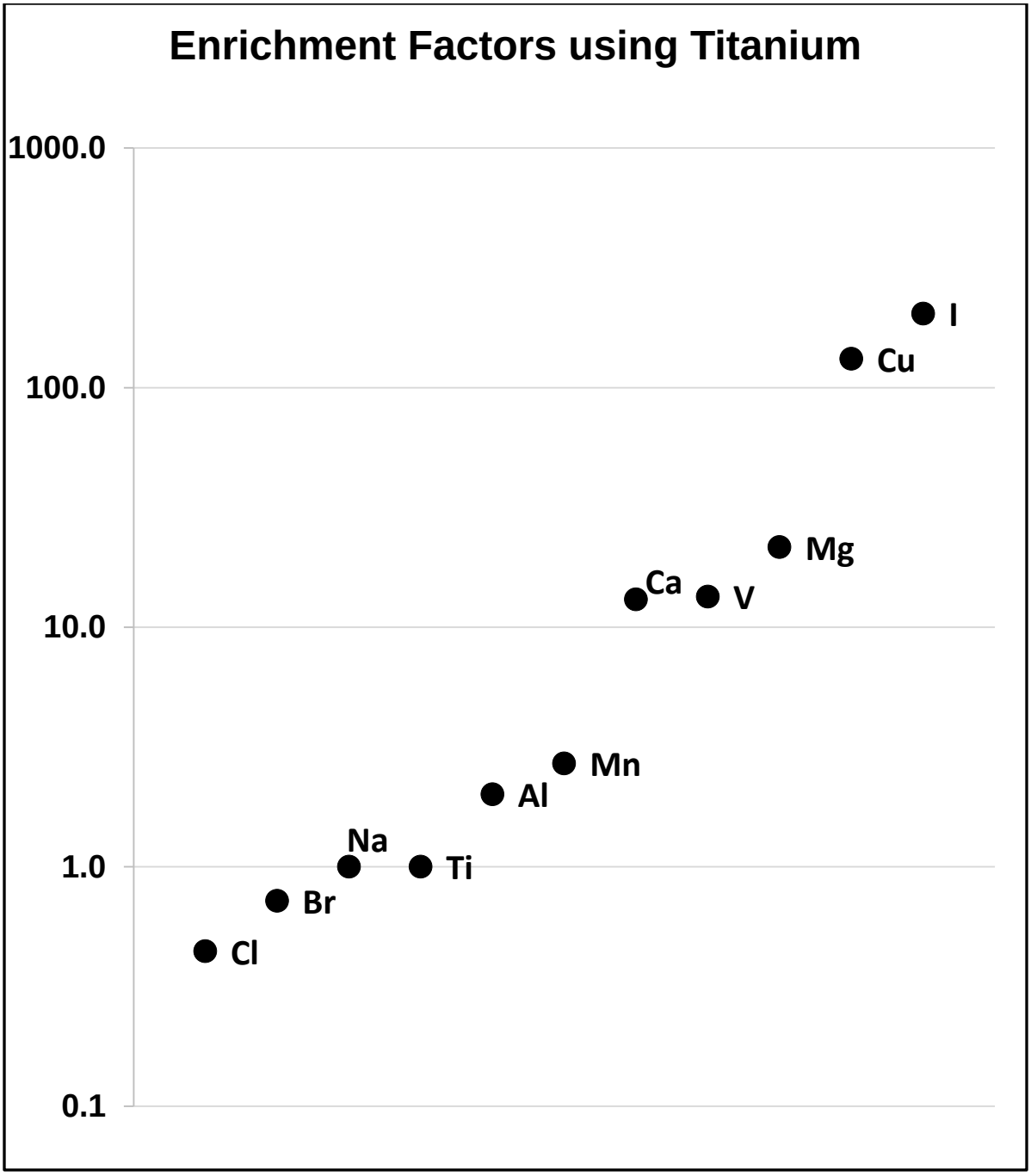

Figure 57 - Enrichment Factors using Titanium

For reference and comparison, Table 27 shows results next to values from two comparable studies.

Table 27 - Enrichment Factor Comparison

Element	Enrichment Factor with Aluminum	Enrichment Factor with Titanium	Enrichment Factor from Ref 1 with Aluminum against global averages from Ref 2	Enrichment Factor using Aluminum for Alert 1985 data in Reference 3
Aluminum (Al)	**1.0**	2.0	1.0	1
Bromine (Br)	**0.7**	0.7	1.3	11
Calcium (Ca)	**5.5**	13.1	2.3	4
Chlorine (Cl)	**0.4**	0.4	0.1	1
Copper (Cu)	**84.1**	131.8	573	N/A
Iodine (I)	**203.5**	203.5	615	1000
Magnesium (Mg)	**8.3**	21.6	N/A	N/A
Manganese (Mn)	**1.4**	2.7	2.9	3
Sodium (Na)	**1.0**	1.0	1.0	1
Titanium (Ti)	**0.9**	1.0	2.8	3
Vanadium (V)	**6.6**	13.4	7.1	8

Reference 1 [Mason, 1966]
Reference 2 [Basunia, 2002]
Reference 3 [Landsberger et al., 1990]

6.2 Excess Concentrations

Excess concentrations are similar in concept to enrichment factors. An elemental component is considered to be in “excess” if its contribution is greater than the expected contribution from natural sources (the sea or the earth’s crust).

6.2.1 Excess Bromine

An excess amount of a chemical such as Bromine, Vanadium, or Manganese, all determined to be an indicators of anthropogenic pollution [Rahn, 1981; Landsberger et al., 1990; Biegalski et al., 1997]. For this study, only Bromine is considered as it is related to previous related work. The Excess concentration for an element is given by the following equation, which can be used with either Aluminum or Titanium [Rahn, 1981], where the Aluminum denominator and Aluminum multiplier would be replaced with Titanium:

$$X_{non_{crustal}} = X_{aer_{total}} - \left(\frac{X}{Al}\right)_{crustal} * Al_{aer}$$

Similarly, for Bromine, taken as a sea component [Landsberger et al., 1990]:

$$Br_{excess} = \left(\frac{Br}{Na}\right)_{sea} * Na_{aer}$$

This “excess Bromine” equation could be used for other elements as needed.

6.2.2 Excess Concentration Results

Excess Bromine results show an average across the sample space to be **1.34** (Figure 58). Note that this is just for the winter average for 1980 through 2010, as the remainder of the seasons are not included in this study. (CABM Section 7 data gives an average Excess Bromine across the entire year and set as **0.85**.) The entire data is shown below for excess Bromine, followed by a point of each yearly average (Figure 59).

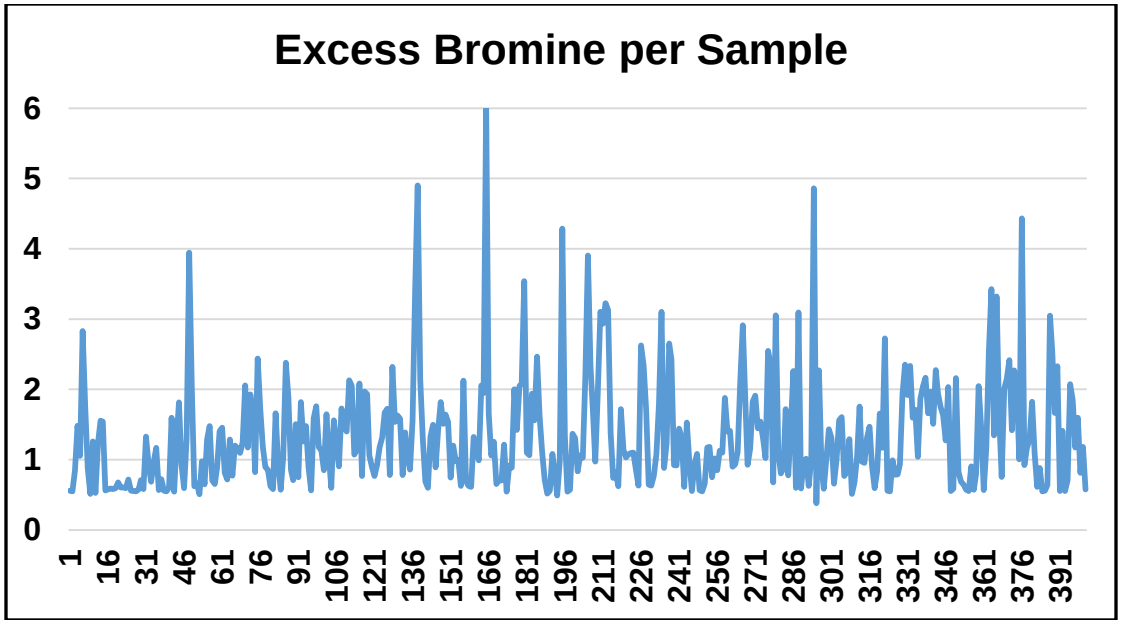

Figure 58 - Excess Bromine per Sample

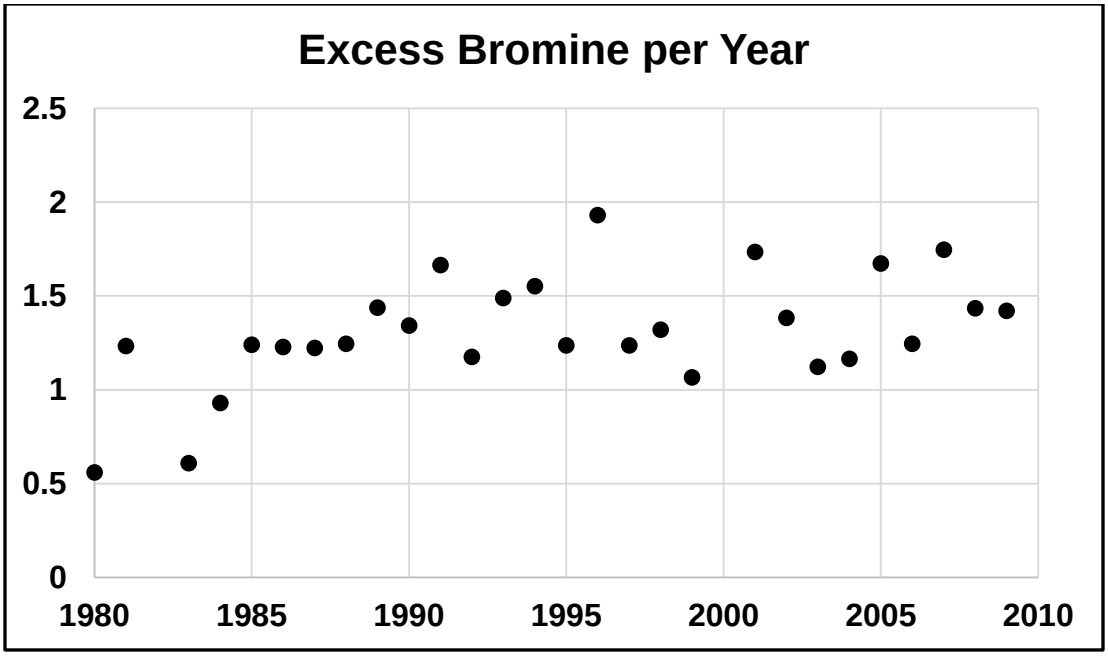

Figure 59 - Excess Bromine per Year

One final study [Landsberger et al., 1990] includes actual Alert data and excess Bromine concentrations for March 1985, a month which this study includes. However, the daily samples therein as compared to the weekly samples herein are not similar in either absolute Bromine concentration levels (in the stated study the Bromine levels recorded in ng/m^3 were much higher) or in the levels or even percentage of excess bromine across that month. The reasons for the disparity are unknown. Additionally, a study of Kevo, Finland data concluded that there was no excess Bromine present in the samples [Basunia, 2002].

Due to the issue with detectability in the samples included in this study (see Table 10), the relevance of the data is indeterminate regarding excess Bromine here.

6.3 Elemental Ratios

Similar to “excess” concentrations that relate aerosol concentrations to the known concentrations in the crust or the sea, ratios of other elements can give clues as to anthropogenic contributions.

6.3.1 Mn/V and xMn/xV

The non-crustal Vanadium (xV) component of the aerosol samples can be taken as a ratio against the non-crustal Manganese (xMn) component to provide a tracer of pollution sources in the Arctic. Excess concentrations of each can be compared against each other, and the difference between Eurasian aerosol xMn/xV ratios has been seen to be ~5 times greater than the ratio in North American sources. [Rahn, 1981] The difference between the average enrichment factor for an element over a data set and the excess of that element may be extremely small. The ratio can be either positive or negative. The average Mn/V ratio in this study is calculated to be **2.57** (for winter), and for comparison, a similar study [Ping, 1996] calculated the winter ratio to be **1.74** whereas spring was calculated to be **2.72**. The similarity in these values are reassuring.

When considering only non-crustal versions of each element, the average xMn/xV ratio for the data in this study is calculated to be **-2.4** as shown in Figure 60. The yearly average of xMn/xV per Year is shown in Figure 61.

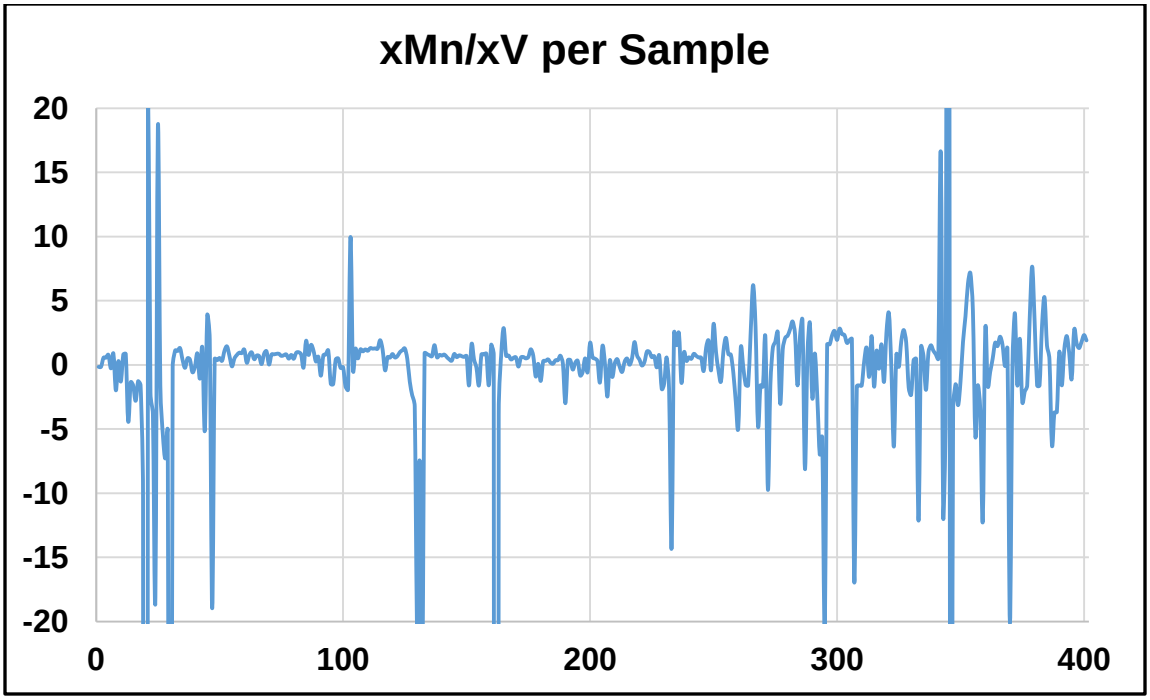

Figure 60 - xMn/xV per Sample

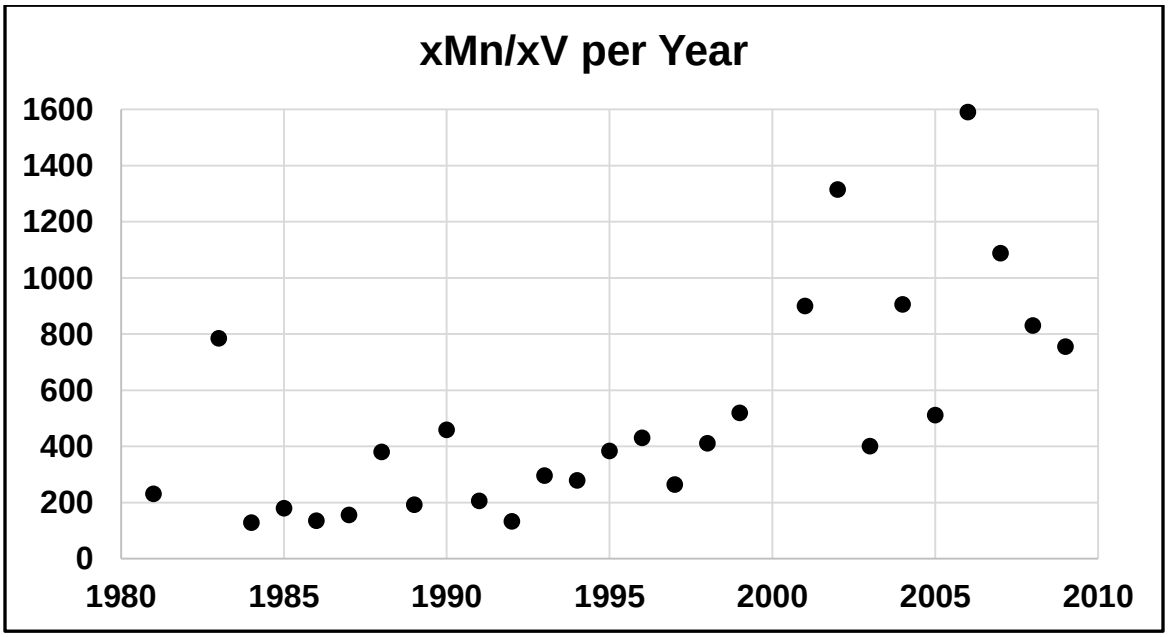

Figure 61 - xMn/xV per Year

For context, a study using similar data [Ping, 1996] results in a mean winter ratio of xMn/xV of **0.7**. Other previous work provides summer and winter xMn/xV geometric means for both summer and winter calculated from data taken at Kevo, Finland. The summer mean provided is **3.76**, and the winter mean provided is **1.45**, providing a seasonal variation in this ratio. [Basunia, 2002] These values do not mesh well with the values calculated herein, nor with each other, even though the stated method of calculation is the same, and the crustal ratios therein are similar.

Other work notes that xMn/xV decreased at Barrow Alaska from 1976 until 2008 (the end of the study) by about 60% [Quinn et al., 2009]. The data presented herein do not support such a decrease. Rather, if any significant change is apparent at all, it is a mild increase that strengthened around the year 2000. The increase of the xMn/xV may give strong indication of the decrease of vanadium over the past two decades.

6.3.2 Cl/Na and Mg/Na Ratios

Chlorine and Sodium are the strongest sea components in the Arctic aerosol. The Cl/Na aerosol ratio tends to be much stronger when wind is direct from open water, as evidenced by High Arctic summer data [Maenhaut et al., 1996]. This is apparent also in Alaskan aerosol data where it is noted that direct airflow from the pacific pushes the Cl/Na from a relatively low value overland

towards the higher seawater ratio of 1.73 [Shaw, 1991]. The ratio is always lower than that of seawater at all locations and in all studies.

The mechanisms that drive the Cl/Na aerosol ratio from 1.73 in the seawater to something much lower over land and ice appear to have one main driver. That driver appears to be volatilization of Chlorine by air pollution. One possible pollutant that may remove chloride from aerosol sea salt is H_2SO_4. The Cl/Na ratio has been inversely correlated to SO_4 in previous literature. Increased pollution has been seen explicitly in some data in conjunction with depressed Cl/Na ratios. [Shaw, 1991]

All other factors being equal, higher pollution should then correlate with a reduced Cl/Na ratio in the Aerosol sample. Increased wind from open water, or increased open water for a consistent wind, should also show an increase in the Cl/Na ratio. Decreasing pollution with time and decreasing ice cover with time are both occurring in the Arctic, and both then combine to result in a significant increase in Cl/Na with time in the Alert samples. In the next table, it can be seen that Cl/Na drops significantly around the arctic sunrise. This indicates that perhaps pollution is less of a factor than wind and ice cover. However, the monthly trend in the CABM Section 7 data is that although depressed around the polar sunrise, the ratio returns in June to the value that it remains at until the following March.

Additionally, the Cl/Na data herein, when correlated to Sulphate data in the CABM Section 7 data, produces an inverse correlation of -0.4, and a negative

correlation of -0.4 with NH_4 as well. These numbers reinforce the relationship described elsewhere [Shaw, 1991] and also reinforce the Sulphate trends related to air quality regulations from the 1970s [Samset, 2018; Voiland, 2009].

There is less of an understanding of the Mg/Na. The Mg/Na ratio has been noted to be higher over ice than near open water [Maenhaut et al., 1996]. Thus, an increase of wind from open water, or a lessening of ice in the upwind direction of the wind (wind at Alert is predominantly East to West) should correlate with a decrease of the Mg/Na ratio. The Cl/Na and Mg/Na trends are shown in Table 28.

Table 28 - Cl/Na and Mg/Na trend Review and Results

	Cl/Na	**Mg/Na**
Alert, Canada (This Work) - Winter	Mean: 0.92 January: 1.11 February: 1.04 March: 0.80 April: 0.60 Not known how this trend changes beyond the 4 months shown.	Mean: 0.42 January: 0.42 February: 0.39 March: 0.41 April: 0.47 No monthly trend seen in this data
Antarctica [Hara et al., 2014] - November through January	Coastal Mean: ~0.4 Landlocked Mean (Over Ice): ~0.1 Extreme dependence on proximity to open ocean.	Coastal Mean: ~0.3 Landlocked Mean: ~0.3 No apparent dependence on proximity to open ocean.
Kevo, Finland [Basunia, 2002] - All Seasons	Mean: 0.41	N/A
High Arctic [Maenhaut et al., 1996] -Summer	<2µm Over Ocean: 1.01 <10µm Over Ocean: 1.37 <2µm Over Ice: 0.40 <10µm Over Ice: 0.88 Reference Sea Level: 0.48 Reference High Altitude: 0.68	<2µm Over Ocean: 0.10 <10µm Over Ocean: 0.10 <2µm Over Ice: 0.30 <10µm Over Ice: 0.43 Reference Sea Level: 0.21 Reference High Altitude: 0.25
Alaska [Shaw, 1991] - March through April	All Data: 0.81 Chinook (overmountain): 0.94 Barrow Data: 0.87 Arctic Air Intrusions: 0.68 Sea-Salt Spikes: 0.53	N/A
Global Averages in Seawater and Crust [Lide, 2000]	Crust: 0.00 Seawater: 1.73 All aerosol ratios are less than the Seawater ratio.	Crust: 0.96 Seawater: 0.12 All ratios are less than the crustal ratio and tend to reach a minimum at the seawater ratio.

In addition to the tabulated data above, when considering yearly-averaged data, the following information can be extracted:

Cl/Na Yearly Average Pearson Correlation: **0.77**

Mg/Na Yearly Average Pearson Correlation: **-0.51**

These statistically-significant trends with time are likely again to be due to changing yearly ice coverage and changing pollution levels. The following plots demonstrate these trends more visually (Figures 62 and 63):

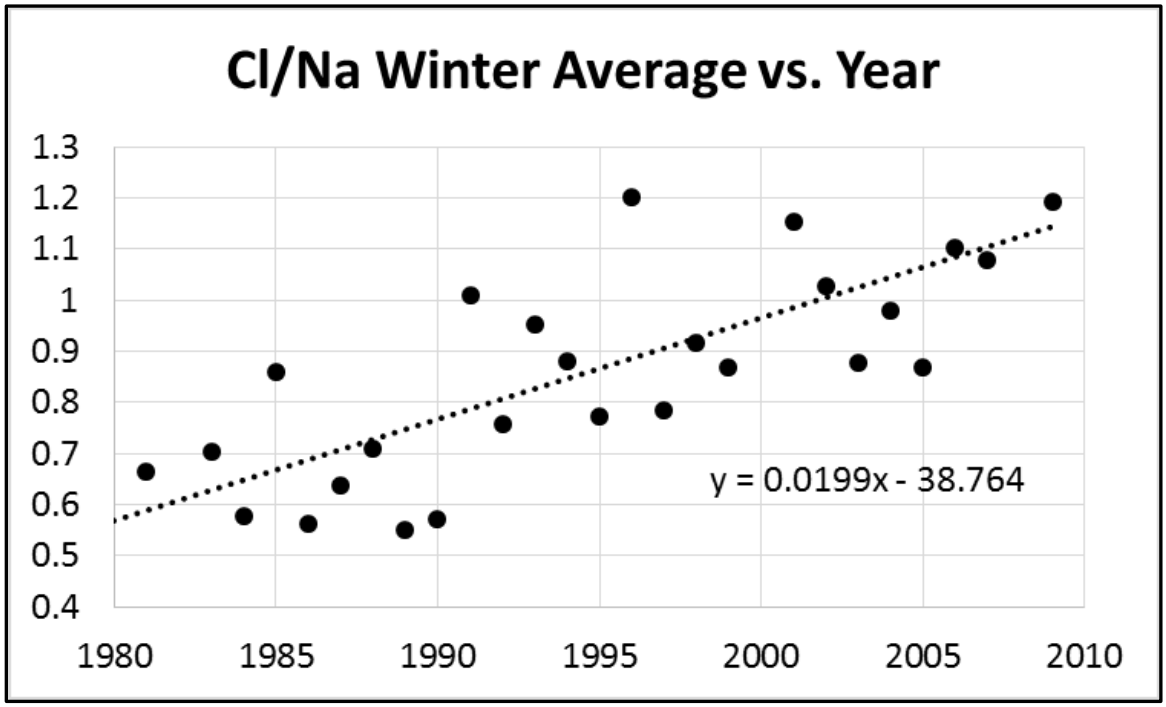

Figure 62 - Cl/Na Winter Averages by Year

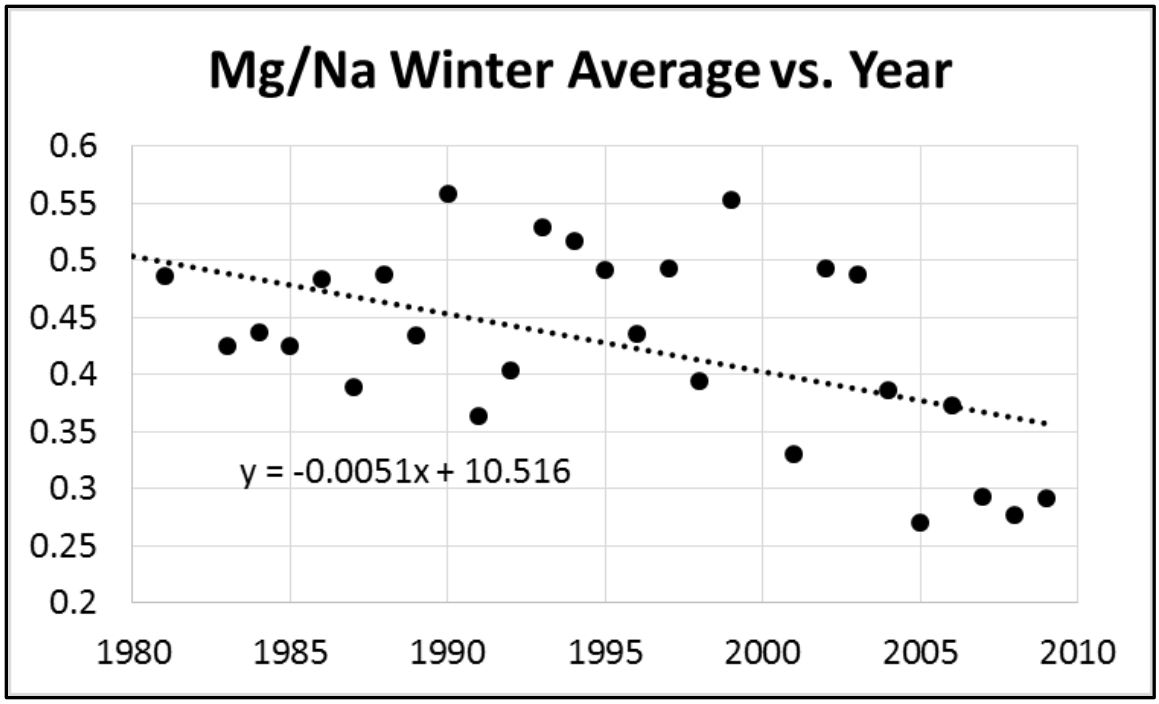

Figure 63 - Mg/Na Winter Averages by Year

The Sen's slope for these two figures are as follows:

Cl/Na: **-0.002**

Mg/Na: **-0.012**

Note that the Cl/Na Sen's slope is contrary to the linear regression slope, whereas the Mg/Na Sen's slope is both the same magnitude and the same direction as the regression line. See Section 5 for reasons why the Sen's slope may be significantly different than the linear regression slope.

When comparing the time-results here with the correlation results for Chlorine vs. Sodium, including the non-parametric slope result, a strong case can be made that: 1) Chlorine and Sodium are highly correlated; 2) a Cl/Na time trend is definitive (if not taking into account the Sen's slope value) and likely due to changing ice cover as well as pollution levels, and 3) the Mg/Na decrease with time is both definitive (including the Sen's slope result) and likely due primarily to changing ice coverage.

7. Canadian Arctic Baseline Measurement Data

To further validate and reinforce the work done herein through NAA on Alert data, the Canadian Aerosol Baseline Measurement (CABM) website is consulted. The CABM site includes data from 1980 through 2006. From the CABM website, located at: https://www.canada.ca/en/environment-climate-change/services/climate-change/canadian-aerosol-baseline-measurement-program.html: “The Canadian Aerosol Baseline Measurement (CABM) Program operates a network of stations that measure the properties of atmospheric aerosols. This observational program tracks long-term changes in aerosol concentration and composition over Canada. Aerosols tend to influence the climate system through their impact on the radiative energy balance and the hydrological cycle.” “CABM measurements help scientists understand the connections between aerosol chemical composition, aerosol radiative properties, cloud formation, and precipitation. These measurements are also used to validate regional and global climate models.”

7.1 CABM Data Specifics

The CABM data is derived from pieces of the same samples used for the NAA analysis, although the methods used to determine concentrations are water extraction Ion Chromatography (IC) and acid extraction Inductively-Coupled

Plasma Atomic Emission Spectra (ICP/AES). As the methodology of composition determination is different, with different capabilities, the resulting information is different in species, and, in some cases, absolute composition.

CABM data runs from 1980 through 2006, and includes every week of every year, unlike the NAA data which includes only winter data. It does not include, however, Titanium, Iodine, or Vanadium, all of which are important for this study. The additional components in the CABM data include: Sulphate, Iron, Nitrate, Lead, Ammonium, and Methanesulphonic Acid (MSA). For long-term trending, the lack of post-2006 data is not helpful as the NAA data runs through 2010, but monthly trends can be gleamed and correlations to these additional components can be made.

The CABM data set includes multiple elements that are identical to those analyzed using NAA. The CABM set is much larger, as it includes analysis of essentially weekly samples throughout the year, as well as additional elements and compounds. Due to the limited seasonal data available in the NAA results, only the sample data corresponding with the exact samples used for NAA are directly compared. All identical elements are compared over those identical samples to validate the scale and trends of the results.

7.2 CABM Data Comparison to NAA Data

Correlations are used between identical samples, and comparison of means among identical elements and identical samples.

The average monthly temperatures in the CABM data are all a couple degrees lower than the official Alert record (Section 2). This is likely due to the fact that most of the samples were taken in the evening. The mean sample time is 1700, and the median is 1746, hence more than 50% of the samples were collected later than 1746. Table 31 and 32 directly compare the two data sets.

Table 29 - CABM to NAA Correlations

Al/Al	**0.906**
Br/Br	**0.900**
Ca/Ca	**0.540**
Cl/Cl	**0.947**
Cu/Cu	**0.878**
Mg/Mg	**0.768**
Mn/Mn	**0.788**
Na/Na	**0.913**

The element that correlates the least well, Calcium, was gathered with water extraction Ion Chromatography, and incomplete solution is the likely cause of the relatively low correlation. As such, it is likely that the NAA data is more accurate for this element.

Table 30 - CABM Means vs. NAA Means

Element	NETL Mean (ng/m^3)	CABM Mean (ng/m^3)
Al	55.6	54.5
Br	9.00	8.84
Ca	114.8	66.4
Cl	190.4	205.2
Cu	2.28	1.98
Mg	96.4	71.1
Mn	0.78	0.82
Na	221.2	206.4

It can be seen that the data is similar with the exception of Calcium, which has a very different mean between the two sets and whose correlation is surprisingly low (see explanation on previous page regarding water extraction: incomplete solution would result in a lower value for the IC mean value). For the other elements, the correlation is strong between the sets, indicating that there is valid data in both sets. The lower comparisons for Manganese and Magnesium may be due to incomplete digestion of the filter paper for ICP. Statistical information and monthly averages for CABM data is given in Tables 33 and 34. CABM and UT/CABM correlations are seen in Tables 35 and 36, respectively.

7.3 CABM Statistical and Correlation Data

Table 31 - Statistical Information from CABM Data (ng/m^3)

	Cl	Br	N	S	S,non	Na	NH4	MSA
Slope (per year)	2.8E+00	-2.1E-02	9.1E-01	-2.1E+01	-2.1E+01	4.6E-01	-1.6E+00	-7.5E-05
Sope (per sample)	5.7E-05	-9.6E-07	1.5E-05	-4.8E-04	-4.8E-04	7.1E-06	-3.8E-05	-1.5E-06
Mean	1.7E+02	4.5E+00	6.4E+01	6.6E+02	6.2E+02	1.4E+02	7.2E+01	6.0E-03
Gemotric Mean	6.1E+01	1.7E+00	5.0E+01	3.6E+02	3.3E+02	1.9E+02	4.8E+01	3.4E-03
	Pb	**Cu**	**Al**	**Ca**	**Fe**	**Mg**	**Mn**	
Slope (per year)	-3.4E-02	-1.0E-02	-1.2E+00	-4.9E+00	-1.7E+00	-1.5E+00	-2.4E-02	
Sope (per sample)	-7.3E-07	-2.1E-07	-2.1E-05	-6.3E-05	-3.1E-05	-2.7E-05	-4.4E-07	
Mean	1.011696	1.385357	38.16502	128.7804	55.38036	69.84411	0.974183	
Gemotric Mean	0.483891	0.597288	20.0489	63.46643	28.20363	39.79158	0.57648	

Table 32 - CABM Monthly Averages (ng/m^3)

	Cl	Br	N	S	S,non	Na	NH4	MSA
January	3.6E+02	5.5E+00	1.0E+02	1.1E+03	9.9E+02	2.6E+02	1.1E+02	1.5E-03
February	2.7E+02	5.4E+00	9.3E+01	1.2E+03	1.1E+03	2.3E+02	1.2E+02	2.1E-03
March	1.9E+02	1.1E+01	8.8E+01	1.4E+03	1.4E+03	2.1E+02	1.4E+02	3.7E-03
April	1.0E+02	1.5E+01	9.0E+01	1.5E+03	1.5E+03	1.8E+02	1.4E+02	9.4E-03
May	6.7E+01	8.8E+00	8.2E+01	7.8E+02	7.6E+02	9.8E+01	8.1E+01	1.4E-02
June	2.6E+01	1.3E+00	5.3E+01	1.9E+02	1.8E+02	1.9E+01	4.3E+01	8.0E-03
July	3.2E+01	5.4E-01	3.7E+01	8.7E+01	8.2E+01	1.9E+01	2.8E+01	9.8E-03
August	5.6E+01	4.7E-01	3.0E+01	8.1E+01	7.2E+01	3.4E+01	2.4E+01	9.3E-03
September	6.1E+01	5.0E-01	2.1E+01	1.4E+02	1.3E+02	3.8E+01	2.0E+01	7.1E-03
October	1.7E+02	7.1E-01	2.9E+01	3.0E+02	2.7E+02	1.1E+02	2.4E+01	3.6E-03
November	3.7E+02	1.8E+00	5.5E+01	5.0E+02	4.4E+02	2.5E+02	4.5E+01	1.8E-03
December	3.7E+02	3.4E+00	9.3E+01	7.6E+02	7.0E+02	2.7E+02	8.3E+01	1.5E-03
	Pb	**Cu**	**Al**	**Ca**	**Fe**	**Mg**	**Mn**	
January	2.2E+00	1.7E+00	2.2E+01	7.9E+01	3.3E+01	9.5E+01	9.0E-01	
February	2.3E+00	1.6E+00	2.5E+01	9.5E+01	3.4E+01	9.4E+01	9.2E-01	
March	2.2E+00	2.6E+00	2.4E+01	7.0E+01	3.2E+01	8.4E+01	8.9E-01	
April	1.3E+00	1.8E+00	4.2E+01	1.0E+02	5.2E+01	6.9E+01	1.1E+00	
May	4.9E-01	9.4E-01	5.3E+01	1.3E+02	7.1E+01	6.1E+01	1.1E+00	
June	4.3E-01	1.0E+00	2.2E+01	6.8E+01	3.1E+01	2.1E+01	4.8E-01	
July	3.9E-01	1.6E+00	2.0E+01	1.0E+02	3.4E+01	2.8E+01	5.3E-01	
August	2.7E-01	8.3E-01	2.3E+01	1.0E+02	3.7E+01	3.0E+01	5.8E-01	
September	2.7E-01	1.1E+00	8.0E+01	2.9E+02	1.2E+02	9.2E+01	1.7E+00	
October	3.1E-01	8.9E-01	6.8E+01	2.8E+02	1.1E+02	9.5E+01	1.5E+00	
November	5.3E-01	1.1E+00	3.9E+01	1.1E+02	5.4E+01	7.3E+01	8.7E-01	
December	1.4E+00	1.5E+00	3.7E+01	1.1E+02	4.9E+01	8.8E+01	9.7E-01	

Table 33 - CABM Data Correlations

	Cl	Br	N	S1	S2	Na	NH4	MSA	Pb	Cu	Al	Ca	Fe	Mg
Cl	1.00													
Br	0.18	1.00												
N	0.44	0.45	1.00											
S1	0.11	0.57	0.47	1.00										
S2	0.06	0.56	0.44	1.00	1.00									
Na	0.92	0.38	0.59	0.39	0.34	1.00								
NH4	0.06	0.46	0.51	0.89	0.90	0.31	1.00							
MSA	-0.24	0.12	-0.05	-0.02	0.00	-0.23	0.00	1.00						
Pb	0.12	0.26	0.40	0.65	0.65	0.28	0.71	-0.15	1.00					
Cu	0.02	0.06	0.06	0.13	0.13	0.07	0.14	-0.04	0.31	1.00				
Al	0.12	-0.02	0.03	-0.01	-0.02	0.10	-0.06	0.08	-0.02	0.00	1.00			
Ca	0.15	-0.09	-0.03	-0.09	-0.10	0.09	-0.12	0.04	-0.03	0.05	0.87	1.00		
Fe	0.11	-0.05	-0.01	-0.02	-0.03	0.08	-0.06	0.07	-0.01	0.01	0.92	0.95	1.00	
Mg	0.53	0.10	0.31	0.17	0.15	0.51	0.12	-0.09	0.19	0.14	0.77	0.84	0.81	1.00
Mn	0.15	0.02	0.10	0.12	0.11	0.15	0.09	0.05	0.14	0.03	0.89	0.93	0.96	0.85

Table 34 - UT-Austin and CABM Data Correlations

	Al	Br	Ca	Cl	Cu	I	Mg	Mn	Na	Ti	V	N	S	S_non-sea	Pb	MSA	NH4	Fe
Al	1.00																	
Br	0.09	1.00																
Ca	0.68	0.06	1.00															
Cl	0.03	0.11	0.17	1.00														
Cu	0.00	0.03	0.00	-0.04	1.00													
I	0.14	0.19	0.08	-0.04	0.56	1.00												
Mg	0.54	0.26	0.71	0.59	0.00	0.10	1.00											
Mn	0.69	0.15	0.55	0.00	0.03	0.19	0.57	1.00										
Na	0.10	0.33	0.25	0.88	-0.01	0.06	0.66	0.15	1.00									
Ti	0.94	0.06	0.61	0.01	0.00	0.16	0.47	0.63	0.08	1.00								
V	0.18	0.04	0.27	-0.04	0.04	0.14	0.26	0.53	0.08	0.17	1.00							
N	0.23	0.29	0.15	0.49	-0.03	0.16	0.41	0.27	0.58	0.18	0.14	1.00						
S	0.08	0.36	0.19	-0.12	0.04	0.15	0.21	0.41	0.12	0.06	0.64	0.09	1.00					
S_non-sea	0.07	0.35	0.18	-0.17	0.04	0.15	0.17	0.41	0.07	0.05	0.64	0.05	1.00	1.00				
Pb	-0.03	0.03	0.08	-0.02	0.50	0.40	0.12	0.37	0.07	-0.03	0.65	0.11	0.52	0.52	1.00			
MSA	0.20	0.29	0.06	-0.17	0.00	0.10	-0.04	0.20	-0.06	0.17	0.00	0.11	0.20	0.21	-0.07	1.00		
NH4	0.03	0.24	0.14	-0.10	0.04	0.24	0.15	0.44	0.09	0.01	0.70	0.17	0.89	0.89	0.62	0.17	1.00	
Fe	0.94	0.10	0.64	0.00	0.00	0.17	0.48	0.66	0.10	0.92	0.25	0.19	0.16	0.16	0.08	0.24	0.13	1.00
Temperature	0.31	0.00	0.15	-0.07	-0.03	0.03	-0.07	-0.01	-0.06	0.30	-0.27	-0.07	-0.25	-0.24	-0.33	0.39	-0.21	0.32

7.4 CABM Data Usage

Copper and Bromine are predominantly below the limit of detection in the NAA results. For the data that overlapped between both sets, all NAA data is used with the exception of Copper. The remaining CABM data was used for every NAA sample through 2006 (the end of the publically-available CABM data). As such, the total number of samples is reduced from those available in the CABM data, but the number of elements and items analyzed in conjunction with the NETL NAA data is greatly increased from 11 to 17. Although NH_4 and MSA are not purely elemental, Nitrogen, Sulphur, Lead, and Iron are. Two sets of sample data was generated for EPA-PMF: one including MSA and NH_4, and the other without, so it would produce a purely elemental result.

7.5 Insights from CABM Data

Insights from CABM comparison to NAA data are mostly validations and verification of other studies and of the of the NAA data. Particular items include:

- Ca/Cl Much higher in summer than winter [Pacyna & Ottar, 1988], 20x higher in the summer per CABM data.
- Chlorine is 2x higher in the summer than the winter, confirming the trend seen in that same study [Pacyna & Ottar, 1988].
- Ca/Cl trend through 1997 is -2.4E-2 in the CABM data, whereas for the

NAA set it is -2.8E-2/yr.

- MSA concentrators are much higher in the summer than for other seasons. It is the only aerosol component that is much higher in the summer than for the other months.
- All components decreasing with time (regression slope) except Nitrogen, Chlorine, and Sodium.

From the correlation data, the following additional insights are gained:

- Iron correlates strongly to Titanium and Aluminum, showing that not only are all three significant crustal tracers, but that the NAA Titanium results are valid.
- Copper and Lead are correlated, giving some validity to the Copper results, as Copper and Lead are both primarily anthropogenic.
- Lead, and particularly NH_4, are strongly correlated to the Sulphate components. A problem this introduces (see Section 8) is that both Sulphates (non-sea-salt and normal) are equally correlated to Lead and NH_4. Therefore, the algorithm than was used to give a split to the two Sulphate components does not truly separate the sea-salt Sulphate from the anthropogenic components.

7.6 CABM Summary

The CABM data is extremely useful for comparing to the NAA data and also for validating the work in the NAA data set. Additional insights are possible due to the additional data that includes anything related to Lead, MSA, Sulphate, Nitrates, and Iron. Monthly and seasonal trending is also possible due to the 12-month nature of the CABM data.

Disadvantages of the CABM data are primarily that the set only goes up to 2006. Thus even if the NAA data is extended to present day, the CABM data will be unable to provide any insights post-2006. Also, there are elements missing from that CABM data that are already included in the NAA data (Iodine, Titanium, and Vanadium). There will be even more elements in the NAA data (Antimony, Arsenic, and Indium) once the Epithermal NAA is completed. These three elements are also not included in the CABM data and will prove valuable for identifying industrial and other anthropogenic sources.

8. Factor Analysis

Factor Analysis is a general term that refers to types of multivariate data analysis methods [Hopke, 2000]. The goal of factor analysis is to determine relationships among the measured data.

The principle of “mass-balance” allows all the relationships described in this section. In all cases of using a mass-balance, a chemical mass-balance is assumed that takes the following form [Hopke, 2000]:

$$x_{ij} = \sum_{k=1}^{top} f_{ik} * g_{kj}$$

where:

x_{ij} is the i^{th} elemental concentration measured in the j^{th} sample,

f_{ik} is the concentration of the i^{th} element in material from the kth source,

g_{kj} is the airborne mass concentration of material from the k^{th} source in the j^{th} sample. [Hopke, 2000]

8.1 Principal Component Analysis

Principal Component Analysis (PCA) is the most common type of factor analysis. PCA became popular for atmospheric analysis after Lorentz published a paper on the subject in 1956 [Wilks, 2006]. PCA Results are typically

calculated using an eigenvalue analysis of a correlation matrix. There are several problems with PCA that newer methods, such as positive matrix factorization (PMF), attempt to solve. [Hopke, 2000] As such, PMF is used for the data in this study as the exclusive type of factor analysis.

8.2 Positive Matrix Factorization

Newer mathematical methods that can be used to connect sample (receptor) data with potential sources attempt to fix problems with older approaches is Positive Matrix Factorization (PMF). PMF results can be used to estimate what the nature of potential sources of Arctic aerosol pollution may be.

PMF is a multivariate receptor model (or a multivariate factor analysis tool) that estimates source contributions as they are related to samples based on a weighted least-squares approach that finds a solution to a set of equations that minimizes the error between the solution and each data point [Laing et al., 2015; Norris et al., 2014]. It has successfully been used as a basis for source-receptor analysis in numerous studies [Laing et al., 2015; Hopke, 2000; Sirois & Barrie, 1999] and is described in great detail throughout atmospheric science literature.

PMF provides inherently better modeling than some other previous methods [Hopke, 2000]. PMF is typically accomplished using software designed for such a task such as PMF2 and EPA PMF, both available online, with online user guides on several researchers' academic and government websites.

The main advantage of PMF is that it provides better modeling than eigenvector-based methods while allowing all of the constraints from other methods to be included. It is a more complex method to use than some other methods, but with ever-increasing computing power, this computational cost is becoming negligible (unlike when PMF2 was written several decades ago). The software designed for this process also eliminates some of the inherent complexity of the methodology as well.

The PMF methodology is essentially the same as that of Factor Analysis in that a principal of mass-balance is used, followed by an eigenvalue solution method. There are a few additional pieces of information needed for PMF which are incorporated into EMP PMF.

8.2.1 EPA PMF

The program EPA PMF (version 5.0) was developed by the U. S. Environmental Protection Agency's Office of Research and Development to replace PMF2 (an older code written by Pentti Paatero). In the words of the EPA's EPA PMF website: "EPA's Positive Matrix Factorization (PMF) Model is a mathematical receptor model developed by EPA scientists that provides scientific support for the development and review of air and water quality standards, exposure research and environmental forensics. The PMF model can analyze a wide range of environmental sample data: sediments, wet deposition, surface

water, ambient air, and indoor air. EPA's PMF model reduces the large number of variables in complex analytical data sets to combinations of species called source types and source contributions. The source types are identified by comparing them to measured profiles. Source contributions are used to determine how much each source contributed to a sample. In addition, EPA PMF provides robust uncertainty estimates and diagnostics." [EPA, 2017]

Further, "Users of EPA's PMF model provide files of sample species concentrations and uncertainties, and the number of sources. The model calculates source profiles or fingerprints, source contributions, and source profile uncertainties. The PMF model results are constrained to provide positive source contributions and the uncertainty weighted difference between the observed and predicted species concentration is minimized." [EPA, 2017]

8.2.2 EPA PMF Procedure

To run EPA PMF, two separate data files are needed. The first is a simple concentration spreadsheet that can use either dates or sample numbers, with columns for each element (which could also be chemical, molecular, or any other pollution tracer). A second spreadsheet is required that includes an uncertainty value for every cell in the first spreadsheet. Both spreadsheets are in the same format, with one including concentration values (units are arbitrary) and the second including the uncertainty/error values for the first (where units are also

arbitrary, but must match the primary concentration spreadsheet). Once the two spreadsheets are in the correct format, opening EPA PMF immediately displays certain information about each element (or input) such as trends, scatter plots, and time series plots.

Computational runs are next set up for factors to be calculated and results to be displayed. There is an art in this step where one must balance the number of runs (too few will give poor results whereas too many will grind the CPU to a halt), the random number method, and most importantly, the number of factors to include in the result. In selecting the number of factors to consider, the runs must be iterated to find a solution that is reasonable with potential factors for sea sources, crustal sources, and anthropogenic sources. Too few factors will conflate sources, and too many will give false results where several components are not grouped correctly with their actual sources. This process requires iteration and analysis to produce reasonable and useful results. The step-by-step instructions are included in the EPA PMF reference material [Norris et al., 2014], although to truly understand and work with the finer points, other references are needed [Hopke, 2000].

To assist with narrowing down the correct number of factors to include, EPA PMF includes a “Q-value,” both robust and true, that will tend to decrease as better fits are found. This critical parameter for is the objective function of the PMF software. EPA PMF displays two versions of the Q-factor: Q(true), a goodness-of-fit parameter that includes all points; and Q(robust) which is a

goodness-of-fit parameter excluding points that are not good fits from thee model results. Q(robust), being uninfluenced by non-fitting points, is a crucial piece of information in determining the optimal run from multiple runs. [Norris et al., 2014]

$$Q = \sum_{i=1}^{n}\sum_{j=1}^{m}\left[\frac{x_{ij} - \sum_{k=1}^{p} g_{ik} f_{kj}}{u_{ij}}\right]^2$$

where:

I = the species (element), and

j = the sample number

These Q-values will necessarily decrease as the number of factors are increased until there are as many factors as there are “elements” in the data. Thus, using the Q-value to help narrow down the correct number of factors is an incorrect use of the metric. Rather, when the program is iterated across 10 runs, for example, the run with the lowest Q-values will indicate the best fit to the model of the iterations performed.

Once results are produced and seem reasonable, uncertainty analysis may be, and should be, performed using the built-in tools. Finally, the results, in conjunction with the uncertainty results can be reviewed to gleam insights and to apply to other areas of the aerosol study.

8.2.3 PMF Results

The results produced by EPA PMF come in numerous forms, all of which serve the same purpose: to show how the elemental composition is distributed among several proposed “sources” that result from the mathematical interpretation of the data. Such results can be displayed in table format using percentages of factor totals, percentage of species sum, and as a concentration of species. The primary graphical element provided for visual representation of each factor is referred to as a “fingerprint plot” which shows a distinct and colorful “fingerprint” for each factor determined by the software. Other data of interest are includes the Q-values (both robust and true), variance explained by the factors, and a variety of error data. Fingerprint plots and tabulated factor profile data is provided for 2-factor, 3-factor, 4-factor, 5-factor, 6-factor, and 7-factor results. Additionally, the Appendix includes Scaled Residual Plots (Figures 74 through 81) which can be used to determine the goodness-of-fit between solutions including different variables. Contribution plots for each factor in the accepted solutions (5-factor) are also included in the Appendix (Figures 82 through 91). Finally, results formatted in the same fashion are included for NAA data combined with CABM data.

8.2.3.1 Two-Factor Results

The two-factor results do not provide any particular insight although they inform the information for the models that include more factors. As can be seen, the two factors in no way differentiate even the sea component from the crustal, thus all information is convoluted.

For all results, Copper shows almost no resolution to the PMF model. The elements with the strongest dependence (resolution) on the model are Chlorine, Magnesium, and Sodium.

Seed: 711 (used for all models and runs to ensure repeatability)

Total Runs: 25 (used for all models to ensure repeatability)

Q (Robust): 32134

Q (True): 115993

Two-factor results are shown in Table 35 while the two-factor fingerprint plot is shown in Figure 64.

Table 35 - Two-Factor Results

Factor Profiles (conc. of species)

	Factor 1	Factor 2
Al	37.196	2.2716
Br	7.6288	0.89444
Ca	87.214	11.798
Cl	43.273	160.11
Cu	0.481	0.03079
I	0.1418	0.02146
Mg	77.129	15.41
Mn	0.63508	0.01011
Na	129	94.781
Ti	2.1007	0
V	0.22575	0.0097

Factor Profiles (% of species sum)

	Factor 1	Factor 2
Al	94.2444	5.75561
Br	89.5059	10.4941
Ca	88.0843	11.9157
Cl	21.2766	78.7234
Cu	93.984	6.01596
I	86.8532	13.1468
Mg	83.3476	16.6524
Mn	98.4327	1.56729
Na	57.6456	42.3544
Ti	100	0
V	95.8797	4.1203

Factor Profiles (% of factor total)

	Factor 1	Factor 2
Al	9.66067	0.79611
Br	1.98138	0.31347
Ca	22.6515	4.13476
Cl	11.239	56.1126
Cu	0.12493	0.01079
I	0.03683	0.00752
Mg	20.0322	5.40063
Mn	0.16495	0.00354
Na	33.5043	33.2172
Ti	0.5456	0
V	0.05863	0.0034

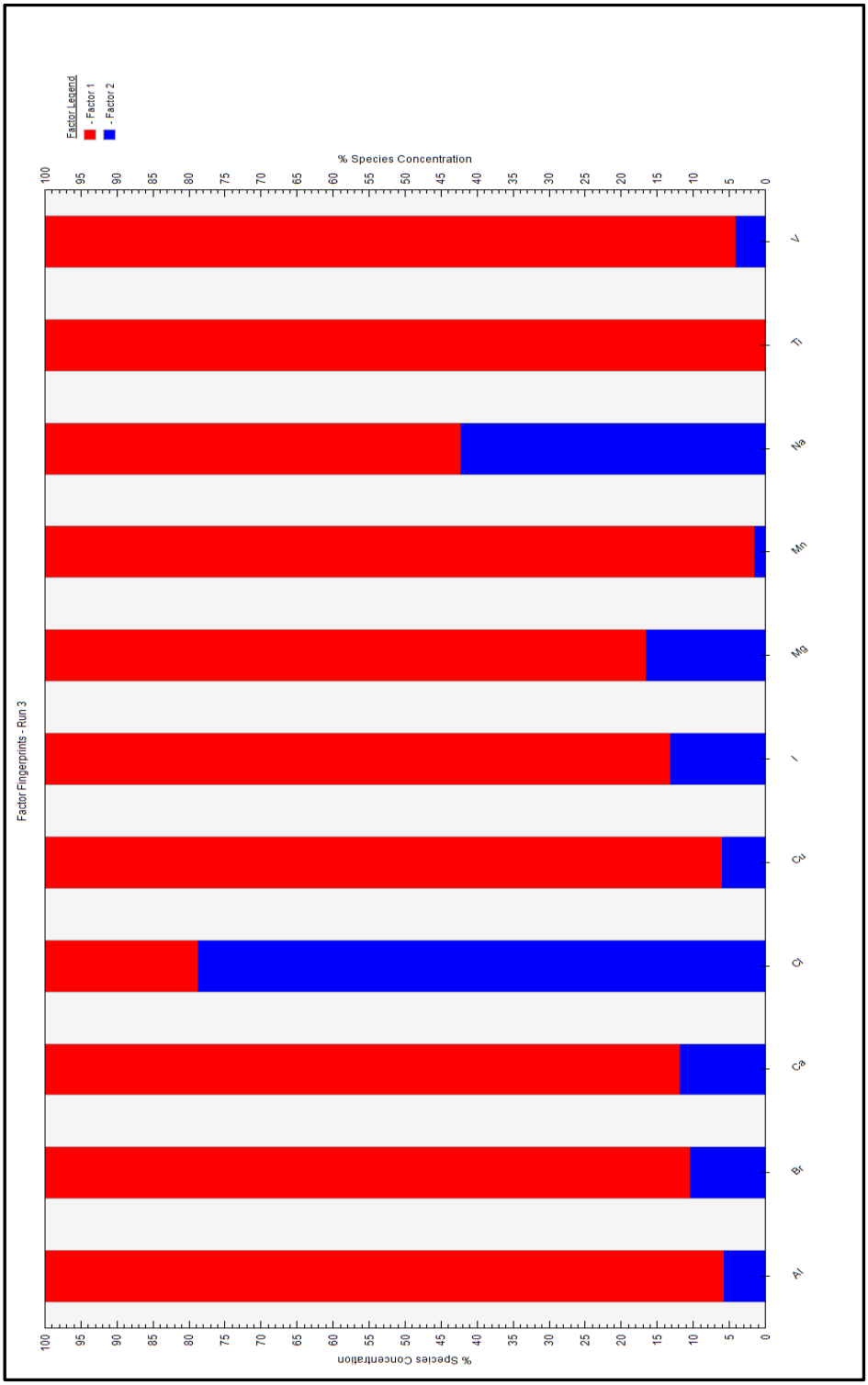

Figure 64 - Two-Factor Fingerprint Plot

8.2.3.2 Three-Factor Results

The 3-factor results are the most straight-forward, assuming that a 2-factor result is without merit (as if conflates any anthropogenic source with either the sea or the crustal source). There is a discernible crustal factor, a sea factor, and an anthropogenic factor in a 3-factor result. The likelihood of conflation, especially of multiple anthropogenic sources, is still high when considering such a small number of factors. However, the usefulness of this simple model lies in the easily discernible components, whereas assessments of the components becomes much harder as the number of factors increases.

From the best run results, the following information is gathered:

Q (Robust): 32134

Q (True): 115993

The three-factor results are shown in Table 36, while the three-factor fingerprint plot is shown in Figure 65.

Table 36 - Three-Factor Results

Factor Profiles (conc. of species)			
	Factor 1	Factor 2	Factor 3
Al	3.2453	40.809	1.3E-06
Br	0.77063	0	8.1307
Ca	13.108	71.769	19.272
Cl	170.66	19.945	12.786
Cu	0	0.24419	0.2406
I	0.01924	0.05725	0.0919
Mg	25.245	62.258	5.6633
Mn	0.03156	0.49067	0.14541
Na	94.901	1.1894	129.74
Ti	0.01255	1.9146	0.35112
V	0.00924	0.11388	0.11382

Factor Profiles (% of species sum)			
	Factor 1	Factor 2	Factor 3
Al	7.36659	92.6334	2.9E-06
Br	8.65747	0	91.3425
Ca	12.5858	68.9099	18.5043
Cl	83.9074	9.80624	6.28641
Cu	0	50.3703	49.6297
I	11.4231	34.0008	54.5761
Mg	27.0967	66.8246	6.0787
Mn	4.72653	73.4936	21.7798
Na	42.0231	0.52668	57.4502
Ti	0.55064	84.0376	15.4117
V	3.89936	48.063	48.0377

Factor Profiles (% of factor total)			
	Factor 1	Factor 2	Factor 3
Al	1.05366	20.5286	7.3E-07
Br	0.2502	0	4.60572
Ca	4.25581	36.1027	10.9168
Cl	55.4086	10.0332	7.24276
Cu	0	0.12284	0.13629
I	0.00625	0.0288	0.05206
Mg	8.19636	31.3183	3.20804
Mn	0.01025	0.24683	0.08237
Na	30.8118	0.59832	73.4926
Ti	0.00407	0.96312	0.1989
V	0.003	0.05729	0.06447

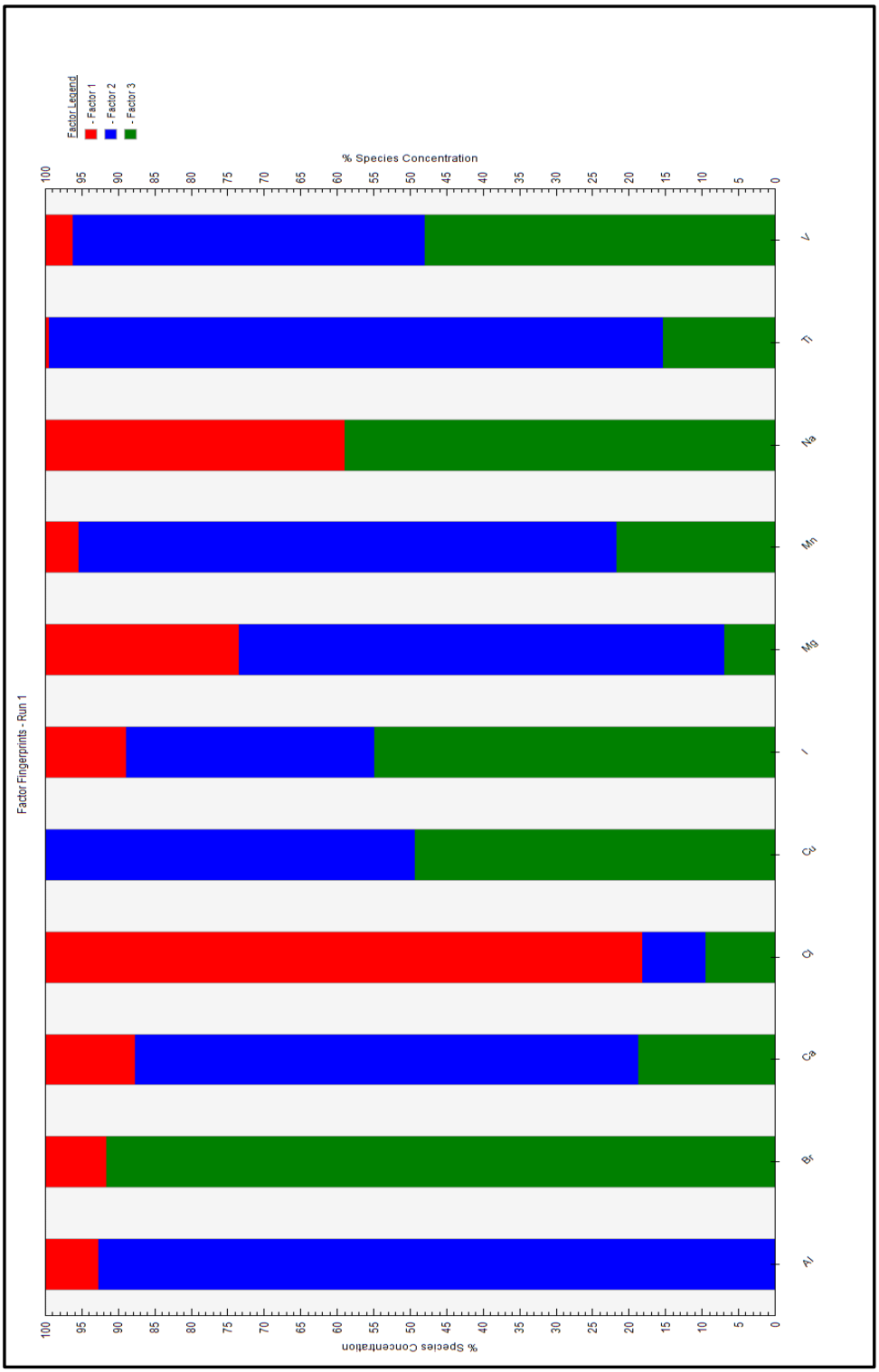

Figure 65 - Three-Factor Fingerprint Plot

Based on these results, Factor 1 is a Sea Component, as it dominated by Chlorine, and contains large amounts of Sodium. Factor 2 is the crustal component, as the vast majority of both Titanium and Aluminum are seen in that factor. Remaining Factor 3 is thus the “anthropogenic” component, although it appears somewhat conflated with a sea component, particularly since Manganese is known to be emitted primarily from coal combustion and yet the majority is linked to Factor 2. Also, Bromine is known to be primarily sea-based, yet is almost completely grouped with Factor 3. This may well be a result of Bromine detection limit problems, but this 3-factor result may still conflate multiple sea sources and multiple anthropogenic sources. Moving into the next section, it is important to observe the changes as a 4th Factor is included in the modeling, and even further as the 5th factor is observed.

Factor 1: Sea Component

Factor 2: Crustal Component

Factor 3: Anthropogenic Component (convoluted with Sea)

8.2.3.3 Four-Factor Results

Assuming that there are at least two anthropogenic sources, the 4-factor results show these multiple sources as well as distinct sea and crustal sources. Because of the poor Copper resolution in the 3-factor results, its dependence

was changed to “weak” in the model. The four-factor results follow:

From the best run results, the following information is gathered:

Q (Robust): 20928

Q (True): 47385

The four-factor results are shown in Table 37, while the four-factor fingerprint plot is shown in Figure 66.

Table 37 - Four-Factor Results

Factor Profiles (conc. of species)

	Factor 1	Factor 2	Factor 3	Factor 4
Al	0	48.513	2.748	0
Br	8.0783	0.56003	0.31178	0
Ca	1.9693	20.059	9.701	73.753
Cl	27.081	10.99	157.75	8.0416
Cu	0.23349	0.15909	0.00037	0.15375
I	0.07312	0.0057	0.01264	0.07663
Mg	0	19.889	22.564	51.529
Mn	0.04077	0.53875	0.01004	0.13476
Na	138.56	0	82.654	4.9521
Ti	0.13884	2.7874	0	0
V	0.08268	0.04351	0.00283	0.10507

Factor Profiles (% of species sum)

	Factor 1	Factor 2	Factor 3	Factor 4
Al	0	94.6392	5.3608	0
Br	90.2592	6.25724	3.48353	0
Ca	1.86695	19.0165	9.1968	69.9198
Cl	13.2839	5.39089	77.3805	3.94462
Cu	42.7091	29.1001	0.06743	28.1234
I	43.4986	3.38989	7.51987	45.5916
Mg	0	21.1626	24.0089	54.8286
Mn	5.62901	74.3802	1.38572	18.6051
Na	61.2647	0	36.5457	2.18959
Ti	4.74466	95.2553	0	0
V	35.3196	18.587	1.20848	44.8848

Factor Profiles (% of factor total)

	Factor 1	Factor 2	Factor 3	Factor 4
Al	0	46.8519	0.99654	0
Br	4.58324	0.54085	0.11306	0
Ca	1.11729	19.3722	3.51798	53.1569
Cl	15.3645	10.6137	57.2066	5.79592
Cu	0.13247	0.15364	0.00013	0.11081
I	0.04148	0.0055	0.00458	0.05523
Mg	0	19.208	8.18264	37.1391
Mn	0.02313	0.5203	0.00364	0.09713
Na	78.6123	0	29.9737	3.56919
Ti	0.07877	2.69196	0	0
V	0.04691	0.04202	0.00103	0.07573

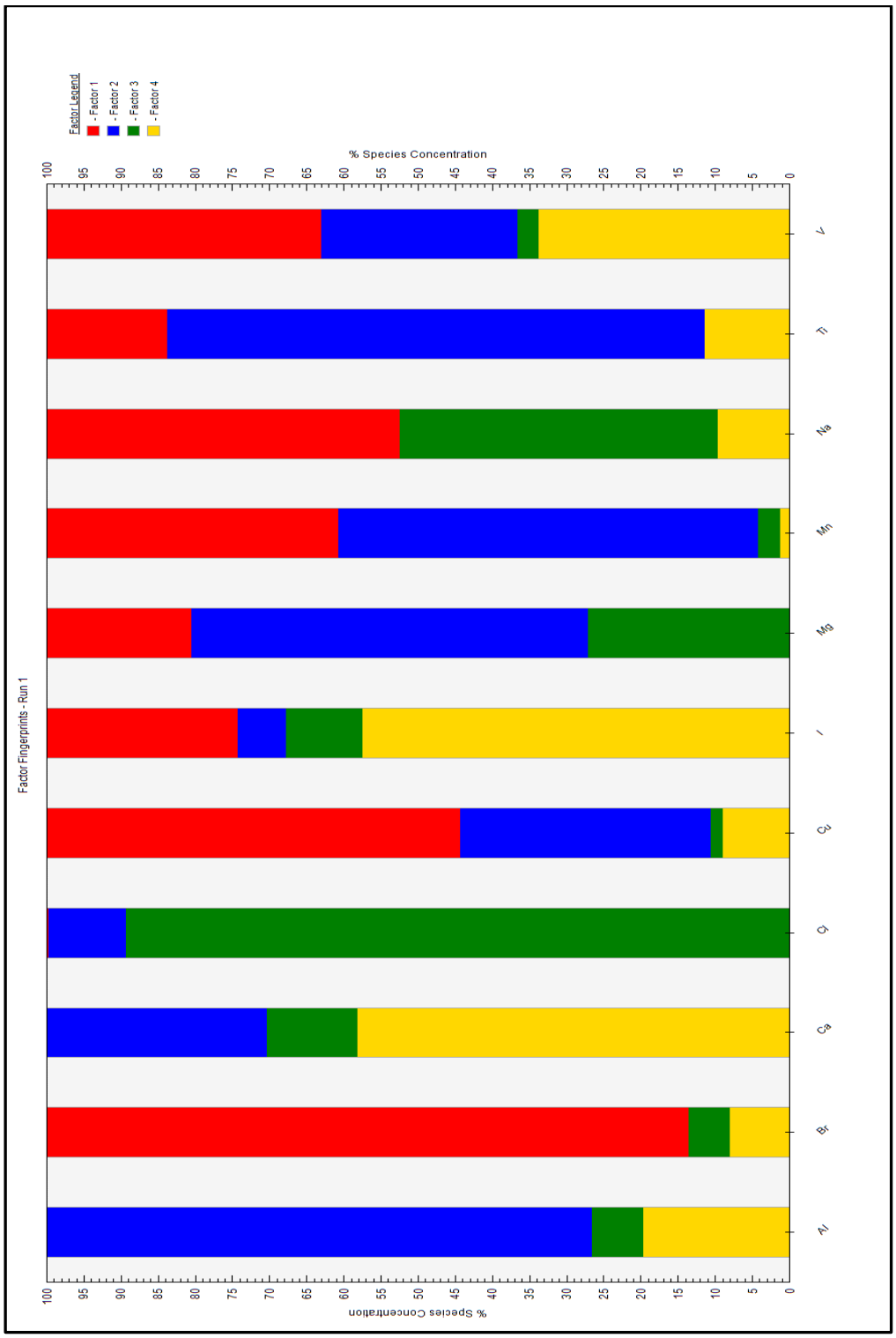

Figure 66 - Four-Factor Fingerprint Plot

Again, Copper shows little to no resolution for the model, and Sodium, Chlorine, and Magnesium show extreme dependence or resolution. The consistent results for Sodium, Chlorine, and Magnesium are encouraging as much of the work and conclusions in this paper are based on those three elements.

Comparing the 4-factor results with the 3-factor results in the previous section, there are still apparent Sea (Factor 3) and Crustal (Factor 2) components as their composition closely matches those in the 3-factor results. The remaining 2 factors appear to be largely anthropogenic. Factor 1 contains the majority of the Bromine (which is linked to seawater, but also to gasoline combustion) and a large quantity of Manganese (which is predominantly linked to combustion). Vanadium is predominately anthropogenic, and predominantly split between Factor 1 and Factor 4. Factor 1 may be convoluted with sea components as there is a very large Bromine component (assuming Bromine has some relevance). Factor 4 appears primarily anthropogenic.

Factor 1: Anthropogenic Component (convoluted with Sea)

Factor 2: Crustal Component

Factor 3: Sea Component

Factor 4: Anthropogenic Component

8.2.3.4 Five-Factor Results

The five-factor results show increased resolution, as expected after considering at least one component from the 4-factor results to be conflated.

Q (Robust): 13514

Q (True): 33658

The five-factor results are shown in Table 38, while the five-factor fingerprint plot is shown in Figure 67:

Table 38 - Five-Factor Results

Factor Profiles (conc. of species)

	Factor 1	Factor 2	Factor 3	Factor 4	Factor 5
Al	0	0	12.229	2.6201	39.114
Br	6.8404	0	1.0987	0	0.95346
Ca	1.1E-06	28.118	60.688	11.846	8.7212
Cl	39.574	0	1.3739	158.78	4.249
Cu	0.20389	0.27738	0.00617	0.00125	0.06487
I	0.06128	0.01913	0.08854	0.00613	0
Mg	0	45.194	2.6069	28.227	16.879
Mn	0.12023	0.29632	0	0.00884	0.30752
Na	136.92	0.75608	21.711	66.925	0
Ti	0	0.30359	0.27426	0	2.5796
V	0.04144	0.26326	0	0.00578	0

Factor Profiles (% of species sum)

	Factor 1	Factor 2	Factor 3	Factor 4	Factor 5
Al	0	0	22.6618	4.85535	72.4829
Br	76.9227	0	12.3553	0	10.722
Ca	9.8E-07	25.7083	55.4871	10.8308	7.9738
Cl	19.4012	0	0.67356	77.8421	2.08308
Cu	36.8323	50.1082	1.11536	0.2257	11.7185
I	35.0018	10.9243	50.5732	3.50064	0
Mg	0	48.6444	2.80593	30.382	18.1676
Mn	16.4045	40.4308	0	1.20571	41.959
Na	60.5005	0.33409	9.59339	29.572	0
Ti	0	9.61504	8.68612	0	81.6988
V	13.347	84.7928	0	1.86019	0

Factor Profiles (% of factor total)

	Factor 1	Factor 2	Factor 3	Factor 4	Factor 5
Al	0	0	12.2197	0.97612	53.6774
Br	3.72244	0	1.09786	0	1.30846
Ca	5.8E-07	37.3772	60.6416	4.41323	11.9684
Cl	21.5356	0	1.37285	59.1535	5.83104
Cu	0.11095	0.36872	0.00617	0.00047	0.08902
I	0.03335	0.02542	0.08847	0.00228	0
Mg	0	60.0762	2.60491	10.516	23.1636
Mn	0.06543	0.3939	0	0.00329	0.42202
Na	74.5097	1.00505	21.6944	24.9329	0
Ti	0	0.40356	0.27405	0	3.54007
V	0.02255	0.34995	0	0.00215	0

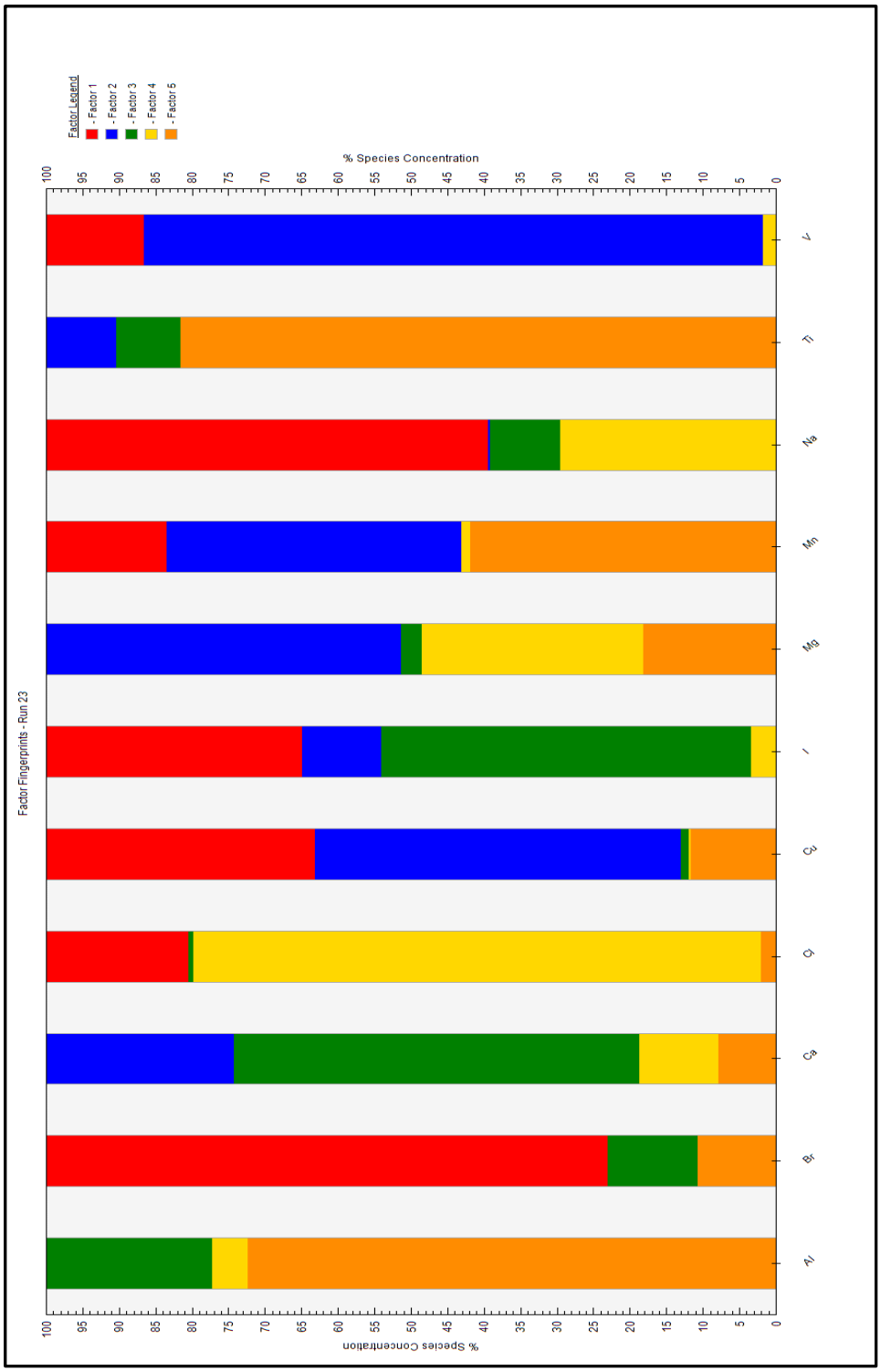

Figure 67 - Five-Factor Fingerprint Plot

Factor 5 in the five-factor results is clearly the crustal term. Titanium and Aluminum are predominantly associated with this factor, Factor 2 has now separated Vanadium largely away from the obvious sea and crustal components, and is solidly anthropogenic. In addition to the Vanadium term, Factor 2 also has large Manganese and even Copper components, all of which are anthropogenic. It seems, however, that the sea component has separated into Factor 1 and Factor 4. One possible reason for the sea-source split could be a blowing snow source in addition to a water source.

Factor 1: Sea Component (1)

Factor 2: Anthropogenic Component (possible smelting industry)

Factor 3: Anthropogenic Component (possible coal combustion)

Factor 4: Sea Component (2)

Factor 5: Crustal Component

8.2.3.5 Six-Factor Results

Not surprisingly at this point, there is a strong crustal term yet again (Factor 1). Factor 3 has become a definitive sea component in these results. The source dependence begins to break down, and two of the 6 factors are indeterminate.

Q (Robust): 7574

Q (True): 17997

Factor 1: Crustal Component

Factor 2: Anthropogenic Component (possibly convoluted with sea)

Factor 3: Sea Component

Factor 4: Indeterminate

Factor 5: Indeterminate

Factor 6: Anthropogenic Component (possible smelting activity)

The six-factor results are shown in Table 39, while the six-factor fingerprint plot is shown in Figure 68.

Table 39 - Six-Factor Results

Factor Profiles (conc. of species)

	Factor 1	Factor 2	Factor 3	Factor 4	Factor 5	Factor 6
Al	44.675	0	1.8941	0	7.1979	0
Br	0.89879	7.9721	0	0	0	0
Ca	0	0	0	73.187	37.283	0
Cl	6.7501	8.6894	153.3	0	34.959	0.55879
Cu	0.05373	0.13231	0.00472	0.09695	0	0.3439
I	0.01038	0.04849	0	0	0.09161	0.03176
Mg	5.4944	15.099	18.18	48.199	0	5.9181
Mn	0.36545	0.07819	0.01913	0	0	0.28184
Na	0	124.29	70.218	1.5255	19.079	10.929
Ti	2.9595	0.17122	0	0	0	0.0382
V	0	0	0	0	0.05978	0.28319

Factor Profiles (% of species sum)

	Factor 1	Factor 2	Factor 3	Factor 4	Factor 5	Factor 6
Al	83.09	0	3.52279	0	13.3872	0
Br	10.1319	89.8681	0	0	0	0
Ca	0	0	0	66.2506	33.7494	0
Cl	3.3047	4.25414	75.0524	0	17.1152	0.27357
Cu	8.50647	20.948	0.74777	15.3499	0	54.4479
I	5.6963	26.6071	0	0	50.2691	17.4275
Mg	5.91492	16.2546	19.5714	51.888	0	6.37105
Mn	49.0793	10.5009	2.56926	0	0	37.8506
Na	0	54.9855	31.0642	0.67488	8.44049	4.83495
Ti	93.3915	5.40311	0	0	0	1.2054
V	0	0	0	0	17.4306	82.5694

Factor Profiles (% of factor total)

	Factor 1	Factor 2	Factor 3	Factor 4	Factor 5	Factor 6
Al	72.9896	0	0.77749	0	7.2949	0
Br	1.46843	5.09462	0	0	0	0
Ca	0	0	0	59.4975	37.7854	0
Cl	11.0283	5.55302	62.9269	0	35.4301	3.03942
Cu	0.08778	0.08455	0.00194	0.07882	0	1.87057
I	0.01696	0.03099	0	0	0.09285	0.17275
Mg	8.9767	9.64911	7.46257	39.1835	0	32.1902
Mn	0.59707	0.04997	0.00785	0	0	1.53301
Na	0	79.4283	28.8232	1.24016	19.3361	59.4459
Ti	4.8352	0.10942	0	0	0	0.20777
V	0	0	0	0	0.06059	1.54035

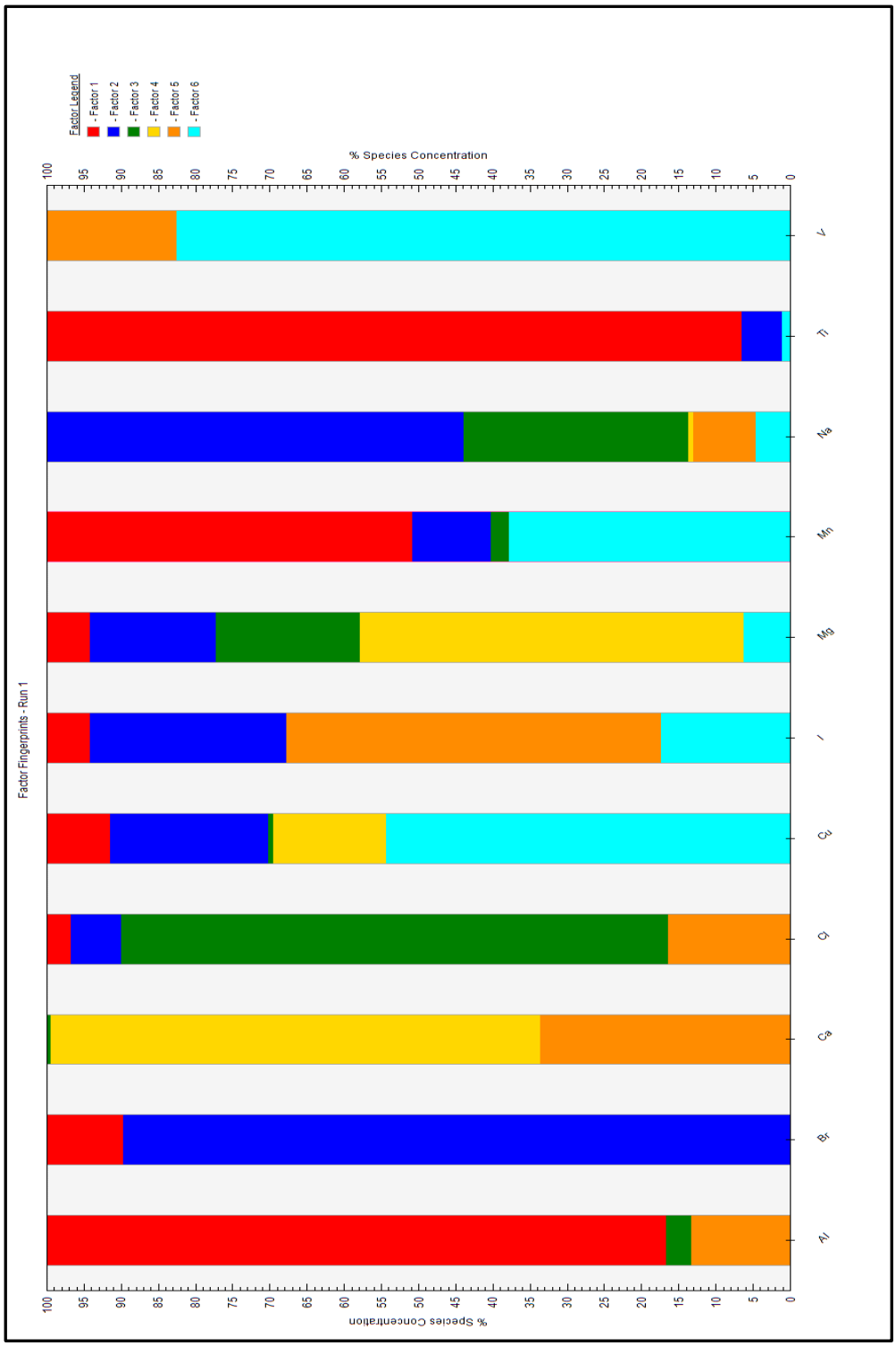

Figure 68 - Six-Factor Fingerprint Plot

8.2.3.6 Seven-Factor Results

As the number of factor increases, and ultimately converges on the number of species in the sample, the results “fit” better and better in that the Q-values continue to decrease, but the results also become harder to make sense of. No formal analysis is thus done of the 7-factor results, but they are left in place for reference. Note, however, that there is still a very strong and definitive crustal component (Factor 7).

Q (Robust): 3581

Q (True): 9347

The six-factor results are shown in Table 40, while the six-factor fingerprint plot is shown in Figure 69.

Table 40 - Seven-Factor Results

Factor Profiles (conc. of species)

	Factor 1	Factor 2	Factor 3	Factor 4	Factor 5	Factor 6	Factor 7
Al	1.3306	2.3659	0	2.1345	0	7.8396	40.519
Br	0	0	0	0	6.5022	1.9765	0.46453
Ca	0	14.077	0	51.75	0	26.805	18
Cl	156.67	10.101	4.607	1.4425	0	21.768	9.5929
Cu	0.0022	0.31461	0.21494	0.03694	0.06669	0.01167	0.01712
I	0	0	0.06867	0	0	0.12688	0
Mg	18.515	0	30.644	31.109	11.587	0	0
Mn	0.00531	0.03383	0.58105	0	0	0.05604	0.08587
Na	75.472	17.29	0	0	94.298	38.958	0
Ti	0	0	0.07795	0	0.60161	0	2.505
V	0	0.27962	0.09939	0	0	0	0

Factor Profiles (% of species sum)

	Factor 1	Factor 2	Factor 3	Factor 4	Factor 5	Factor 6	Factor 7
Al	2.45545	4.36597	0	3.93895	0	14.467	74.7727
Br	0	0	0	0	72.7053	22.1005	5.19421
Ca	0	12.7242	0	46.7767	0	24.229	16.2702
Cl	76.7308	4.94707	2.25633	0.70648	0	10.6611	4.69822
Cu	0.33151	47.3693	32.3625	5.56128	10.0409	1.7574	2.57708
I	0	0	35.1163	0	0	64.8837	0
Mg	20.1568	0	33.3613	33.8675	12.6144	0	0
Mn	0.69619	4.43869	76.2438	0	0	7.35381	11.2675
Na	33.392	7.64983	0	0	41.7215	17.2367	0
Ti	0	0	2.44787	0	18.8914	0	78.6607
V	0	73.7766	26.2234	0	0	0	0

Factor Profiles (% of factor total)

	Factor 1	Factor 2	Factor 3	Factor 4	Factor 5	Factor 6	Factor 7
Al	0.52803	5.32118	0	2.4684	0	8.03718	56.9212
Br	0	0	0	0	5.75133	2.02631	0.65257
Ca	0	31.6608	0	59.8453	0	27.4806	25.2864
Cl	62.1718	22.7183	12.6939	1.66815	0	22.3166	13.4761
Cu	0.00087	0.70759	0.59224	0.04271	0.05899	0.01197	0.02404
I	0	0	0.18921	0	0	0.13008	0
Mg	7.34736	0	84.435	35.9754	10.2489	0	0
Mn	0.00211	0.07608	1.601	0	0	0.05746	0.12063
Na	29.9498	38.8872	0	0	83.4086	39.9398	0
Ti	0	0	0.21479	0	0.53214	0	3.51903
V	0	0.6289	0.27385	0	0	0	0

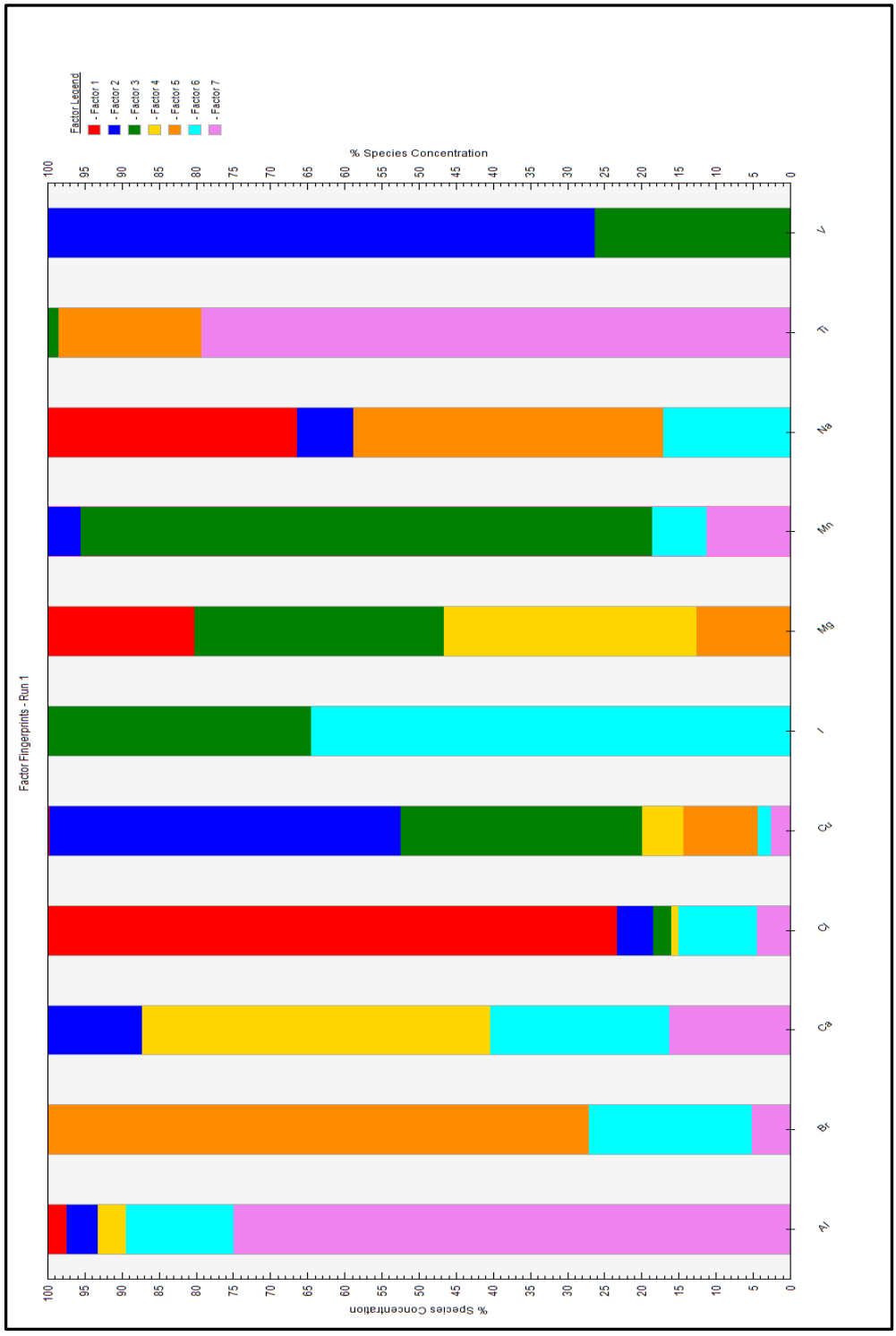

Figure 69 - Seven-Factor Fingerprint Plot

8.2.4 CABM Combined PMF Results

The CABM data set combined with the NAA data results in a much larger data set, whose PMF results could potentially include more factors. Using the combined data, 4, 5, 6, and 7-factor runs are performed. All CABM uncertainties are expressed as 10% of the sample mean, as was Bromine from the NAA data as it did not resolve well previously.

Copper is used from the new CABM data in all the combined PMF runs instead of from the NAA data, as results in the NAA data were largely below detection and did not resolve well. It apparently does not resolve well with the CABM data either.

The CABM data separates “S” and “S-non-sea-salt” using an undefined algorithm. However, because the correlation of the two in the CABM data is identically “1” there is no benefit to be had by including both in the same set. They trend together perfectly, and as such, will correlate to other elements in the CABM runs in exactly the same manner.

8.2.4.1 Four-Factor Results

For the first run, four factors are used with the understanding that the results are only useful for comparing to subsequent runs. By adding more data types the results should not result in fewer factors, but rather should results in 5

or more factors as a relevant solution (as the 5-factor results from the NAA data is the most logical). The results may give more factors if a single new component proves to be stand-alone.

Q (Robust): 57275.8

Q (True): 109867

Factor 1: Sea Component

Factor 2: Crustal Component

Factor 3: Sea Component convoluted with Anthropogenic

Factor 4: Sea Component convoluted with Anthropogenic (Indeterminate)

The CABM four-factor results are shown in Table 41, while the CABM four-factor fingerprint plot is shown in Figure 70.

Table 41 - CABM Four-Factor Results (Part 1 of 2)

Factor Profiles (conc. of species)

	Factor 1	Factor 2	Factor 3	Factor 4
Al	0	49.519	0	0
Br	0.67806	0.099118	3.9231	0
Ca	10.379	65.286	21.155	9.6794
Cl	153.54	16.325	2.5071	17.837
I	0.013227	0.039149	0.087036	0.030413
Mg	23.71	55.24	0	16.376
Mn	0.007976	0.44884	0.037597	0.21552
Na	86.246	0.23034	121.88	13.192
Ti	0.086729	2.3097	0.45123	0
V	0	0.058438	0.052758	0.22524
N	23.318	9.2043	23.016	16.439
S	34.119	0	334.72	718.28
NH4	0	1.0454	34.176	67.02
MSA	1.75E-05	0	0	0.001497
Pb	0.038397	0	0.23849	1.0804
Cu_CBD	0.029821	0.037245	0.10575	0.33403
Fe	0.075814	22.446	0	3.4764

Factor Profiles (% of species sum)

	Factor 1	Factor 2	Factor 3	Factor 4
Al	0	100	0	0
Br	14.42596	2.108769	83.46528	0
Ca	9.745595	61.30175	19.86396	9.08869
Cl	80.72169	8.58266	1.318076	9.377574
I	7.788606	23.05255	51.2504	17.90844
Mg	24.87254	57.94851	0	17.17894
Mn	1.123431	63.2229	5.295855	30.35781
Na	38.92875	0.103968	55.01282	5.954457
Ti	3.045624	81.10873	15.84565	0
V	0	17.36972	15.68144	66.94884
N	32.39632	12.78778	31.97675	22.83915
S	3.138479	0	30.78964	66.07188
NH4	0	1.022482	33.42677	65.55075
MSA	1.156988	0	0	98.84301
Pb	2.828952	0	17.57108	79.59997
Cu_CBD	5.883641	7.348386	20.86433	65.90365
Fe	0.291612	86.3367	0	13.37169

Table 41 - CABM Four-Factor Results (Part 2 of 2)

	Factor Profiles (% of factor total)			
	Factor 1	Factor 2	Factor 3	Factor 4
Al	0	22.2769	0	0
Br	0.204086	0.04459	0.723352	0
Ca	3.123927	29.36994	3.900617	1.120059
Cl	46.2133	7.344059	0.462266	2.064021
I	0.003981	0.017612	0.016048	0.003519
Mg	7.136364	24.85058	0	1.89496
Mn	0.002401	0.201918	0.006932	0.024939
Na	25.95879	0.103622	22.47257	1.526522
Ti	0.026104	1.039055	0.083199	0
V	0	0.026289	0.009728	0.026064
N	7.018377	4.140699	4.243754	1.902251
S	10.26932	0	61.7166	83.11628
NH4	0	0.47029	6.301465	7.755267
MSA	5.27E-06	0	0	0.000173
Pb	0.011557	0	0.043973	0.125019
Cu_CBD	0.008976	0.016755	0.019498	0.038653
Fe	0.022819	10.09769	0	0.402274

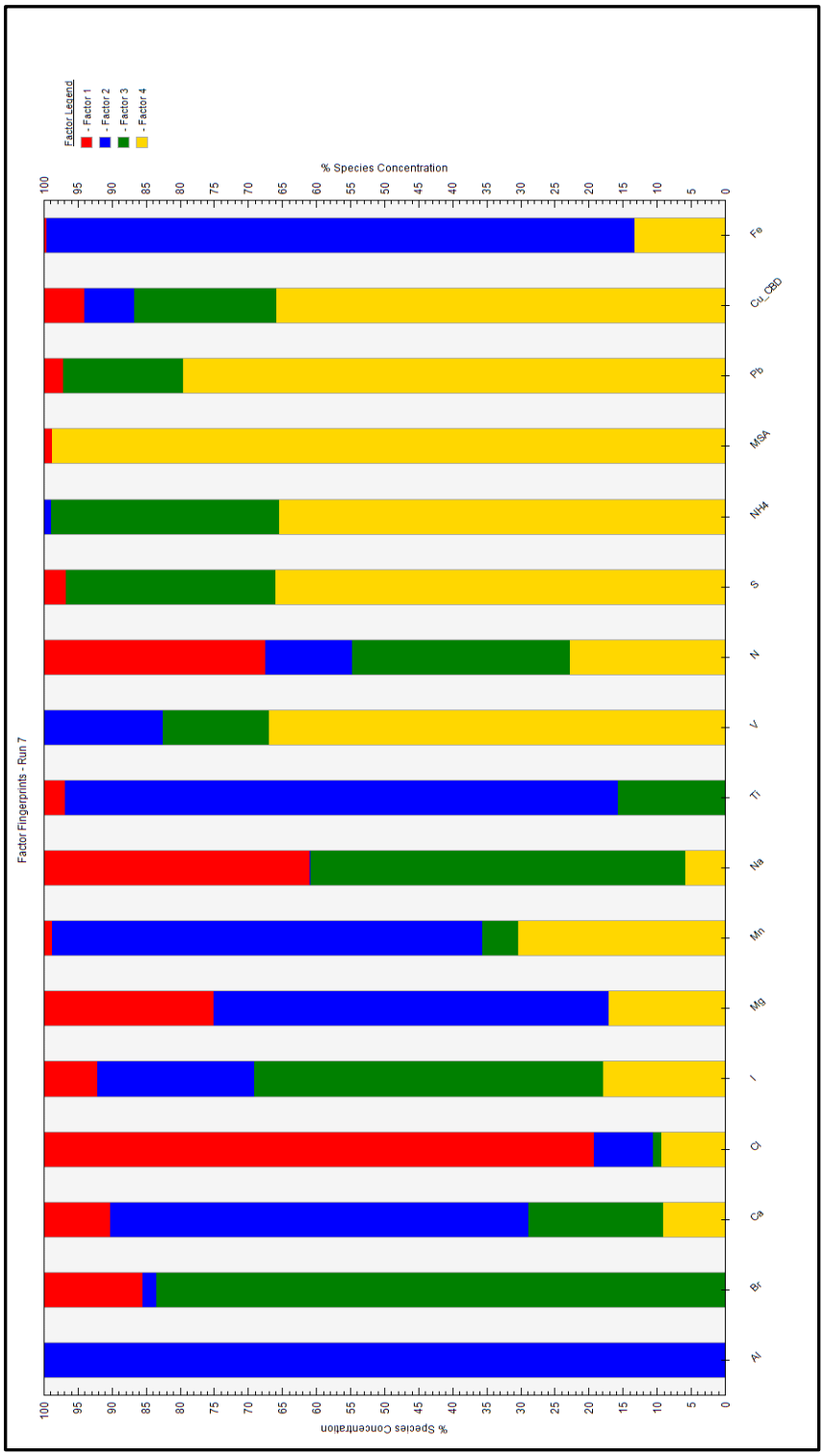

Figure 70 - CABM Four-Factor Fingerprint Plot

8.2.4.2 Five-Factor Results

The Five-Factor results more reasonably group Copper and Lead away from MSA and other sea components. Thus moving from four to five factors already reveals a more plausible solution. As a result, Vanadium, Copper, Lead and Ammonium are shared by the same factor, ensuring that the factor is anthropogenic. The sea components, previous assumed as one being open water and one being from iced-over water, can now be confirmed because MSA is a marker of open water.

Q (Robust): 45852

Q (True): 81951

Factor 1: Anthropogenic (possible combustion)

Factor 2: Anthropogenic (possible smelting or other industrial activity)

Factor 3: Crustal Component

Factor 4: Sea Component (open water)

Factor 5: Sea Component (blowing snow)

The CABM five-factor results are shown in Table 42, while the CABM five-factor fingerprint plot is shown in Figure 71.

Table 42 - CABM Five-Factor Results (Part 1 of 2)

Factor Profiles (conc. of species)					
	Factor 1	Factor 2	Factor 3	Factor 4	Factor 5
Al	11.463	3.0747	37.304	0.45201	0
Br	3.1809	0	0	2.4292	0.057758
Ca	26.112	16.529	37.315	16.652	8.8767
Cl	22.297	6.5349	0.096443	18.034	143.22
I	0.062415	0.038005	0.015272	0.044776	0.006684
Mg	0	13.43	21.38	30.855	27.098
Mn	0.000182	0.25351	0.29043	0.17073	0.027139
Na	111.61	39.241	0.34846	6.6079	63.614
Ti	0.88466	0	2.0678	0.18378	0.005566
V	0	0.27392	0.055088	0.031999	0.001672
N	15.867	11.222	3.3004	22.395	20.309
S	106.3	547.97	0	400.17	25.241
NH4	8.9024	62.084	1.5797	31.321	0
MSA	0	0	0	0.002259	0
Pb	0.025825	1.2737	0.076652	0.087424	0.044596
Cu_CBD	0.057187	0.47835	0.069473	0	0.016588
Fe	4.6075	4.8986	18.939	0	0.25237
Factor Profiles (% of species sum)					
	Factor 1	Factor 2	Factor 3	Factor 4	Factor 5
Al	21.92042	5.879675	71.33554	0.864368	0
Br	56.12173	0	0	42.85922	1.019045
Ca	24.7543	15.66957	35.3748	15.78618	8.415154
Cl	11.72401	3.436123	0.050711	9.482479	75.30668
I	37.34038	22.73686	9.136622	26.78767	3.998468
Mg	0	14.47776	23.04798	33.26218	29.21208
Mn	0.024476	34.1662	39.142	23.00973	3.657593
Na	50.40616	17.72232	0.157374	2.98431	28.72984
Ti	28.15769	0	65.81565	5.849502	0.177159
V	0	75.52686	15.18919	8.822956	0.460986
N	21.70784	15.35296	4.515319	30.63888	27.785
S	9.845501	50.75295	0	37.06373	2.33782
NH4	8.569303	59.76103	1.520593	30.14908	0
MSA	0	0	0	100	0
Pb	1.712309	84.45183	5.08236	5.79659	2.956908
Cu_CBD	9.199997	76.95488	11.17652	0	2.668606
Fe	16.05542	17.0698	65.99536	0	0.879416

Table 42 - CABM Five-Factor Results (Part 2 of 2)

Factor Profiles (% of factor total)					
	Factor 1	Factor 2	Factor 3	Factor 4	Factor 5
Al	3.681471	0.434708	30.36852	0.085376	0
Br	1.021582	0	0	0.458827	0.020001
Ca	8.386163	2.336909	30.37748	3.145227	3.073957
Cl	7.160932	0.92392	0.078513	3.406259	49.59638
I	0.020045	0.005373	0.012433	0.008457	0.002314
Mg	0	1.898765	17.40508	5.827888	9.383904
Mn	5.83E-05	0.035842	0.236434	0.032247	0.009398
Na	35.84481	5.547986	0.283675	1.248099	22.02921
Ti	0.284119	0	1.683359	0.034712	0.001927
V	0	0.038727	0.044846	0.006044	0.000579
N	5.095866	1.586593	2.686797	4.229964	7.032907
S	34.13944	77.47331	0	75.58405	8.740834
NH4	2.859106	8.777584	1.286006	5.915906	0
MSA	0	0	0	0.000427	0
Pb	0.008294	0.180079	0.062401	0.016513	0.015443
Cu_CBD	0.018366	0.06763	0.056557	0	0.005744
Fe	1.47975	0.692576	15.4179	0	0.087394

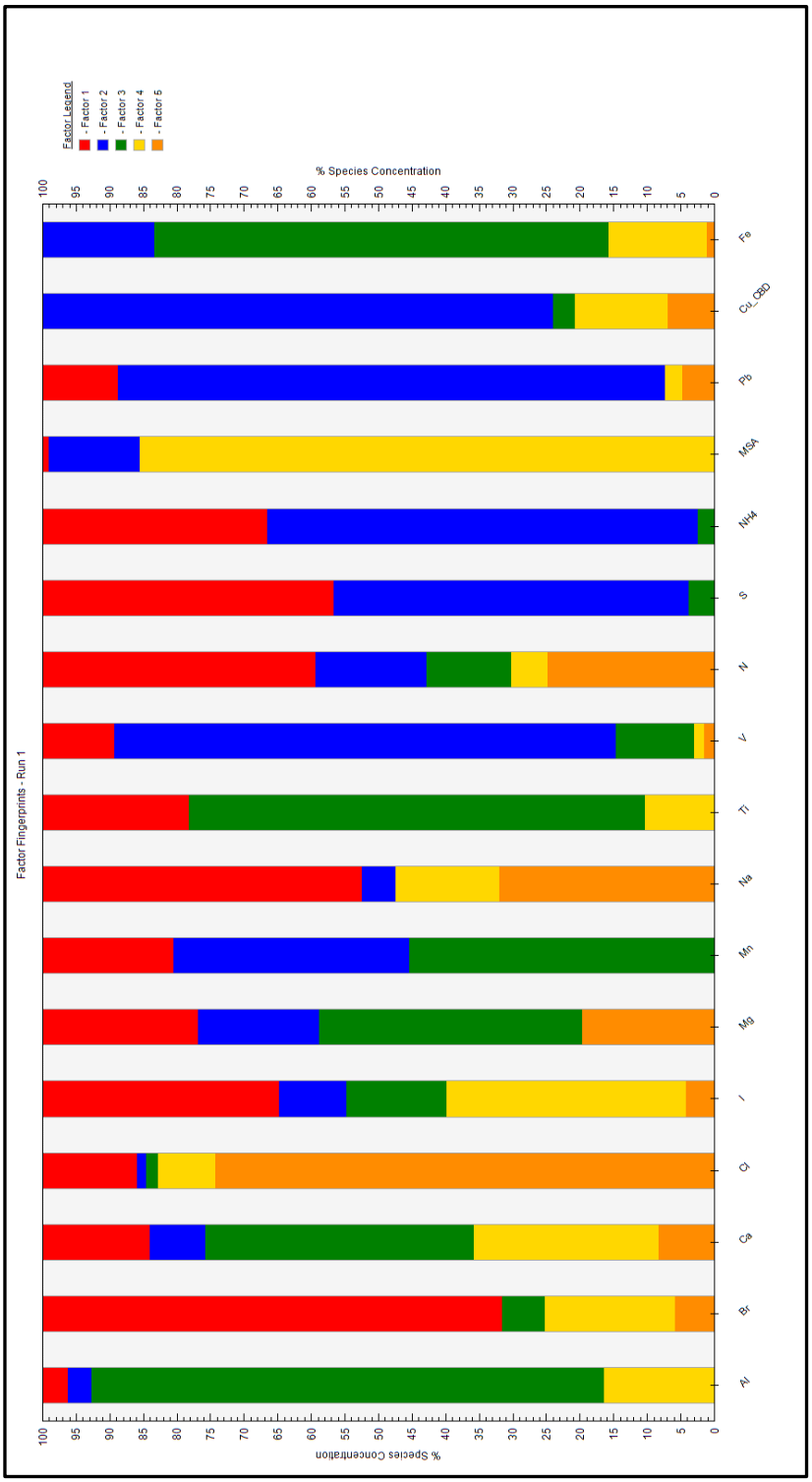

Figure 71 - CABM Five-Factor Fingerprint Plot

8.2.4.3 Six-Factor Results

Moving to six factors, more contributors seem to break away. MSA is now essentially a stand-alone component (it does not correlate well in the CABM data). The results now include an “indeterminate” factor, as do all results with more factors. This result lends credibility to the assumption that the 5-factor result is the most logical solution for the combined data, as well as the assumption that the 5-factor results for the NAA data was valid.

Q (Robust): 36302

Q (True): 60557

Factor 1: Sea Component (open water)

Factor 2: Anthropogenic (possible smelting)

Factor 3: Sea Component (blowing snow)

Factor 4: Indeterminate

Factor 5: Crustal Component

Factor 6: Anthropogenic (possible combustion)

The CABM six -factor results are shown in Table 43, while the CABM six-factor fingerprint plot is shown in Figure 72.

Table 43 - CABM Six-Factor Results (Part 1 of 2)

Factor Profiles (conc. of species)

	Factor 1	Factor 2	Factor 3	Factor 4	Factor 5	Factor 6
Al	0	0	0	11.854	39.221	3.4018
Br	1.5142	0	0.12348	2.0091	0	1.8783
Ca	0	13.009	4.905	0	31.242	59.312
Cl	20.798	0.38703	165.3	0	3.8459	0
I	0.025921	0.031924	0.00534	0.029486	0.008244	0.06426
Mg	3.861	9.0035	21.218	0.97605	19.237	42.314
Mn	0.12189	0.19108	0	0	0.28059	0.15513
Na	0	28.216	74.498	83.639	1.6289	33.283
Ti	0.15761	0	0	0.82803	2.0329	0.29002
V	0.029562	0.2536	0.001566	0	0.050398	0.035517
N	23.239	7.8268	24.51	5.7606	3.3749	10.023
S	244.42	469.09	0	22.555	0	330.71
NH4	27.581	57.767	0.18976	2.3191	1.0913	16.037
MSA	0.002669	7.2E-05	0	0	0.000163	0
Pb	0.17817	1.1743	0.074726	0.024625	0.057658	0.025407
Cu_CBD	0	0.47787	0.028089	0.096377	0.071308	0
Fe	2.1398	2.7803	0.40084	5.7357	19.227	0

Factor Profiles (% of species sum)

	Factor 1	Factor 2	Factor 3	Factor 4	Factor 5	Factor 6
Al	0	0	0	21.75972	71.99579	6.244493
Br	27.40594	0	2.2349	36.36327	0	33.99589
Ca	0	11.9934	4.522071	0	28.80296	54.68157
Cl	10.92728	0.203346	86.84873	0	2.020638	0
I	15.69305	19.32738	3.232814	17.85137	4.991191	38.90419
Mg	3.996499	9.319472	21.96263	1.010304	19.91211	43.79898
Mn	16.28044	25.52191	0	0	37.47746	20.72019
Na	0	12.75214	33.66914	37.80039	0.736176	15.04215
Ti	4.763704	0	0	25.0269	61.44365	8.765747
V	7.975873	68.42167	0.422455	0	13.59746	9.582541
N	31.09549	10.47284	32.79619	7.708107	4.515865	13.41151
S	22.91205	43.97272	0	2.114317	0	31.00091
NH4	26.27133	55.02397	0.180749	2.208979	1.03948	15.27549
MSA	91.89608	2.478196	0	0	5.625722	0
Pb	11.60803	76.50731	4.868505	1.604354	3.7565	1.655302
Cu_CBD	0	70.93806	4.16971	14.30681	10.58541	0
Fe	7.065861	9.180865	1.323619	18.93993	63.48973	0

Table 43 - CABM Six-Factor Results (Part 2 of 2)

	Factor Profiles (% of factor total)					
	Factor 1	Factor 2	Factor 3	Factor 4	Factor 5	Factor 6
Al	0	0	0	8.727274	32.31543	0.683738
Br	0.467246	0	0.042396	1.47916	0	0.377525
Ca	0	2.204136	1.684092	0	25.74128	11.9213
Cl	6.417773	0.065575	56.75443	0	3.168759	0
I	0.007999	0.005409	0.001833	0.021708	0.006793	0.012916
Mg	1.191414	1.525478	7.28503	0.718598	15.84998	8.504823
Mn	0.037612	0.032375	0	0	0.231187	0.03118
Na	0	4.780684	25.57829	61.57756	1.342103	6.689654
Ti	0.048635	0	0	0.609621	1.674971	0.058292
V	0.009122	0.042968	0.000538	0	0.041525	0.007139
N	7.171008	1.326108	8.415312	4.241128	2.780688	2.014554
S	75.42225	79.4787	0	16.60567	0	66.47044
NH4	8.510846	9.787559	0.065153	1.707392	0.899157	3.223327
MSA	0.000824	1.22E-05	0	0	0.000135	0
Pb	0.054979	0.198964	0.025657	0.01813	0.047506	0.005107
Cu_CBD	0	0.080966	0.009644	0.070956	0.058753	0
Fe	0.660292	0.471071	0.137625	4.222796	15.84174	0

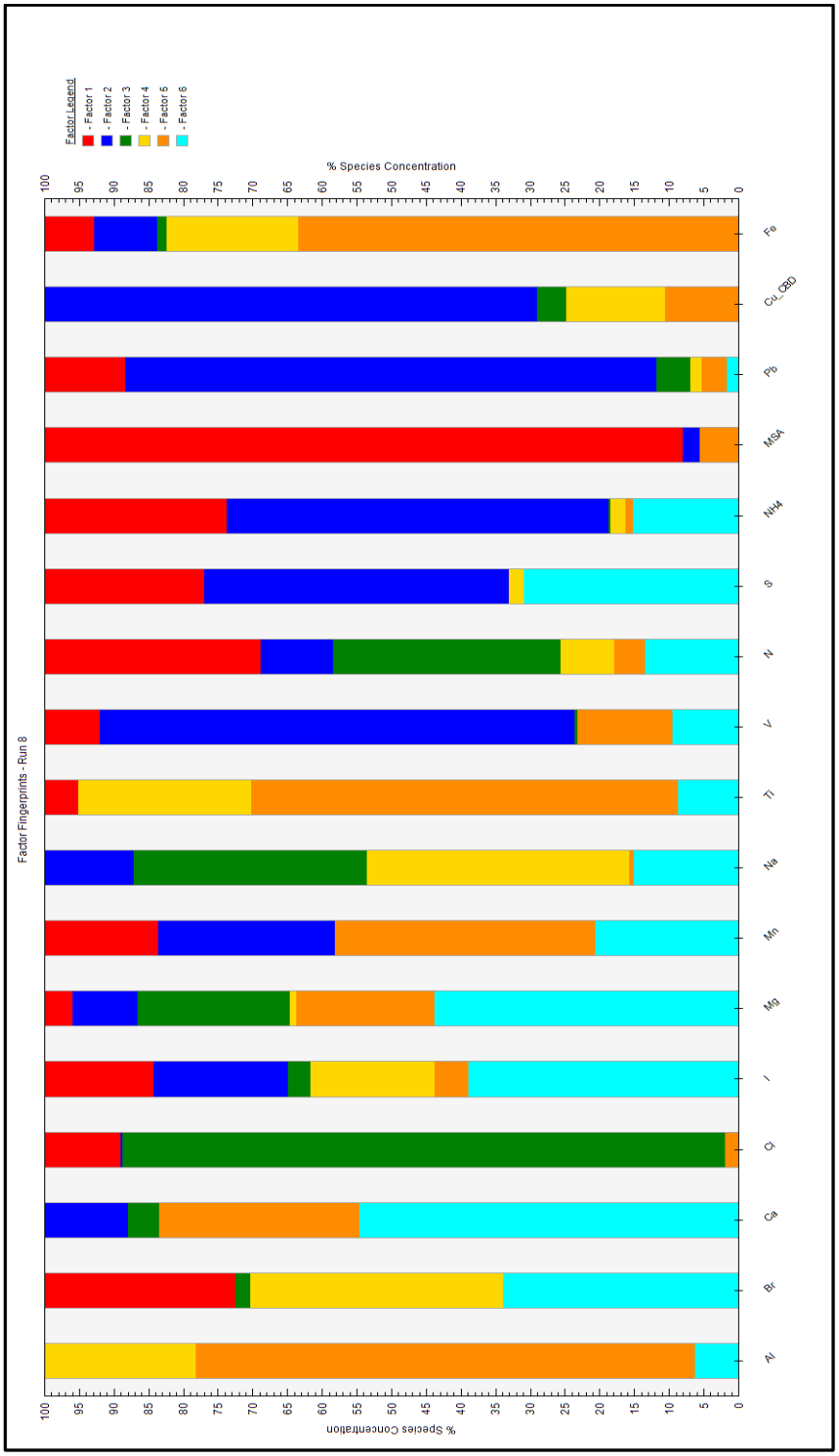

Figure 72 - CABM Six-Factor Fingerprint Plot

8.2.4.4 Seven-Factor Results

Moving to Seven factors, it is no longer obvious what all the factors are, or their relevance. There is a clear Crustal factor, and at least two apparent sea terms, but the others are too scattered and convoluted to be useful. The results from the seven-factor runs are included herein for comparison purposes only.

Q (Robust): 28723

Q (True): 42354

The CABM seven -factor results are shown in Table 44, while the CABM seven-factor fingerprint plot is shown in Figure 73.

Table 44 - CABM Seven-Factor Results (Part 1 of 2)

Factor Profiles (conc. of species)

	Factor 1	Factor 2	Factor 3	Factor 4	Factor 5	Factor 6	Factor 7
Al	0	10.766	0.55276	0.20113	3.2164	1.9846	38.214
Br	0.000502	0	2.8243	0.15457	1.2858	1.1689	0.13762
Ca	0	31.559	0	0	53.884	10.9	18.206
Cl	0	20.088	0	142.26	10.602	17.413	0
I	0.007343	0.041289	0.039556	8.06E-05	0.044158	0.041293	0
Mg	13.603	0	11.782	18.6	31.446	0	19.347
Mn	0.27655	0	0.071072	0.013466	0.052669	0.021317	0.32712
Na	0	47.625	99.234	62.527	0	10.822	1.3062
Ti	0.065446	0.34825	0.6697	0	0	0.057095	2.2384
V	0.24682	0.060904	0.002181	0.003986	0.020417	0	0.034627
N	11.11	0	18.608	20.83	4.174	12.387	7.4523
S	539.88	10.554	299.7	0	141.08	45.841	41.502
NH4	65.535	2.0427	18.864	1.099	6.2251	8.6049	4.4585
MSA	7.36E-05	0.00034	0	0	0	0.002957	3.13E-05
Pb	1.1212	0.25197	0.049717	0.063307	0	0.033781	0
Cu_CBD	0.36708	0.38596	0	0	0	0	0.006744
Fe	3.1527	6.1758	0	0.5225	0	1.991	18.469

Factor Profiles (% of species sum)

	Factor 1	Factor 2	Factor 3	Factor 4	Factor 5	Factor 6	Factor 7
Al	0	19.59775	1.006209	0.366124	5.854931	3.61264	69.56235
Br	0.009016	0	50.69016	2.774202	23.07737	20.97926	2.469986
Ca	0	27.55066	0	0	47.04013	9.515578	15.89364
Cl	0	10.55247	0	74.73091	5.56936	9.147261	0
I	4.227038	23.76759	22.77001	0.046371	25.4191	23.76989	0
Mg	14.35249	0	12.43115	19.62481	33.17859	0	20.41297
Mn	36.28341	0	9.32466	1.766742	6.910183	2.796795	42.91821
Na	0	21.49975	44.79803	28.22708	0	4.885466	0.589669
Ti	1.936908	10.30664	19.82011	0	0	1.689756	66.24659
V	66.90071	16.50807	0.591134	1.080381	5.53404	0	9.385669
N	14.90049	0	24.95665	27.93674	5.598078	16.61318	9.994863
S	50.05577	0.97853	27.78713	0	13.08044	4.250216	3.847919
NH4	61.34559	1.912118	17.65809	1.028745	5.827152	8.05482	4.173484
MSA	2.162537	10.0005	0	0	0	86.91765	0.919316
Pb	73.76437	16.57725	3.270909	4.165003	0	2.222471	0
Cu_CBD	48.31375	50.79867	0	0	0	0	0.887582
Fe	10.40117	20.37478	0	1.723797	0	6.568572	60.93167

Table 44 - CABM Seven-Factor Results (Part 2 of 2)

	Factor Profiles (% of factor total)						
	Factor 1	Factor 2	Factor 3	Factor 4	Factor 5	Factor 6	Factor 7
Al	0	8.287964	0.122185	0.081669	1.276195	1.783608	25.19058
Br	7.91E-05	0	0.624296	0.062763	0.510176	1.050519	0.090719
Ca	0	24.29499	0	0	21.37995	9.796094	12.00135
Cl	0	15.4643	0	57.76468	4.206633	15.64948	0
I	0.001156	0.031785	0.008744	3.27E-05	0.017521	0.037111	0
Mg	2.140972	0	2.604348	7.552532	12.47706	0	12.7535
Mn	0.043526	0	0.01571	0.005468	0.020898	0.019158	0.215637
Na	0	36.66304	21.93514	25.38909	0	9.725993	0.861044
Ti	0.010301	0.268092	0.148034	0	0	0.051313	1.475548
V	0.038847	0.046886	0.000482	0.001618	0.008101	0	0.022826
N	1.748599	0	4.113199	8.458023	1.656148	11.1325	4.91254
S	84.97153	8.124761	66.24708	0	55.97734	41.19842	27.35803
NH4	10.31453	1.572527	4.169786	0.446249	2.469978	7.733432	2.939033
MSA	1.16E-05	0.000262	0	0	0	0.002658	2.06E-05
Pb	0.176465	0.193973	0.01099	0.025706	0	0.03036	0
Cu_CBD	0.057775	0.297123	0	0	0	0	0.004445
Fe	0.496202	4.754301	0	0.212161	0	1.78936	12.17472

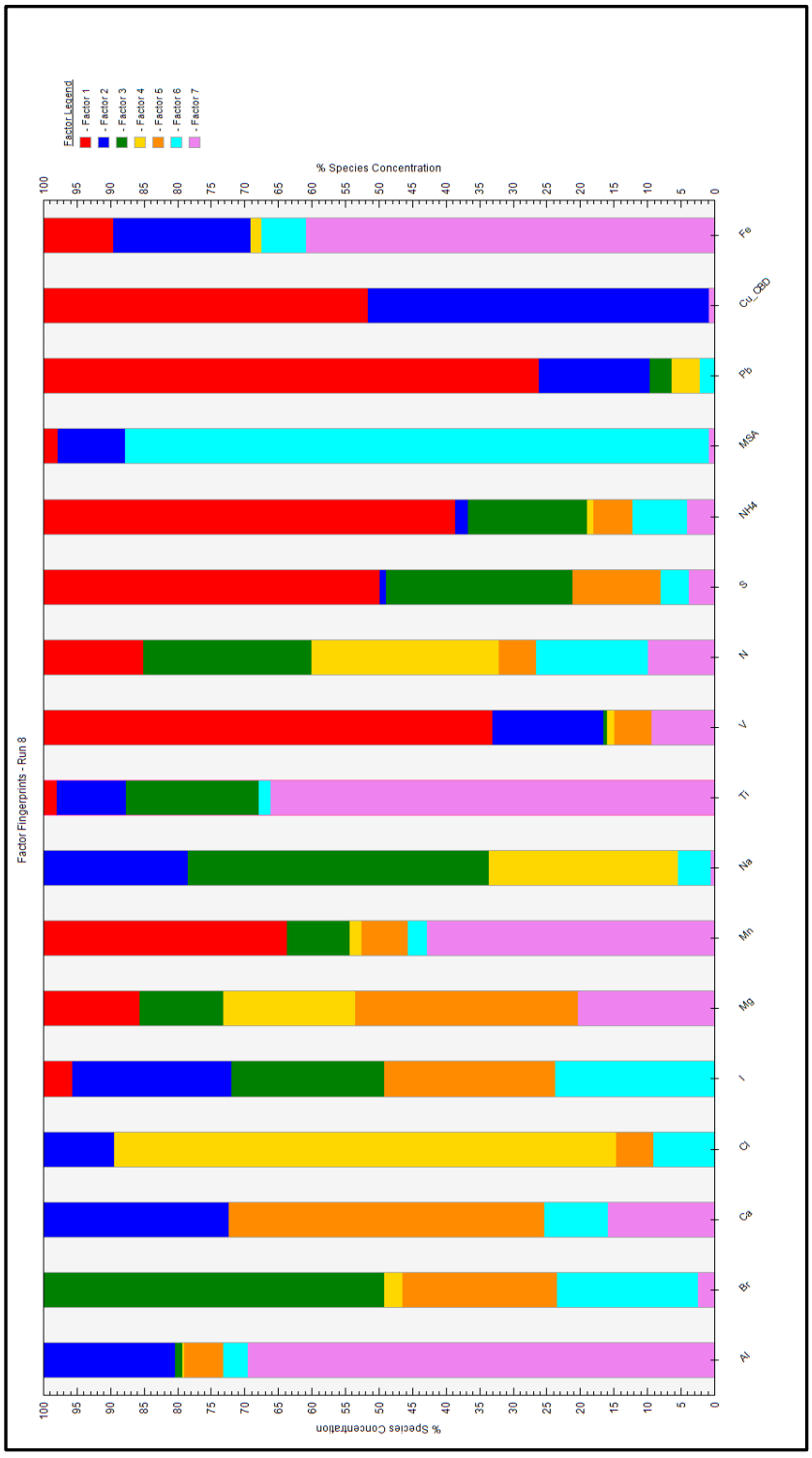

Figure 73 - CABM Seven-Factor Fingerprint Plot

8.2.4.5 CABM Combined PMF Conclusions

As with the PMF results from the NAA data, the most logical solution results in 2 sea components, 2 anthropogenic components, and a strong crustal component. The scaled residuals plots in the Appendix (Figures 74 through 77) validate that the 5-factor solution is more coherent than either the 4-factor solution or the 6-factor solution. The combined 5-factor results are as follows:

Factor 1: Anthropogenic (possible combustion)

Factor 2: Anthropogenic (possible smelting/other industrial activity)

Factor 3: Crustal Component

Factor 4: Sea Component (open water)

Factor 5: Sea Component (blowing snow)

8.2.5 PMF Results Conclusions

In all of the models including 3 or more factors, there is a strong and definitive crustal factor. Also, Chlorine, Magnesium, and Sodium all show extreme dependence on the models, which is encouraging based on the importance of these three elements in the conclusions of this work.

The sea components are less definitive in the NAA data results, but with the addition of the CABM data, some clarity can be gained. It appears that there

are two sea components, with one being an open-water source, and the other being a blowing snow, or iced-over water source. Based on the extreme dependence to the model of the elements Chlorine and Sodium (the strongest sea terms) for every model regardless of the number or runs, the fact that Bromine becomes strongly linked to non-sea factors leads one to the conclusion that Bromine is more of an anthropogenic term in the results herein, regardless of most studies linking it only with the Sea. Bromine is known to be linked to leaded gasoline combustion, and although leaded gasoline was phased out in most countries decades ago, it still seems more linked to combustion factors in these results than to sea components.

It should be noted here that Copper is essentially all below the limit of detection. The fact that Cu is unresolved in all models may be attributed this this fact. Bromine is also not strongly resolved, but still appears somewhat relevant in the PMF results, so it will be assumed that the data is still relevant.

The third element with potential detection limit problems is Titanium. All Titanium results in every section is within expectations and consistent with other literature. In addition, it is reasonably well resolved in the PMF results and consistently tracks into the crustal component, which is expected.

Finally, the 5-factor results make the most sense, and do not mix the sea and anthropogenic components as significantly. The same 5-factor solution falls out of both the NAA runs and the combined CABM data runs. The 5 dominant sources in the sample set most strongly appear to be:

Factor 1: Anthropogenic (possible combustion)

Factor 2: Anthropogenic (possible smelting/other industrial activity)

Factor 3: Crustal Component

Factor 4: Sea Component (open water)

Factor 5: Sea Component (blowing snow)

9. Conclusion and Summary of Findings

9.1 Conclusion

Three decades of winter Arctic aerosol samples from Alert, Canada (1980-2010) have been analyzed using neutron activation analysis to determine concentrations of Aluminum, Bromine, Calcium, Chlorine, Copper, Iodine, Magnesium, Manganese, Sodium, Titanium, and Vanadium. The elemental results have been characterized statistically and through several other methods including PMF. As seen in other research, the data was found to be primarily log-normally distributed.

This work represents a comprehensive look not only 11 elements captured in the Alert Arctic aerosol samples, but also at climatological data. This work then compares the elemental results with that climatological data. This comparison includes temperature trends as well as sea ice, ice shelves, and snow cover trends. Gaseous data is included in this study, although the correlations with the elemental information is not conducted for this study. CABM data is included for comparison and clarification on PMF results.

The NAA results are compared to other known research and available CABM data. Many similarities and many unexpected results are found. For expected results, conclusions can be drawn as to the validity of the processes being used in as much as most values found for the data represented herein are

within expected ranges based on other research available.

Examples of specific results seen previously include certain enrichment factor data, specific elemental ratios, and long term trends including a strong decrease in both Manganese and in Vanadium in Alert Arctic aerosol samples. Unexpected and interesting results of interest include noted divergence in sea-salt components in the PMF results and sea component ratio trends not seen in other literature.

New information of particular interest includes correlations between ice, snow, wind, and winter-averaged data and elemental ratios in the Arctic. This particular area of inquiry represents completely new information in the growing body of climate science and may influence studies that relate to the Arctic climate and environment.

9.2 Summary of Findings

The data herein is mostly lognormally distributed per the boxplots shown with the possible exceptions of Copper and Iodine. This type of distribution is consistent with other literature [Basunia, 2002; Cheng et al., 1991]. Means and geometric means, as well as other descriptive statistical information, is generally consistent with previously published research and do not result in any notable observations to be included in these conclusions. Enrichment factors calculated are also consistent with previously published data, and show no unexpected or

otherwise notable information. Mn/V ratios are somewhat similar to previously published data, and do not relate to any notable observations or findings. The general data, overall, is within the expected bounds and norms, so the following conclusions are considered both significant and valid.

9.2.1 Statistical Results

The means, medians, and all other descriptive statistical data can be reviewed in Chapter 5. None of the data is distributed normally per the tests (box plots indicate that most is distributed approximately log-normally), whereas much of the yearly-averaged data is, in fact, distributed normally. Elements with no aspect of normality are Br, Cu, and Ca. Of the three, Br and Cu are predominantly below the limit of detection, and thus this can be expected. Titanium is also below the limit of detection, but it passed both the normality tests for the yearly averaged data.

Light and dark months are split, and trends seen therein are consistent with those noted in prior literature. They can be reviewed in Chapter 5. Scatter plots and correlation results show many items of interest, specifically how elements are interrelated. Aluminum and Titanium are highly correlated (As is Iron), and Chlorine is highly correlated with Sodium; general inter-elemental correlations reinforce assumptions and understandings about aerosol sources such as a strong correlation between Magnesium and Calcium.

Several time trends of interest appear in the time correlation results. The most interesting is the fact that include the fact a very strong inverse correlation in Vanadium to time, and to a lesser extent but still significant, Manganese and Magnesium both exhibit a significant negative time correlation. Positive correlations with time include Chlorine and Iodine. Detailed inter-elemental correlation results can also be reviewed in Chapter 5.

9.2.2 Climatological Correlations

From the wind, ice, snow, and temperature data that is correlated with the Alert aerosol data set, many remarkable observations and results were found.

- Vanadium, Chlorine, Cl/Na and Mg/Na are all highly correlated to ice cover.
- No correlation is seen between wind speed and an element or ratio with the notable exception of Vanadium.
- Only Chlorine and Cl/Na seem to be correlated with temperature.
- Chlorine, Cl/Na, and Mg/Na are all correlated with time: strong temporal trends exist. Specifically, Chlorine and Cl/Na are increasing with time, whereas Mg/Na is decreasing with time and Magnesium has a decrease with time as well.
- Chlorine is more strongly correlated with Na during the dark months

9.2.3 PMF Results

Sodium, Chlorine, and Magnesium are extremely well resolved in all of the PMF models and results, which is encouraging as many conclusions are drawn herein based on those three elements. Other elements are less well resolved, and Copper shows almost no resolution. This is likely due to the fact that Copper is predominately below detection limits, yet the other two elements that are also primarily below detectable (Titanium and Bromine) do not show such a lack of modeling resolution.

The PMF results (both NAA-specific, and CABM combined results) point to there being 5 primary sources of the aerosol sampled at Alert, Canada. These include:

1: Anthropogenic source (possible combustion)

2: Anthropogenic source (possible smelting/other industrial activity)

3: Crustal source

4: Sea source (open water)

5: Sea source (blowing snow)

The apparent presence of two sea sources could mean that one is from salt entrainment from wind across ice and snow [Huang & Jaeglé, 2017] and the other is from more distant open waters. It is well known that certain sea

components reach a yearly maximum when the local ocean is frozen over [Huang & Jaeglé, 2017], so this number of sea-source components may partially explain that phenomenon. It is also likely that this type of verification of independent sources from both water and snow has not been explicitly seen before.

The presence of two anthropogenic sources is also somewhat expected based on the fact that much of the Arctic aerosol literature discusses black carbon, which is a combustion product [Stone et al., 2014; Cole & Steffen, 2010], whereas other literature focuses on smelting and other industrial activities in the Arctic [Basunia, 2002; Sirois & Barrie, 1999]. These results point to a similar conclusion that there are significant products from both combustion and aerosol elements released from smelting (or other industrial activities) as well, albeit more distant than from the sampling locations used in some prior research [Basunia, 2002].

9.3 Summary

Two apparent sea sources exist that produce aerosol pollution in the Arctic, based on the PMF data, which have not been noted in previous literature. Of these, one is likely snow, and one is more distant open water. Two predominant anthropogenic aerosol pollution sources also exist, contributing to the aerosol pollution at Alert, Canada. One is combustion, and the other is

smelting or other distant industrial activities.

Time trends exist in Cl/Na and Mg/Na which are consistent with other literature in that they reflect a changing Arctic. What is new in this research is the direct linkage of these ratios to Sulphate pollution, ice cover, and a direct correlation to temperature. There can now be seen an interplay between temperature, driven up by a decrease in Sulphates, which results in less ice as well as more sea-salt-components in the aerosol. The increased sea-salt components are not scrubbed by Sulphates as readily since clean air standards were enacted in the 1970s, and thus the Cl/Na ration increases as well.

Vanadium and other anthropogenic components have been decreasing for decades. Ultimately, as pollution has gone down, sea components and specific sea-component ratios in the Arctic Aerosol sample have gone up due to that decrease. Decreasing ice trends and increasing temperature trends in the Arctic also contribute to the trends and conclusions herein. Dominant factors affecting trends seen in the Arctic aerosol record from 1980 until at least 2010, validated and confirmed by the results herein, include:

1. Increasing Arctic air temperature
2. Decreasing Arctic ice cover
3. Decreasing general anthropogenic pollution
4. Stricter global gasoline standards
5. Stricter global coal combustion standards

10. Future Work, Impact, and Applications

The work performed herein is by no means fully comprehensive when all possible perturbations and applications are considered. Rather, a reasonable effort has been made to follow multiple lines of research that became apparent as the Alert data was considered and examined. As the results show, much has been learned from this investigation; however, those insights do not rule out additional information that can be extrapolated from the Alert aerosol record, or from the larger Arctic aerosol record. Rather, it is the belief of the author that both the Alert Arctic aerosol samples and the larger Arctic aerosol records should be further studied to gleam more knowledge and make potential judgments about our planet related to those records and their extrapolated insights.

In this section, some ideas and potential applications are laid out. There are likely many more avenues of discovery that the ambitious or resourceful researcher may follow in addition to those laid out herein. Hopefully more work will be done on the Arctic aerosol record in the future.

10.1 Follow-On Work

An examination of the data and results, combined with a general understanding of those data and the results, yields clues into the most likely fruitful and most logical areas of further research. Additionally, it was originally

expected that there would be Epithermal NAA results to compare with the Thermal NAA results. This additional NAA work did not occur due to staffing considerations, but would immediately lend itself to a more thorough knowledge of anthropogenic components and trends as related to other aerosol components, climate, ice, and all other areas considered herein.

If all of the following suggested areas of research were to be completed, many additional insights would be extracted, whereas completing even single items on the list would produce useful and interesting information. Thus, known areas open for (further) exploration include, but are not limited to the following:

1. The analysis results should be expanded to include NAA results of all samples available from Alert (January through December rather than just winter data), thus performing similar trending and analysis across all seasons. This would also include samples more recent than 2010, as the sample collection is ongoing.
2. The analysis results should be expanded to include Epithermal NAA data, which would include more elements such as Arsenic, Indium, and Antimony, all of which are anthropogenic tracers of pollution and industrial activity. The data set on hand includes only weaker anthropogenic elements of the aerosol record.

3. Gaseous trend analysis and correlation with the aerosol record (see Section 2.5) may provide correlations both previously observed and not predicted.
4. Black carbon and other data could be collected and compared to the data used for this study. Black carbon is linked to human activity, and thus would be a good addition to the current anthropogenic elements in the sample, as well as a good addition to any epithermal NAA results and data.
5. A comparison of the results and trends could be compared to additional well-documented global events releasing gasses and aerosols into the environment, most notably volcanism. For example, the Mount Pinatubo eruption in 1991 changed the optical thickness in the stratosphere significantly, as have other eruptions during the sample span, particularly the Mt. St. Helens eruption in 1980. [Keen, 2017]. Thoroughly comparing the information in this study to the reference given may imply a link between the Calcium (and other components) in the Arctic aerosol and volcanic activity, but insufficient information has been gathered to draw any comparisons or conclusions.
6. Back-Trajectory analysis would help identify local or specific regional sources, which may include oil consumption at Alert and changes in such consumption relating to the changes in Vanadium levels that can be seen

in this study. Such analysis would also help identify sources or interr-elemental spikes seen in the time-series data collected.

All of the aforementioned areas of exploration should result in insights and a better understanding of the Arctic aerosol record, Earth's climate, and human contributions to pollution in the Arctic. It is important to reiterate that there are numerous additional areas of potential work that are not covered here. Many additional publications and dissertations could be written from the many avenues of further study available, not limited to the few described above.

10.2 Impact and Applications

The results of this study and similar studies are instrumental to the further development of climate science. The complex response mechanisms from the climate due to different atmospheric and aerosol components are not fully understood, and every new piece of information aids in helping to understand the functions of a very complex system. Areas of science that have become of great concern over the past few decades include climate change in conjunction with pollution trending. This research will help further include linkages between some of the many contributing factors in both. Pollution monitoring and weather trend analysis are integrally linked with all other fields of climate science, all of which can benefit from the information in this study.

This work should have an impact on the particular fields of Arctic Aerosol Monitoring, Atmospheric Transport, Global Diffusion and Dispersion, Arctic Climate Science, Pollution Monitoring, Atmospheric Chemistry, and Source-Receptor Analysis. Of these fields at the present time there is a great deal of interest in Arctic Climate Science, and thus the previous sections and conclusions herein emphasize potential connections between the Arctic climate and the Arctic aerosol record. In summary, the primary scientific interest lies in the correlation between actual Arctic aerosol trends and predicted trends as they correlate to temperature, ice, and other trends recorded in the Arctic as well as in validation of other research.

Table 45 summarizes the immediate applications that can be taken from this work:

Table 45 - Research Applications

Field of Application	Purpose/Benefit to Science
1. Arctic Aerosol Monitoring	This work is an additional piece of the growing body of research and data of the Arctic aerosol record.
2. Atmospheric Chemistry	In addition to the aerosol record, there is a large body of research on atmospheric chemistry that involves chemical changes. Some research involves aerosol interactions, and some involves gaseous interactions. Components of each can interchange and interact; the Aerosol record is an important part of that study.
3. Anthropogenic Pollution Monitoring	This work is an additional piece of the growing body of research and data of the Arctic aerosol record.
4. Arctic and General Climate Science	Trends and correlations calculated in this work can be directly applied to other areas of the growing body of Climate Science research and data.

APPENDIX

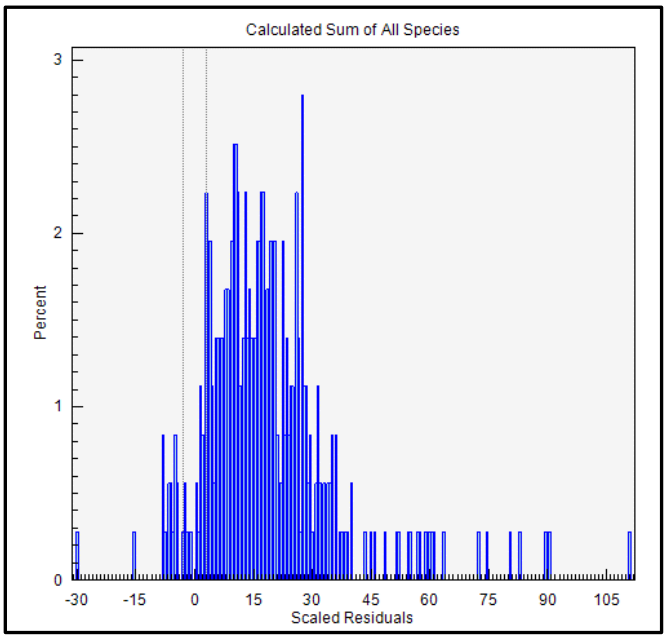

Figure 74 - NAA+CABM PMF 4-Factor Scaled Residuals

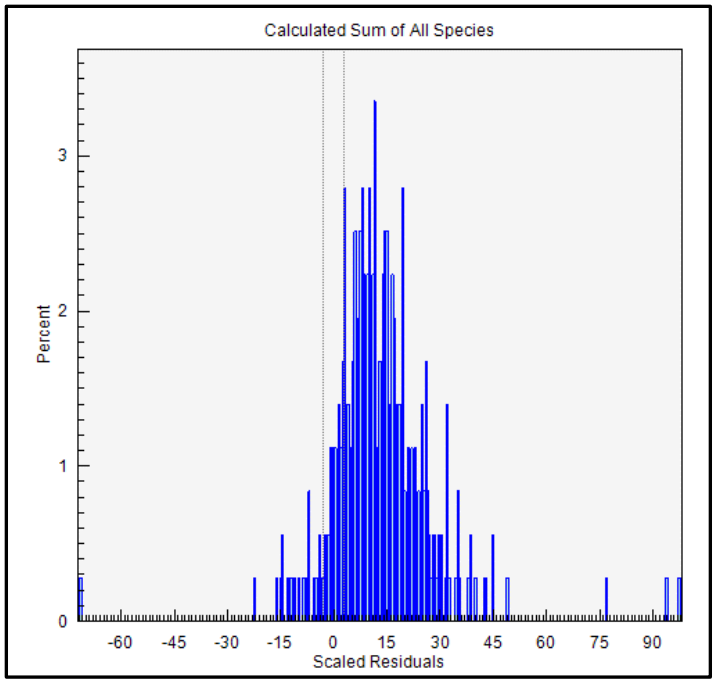

Figure 75 - NAA+CABM PMF 5-Factor Scaled Residuals

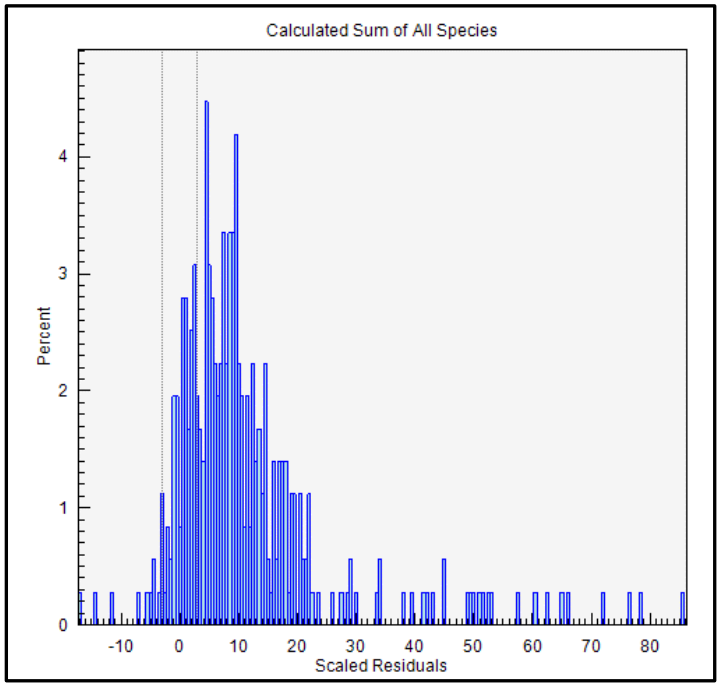

Figure 76 - NAA+CABM PMF 6-Factor Scaled Residuals

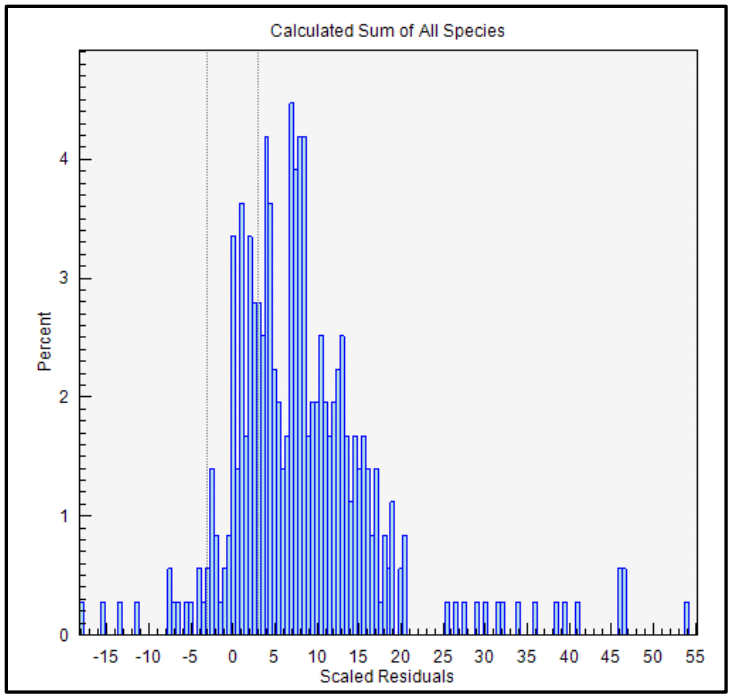

Figure 77 - NAA+CABM PMF 7-Factor Scaled Residuals

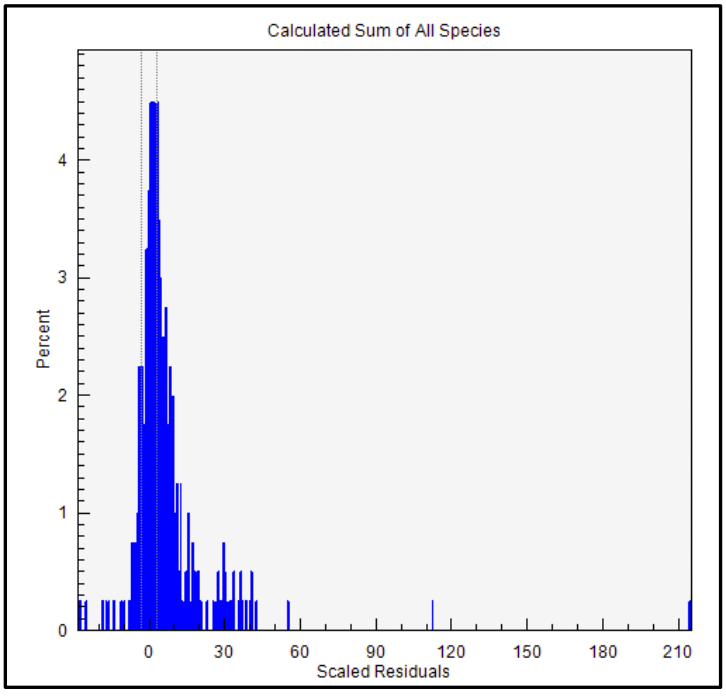

Figure 78 - NAA PMF 4-Factor Scaled Residuals

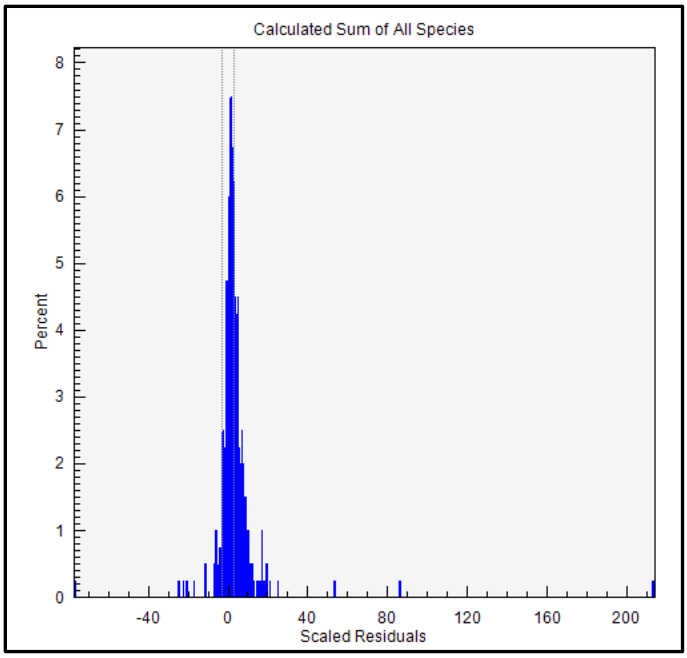

Figure 79 - NAA PMF 5-Factor Scaled Residuals

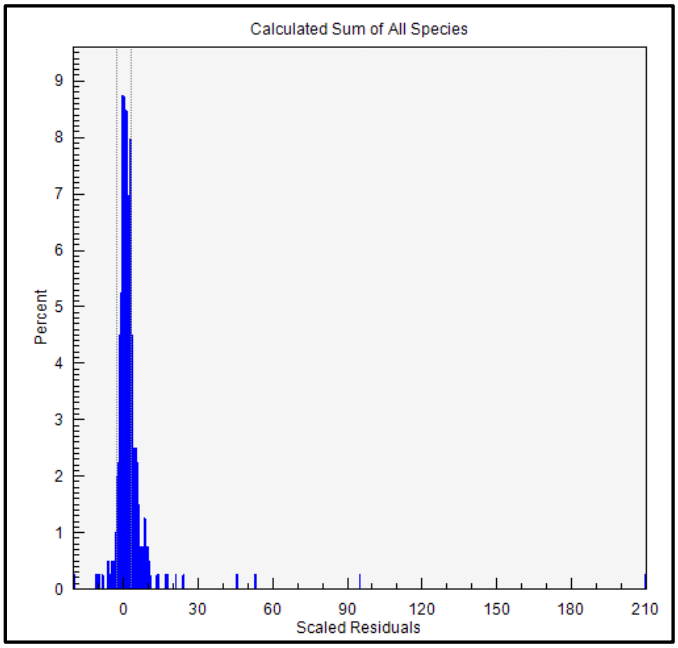

Figure 80 - NAA PMF 6-Factor Scaled Residuals

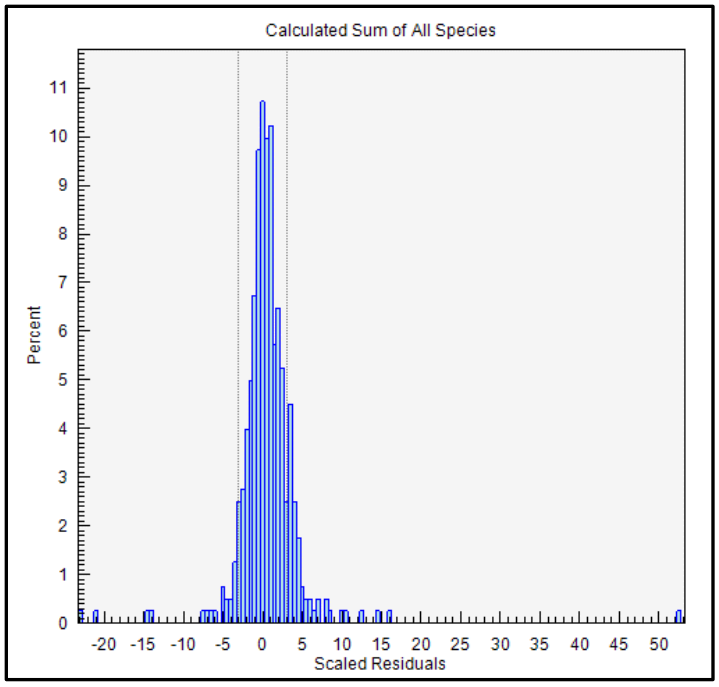

Figure 81 - NAA PMF 7-Factor Scaled Residuals

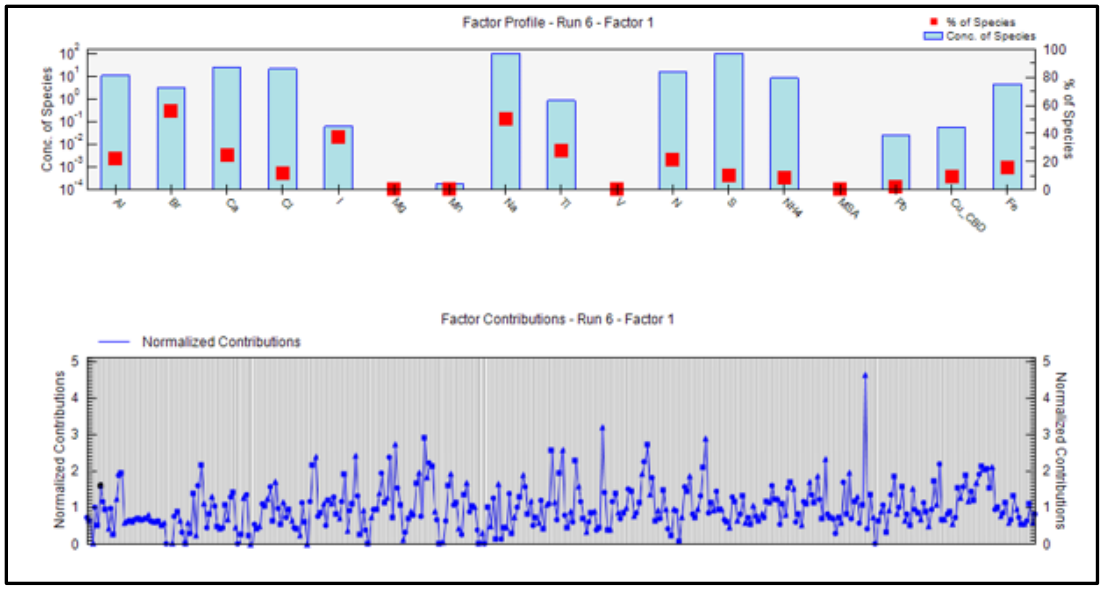

Figure 82 - NAA+CABM Factor 1 Profile and Contributions

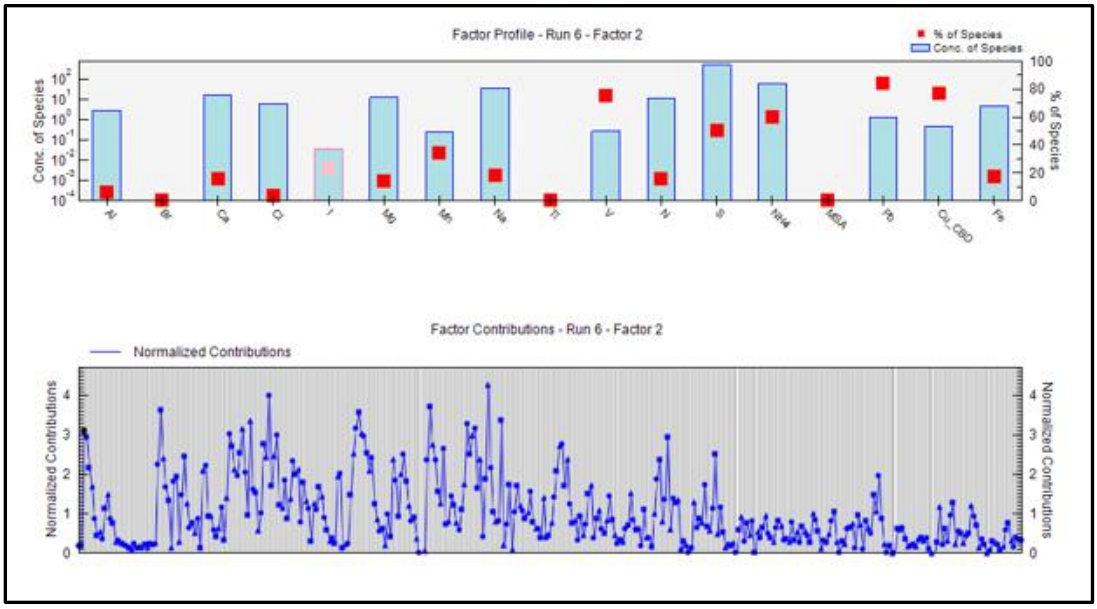

Figure 83 - NAA+CABM Factor 2 Profile and Contributions

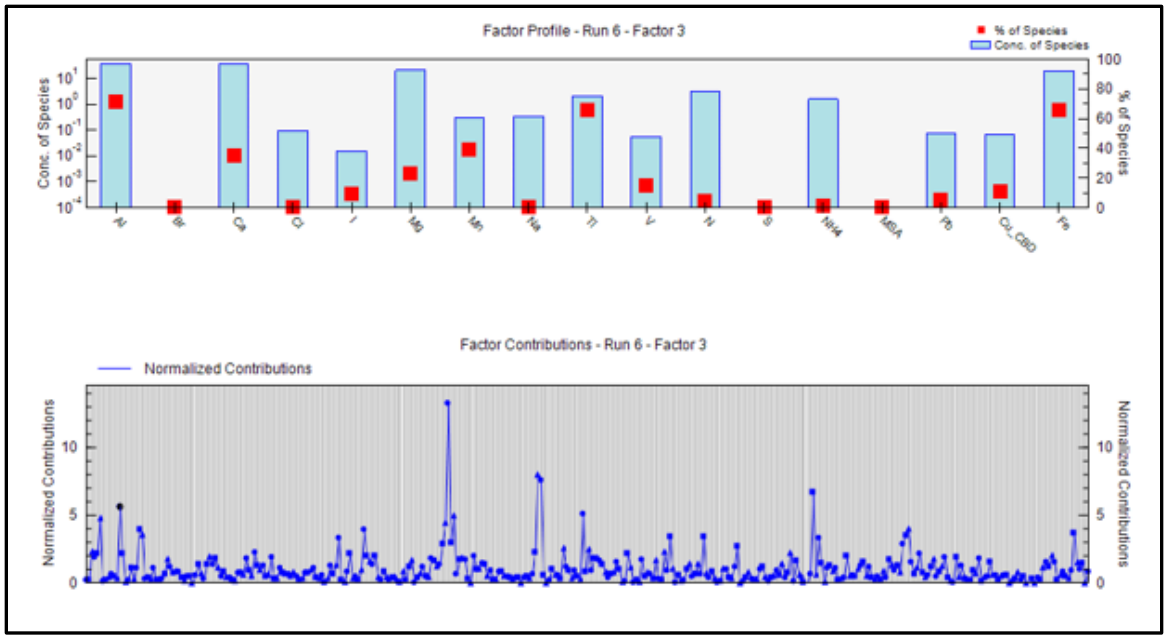

Figure 84 - NAA+CABM Factor 3 Profile and Contributions

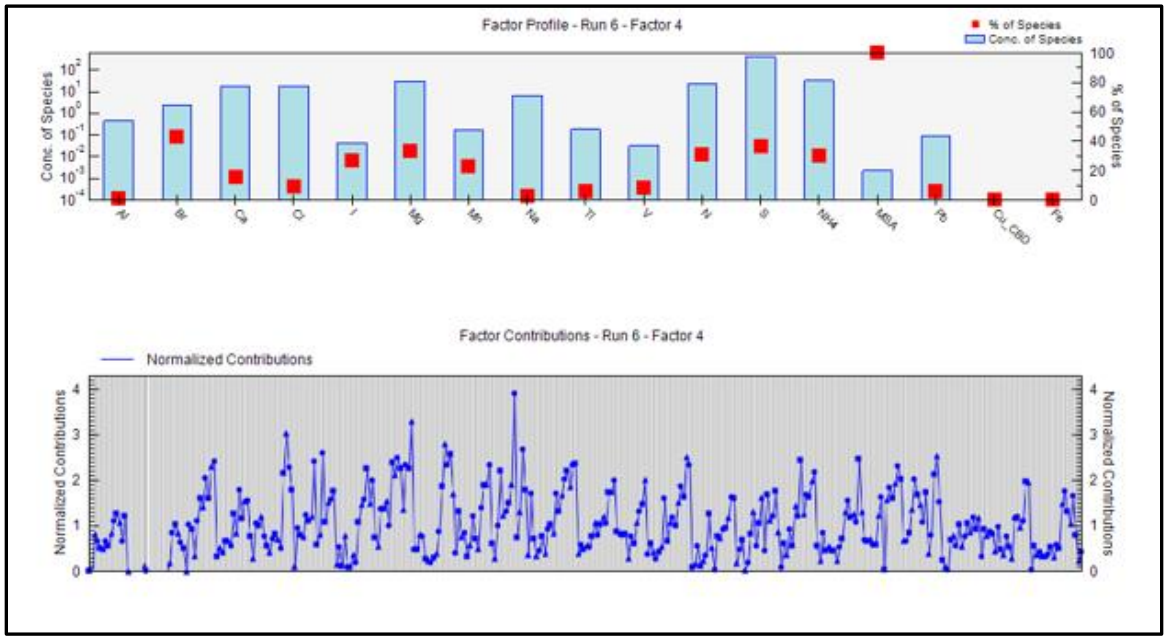

Figure 85 - NAA+CABM Factor 4 Profile and Contributions

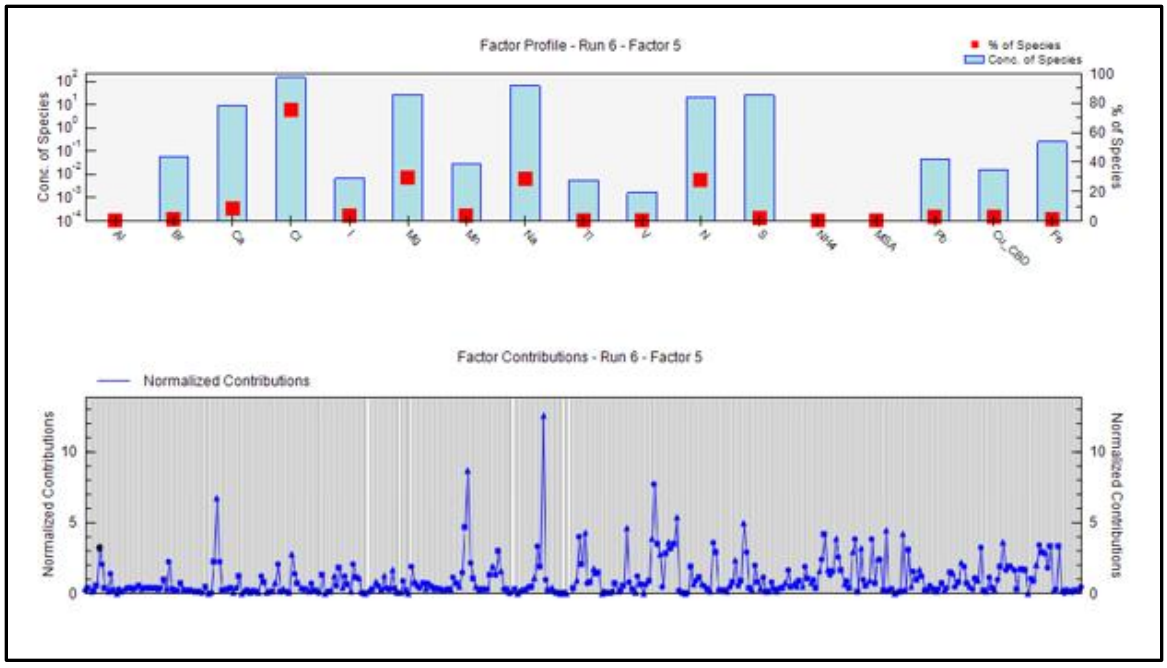

Figure 86 - NAA+CABM Factor 5 Profile and Contributions

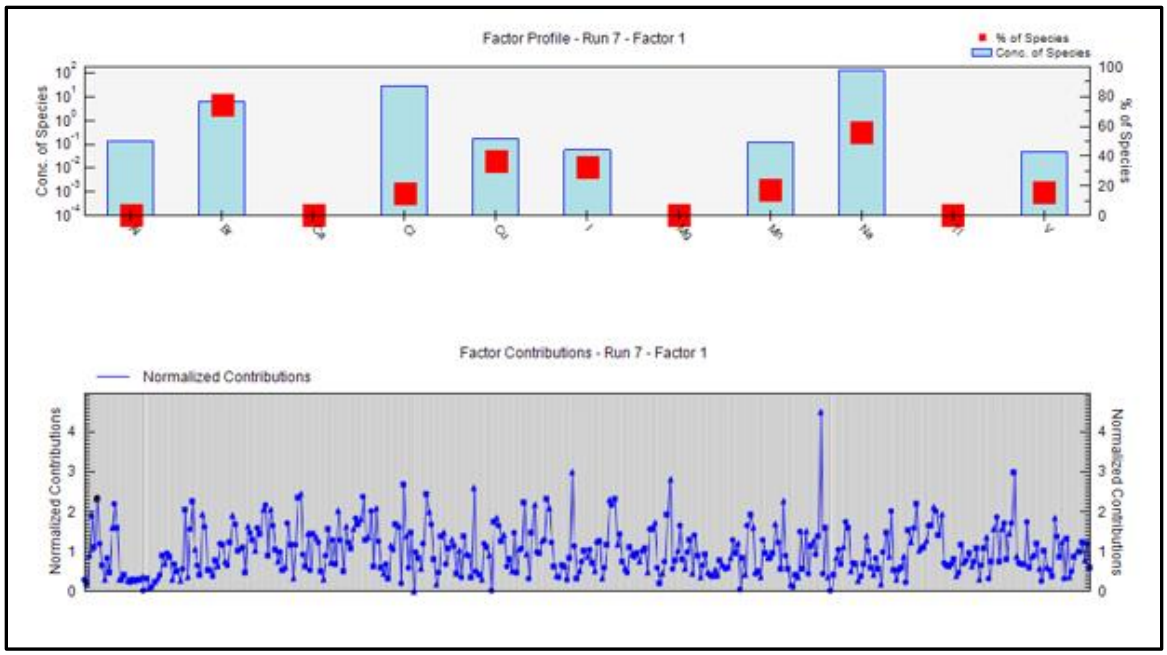

Figure 87 - NAA Factor 1 Profile and Contributions

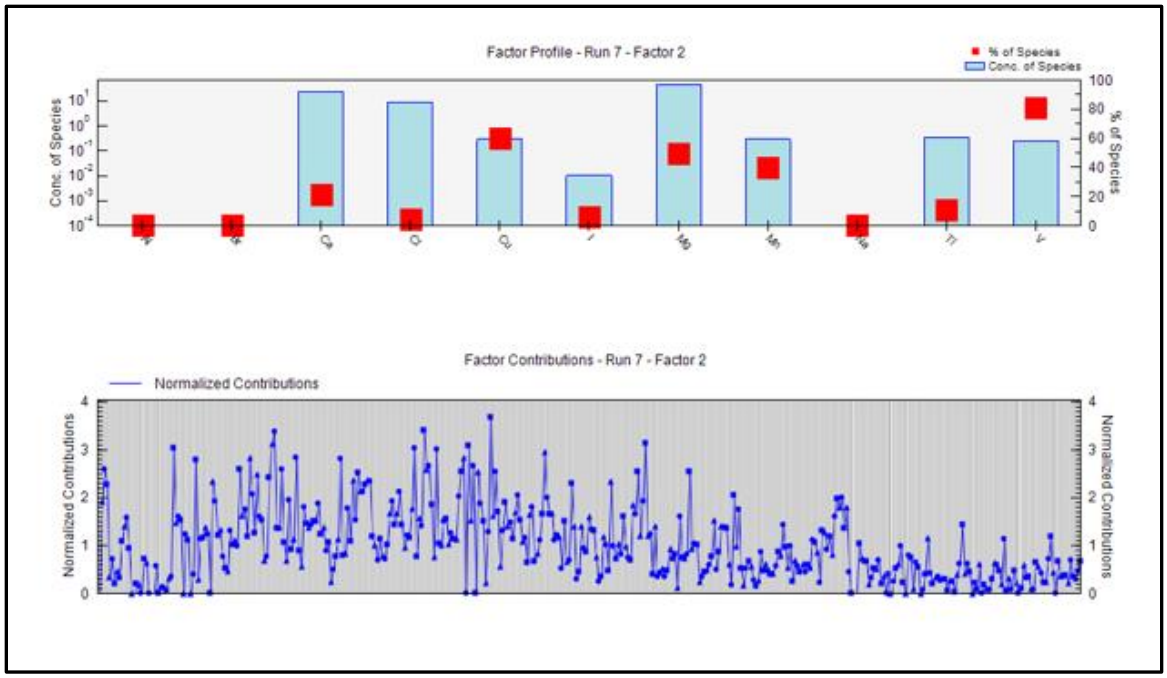

Figure 88 - NAA Factor 2 Profile and Contributions

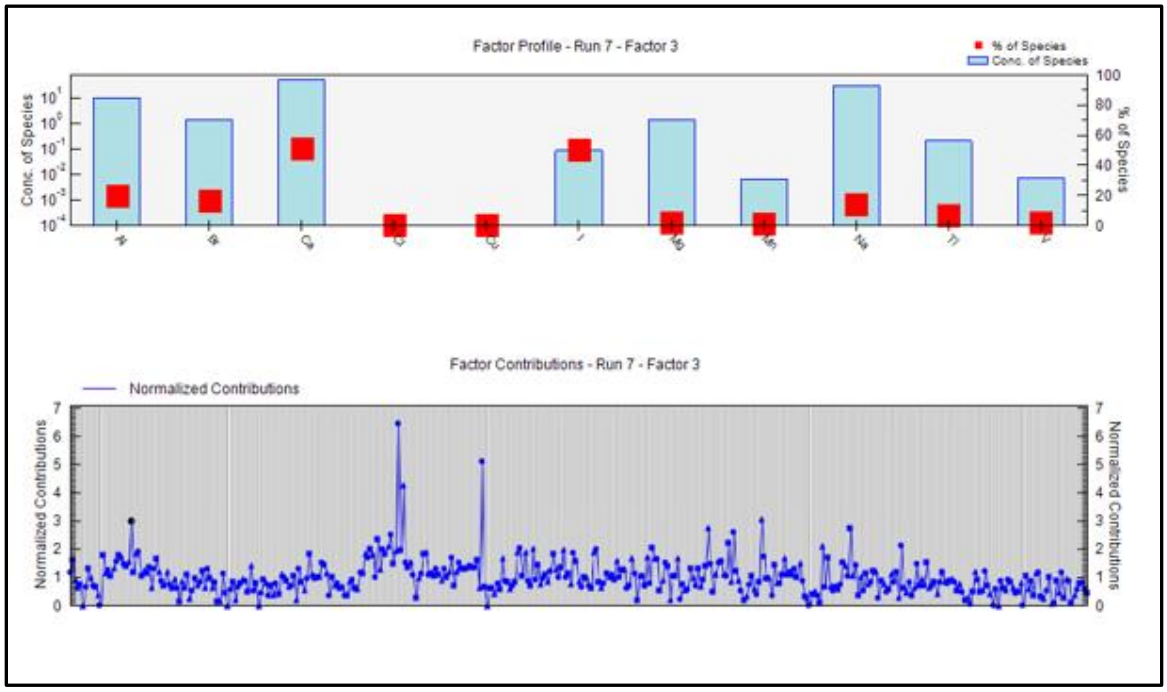

Figure 89 - NAA Factor 3 Profile and Contributions

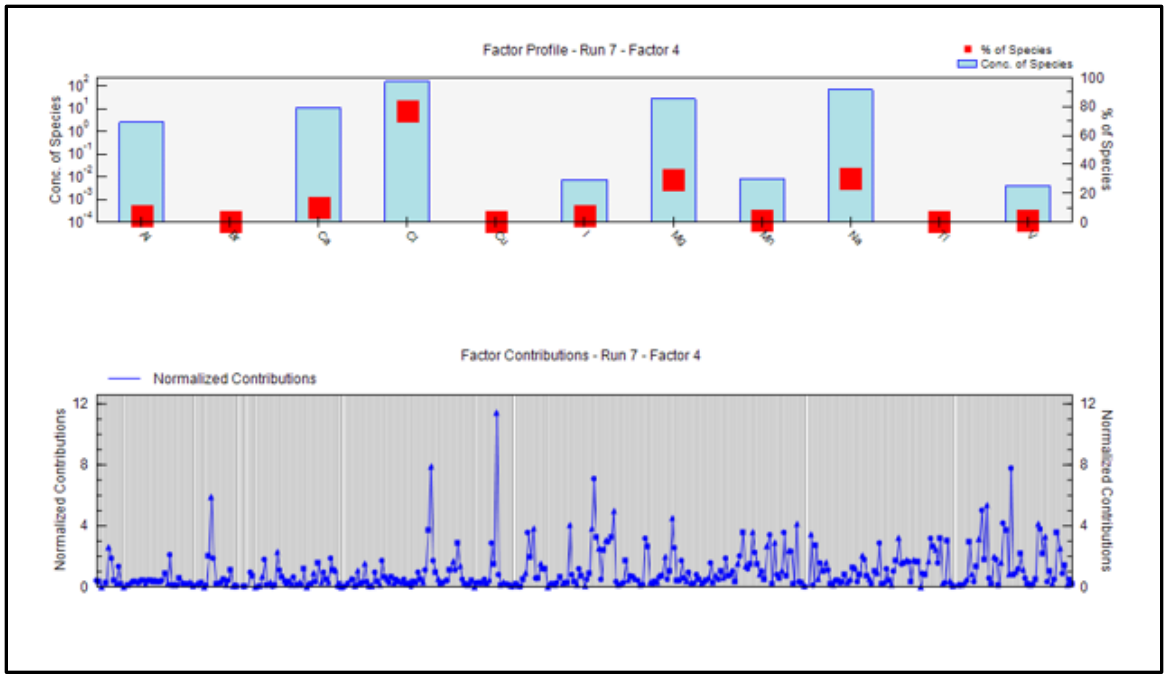

Figure 90 - NAA Factor 4 Profile and Contributions

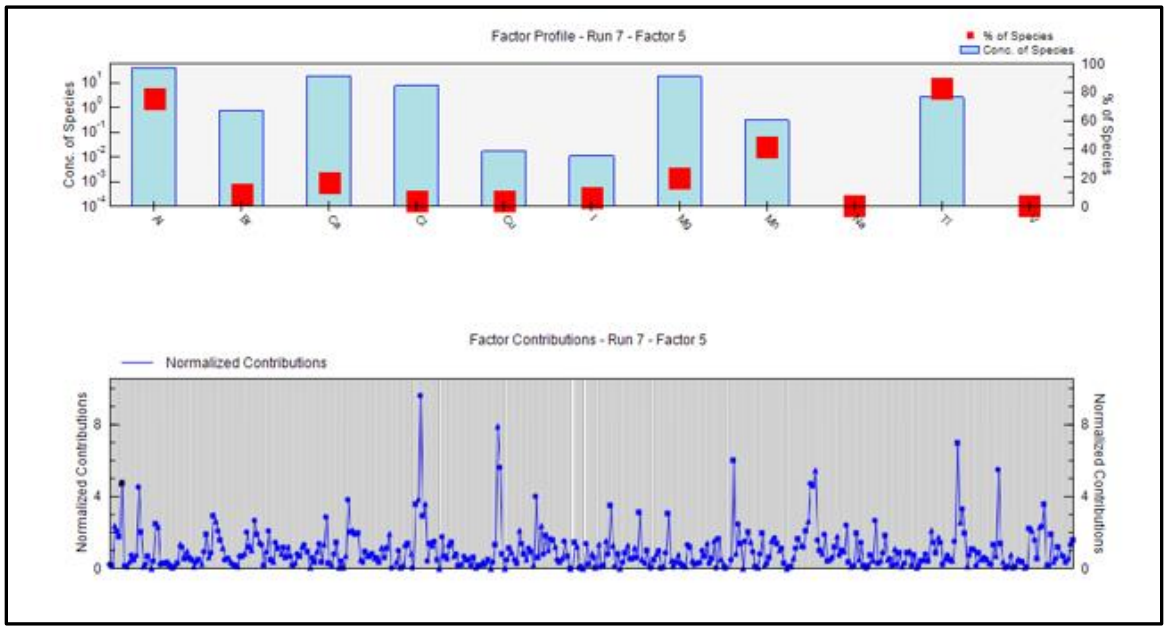

Figure 91 - NAA Factor 5 Profile and Contributions

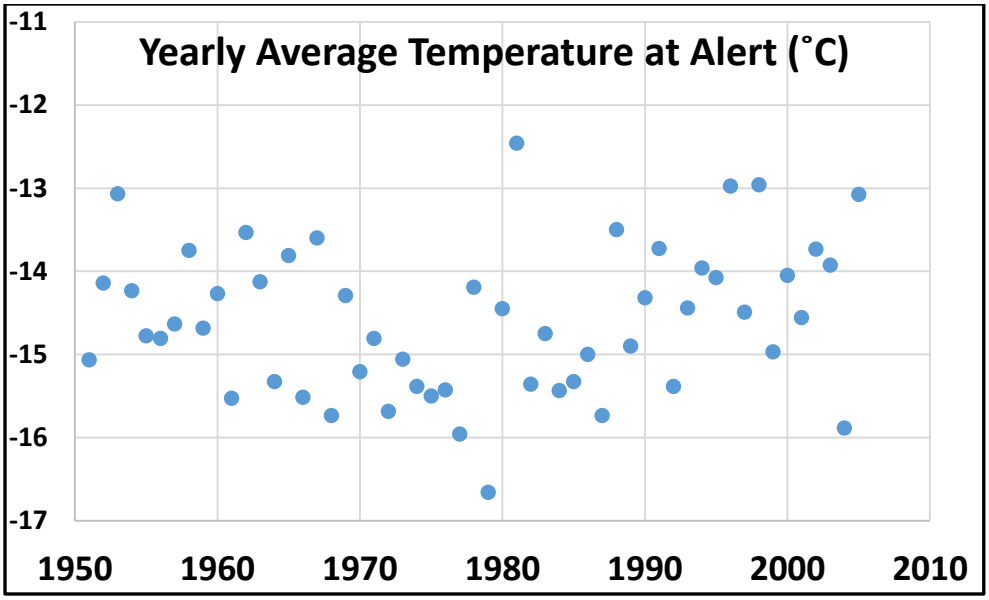

Figure 92 - Yearly Average Temperature at Alert

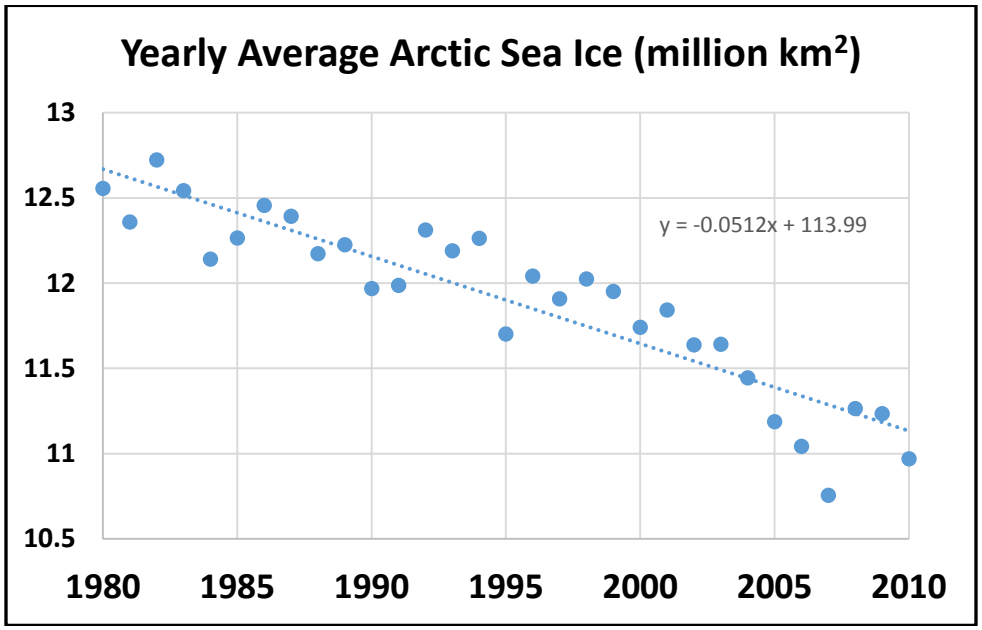

Figure 93 - Yearly Average Arctic Sea Ice

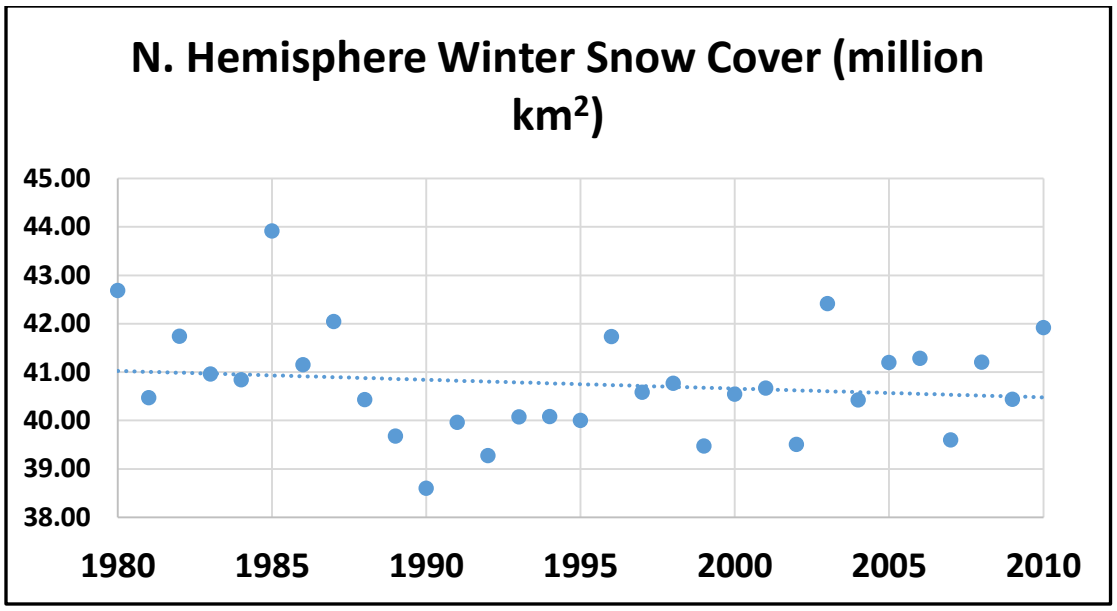

Figure 94 - N. Hemisphere Winter Snow Cover

Table 46 - Monthly Averaged Data Correlations

	January	Al	Br	Ca	Cl	Cu	I	Mg	Mn	Na	Ti	V
January	1.00											
Al	0.01	1.00										
Br	0.45	0.10	1.00									
Ca	-0.22	0.73	0.05	1.00								
Cl	0.44	0.09	0.58	-0.01	1.00							
Cu	-0.21	-0.03	0.21	0.17	0.11	1.00						
I	0.24	0.63	0.14	0.46	0.25	0.34	1.00					
Mg	0.12	0.72	0.50	0.69	0.46	0.16	0.53	1.00				
Mn	-0.18	0.75	0.04	0.66	-0.03	0.20	0.49	0.68	1.00			
Na	0.35	0.15	0.56	0.07	0.94	0.26	0.31	0.53	0.16	1.00		
Ti	-0.07	0.94	-0.03	0.68	-0.02	-0.08	0.56	0.57	0.66	0.02	1.00	
V	-0.80	0.15	-0.49	0.24	-0.37	0.27	0.10	0.01	0.45	-0.27	0.24	1.00
	February	Al	Br	Ca	Cl	Cu	I	Mg	Mn	Na	Ti	V
February	1.00											
Al	-0.19	1.00										
Br	0.47	-0.01	1.00									
Ca	-0.49	0.68	-0.05	1.00								
Cl	0.38	0.24	0.56	0.10	1.00							
Cu	-0.35	-0.11	-0.20	0.02	-0.21	1.00						
I	0.33	0.21	0.12	0.13	0.09	0.28	1.00					
Mg	-0.15	0.67	0.26	0.71	0.56	-0.07	0.26	1.00				
Mn	-0.47	0.60	-0.03	0.72	0.04	0.50	0.45	0.62	1.00			
Na	0.18	0.37	0.52	0.26	0.94	-0.06	0.07	0.63	0.21	1.00		
Ti	-0.06	0.79	0.07	0.46	0.28	0.06	0.17	0.54	0.55	0.39	1.00	
V	-0.69	0.35	-0.28	0.57	-0.16	0.57	0.24	0.34	0.73	0.05	0.19	1.00
	March	Al	Br	Ca	Cl	Cu	I	Mg	Mn	Na	Ti	V
March	1.00											
Al	0.04	1.00										
Br	-0.28	0.04	1.00									
Ca	-0.29	0.57	0.42	1.00								
Cl	0.49	-0.16	0.01	-0.16	1.00							
Cu	-0.01	-0.09	-0.02	0.00	-0.13	1.00						
I	0.35	-0.11	0.10	-0.11	0.01	0.85	1.00					
Mg	-0.06	0.30	0.55	0.64	0.44	0.01	0.02	1.00				
Mn	-0.10	0.59	0.43	0.48	-0.39	0.01	0.17	0.30	1.00			
Na	0.25	-0.04	0.44	0.24	0.82	-0.06	0.08	0.71	-0.09	1.00		
Ti	-0.10	0.77	0.05	0.43	-0.12	-0.09	-0.18	0.28	0.42	-0.07	1.00	
V	-0.59	0.16	0.72	0.45	-0.45	0.06	0.03	0.30	0.63	-0.06	0.14	1.00
	April	Al	Br	Ca	Cl	Cu	I	Mg	Mn	Na	Ti	V
April	1.00											
Al	-0.06	1.00										
Br	-0.47	-0.07	1.00									
Ca	-0.29	0.86	0.12	1.00								
Cl	0.30	0.01	0.19	0.06	1.00							
Cu	-0.07	0.54	0.38	0.51	0.13	1.00						
I	0.59	0.16	-0.34	-0.09	0.06	0.37	1.00					
Mg	-0.22	0.87	0.18	0.91	0.26	0.57	-0.04	1.00				
Mn	-0.09	0.94	-0.06	0.75	-0.04	0.55	0.22	0.81	1.00			
Na	-0.06	0.23	0.35	0.28	0.76	0.45	0.02	0.50	0.23	1.00		
Ti	-0.06	0.99	-0.03	0.86	0.05	0.57	0.14	0.89	0.94	0.26	1.00	
V	-0.67	0.48	0.28	0.58	-0.19	0.27	-0.27	0.57	0.60	0.23	0.50	1.00

REFERENCES

Alert, Nunavut (2017), https://en.wikipedia.org/wiki/Alert,_Nunavut

Barrie, L. A., Hoff, R. M., and Daggupaty, S. M. (1980) The Influence of Mid-Latitudinal Pollution Sources on Haze in the Canadian Arctic, Atmospheric Environment, 15, 8, 1407-1419

Barrie, L. A., and Hoff, R. M. (1985) Five Years of Air Chemistry Observations in the Canadian Arctic, Atmospheric Environment, 19, 12, 1995-2010

Barrie, L. A., Staebler, R., Toom, D., Georgi, B., den Hartog, G., Landsberger, S., and Wu, D. (1994) Arctic Aerosol Size-Segregated Chemical Observations in Relation to Ozone Depletion during Polar Sunrise Experiment 1992, Journal of Geophysical Research, 99, D12, 25439-25451

Basunia, M. S. (2002) Characterization of Finnish Arctic Aerosols and Receptor Modeling, Ph.D. Dissertation, University of Texas at Austin

Baum, E. M., Ernesti, M. C., Knox, H. D., Miller, T. R., and Watson, A. M. (2009) Chart of the Nuclides, Seventeenth Edition, Bechtel Marine Propulsion Corporation

Becagli, S., Lazzara, L., Marchese, C., Daya, U., Ascanius, S. E., Cacciani, M., Caiazzao, L., Di Biagio, C., Di Iorio, T., di Sarra, A., Eriksen, P., Fani, F., Giardi, F., Meloni, D., Muscari, G., Pace, G., Sevari, M., Traversi, R., and Udisti, R. (2016) Relationships Linking Primary Production, Sea Ice Melting, and Biogenic Aerosol in the Arctic, Atmospheric Environment, 136, 1-15

Begum, B. A., Kim, E., Jeon, C. H., Lee, D. W., and Hopke, P. K. (2005) Evaluation of the Potential Source Contribution Function using the 2002 Quebec Forest Fire Episode, Atmospheric Environment, 39, 3719-3724

Biegalski, S. R., Landsberger, S., and Hoff, R. (1997) High Bromine Aerosol Concentrations near Lake Huron from Long-Range Transport from the Arctic during Polar Sunrise, Journal of Geophysical Research, 102, D19, 23337-23343

Biegalski, S. R., Landsberger, S., and Hoff, R. M. (1998) Source-Receptor Modeling using Trace Metals in Aerosols Collected at Three Rural Canadian Great Lakes Sampling Stations, Journal of Waste Management Association, 48, 3, 227-237

Biegalski, S. R., and Landsberger, S. (1995) Improved Detection Limits for trace Elements on Aerosol Filters using Compton Suppression Counting and Epithermal Irradiation Techniques, Journal of Radioanalytical and Nuclear Chemistry, 192, 2, 195-204

Bilello, M. A. (1961) Formation, Growth, and Decay of Sea-Ice in the Canadian Arctic Archipelago, Journal of the Arctic Institute of North America, 14, 1, 1-23

Bodhaine, B. A., and Dutton, E. G. (1993) A Long-Term Decrease in Arctic Haze at Barrow, Alaska, Geographical Research Letters, 20, 10, 947-950

Boé, J., Hall, A., and Qu, X. (2009) September Sea-Ice Cover in the Arctic Ocean to Vanish by 2100, Nature Geoscience, 2, 341-343

Bowen, H. J. M. (1966) Trace Elements in Biochemistry, Academic Press, New York, NY

Browse, J., Carslaw, K. S., Mann, G. W., Birch, C. E., Arnold, S. R., and Leck, C. (2014) The Complex Response of Arctic Aerosol to Sea-Ice Retreat, Atmospheric Chemistry and Physics, 14, 7543-7557

Chang, R. Y.-W., Leck, C., Graus, M., Müller, M., Paatero, J., Burkhart, J. F., Stohl, A., Orr, L. H., Hayde, K., Li, S.-M., Hansel, A., Tjernström, M., Leaitch, W. R., and Abbatt, J. P. D. (2011) Aerosol Composition and Sources in the Central Arctic Ocean during ASCOS, Atmospheric Chemistry and Physics, 11, 10619-10636

Cheng, M. D., Hopke, P. K., Landsberger, S., and Barrie, L. A. (1991) Distribution Characteristics of Trace Elements and Ionic Species of Aerosol Collected at Canadian High Arctic, Atmospheric Environment, 25A, 12, 2903-2909

Cole, A. S., and Steffen, A. (2010) Trends in Long-Term Gaseous Mercury Observations in the Arctic and Effects of temperature and Other Atmospheric Conditions, Atmospheric Chemistry and Physics, 10, 4661-4672

Copland, L., Mueller, D. R., and Weir, L. (2007) Rapid Loss of the Ayles Ice Shelf, Ellesmere Island, Canada, Geophysical Research Letters, 34, L21501

Draxler, R. R., and Hess, G. D. (1997) Description of the HYSPLIT_4 Modeling System (2014 revision), NOAA Technical Memorandum ERL ARL-224

Draxler, R., Stunder, B., Rolph, G., Stein, A., and Taylor, A. (2016) HYSPLIT4 User's Guide, Air Resources Laboratory, National Oceanic and Atmospheric

Administration

Ellesmere Island (2017) The Canadian Encyclopedia Online, http://www.thecanadianencyclopedia.ca/en/

EPA PMF (2017) website: https://www.epa.gov/air-research/positive-matrix-factorization-model-environmental-data-analyses

Eslinger, P. W., Biegalski, S. R., Bowyer, T. W., Cooper, M. W., Haas, D. A., Hayes, J. C., Hoffman, I., Korpach, J., Yi, J., Rishel, J. P., Ungar, K., White, B., and Woods, V. T. (2014) Source Term Estimation of Radioxenon Released from the Fukushima Dai-ichi Nuclear Reactors using Measured Air Concentrations and Atmospheric Transport Modeling, Journal of Environmental Radioactivity, 127, 127-132

Fisher, J. A., Jacob, D. J., Wang, Q., Bahreini, R., Carouge, C. C., Cubison, M. J., Dibb, J. E., Diehl, T., Jimenez, J. L., Leibensperger, E. M., Lu, Z., Meinders, M. B. J., Pye, H. O. T., Quinn, P. K., Sharma, S., Streets, D. G., von Donkelaar, A., and Yantosca, R. M. (2011) Sources, Distribution, and Acidity of Sulfate-Ammonium Aerosol in the Arctic in Winter-Spring, Atmospheric Environment, 45, 7301-7318

Garrett, T. J., and Verzella, L. L. (2008) An Evolving History of Arctic Aerosols, American Meteorological Society, 299-302

Glascock, M. D. (2016) Overview of Neutron Activation Analysis, archaeometry.missouri.edu/naa_overview.html

Gong, S., and Barrie, L. A. (2005) Trends of Heavy Metal Components in the

Arctic Aerosols and their Relationship to the Emissions in the Northern Hemisphere, Science of the Total Environment, 342, 175-183

Hara, K., Nakazawa, F., Fujita, S., Enomoto, H., and Sugiyama, S. (2014) Horizontal Distributions of Aerosol Constituents and their Mixing States in Antarctica during the JASE Traverse, Atmospheric Chemistry and Physics., 14, 10211-10230

Heidam, N. Z. (1985) Crustal Enrichments in the Arctic Aerosol, Atmospheric Environment, 19, 12, 2083-2097

Hopke, P. K. (2000) A Guide to Positive Matrix Factorization, Clarkson University Department of Chemistry

Hopke, P. K. (2016) Review of Receptor Modeling Methods for Source Apportionment, Journal of the Air & Waste Management Association, 66, 3, 237-259

Howell, S. E. L., Laliberte, F., Kwok, R., Derson, C., and King, J. (2016) Landfast Ice Thickness in the Canadian Arctic Archipelago from Observations and Models, The Cryosphere, 10, 1463-1475

Huang, J., and Jaeglé, L. (2017) Wintertime Enhancements of Sea Salt Aerosol in Polar Regions Consistent with a Sea Ice Source from Blowing Snow, Atmospheric Chemistry and Physics, 17, 3699-3712

HYSPLIT (2017) General Information about HYSPLIT, http://ready.arl.noaa.gov/HYSPLIT.php

Keen, R. A. (2017) Two Centuries of Volcanic Aerosols Derived from Lunar

Eclipse Records 1805-2015, NOAA Global Monitoring Annual Conference (2017) Proceedings

Koch, R. C. (1960) Activation Analysis Handbook, Academic Press, New York, NY

Knoll, G. F. (2000) Radiation Detection and Measurement, Third Edition, John Wiley and Sons, New York, NY

Krachler, M., Zheng, J., Koerner, R., Zdanowicz, C., Fisher, D., and Shotyk, W. (2005) Increasing Atmospheric Antimony Contamination in the Northern Hemisphere: Snow and Ice Evidence from Devon Island, Arctic Canada, Journal of Environmental Monitoring, 7, 1169-1176

Landsberger, S., Cizek, W. D., and Campbell, R. H. (1994) NADA92: An Automated, User-Friendly Program for Neutron Activation Data Analysis, Journal of Radioanalytical and Nuclear Chemistry, Articles, 180, 1, 55-63

Landsberger, S., Vermette, S. J., and Barrie, L. A. (1990) Multielemental Composition of the Arctic Aerosol, Journal of Geophysical Research, 95, D4, 3509-3515

Landsberger, S., Vermette, V. G., Stuenkel, D., Hopke, P. K., Cheng, M. D., and Barrie, L. A. (1992) Elemental Source Signatures of Aerosols from the Canadian High Arctic, Environmental Pollution, 75, 181-187

Landsberger, S., Zhang, P., Wu, D., and Chatt, A. (1997) Analysis of the Arctic Aerosol for a Ten Year Period using Various Neutron Activation Analysis Methods, Journal of Radioanalytical Chemistry, 1, 11-15

Lawson, D. R., and Winchester, J. W. (1979) A Standard Crustal Aerosol as a Reference for Elemental Enrichment Factors, Atmospheric Environment, 13, 925-930

Laing, J. R., Hopke, P. K., Hopke, E. F., Husain, L., Dutkiewicz, V. A., Paatero, J., and Viisanen, Y. (2014a) Long-Term Particle Measurements in Finnish Arctic: Part I – Chemical Composition and Trace Metal Solubility, Atmospheric Environment, 88, 275-284

Laing, J. R., Hopke, P. K., Hopke, E. F., Husain, L., Dutkiewicz, V. A., Paatero, J., and Viisanen, Y. (2014b) Long-Term Particle Measurements in Finnish Arctic: Part II – Trend Analysis and Source Location Identification, Atmospheric Environment, 88, 285-296

Laing, J. R., Hopke, P. K., Hopke, E. F., Husain, L., Dutkiewicz, V. A., Paatero, J., and Viisanen, Y. (2015) Positive Matrix Factorization of 47 Years of Particle Measurements in Finnish Arctic, Aerosol and Air Quality Research, 15, 188-207

Lide, D. R. (2000) CRC Handbook of Chemistry & Physics, CRC Press, USA

Lodge, J. P. (1986) Editorial: Use of Whatman 41 Filter Papers in Particle Sampling, Atmospheric Environment, 20, 9, 1657

Lowenthal, D. H., and Rahn, K. A. (1987) Further Comments on the Use of Whatman 41 Filter Papers for High Volume Aerosol Sampling, Atmospheric Environment, 21, 12, 2732-2734

Lucey, D., Hadjiiski, L., Hopke, P. K., Scudlark, J. R., and Church, T. (2001)

Identification of Sources of Pollutants in Precipitation Measured at the Mid-Atlantic US Coast using Potential Source Contribution Function (PSCF), Atmospheric Environment, 35, 3979-3986

Ma, Y., Mao, R., Feng, S., Gong, D., and Kim, S. (2017) Does the Recent Warming Hiatus Exist over Northern Asia for Winter Wind Chill Temperature? International Journal of Climaology, 37, 3138-3144

Maenhaut, W., Ducastel, G., Leck, C., Nilsson, E. D., and Heintzenberg, J. (1996) Multi-Elemental Composition and Sources of the High Arctic Atmospheric Aerosol during Summer and Autumn, Tellus, 48B, 300-321

Maslanik, J., Drobot, S., Fowler, C., Emery, W., and Barry, R. (2007) On the Arctic Climate Paradox and the Continuing Role of Atmospheric Circulation in Affecting Sea Ice Conditions, Geophysical Research Letters, 34, L03711

Mason, B. (1966) Principles of Geochemistry, 3rd Edition, John Wiley &Sons, Inc., New York, NY

Miller, I., Freund, J. E., and Johnson, A. (1990) Probability and Statistics for Engineers: Fourth Edition, Prentice-Hall

Nilsson, E. D., Rannik, Ü., Swietlicki, E., Leck, C., Aalto, P. P., Zhou, J., and Norman, M. (2001) Turbulent Aerosol Fluxes over the Arctic Ocean 2. Wind-Driven Sources from the Sea, Journal of Geophysical Research, 106, D23, 32,139-32,154

Norris, G., Brown, S., and Bai, S. (2014) EPA Positive Matrix Factorization (PMF) 5.0 Fundamentals and User Guide, EPA/600/R, U. S. Environmental

Protection Agency, Office of Research and Development, Washington, DC

Pacyna, J. M., and Ottar, B. (1988) Origin of Natural Constituents in the Arctic Aerosol, Atmospheric Environment, 23, 4, 809-815

Ping, Z. (1996) Relative Composition of Crustal and Anthropogenic Trace Element Constituents in Canadian Arctic Aerosol from 1982-1992 as Determined by Neutron Activation Analysis, M.S. Thesis, University of Illinois at Urbana-Champaign

Polissar, A. V., Hopke, P. K., Paatero, P., Kaufmann, Y. J., Hall, D. K., Bodhaine, B. A., Dutton, E. G., and Harris, J. M. (1999) The Aerosol at Barrow, Alaska: Long-Term Trends and Source Locations, Atmospheric Environment, 33, 2441-2458

Polissar, A. V., Hopke, P. K., Malm, W. C., and Sisler, J. F. (1998) Atmospheric Aerosol over Alaska 1. Spatial and Seasonal Variability, Journal of Geophysical Research, 103, 19, 035-19, 044

Pope, S., Copland, L., and Mueller, D. (2012) Loss of Multiyear Sea Ice from Yelverton Bay, Ellesmere Island, Nunavut, Canada, Arctic, Antarctic, and Alpine Research, 2, 210-221

Quinn, P. K., Bates, T. S., Shulz, K., and Shaw, G. E. (2009) Decadal Trends in Aerosol Chemical Composition at Barrow, Alaska: 1976-2008, Atmospheric Chemistry and Physics, 9, 8883-8888

Quinn, P. K., Shaw, G., Andrews, E., Dutton, E. G., Ruoho-Airola, T., and Gong, S. L. (2007) Arctic Haze: Current Trends and Knowledge Gaps, Tellus, 59B,

99-114

Rahn, K. A., and McCaffrey, R. J. (1980) On the Origin and Transport of the Winter Arctic Aerosol, Annals of the New York Academy of Sciences, 338, 486-503

Rahn, K. A. (1981) The Mn/V Ratio as a Tracer of Large-Scale Sources of Pollution Aerosol for the Arctic, Atmospheric Environment, 15, 8, 1457-1461

Randerson, D. (1984) Atmospheric Science and Power Production, Technical Information Center, Office of Scientific and Technical Information, United States Department of Energy

Rothrick, D. A., Yu, Y., and Maykut, G. A. (1999) Thinning of the Arctic Sea-Ice Cover, Geophysical Research Letters, 26, 23, 3469-3472

Samset, B. H. (2018) How Cleaner Air Changes the Climate, Science, 360, 6385, 148-150

Serreze, M. C., Holland, M. M., and Stroeve, J. (2007) Perspectives on the Arctic's Shrinking Sea-Ice Cover, Science, 315, 1533-1536

Shaw, G. (1991) Aerosol Chemical Components in Alaska Air Masses 2. Sea Salt and Marine Product, Journal of Geophysical Research, 96, D12, 22369-22372

Shelley, R. U., Morton, P. L., and Landing, W. M. (2014) Elemental Ratios and Enrichment Factors in Aerosols from the US-GEOTRACES North Atlantic Transects, Deep Sea Research Part II: Topical Studies in Oceanography, 116, 262-272

Shevchenko, V., Lisitzin, A., Vinogradova, A., and Stein, R. (2003) Heavy Metals in Aerosols over the Seas of the Russian Arctic, The Science of the Total Environment, 306, 11-25

Sirois, A., and Barrie, L. A. (1999) Arctic Lower Tropospheric Aerosol Trends and Composition at Alert, Canada, 1980-1995, Journal of Geophysical Research, 104, D9, 11599-11618

Sprovieri, F., Pirrone, N., and Hedgecock, I. M. (2002) Intensive Atmospheric Mercury Measurements at Terra Nova Bay in Antarctica during November and December 2000, Journal of Geophysical Research, 107, D23, 4722

Stone, R. S., Sharma, S., Herber, A., Eleftheriadis, and Nelson, D. W. (2014) A Characterization of Arctic Aerosols on the Basis of Aerosol Optical Depth and Black Carbon Measurements, Elementa, 2, 000027, 1-22

Struthers, H., Ekman, A. M. L., Glantz, P., Iverson, T., Kirkevåg, A., Mårtensson, E. M., Seland, Ø., and Nilsson, E. D. (2011) The Effect of Sea Ice Loss on Sea Salt Aerosol Concentrations and the Radiative Balance in the Arctic, Atmospheric Chemistry and Physics, 11, 3459-3477

Thropp, J., Smith, S. L., and Lewkowicz, A. G. (2010) Observed Recent Changes in Climate and Permafrost Temperatures at Four Sites in Northern Canada, GEO2010 Proceedings, 1265-1272

TraPSA (2017) https://adweb.clarkson.edu/projects/TraPSA/public_html/

Voiland, A. (2009) Aerosols may Drive a Significant Portion of Arctic Warming, NASA's Earth Science News Team, www.nasa.gov

Wedepohl, K. H. (1967 [German edition]/1971) Geochemistry, Holt, Rinehart and Winston, Inc., USA

Wilks, D. S. (2006) Statistical Methods in the Atmospheric Sciences: Second Edition, Elsevier & Academic Press

Wofsy, S. C., McElroy, M. B., and Yung, Y. L. (1975) The Chemistry of Atmospheric Bromine, Geophysical Research Letters, 2, 6, 215-218

Ye, P., Xie, Z., Yu, J., and Kang, H. (2015) Spatial Distribution of Methanesulphonic Acid in the Arctic Aerosol Collected during the Chinese Arctic Research Expedition, Atmosphere, 6, 699-712

Yli-Tuomi, T., Venditte, L., Hopke, P. K., Basunia, M. S., Landsberger, S., Viisanen, Y., and Paatero, J. (2003a) Composition of the Finnish Arctic Aerosol: Collection and Analysis of Historical Filter Samples, Atmospheric Environment, 37, 17, 2355-2364

Yli-Tuomi, T., Hopke, P. Pk., Paatero, P., Basunia, M. S., Landsberger, S., Viisanen, Y., and Paatero, J. (2003b) Atmospheric Aerosol over Finnish Arctic: Source Analysis by the Multilinear Engine and the Potential Source Contribution Function, Atmospheric Environment, 37, 31, 4381-4392

Yu, Y., Stern, H., Fowler, C., Fetterer, F., and Maslank, J. (2014) Interranual Variability of Arctic Landfast Ice between 1976 and 2007, Journal of Climate, 27(1), 227-243

Zwillinger, D. (2003) CRC Standard Mathematical Tables and Formulae, Chapman & Hall, USA

VITA

Eric Compher was born in a suburb of Cincinnati, Ohio. After 6 years in the U. S. Navy operating nuclear reactors on submarines, he began his college career, earning the degree of Bachelor of Science in Physics from Lynchburg College in 2008, followed by the degree of Master of Science in Electrical Engineering from the University of Virginia in 2010. Upon completion of the M. S., he moved to Pittsburgh, Pennsylvania and began working at the Bettis Atomic Power Laboratory as a Reactor Safety Engineer. In 2015 he transferred to the Bettis Reactor Engineering School to teach Naval Reactors Engineers both Nuclear Physics and Shipboard Electrical Engineering.

Address: ecompher@utexas.edu

This manuscript was typed by the author.